A thesis submitted to University of Hyderabad for the award of

Doctor of Philosophy (Ph.D.)
by

Akash
Enrollment Number 17LPPH10

Department of Plant Sciences
School of Life sciences
University of Hyderabad
Hyderabad

December 2022

Certificates

University of Hyderabad
(A Central University established in 1974 by act of parliament)

Department of Plant Sciences

School of Life Sciences

Hyderabad– 500 046, INDIA

DECLARATION

I, **Akash**, hereby declare that this thesis entitled ***"Functional characterization of SlRbohH and SlFBX2L1 genes for their roles in phosphorus starvation response in tomato"*** submitted by me is based on the results of the work done under the guidance and supervision of **Dr. Rahul Kumar** at the Department of Plant Sciences, School of Life Sciences, University of Hyderabad. The work presented in this thesis is original and plagiarism free. I also declare that no part or in full of this thesis has been submitted previously to this University or any other University or Institution for the award of any degree or diploma.

Akash

Regd. No: 17LPPH10

Certificates

University of Hyderabad

Hyderabad– 500 046, INDIA

CERTIFICATE

This is to certify that the thesis entitled *"**Functional characterization of SlRbohH and SlFBX2L1 genes for their roles in phosphorus starvation response in tomato"*** submitted by **Akash** bearing registration number **17LPPH10** in partial fulfilment of the requirement for the award of Doctor of Philosophy in the School of Life Sciences is a bonafide work carried out by him under my supervision and guidance.

The thesis is free from plagiarism and has not been submitted previously in part or in fully to this or any other university or institution for the award of any degree or diploma.

Part of the thesis have been published in the following publications:

1. **Akash.,** Rajat Srivastava and Kumar, R. (2021). VIGS-based gene silencing for assessing mineral nutrient acquisition. Plant gene silencing. Methods in Molecular Biology, 2nd edition vol. 2408. DOI: 10.1007/978-1-0716-1875-2_11.
2. **Akash.,** Parida, A. P., Srivastava, A., Mathur, S., Sharma, A. K., & Kumar, R. (2021). Identification, evolutionary profiling, and expression analysis of F-box superfamily genes under phosphate deficiency in tomato. Plant Physiology and Biochemistry, 162, 349-362. DOI: 10.1016/j.plaphy.2021.03.002.

Presented the poster in the following conferences:

1. **Akash** and Rahul Kumar "**Functional elucidation of a Phosphorus starvation inducible Respiratory burst oxidase *SlRbohH* gene in the reprogramming of root system architecture"** at the International Conference on Frontier Areas of Science and Technology (ICFAST-2022), September 9 - September 10, 2022, organized by Indian JSPS Alumni Association (IJAA), University of Hyderabad, Hyderabad, India-500046
2. **Akash** and Rahul Kumar **"Identification and functional characterization of low Phosphate inducible *FBX2L1* gene in tomato"** at National Conference on Frontiers in Plant Biology, January 31 - February 1, 2020, organized by the Department of Plant Sciences, School of Life Sciences, University of Hyderabad.
3. **Akash** and Rahul Kumar **on "Genome-wide identification of F-box members and functional characterization of F-box gene for its role under phosphate starvation in tomato"** at National conference on Integrative Plant Biochemistry and Biotechnology, November 8-9 November 2019, organized by Society for Plant Biochemistry and Biotechnology, New Delhi and IICAR-IRR, Hyderabad.
4. **Akash,** Rajat Srivastava and Rahul Kumar entitled "**Understanding the molecular circuitry underlying low phosphorous response in tomato"** in BioQuest-2017 held on October 12 - 132017 at School of Life Sciences, University of Hyderabad, Hyderabad, India-500046.

Further, the student has passed the following courses towards the fulfillment of the coursework requirement for Ph. D.

Course code	Name	Credits	Pass/Fail
PL 801	Research Methodology/Analytical techniques	4	Pass
PL 802	Research ethics, Biosafety, Data analysis, and Biostatistics	4	Pass
PL 803	Scientific Writing and Research Proposal	4	Pass

R. Kumar
Supervisor

Dr. RAHUL KUMAR
Assistant Professor
Department of Plant Sciences
School of Life Sciences
University of H...
Hyderabad

Dr. Y. Srinivasulu 14.12.22
Head of the Department

HEAD
Dept. of Plant Sciences
School of Life Sciences
University of Hyderabad
Hyderabad-500 046. INDIA

Nirmal Kumar 14/12/22
Dean of the School

DEAN
School of Life Sciences
University of Hyderabad
Hyderabad-500 046.

Table of Contents

Abbreviation:

Fe=Iron. Zn=Zinc. gm=Gram. B=Breaker. kb=kilobase. sec=Second. no=Number. N=Nitrogen. min=Minute. Ca=Calcium. bp=Base pair. ml=Milli liter. µL=Micro liter. Ab=Antibiotic. PR=Pusa ruby. KO=Knockout. O/N=Overnight. cm=Centimeter. EXP=Expansin. Rif=Rifampicin. mm=Milli meter. µm=Micro meter. DW=dry weight. Mg=Magnesium. nM=Nano Molar. µM=Micro Molar. Kan=Kanamycin. CEL2=Cellulose2. Hyg=Hygromycin. Col-0=Columbia-0. C=Degree Celsius.	HM=Homozygous. FW=Fresh weight. WP=Whole Plants. PE=Pectin esterase. MG=Mature Green N2=Liquid Nitrogen. ns=Non-significance. GUS=β-glucuronidase. RH=Relative humidity. CDS=Coding sequence. PM=Plasma membrane. Pi=Inorganic phosphate. NaCl=Sodium Chloride. RIN=Ripening inhibitor. PSY=Phytoene synthase. Liq. N_2=Liquid Nitrogen. LP=Low Phosphate (µM). DAT=Day after treatment. Com cell=Competent cell. APase=Acid Phosphatase. PDS=Phytoene desaturase. NaOH=Sodium Hydroxide. MCT=Microcentrifuge tube. LCYB=Lycopene β-cyclase NBT=Nitroblue tetrazolium. EI=Ethylene insensitive like. DDW=Double distilled water. DAB=3,3′-Diaminobenzidine. HP=High Phosphate 1.25mM). ZDS=Zeta-carotene desaturase. SAP=Secretary Acid Phosphatase.	pNPP=Para-Nitrophenyl phosphate. PSI=Phosphate Starvation Inducible. DPI=Diphenyleneiodonium chloride. VIGS=Virus-induced gene silencing. PSR=Phosphate Starvation Response. TEM=Transmission Electron Microscope. Rboh=Respiratory burst oxidase homologue. BCIP=5-Bromo-4-chloro-3-indolyl phosphate. ACO=Aminocyclopropanecarboxylate Oxidase. qPCR=Quantitative Polymerase Chain reaction. HPLC=High-performance liquid chromatography. GC-MS=Gas Chromatography Mass Spectrometry. P1BS=Phosphate Starvation Response1 binding site. H2DCFDA=2',7'-Dichloro Dihydro Fluorescein Diacetate. 2D PCA=Two-dimension Principal Component Analysis. 3D PCA=Three-dimension Principal Component Analysis. CRISPR=Clustered regularly interspaced short palindromic repeats. NADPH oxidase=Nicotinamide Adenine Dinucleotide Phosphate Oxidase. pSlRbohH=SlRbohH promoter construct

1. Introduction

Phosphorus (P), is the 11th most common element on earth. It is the second limited element, after Nitrogen (N) in the plants. It is an essential and fundamental nutrient for all living organisms for their growth and development. P is a key constituent of nucleic acids, as it forms the phosphate backbone of the DNA and RNA in living organisms. P also exists in the form of phospholipids in cell membrane to maintain its integrity and protect against different environmental stresses. P is a primary component of ATP, also known as the "energy currency of cell." Orthophosphate or inorganic phosphate (Pi) is also a regulator of cell signaling, as phosphorylation/dephosphorylation of proteins controls many signal transduction pathways [1]. Pi also plays an important role in different metabolic pathways like the pentose phosphate pathway, hexose monophosphate shunt, glycolysis pathway, glycogen metabolism, and TCA cycle. Due to the widespread involvement of P in different cellular processes, its limited availability often results in a penalty in plant growth and development. In agroecosystems, the scarcity of bioavailable Pi is mitigated by routine application of phosphatic fertilizers.

1.1. P fixation in soil

Soil P is divided into two subgroups: organic and inorganic pools. Soil organic P is mainly present in flora rests, fertilizers, and microbial and insect tissues. Evidence suggests that almost 60-70 % of total applied Pi in field soil is fixed either in its organic form (Po) or insoluble inorganic complexes with aluminum (Al), iron (Fe), cadmium (Cd) or calcium (Ca), rendering it unavailable to plants [2,3]. Due to its highly reactive nature, Pi is rapidly fixed in the soils. Thus, Pi is mostly immovable in the soils as it remains in water-insoluble forms, making it unavailable to plants. Pi uptake by plants is the highest at neutral pH as the unfixed P remains majorly in its water-soluble $H_2PO_4^-$ state and is readily absorbed by the roots.

1.2. Status of global P reserves

Rock phosphate (RP) is mined and processed to produce Pi fertilizers. Global P reserves are a non-renewable resource and are anticipated to be critically exhausted in the next 100-200 years [4]. Almost 90 % of total global RP reserves are confined to 5 major countries, including Morocco, China, S. Africa, USA and Jordon. The uneven distribution of international RP reserves and the lack of large indigenous resources in most nations add to the worry about securing the long and

uninterrupted supply of affordable Pi fertilizers by Pi importing countries. India is the second-largest Pi-fertilizers importing country in the world after USA.

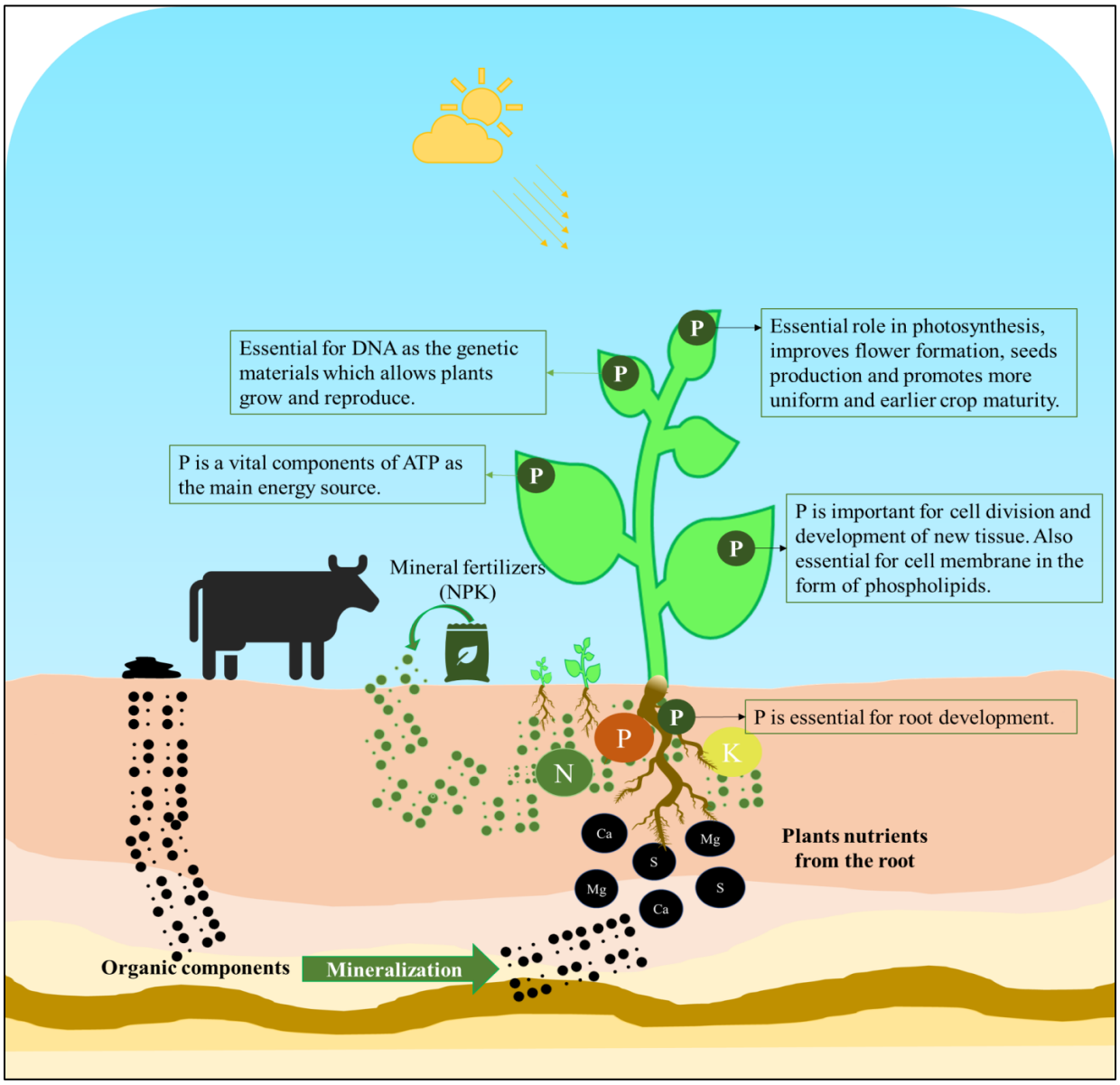

Fig. 1: General schematic diagram for the mineralization of organic P sources in the rhizosphere and the important role of phosphorus (P) in plants.

1.3. Plant adaptations under Pi deficiency

Cellular Pi status is known to influence plant carbon reserves because its deficiency perturbs the balance between carbon assimilation and its metabolism of carbon metabolites. Heldt et al. (1977) demonstrated that low Pi levels favor starch accumulation and inhibit CO_2 fixation [5]. Foyer et al. (1986) reported inhibited photosynthesis and lower sucrose/starch ratio in the leaves of Pi-

deficient barley seedlings [6]. Overall, Pi deficiency inhibits shoot growth and causes enhanced sugar remobilization from shoot to root to favor the growth of the latter. Due to differential root and shoot growth response, a higher root-to-shoot ratio is favored in Pi-deficient plants. Plants have evolved a variety of surviving strategies to cope with Pi limitation and increase its accessibility in the rhizosphere. Two types of adaptive strategies underlie the plant response to Pi deficiency, local and systemic. Local responses are fast responses that are employed immediately after sensing of Pi starvation by root tips. These are associated with reprogramming of root system architecture (RSA), including growth of primary and lateral roots growth, and root hairs (RH). In contrast, the systemic responses kick in once root-derived signals are conveyed to shoots. The systemic response control Pi homeostasis by influencing Pi transport, Pi recovery and its recycling within plants [7,8]. Thus, local and systemic responses determine the magnitude of plant adaptations to Pi starvation.

1.3.1. Morpho-physiological adaptations

Roots are the main organ that acquires the essential mineral nutrients for plant development and growth (Gregory, 2008). Root system changes their configuration in all three-dimension in soil for better uptake of mineral nutrients [9,10]. Root growth and development are very plastic and are influenced by different edaphic factors such as the quality of soil, the availability of varying mineral nutrients along with Pi, oxygen concentration, water accessibility, soil density, and pH [11,12]. Change in RSA is a fundamental strategy to enhance Pi utilization efficiency (PUE) under low Pi conditions for improving plant growth and development [10,13]. RSA adaptation, including shallower growth angle of the axial root, horizontal growth of root, enhanced adventitious roots, lateral root, and promoted RHs density, have been shown to improve axial root length [14–19]. Pi-starved plants respond in many ways, including the distribution of more carbon sources from shoot to root for enhancing the root-to-shoot ratio and promoting changes in lateral root development, increasing root length and RHs density to mitigate low Pi levels [14,20].

Once the root tip senses Pi scarcity in the rhizosphere, the roots of Pi-deficient plants undergo a wide range of local adaptive reprogramming of RSA, which increases the total root surface area to explore the larger Pi catchment region. Altering root growth angle also maximize Pi uptake from top soil layers [21]. Some of the most notable local changes shown by Pi-deficient Arabidopsis seedlings roots are inhibition of primary root length, promotion in the number and growth of

lateral roots, and increased RH density and length [11]. It is important to mention that inhibition of the primary root, a visual difference observed in many Arabidopsis seedlings under Pi unavailability, is not a universal response. Several Arabidopsis genotypes and most crop plants, such as rice, maize, tomato, and barley, show an increase in primary root length upon Pi starvation [22,23]. Altogether, these observations reveal different adaptive strategies by different species for reprogramming RSA in Pi-deficient plants [20,24,25]. Because most of the Pi-sources are present in the top soil layers, Pi-deficient plants of many species also modify their root growth angles to promote horizontal growth. Such altered growth angles enable them to explore and exploit shallower soil horizons [14]. Evidence suggests that maize, soybean, and bean show thinner root growth angles in the efficient genotypes than the inefficient genotypes that uptake high Pi from P-enriched soils [26–28]. In rice, the actin-binding protein Rice Morphology Determinant (RMD) has been found to link actin filaments with statoliths to control root growth angle [29]. In some species, especially members of Fabaceae (*Lupinus albus*) or Proteaceae (*Hakea prostrata*) families, cluster roots (CRs) are formed in response to a meager Pi supply. These species exhibit this extreme response to maximize Pi uptake from the Pi-rich soil patches. CRs release large amounts of carboxylates in confined patches for mining of insoluble forms of Pi from its enriched soil patches [30,31].

RHs are one of the most important parts of root architecture to acquire most soil nutrients. Trichoblasts are the tubular-shaped cells towards the exterior part of the plant's root responsible for the RHs formation [32,33]. For the major contribution of minerals uptake, RHs are a straightforward way to investigate prominent rhizosphere regions in plants. In Arabidopsis, approximately 77 % of the root surface zone is covered by RHs. Formation of RH and growth are linked with minimal mobile nutrients like P. The accumulated literature suggests that enhanced lateral root growth and RH density enhance PAE [32,34,35]. Trichoblast numbers improve, leading to more RH formation in low Pi-grown plants [36]. The number of RHs and density are five times more in Pi-depleted soil-grown plants than in Pi-enriched soils [36,37]. Total root length and denser RHs were observed in the basal root of soybean as compared to taproots [38]. RHs also help the secretion of enzymes and carboxylic acid from roots which release Pi from the organic sources and exploit patches of inorganic and organic Pi sources [39]. Low soil P also promotes the formation of longer and denser RHs in Pi-deficient roots. RH is vital for nutrient acquisition because these epidermal extensions facilitate half of the total Pi uptake [40,41]. The robust proliferation of RH in Pi-deprived plants is favored because, being the single-celled extension of the epidermal cell, elongation

of RH comes with lower carbon cost [42–44]. Therefore, breeding crop germplasm for cultivars with longer and denser RH hairs has been suggested as an effective strategy to develop Pi-use efficient plants.

Plants also develop beneficial interrelationships with some soil microorganisms, such as arbuscular mycorrhizal fungi (AMF), to promote Pi uptake. A body of evidence suggests that root mycorrhization by AMF also influences PAE and PUE in plants [23,45–48]. In this symbiotic association, plants transfer carbon sources such as carbohydrates and lipids to the fungal partner in exchange for Pi. The extent of plant-AMF association is known to be directly influenced by soil P levels, as several lines of evidence suggest inhibition of root mycorrhization under the excessive availability of P [49–53]. AMF associations are not always suitable for plants as edaphic factors supporting fungal growth sometimes lead to over-mycorrhization of roots by AMF, leading to an imbalance between low Pi gain and high carbon cost [48,54]. Besides AMF, soil P solubilizing bacteria (PSBs) also play an essential role in the cycling of bioorganic and inorganic phosphate in the rhizosphere [55–57]. Evidence suggests that plant growth-promoting bacteria (PGPB) infected roots exhibit enhanced soil organic phosphate, like inositol phosphate [57,58]. Inoculation of microbes such as phosphate solubilizing fungi, *Penicillium*, has been reported to play an important role in enhancing Pi availability to plants [55,57].

1.3.2. Metabolic adaptations

1.3.2.1. Glycerolipid metabolism

Phospholipids levels decrease in cell membranes upon Pi starvation. Such change in cell membrane composition was first reported in the non-photosynthetic bacterium, followed by *Rhodobacter sphaeroides*. Benning et al. (2002) reported that Pi starvation sturdily reduces the total phospholipids' relative quantity by increasing specific non-phosphorous lipids, such as galactolipids and sulfolipids [59]. Pi-starved plants activate hydrolysis of phospholipids, resulting in the release of precursor molecules like diacylglycerol (DAG), which in turn are consumed in the biosynthesis of P-free lipids such as galactolipids (monogalactosyldiacylglycerol (MGDG), sulfolipids (sulfoquinovosyldiacylglycerol (SQDG) and digalactosyldiacylglycerol (DGDG). In plastids and extra-plastidial membranes, these glycerol lipids substitute for phospholipids and support the Pi availability to other vital cellular processes. Most of the genes involved in this process are triggered by Pi deficiency [59–64]. One such highly up-regulated PSI gene in plants belongs to the

Glycerophosphodiester phosphodiesterase (GDPD) group of proteins. GDPDs are highly conserved proteins expressed ubiquitously from bacteria to humans and perform diverse functions [65]. The first GDPD encoding gene was identified in the *glp* regulon of *E. coli* [66]. The glycerol synthesis and its metabolism by *E. coli* play a significant role during phospholipid biosynthesis or so-called lipid remodeling (recycling) [67]. Further, YPL110c and YPL206c GDPD genes were recognized in yeast where glycerophosphocholine (GPC) was hydrolyzed by YPL110c or GDE1 (new nomenclature Glycerophosphodiesterase 1). In the Pi-starved condition, GDE1 expression is higher than in normal conditions. GlpQ is a periplasmic enzyme that exhibits an extensive range of substrate specificity for different types of glycerophosphodiesters, namely, glycerophosphocholine (GPC), glycerophosphoethanolamine (GPE) [68]. The other GDPD (UgpQ) from *E. coli* was identified from *upg* operon, which also allows glycerophosphodiesters to be utilized as a source of phosphate [69]. In plants, GDPDs or GPX-PDEs were first identified in carrots, followed by Arabidopsis [69]. Low Pi promotes its utilization from different endogenous phosphate-holding molecules, and multiple groups of enzymes catalyze the phospholipids in cellular membranes to release Pi. Two central pathways release Pi from its membrane-bound P, i.e., PLD-mediated or PLC (NPC4/5)-mediated hydrolysis of phospholipids. In plants, a third pathway involving GDPDs is present, which catalyzes the hydrolysis of glycerophosphodiester to G-3-P [69]. Thus, the lipid remodeling under Pi stress occurs majorly via 3-distinct pathways in plants. The first pathway is mediated by Phospholipase D (PLDs), which separates the phospholipids' polar head groups and gives rise to phosphatidic acid (PA). Consequently, PA gets dephosphorylated by PA phosphatase to form DAG and release Pi (Nakamura and Ohta, 2010). Phospholipid degradation and DGDG accumulation level deteriorated in *Arabidopsis pldζ2* and *pldζ1pldζ2* mutants' roots under low Pi conditions [70]. Another group of lipases, Phospholipase C (PLC), modulates the second pathway of lipid remodeling which is a one-step conversion of phospholipids into DAG, without converting the lipids into PA first. Depending on the substrate specificity, PLCs can be of two types; Phosphoinositide-specific PLC (PI-PLC) and Non-specific PLC (NPC). PI-PLCs are presumed to be preferentially involved in lipid signaling whereas NPC is involved in direct conversion of Phosphatidylcholine to DAG [70]. Synthesis of glycerophosphodiester (GPD) and free fatty acid chains via hydrolysis of phospholipid by Lipid acyl hydrolase (LAH) and GPDs are converted into sn-glycerol-3-phosphate (G3P) and respective alcohols by GDPDs [69]. Further, G3P is converted

into DAG through acyl transferase phosphatidic acid phosphatase. This G3P could be dephosphorylated and release glycerol [71] thereby providing extra P in Pi-depleted cells. GDPDs have been reported to be induced under Pi deficiency in several plant species [72]. Overexpression of *OsGDPD2* gene promoted Pi deficit tolerance in transgenic lines [73]. Recent characterization of another GDPD gene revealed that overexpression of *AtGDPD6* promotes root growth under low Pi condition [74].

1.3.2.2. Secretion of organic acids/carboxylates

Roots secrete different organic chemicals such as phenolics, proteins, polysaccharides, amino acids and sugars in the rhizosphere during normal growth and development by influencing nutrient availability, plant-microbe signaling, and minerals acquisitions [75,76][2,77,78]. These secretory products differ in abundance and composition during biotic and abiotic stress conditions [2,30,77]. For example, the synthesis and exudation of numerous organic acids, including malic acid, oxalic acid, cis-aconitic acid, citric acid, tartrate, succinate, γ-aminobutyric acid have been reported during Pi depleted conditions to promote plant growth and development and root-rhizosphere interactions including soil microorganisms [76,79–86]. These root exudates help release Pi from the organic P reserves or metal-phosphate complexes to improve phosphate availability near the root surrounding areas in soils [77,87]. Likewise, roots secreted organic acids convert the organic substances and promote Pi recycling in the soils [88]. Low Pi-grown lupin roots show increased citrate, oxalate, and malate secretion in root exudates. Among these, citrate was the most effective in releasing Pi from chelated aluminum-phosphate complexes in acidic soils [88]. It has also been demonstrated that maize plants with externally applied oxalate and citrate showed higher Pi uptake and enhanced Pi diffusion in the soil [89]. Transgenic tobacco plants also exhibited more citrate exudation for enhanced Pi acquisition and improved PAE under Pi deficiency [90]. Thus, the crops genotype with high root exudation potential under low Pi availability may be better suited to soils with poor Pi status.

1.3.2.3. Secretion of phosphatases

In another adaptive strategy, roots secrete acid phosphatases in the soil to promote the breakdown of organic phosphate and metal-bound phosphate complexes into the inorganic phosphate or organic phosphate anion. For example, overexpression of a secretary phytase and an acid phosphatase-related gene exhibited more Pi accumulation and plant growth promotion on media where phytate was used as the P source in Arabidopsis and soybean, respectively [51,91,92]. In addition, phosphatase *under-producer3 (pup3) Arabidopsis* mutant plants secret lower APase in roots. These seedlings were found to accumulate less Pi in the shoot than the wild type when grown in the soil with organic P composites as a P source [93]. Many APase activity-related genes have been characterized in vascular plants, such as *Lupinus albus* (Ozawa et al. 1995; Li et al. 1996; and Miller et al. 2001), *Solanum lycopersicum* (Bozzo et al. 2004, 2006), *Phaseolus vulgaris* (Liang et al. 2010), *N. benthamiana* (Lung et al. 2008), and *Arabidopsis thaliana* (Tran et al. 2010) [94–96] [97,98] [99] [100],[101]. The first putative purple acid phosphatase (PAP) was characterized in Arabidopsis, where this protein was found to be present in the apoplastic region [102]. Characterization of Arabidopsis *PAP17* revealed that it is a dual-localized (extracellular matrix as well as lytic vacuoles localized protein) PAP which is upregulated at the low Pi condition and is involved in leaf senescence and oxidative stress condition [103]. *AtPAP12* and *AtPAP26* are predominant PSI-secreted APase in *Arabidopsis thaliana* [101]. *AtPAP10* is another important PAP, a root surface associated with PSI PAP [104]. Another class of protein called haloacid dehalogenase-like APase is also induced in Pi-deficient plants [105]. The HAD family of proteins is composed of several epoxide hydrolases, ATPase, dehalogenase, phosphatases, phosphomutases, phosphoserine, and other phosphatase domains [106,107]. The tomato *PS2* gene, belonging to HAD family, is induced by Pi-limited growth conditions. Overexpression of this gene led to enhanced APase activity, total anthocyanins contents, and delayed flowering phenotype in tomato plants [108,109]. Further, common bean (*Phaseolus vulgaris HAD1., PvHAD1)* is also induced by low Pi with Ser/Thr phosphatase activity [110]. *PvPS2:1* was found to be involved in Pi accumulation and root growth in Arabidopsis plants overexpressing this gene [111]. Rice *OsHAD1* having kinase activity has been characterized for its role in maintaining Pi homeostasis under low Pi supply [112].

1.3.2.4. Sugar metabolism

Pi levels are tightly associated with the intracellular levels of ATP, ADP, and related nucleoside P sources, and severe Pi stress is known to reduce their quantity in the cell [113,114]. Activation of inorganic pyrophosphate-dependent bypass enzymes is crucial for the metabolic adaptations of plants under depleted intracellular Pi [115]. Such changes facilitate the C flux for the enhanced synthesis of organic acids in the glycolytic pathway under chronic Pi limitation and help plant survival under depleted ATP levels [115]. With such adaptations, plants can maintain the the proper functioning of the mitochondrial citric acid cycle and electron transport chain with impaired ATP production [114,116]. Higher levels of several sugars and total carbohydrates in Pi-deficient plants are also required to activate PSI genes under low Pi conditions [117,118]. A mutation in the sucrose transporter *SUC2* gene in Arabidopsis was found to reduce the secretion of total acid phosphatases by 30 % in the roots, indicating the importance of enhanced sugar remobilization to roots under Pi starvation.

1.3.2.5. Anthocyanins/flavonoids accumulation

In maize, the production of most of the organic acids such as malic acid, citrate, and succinate in TCA cycle is increased in roots under Pi stress [119]. Flavonoids such as benzoxazinoids are strongly decreased in Pi-resistant roots in maize. In contrast, the flavonoids such as quercetin-3,4-O-di-b-glucopyranoside accumulated at higher levels in leaves of Pi-sensitive maize genotypes [120]. The concentration of many phenylpropanoids, flavonoids, and their derivatives increases during Pi-limitation in both roots and shoots of Arabidopsis plants [121]. Glucosinolate levels also increase under salt, light, and drought stress and during Pi limitation [122]. The concentration of C-glycosylflavones was found to be significantly high under PI-limited conditions, which also promoted mycorrhizal colonization in melon roots [123]. Quercetin, a flavonoid, was found to be effective in promoting mycorrhizal associations in plants. The root-secreted flavonoids are helpful in solubilizing P and also serve as metal-chelating operatives to increase the availability of micronutrients in the rhizosphere. Similarly, flavonoid exudates from white lupin roots were also reported to enhance P acquisition by plants. In Pi-deficient Stylosanthes (a genus of the legume family) plants, increased accumulation of flavonoids, phenylamides, and phenolic acid in roots was found to help Pi remobilization and promote interaction between plants and microorganisms. An isoflavonoid present in root exudates of alfalfa was shown to dissolve phosphate complexes of iron, making both Fe and P available to the Pi-deficient plant [124]. The synthesis and exudation of piscidic acid by the roots of some plants, such as pigeon pea (*Cajanus cajan*), have been reported

to be highly effective in releasing Pi from iron and aluminum Pi complexes. All these studies emphasize the importance of flavonoids in increasing the availability of Pi in the soil.

1.3.3. Molecular adaptations in Pi-deficient plants

1.3.3.1. Transcriptomic studies

The extent of both local and systemic responses may vary in different and within the same species. For example, RSA is a highly plastic trait, and its modulation varies in various plant species, indicating species-specific divergent genetic regulatory mechanisms controlling this trait [125,126]. Similarly, distinct genetic regulatory networks are responsible for the variations observed in the PUE within species [126–130]. Genome-wide transcriptional analyses in model dicot plant, Arabidopsis (Mission et al., 2005, Bustos et al., 2010; Thibaud et al., 2010) and tomato (Peng Tian et al. 2021, J. Pfaff et al., 2020, V. Satheesh 2022), cereal crops such as rice, wheat, maize, sorghum, barley (Wang et al., 2019; Wasaki et al., 2006; Li et al., 2010; Secco et al., 2013; Oono et al., 2013; Du et al., 2016, Deng et al., 2018, Zhang et al., 2019) and leguminous plants, including common bean, white lupin, and soybean (Aparicio-Fabreetal.,2013; O'Rourke et al., 2013; Wang et al., 2014; Zeng et al. 2016) under low-Pi stress have greatly improved our knowledge of phosphate starvation response (PSR) in plants [7,131,140–147,132–139]. These studies captured the genome-wide changes at the transcripts level and provided comprehensive information on the molecular regulation of PSR in plants. A list of conserved candidate regulators and effector genes, both PSI and non-PSI, in different species also emerged from these studies. Altogether, these studies revealed that extensive remodeling of transcriptomes coordinates the requisite morphological and physiological adaptations in plants [115].

1.3.3.2. Local Pi response (local response) and signaling

Sensing Pi unavailability by roots activates the different adaptive responses in Pi-deficient plants. Reports suggest that Pi deficiency is monitored by root tips in soil [148]. Studies also suggest that PSR genes perform a critical role during Pi stress sensing in roots under Pi-limited conditions [149]. For example, a high-affinity Pho84 Pi transporter has been proposed as a Pi "transceiver" for its role in Pi sensing under the low Pi condition in yeast [150,151]. Several Pi transporters help Pi uptake from the soil and promote translocation of absorbed Pi from root to shoot under both Pi-

sufficient/deficient conditions in plants. These Pi transporters are sub-categorized into two sub-families, high-affinity Pi transporters, and low-affinity Pi transporters. High-affinity Pi transporters show their expression in root epidermal cells during low Pi conditions. In contrast, low-affinity Pi transporters are expressed in the chloroplast. PHT1 subfamily members belong to the high-affinity class Pi-H^+ cotransporter and are located on the plasma membrane of the cell [152–154]. These genes also showed strong induction under Pi-deplete conditions to increase Pi uptake from the soil [155]. There are nine PHT1 members in Arabidopsis. *AtPHT1;1* and *AtPHT1;4* are highly expressed in all parts of the root (root hairs, root cap, and epidermal cells) under Pi-depleted conditions [156]. There is a penalty in Pi uptake from the low Pi growth media in *AtPHT1;1* and *AtPHT1;4* mutants [157,158]. Similarly, there are 13 PHT1 members in rice. Among these, 10 PHT1 show their expression in root. *OsPHT1*;*11* is highly induced by mycorrhiza symbiosis [159]. *OsPHT1*;2 and *OsPHT*;6 show a significantly enhanced transcript accumulation in low Pi-grown rice root. Similarly, 11 PHT1 genes were identified in barley root under Pi-deprived conditions [160,161]. Along with this, sorghum *SbPSTOL1,* a homolog of *OsPSTOL1,* exhibited a change in root system architecture and improved grain yield in Pi-deprived conditions [162].

The intracellular translocation of phosphate is regulated by four other classes of Pi transporters, namely PHT2, PHT3, PHT4, and PHT5. These transporters are localized in the plastid, mitochondrial membranes, Golgi compartments, and tonoplast [125,163]. These transporters are important for the transport of the Pi to each organelle. Thus, together these proteins maintain cytosolic P homeostasis and support various metabolic pathways. The PHT2 family belongs to low-affinity Pi transporters with P-loading and unloading functions in vascular tissues [164,165]. The ubiquitination and phosphorylation are involved in controlling the *PHT1s* at the post-translational level. The protein coded by the *AtPHO2* gene, which belongs to the E2 ubiquitin category and is regulated by miRNA399, interacts with AtPHT1s and then facilitates proteasomal degradation by ubiquitination pathway [166–168]. It has been suggested that Casein kinase-2 (CK2) phosphorylates the PHO2 and OsPHF1 to maintain phosphate homeostasis in rice [86,169]. Thus, plants require a higher expression level of active transporter to increase PAE and better PUE in low P soil.

Another class of proteins plays an important role in Pi transfer from root to shoot [170]. The *PHO1 Arabidopsis* mutant showed less P content in leaves and shoots because of an error in Pi loading into the xylem. In rice, three homologs, OsPHO1;1, OsPHO1;2, and OsPHO1;3, where OsPHO1;1,

OsPHO1;2 are involved in internal Pi distribution to the grains [171]. However, OsPHO1;2 over-expression lines showed increased grain yield and better PUE on Pi-deplete soil in field conditions suggesting that this is a candidate gene for increasing grain yield for supportable agriculture [172]. In the plant cell, the vacuole is the largest Pi-storing organelle. The Pi transport across the tonoplast is mediated by the PHT5 transporters [173–175]. Under Pi-sufficient levels, about 70-95 % of Pi is stored in vacuoles of vegetative cells and phytate in mature seeds [176]. Further, the overexpression of PHT5, also called Vacuolar Phosphate Transporter (VPT), showed huge Pi absorption in the vacuole and changed the expression of PSR genes in Arabidopsis [174]. The PHT5 group of the family, with three members (PHT5;1, PHT5;2 and PHT5;3), belongs to SPX-MFS proteins in Arabidopsis [174]. Sahu et al. (2020) have also demonstrated that PHT5 controls the root development by Pi uptake, recycling, and sequestration in Arabidopsis [177].

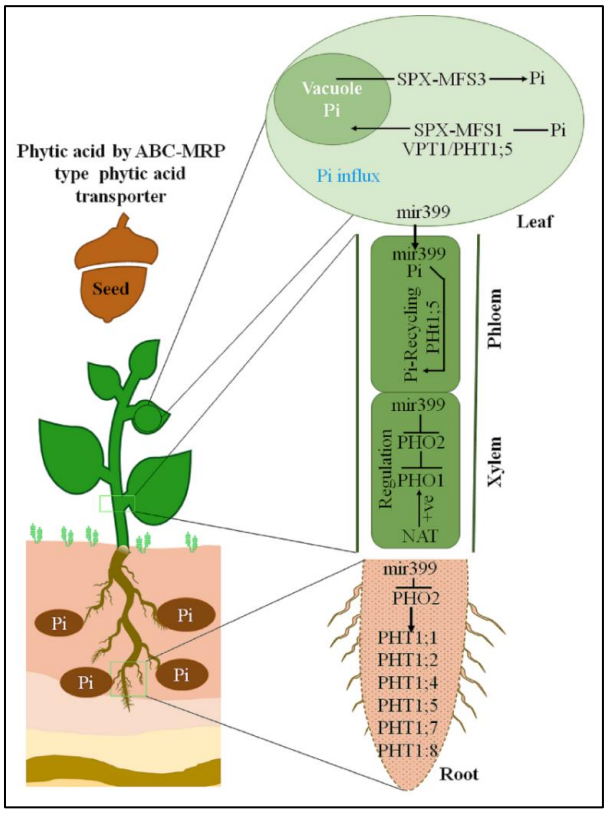

Fig. 2: A summary of Pi transport in plants. Phosphate transport is represented in four different compartments: Pi uptake from soils and media by the roots. The absorbed Pi is transported from roots to shoots by its loading into the xylem. Next, Pi is unloaded in the shoot, reaches different organelles, and is finally transported to seeds in phytate form. The high-affinity Pi transporter PHT1 family (PHT1;1 and PHT1;4) plays a main important role during Pi uptake from the soil/media in roots. Loading of Pi in the root xylem is increased by PHO1 protein and PHT1;5 has an important character in Pi translocation from shoot to root. SYG1/PHO81/XPR1 major facility

superfamily 3 (SPX-MFS3/PHT5;1) and SPX major facilitator superfamily (SPX-MFS1) proteins are important for the vacuolar Pi efflux and influx, correspondingly. Further, ABC-MRP-type (ABC-MRP, ATP binding cassette-multidrug resistance-associated protein) phytate transporter helps transport the phytate from leaves to seeds. The expression level of PHT1, PHO1, and PHO2 is controlled by cis-natural antisense transcript of phosphate transporter 1;2; (cis-NATPHO1;2) and miR399 in the xylem and roots.

1.3.3.3. Molecular regulators of Pi starvation response

Phosphate starvation response1 (PHR1) homologs

Several transcriptome-level studies have identified hundreds of Phosphorus Starvation Response (PSR) genes in plants. As a result, six main classes of P starvation regulator (PSR) transcription factors, including MYB, ERF/AP2, zinc finger, WRK, NAC and CCAAT-binding groups, have been identified in plants [178]. Among these, Phosphate starvation Response 1 (PHR1), which belongs to MYB class, is known as a master regulator of PSRs [179]. Interestingly, the transcript level of the PHR1 gene showed weak induction under the low Pi condition in plants. But it undergoes significant changes at the post-translational modification level [180]. A subdued PSR has been reported in *Arabidopsis phr1* mutant seedlings under Pi-depleted condition, as evidenced by the reduced level of PSI genes, sugar levels, anthocyanins content, altered root-to-shoot ratio, and Pi content, in comparison to the wild-type counterpart [179,181]. On the contrary, AtPHR1 overexpression lines showed derepression of PSR even under Pi-sufficient conditions and exhibited higher expression levels of PSI genes, leading to higher Pi levels in the shoot [181]. Similarly, overexpression of AtPHR1 homolog in rice, *OsPHR2*, caused a higher accumulation of Pi in the shoot by upregulating many phosphate transporters and micro-RNA399 (miR399) during high phosphate conditions in transgenic lines [182]. Increased upregulation of many PSI genes, enhanced root length, and root hair development were also observed in *OsPHR2-OX* plants [182]. A close homolog of PHR1, PHL1 (PHR-like1), has also been identified in Arabidopsis. Compared to WT plants, the phr1 phl1 double mutant plants showed the downregulation of PSI genes under Pi-deprived conditions. These studies suggest the central role of PHR1 and PHL1 in the transcriptional activation/repression of PSR genes in Pi-starved Arabidopsis plants [183]. Other PHR1 homologs such as PHL2, PHL3, and PHL4 in Arabidopsis and other plant species such as rice, Medicago, tomato, and soybean have also been reported [182,184–187]. Many cis-elements such as TATA-like, PHO-like, and identified PHO motif (CACGTC/C) had been reported in the pro-

moters of early PSR genes [188,189]. Among these elements, the PHR1 binding site (P1BS: GNATATN) is enriched in the promoters of PSI genes [179,181]. P1BS element is a direct binding site for AtPHR1 and its homologs in other plant species. The P1BS cis-element is significantly enriched in most PSI genes, but their high number is not observed in Pi-starvation-repressed genes [183,190]. Another class of proteins, namely SPX, named after the yeast Syg1, Pho81, and the human XPR1 proteins, are involved in intracellular Pi homeostasis. These are negative regulators of PHR1 activity. Some SPX members such as SPX1, SPX2, SPX3 and PHO1;H1 are direct target of PHR1 [179,181,191–194].

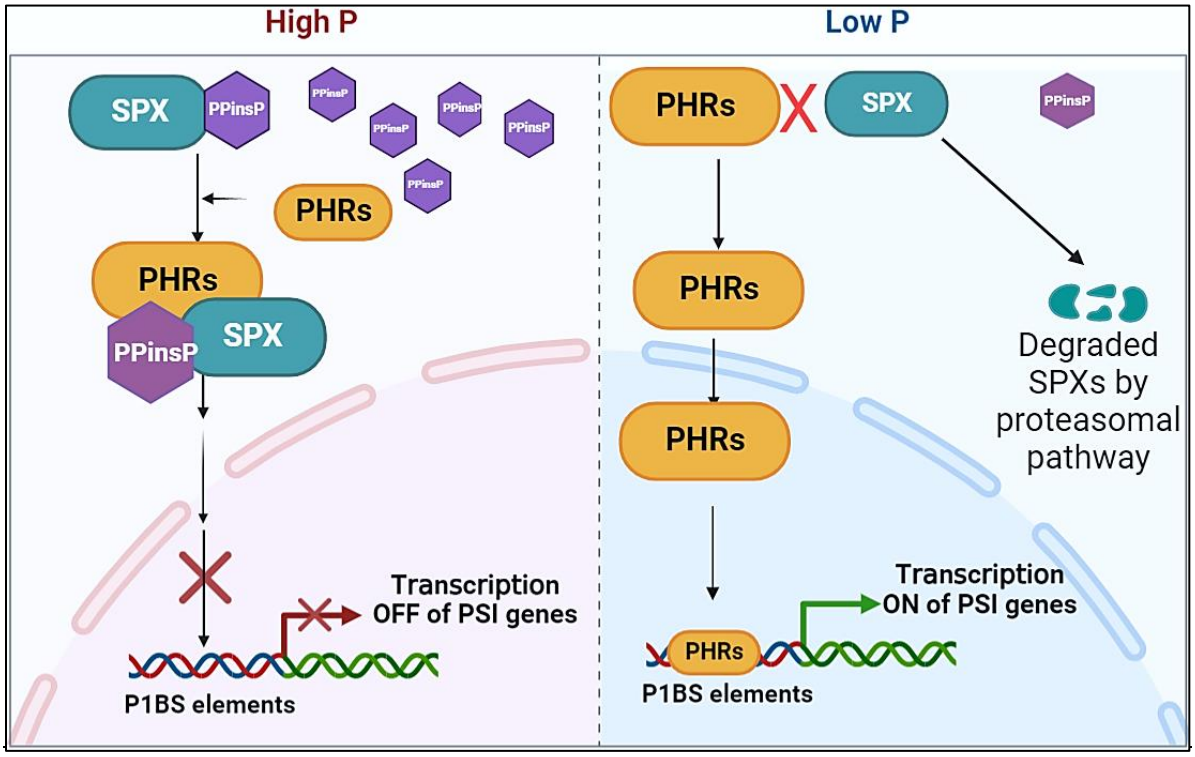

Fig. 3: Schematic diagram of plants' molecular regulatory cascade of phosphorus starvation responses. The left side of the figure represents high P, and the right panel represents low P. Under HP conditions, SPX proteins control PHRs activity by physically interacting with them. SPX-PHR complex does not allow PHR to bind to the promoters of the phosphate starvation inducible genes (PSI) transcription. Under LP conditions, SPX proteins are degraded, releasing PHRs to activate PSI genes and start PSR consequently. The Arrow line denotes positive regulation and crosses present inhibition/blockage of pathways.

PHRs have also been found to control the expression of PSI genes of glycerolipid metabolism and purple acid phosphatases such as *OsGDPD2* and *OsPAP21b* in rice during Pi starvation [73]. Recently, the physical between PtoWRKY40 and PtoPHR1-LIKE3 (PtoPHL3), a PHR1 homolog in

poplar, blocked PSRs by inhibiting the binding of the latter to the P1BS element of target genes [195]. In tomato, SlPHL1, a homolog of AtPHR1 and OsPHR2, was shown to bind the P1BS elements of the promoters of *SlPht1*;*2* and *SlPht1*;*8* Pi transporters. Its overexpression in the *Atphr1* mutant background successfully compensated for the activity of its Arabidopsis homolog under Pi starvation [135].

1.3.3.4. Non-PHR transcription factors

Apart from PHR1 homologs, the regulatory role of several other transcription factors has also emerged in PSR in plants. For example, Huang et al. (2018) reported that PHR1 is a direct target of AUXIN RESPONSE FACTOR7 (ARF7) and ARF19 in *Arabidopsis thaliana* [196]. PHR1 expression was found to be down-regulated in the *arf7* and *arf19* single and *arf7/arf19* double mutants. The inhibited PHR1 levels consequently inhibited the expression of downstream Pi starvation-induced genes in the roots in the mutant backgrounds. These mutants were also reported to be defective in Pi uptake, exhibited exacerbated stress phenotype, and accumulated higher levels of anthocyanins in shoots. Besides MYBs, other classes of TFs, such as WRKY, AP2/ERF, and bHLH, actively regulate PSRs in plants [197–199]. In rice and soybean, OsWRKY74 and GmWRKY35 have been reported to modulate P starvation response [197,199]. He et al. (2020) recently highlighted the importance of the interaction between OsbHLH6 with OsSPX4 in regulating PSR in rice [200]. Similarly, bHLH32 has been implicated in regulating multiple aspects of plant response under Pi deficiency [201]. Similarly, NiMYB12 was found to positively regulate flavonol biosynthesis and confer improved tolerance to Pi starvation in *N. benthemiana* [119]. Similarly, overexpression of a *Jatropha curcas* ethylene response factor *JcERF035* altered root system architecture and enhanced anthocyanins accumulation in Arabidopsis under low Pi conditions [198]

1.3.3.5. SPX domain-containing proteins

Though initially identified in yeast, plant SPX domain-containing protein members such as AtSPX1, AtPHO1;H1, and AtSPX3 were identified for their conserved functions regulating PSRs. Based on the no or additional c-terminal domains, plant SPX-domain members belong to four groups: SPX, SPX-EXS, SPX-RING, and SPX-MFS [202]. These proteins physically interact with

PHR1 homologs and have been suggested to perform Pi-sensing functions [203]. Their intracellular Pi sensing function is attributed to their binding affinity with InsP/PP-InsP as their ligand [204]. It is now known that in the presence of Pi sufficient condition, which also supports high cellular InsP/PP-InsP levels, the InsP-activated SPX members bind to PHR1 homologs and sequester them from binding to their target genes to block PSR. On the contrary, under Pi-depleted conditions, when InsP levels decline considerably, the SPX-PHR physical interaction is not promoted in the nucleus. In such conditions, SPX members undergo proteasomal mediated degradation, thereby releasing PHRs to freely bind to target PSI genes and initiate PSR in plants [205,206]. Alternatively, cytosolic SPX members have been suggested to sequester PHR homologs in the cytoplasm, thus not allowing the latter to move into the nucleus for initiating PSR [207]. In contrast to SPX1 members, SPX-EXS (PHO1) and SPX-MFS (PHT5) members are generally involved in Pi transport in plants [208].

1.3.3.5. Hormone signaling during Pi starvation

Phytohormones mediate the expression level of many PSR genes and RSA changes in plants under low Pi availability. The hormone biosynthesis, transport, and sensitivity are altered under Pi-depleted conditions. Auxin, gibberellic acid (GA), cytokinins (CKs), strigolactone (SLs), ethylene and abscisic acid (ABA) are well explored for their roles in the regulation of PSR.

Auxin

Auxin actively participates in root system architecture (RSA) modifications under Pi-deprived conditions, as evidence suggests that both auxin levels and auxin sensing is increased in roots, especially in tips and lateral root primordia [209]. Such changes in RSA are also influenced in an auxin dosage-dependent manner [131]. The induction of more lateral roots, leading to more root tips, has been suggested as an improved fitness trait under Pi-starvation [28,122,210]. Another striking example of auxin involvement in RSA is the formation of cluster roots in a wide range of species [211]. However, such induction in lateral roots does not represent a universal phenomenon. Many studies, including in Arabidopsis and other plant species, do not always show a positive correlation between increased lateral roots and Pi starvation [20,212–214].

The increased auxin sensing upon Pi-starvation can be correlated with the increased expression of auxin receptor TRANSPORT INHIBITOR RESPONSE1 (TIR1) in both root tips and lateral root

primordia [122,209]. Recently, Pérez-Torres et al. (2008) demonstrated a correlation between the higher expression of auxin receptor TRANSPORT INHIBITOR RESPONSE1 (TIR1) and enhanced degradation of AUXIN/INDOLE-3-ACETIC ACID (AUX/IAA) in Pi-deficient Arabidopsis seedlings. This caused the release of transcription factor AUXIN RESPONSE FACTOR19 (ARF19) from the ARF-AUX/IAA protein complex, leading to the activation or repression of the genes responsible for lateral root (LR) formation. In their findings, Pérez-Torres et al. (2008) implicated ARF7 and ARF19 as the possible transcriptional regulator of PHR1. Recent evidence indicates that TIR1 may be a direct target of PHR1, arguing for a relatively direct link between Pi starvation, auxin signaling, and lateral root formation [215,216]. IAA14, another component of auxin signaling, is also required for Pi starvation signaling in both Arabidopsis and rice [217–219].

Root hairs are the main site for nutrient and water uptake [32]. In rye, over 60 % of Pi is absorbed by root hairs under Pi deficiency [220]. Pi-limitation also causes increased density and longer root hairs to increase root surface area for better Pi uptake in plants [221–223]. Root hairs also serve as the primary site for releasing root exudates such as organic acids, enzymes, mucilage, and secondary metabolites and help mobilize nutrients [224]. Evidence suggests a direct role of PHRs in regulating this trait as shorter root hairs are observed in *phr1;phl1* mutants [132]. Several other presumptive targets of PHR1, such as PLDΣ11, a phospholipase, have also been implicated in root hair development. Several ARFs, including ARF5, 7, 8 and 19 are known to induce RSL4 [225,226]. The promotion of root hair elongation under low Pi conditions is attenuated in ARF19 knock out alleles (*arf19-a* and *arf19-b*). More recently, role of *Aux1* in promoting auxin gradient formation and root hair elongation under Pi-deficiency was demonstrated in Arabidopsis and rice [21,212]. Not only auxin signaling genes but biosynthesis and metabolism, such as TAA and DAO, respectively, appear to promote root hair elongation during low external P. While *taa1* mutation decreases the promotion of root hair elongation under low Pi by more than 60 % in both Pi-sufficient and Pi-deficient conditions, the *dao1.2D* (dominant allele) mutant plants exhibited shorter root hairs under only Pi-deficient conditions [212].

Ethylene

Ethylene production under nutrient deficiency was initially debatable as both higher and lower ethylene production were reported under low Pi in different plant species. He et al. (1992), Borch et al. (1999), and Gilbert et al. (2000) reported that the presence of low levels of ethylene was able to promote rapid and extensive aerenchyma formation in the roots of *Zea mays L*., pre-exposed to N and P-deprivation [227–229]. In Arabidopsis, increased expression of three ethylene biosynthesis ACS genes, *ACS2*, *ACS4* and *ACS6,* indicates its higher production under low Pi conditions [230]. P scarcity and ethylene cause analogous alterations in RSA, such as aerenchyma development, altered root growth angle, induced root hair development, and increased density [228,231]. Formation of adventitious roots in WT but not in an ethylene-insensitive mutant cultivar *Never-ripe* in tomato under Pi deficiency also supports a role for ethylene in adventitious root development. The authors also reported increased ethylene production by tomato shoots and reduced ethylene biosynthesis in roots under low Pi availability [232]. Unlike in tomato, Pi-limitation resulted in lesser lateral roots and reduced lateral root density in common bean, suggesting both promoting and inhibitory roles of ethylene on lateral root production in different species [228]. Evidence from white lupin also implicates ethylene in cluster-roots (CR) formation. Treatment of the ethylene antagonist $CoCl_2$ was found to reduce the number of CR formations under P-limitation [233]. Limited evidence also suggests that ethylene may also regulate the root growth angle to promote plagiogravitropic growth of roots in Pi-deficient plants [234].

Besides LRs, evidence shows a largely promoting effect of ethylene on root hair production and length in stressed and unstressed conditions, including Pi starvation. Zhang et al. (2003), through pharmacological experiments, demonstrated that the application of inhibitors of ethylene biosynthesis or ethylene signaling caused a reduction in root hair density and root hair Length [235]. This observation was further corroborated by the scantier and shorter root hairs phenotype in the ethylene-insensitive mutants, *ein2,* and *etr1*, which could not be fully restored upon Pi starvation [443]. The authors using different ethylene biosynthesis inhibitors during simultaneous Pi starvation, found that only Co^{2+} and not AVG and aminooxy acetic acid effectively blocked the Pi deficiency-induced increase in the root hair density of the WT plants. Like auxin mutants, ethylene-insensitive Arabidopsis mutants respond to Pi deficiency with denser and longer root hairs, albeit the extent of such response in the mutants varies from that observed in WT. Although, it was found that ethylene-mediated root hair formation is not accompanied by the increased number of cortical

cells but only by the increased percentage of root hair forming H-cells. This indicates the existence of different gene activation mechanisms, at least partially, underlying root hair formation by ethylene and low Pi. Recent evidence by Song et al. (2016) provided further insights into such molecular mechanisms in Arabidopsis. Seedlings of a hypersensitive-to-phosphate-starvation 5 (*hps5*) mutant, a mutated ethylene receptor ERS1, exhibited constitutive ethylene responses and enhanced sensitivity to low Pi [236]. These seedlings were found to over-accumulate EIN3 protein, which is further stabilized by Pi starvation. By employing various approaches, the authors demonstrated that EIN3 and RSL4 share a set of common target genes. The combinatorial action of these two transcriptional regulators, especially the stabilized EIN3, is responsible for the exacerbated response of denser and longer root hairs under Pi starvation. Further, it was proposed that the stability of EIN3 likely regulates the differential root hair development paradigms under unstressed and stressed conditions. Recent imaging studies have disclosed the inter-relationships between ethylene and RSA modulation under low Pi conditions in Arabidopsis. Ma et al. (2003) showed the altitudinal outline of the relative elongation of root cells and biogenesis rates of cortical cells, trichoblasts, and atrichoblasts [237]. They have also reported that P deficiency temperately reduces the optimal rate of relative elongation, ceases the growth zone, and lessens the production rate of both epidermal cell types towards the cortical cells. Blocking ethylene production (with aminoetoxyvinyl-glycine) or its action (with 1-methyl cyclopropane) revealed enhanced elongation in high P and substantially decreased in low P conditions. To further validate whether the effects are explicitly related to ethylene, the authors further validated by reversing the effect of repressed ethylene production with concurrent exogenous treatment with an ethylene precursor (1-aminocyclopropane-1-carboxylic acid). It was observed that ethylene predominantly regulates the elongation rather than the maturation of the growth zone. It was concluded from their study that, a fine-tuning is needed between the ethylene levels and its subsequent signal transduction pathway for the acclimatization to the low P ambiance, which directly correlated with the root growth and division under P stress. Borch et al. showed in bean (*Phaseolus vulgaris*) that ethylene limits root elongation in phosphorus-adequate conditions but sustains elongation under phosphorus deficiency [228]. This finding recommends that roots respond to P stress by shifting ethylene signal transduction pathways involved in regulating growth.

Strigolactone

The carotenoid-derived terpenoid lactones play important roles in Pi acquisition by establishing symbiotic associations and manipulating plant architecture [441,442]. It is already well-documented that low Pi condition induces SL biosynthesis in plants which helps establish the symbiosis associations through the exudation in the rhizosphere as an inductive signal [238–240]. SL also stunts the shoot branching pattern to utilize available Pi judiciously. Further, SLs induce branching in the root to increase total surface area and enhance the probability of Pi uptake. SLs are synthesized once roots sense low Pi. SL-signaling mutant (*max2*) and deficient mutants (*max3*, *max4*) and exogenous synthetic SL analog lead to inhibition of primary root development, lateral root, root hairs elongation, and adventitious root growth [241–243]. It is observed that the exogenous application of SLs mimics the Pi deficiency symptoms in rice [438] and Arabidopsis [244]. Under low Pi, plants showed compromised growth in the primary root but exhibited enhanced lateral root density in the *max2-1* mutant compared to WT plants. Yoneyama et al. reported that orobanchol exudation from the roots of *Trifolium pratense* in hydroponic media is negatively proportionate with the increasing concentration of Pi in the medium [245]. SLs also participate in the cross-talks between the plants' P and Nitrogen (N) status. A low P condition is created under the suboptimal N condition, leading to induction in SL biosynthesis. Interestingly, the opposite does not happen, indicating basal SL levels for maintaining plant growth when N starvation is created either in P-sufficient or deficient conditions in tomato [246]. Surprisingly, SLs regulate LR and RH growth by controlling auxin supply [247,248]. In rice, an exogenous supply of GR24, a synthetic SL, causes the down-regulation of PIN family genes and reduces the IAA supply to control LR formation [249]. However, the expression of the PIN gene was not altered by GR24 treatment in the primary root (PR) tip in Arabidopsis [242]. A similar interaction between auxin and SLs was found to regulate root hair development. High SLs concentrations caused a decreased level of auxin accumulation in the root, resulting in high root hair density [250]. Such root responses generally occur during Pi-depleted conditions [251]. SLs acts as sensor under low nitrogen and phosphate conditions in early-grown seedlings indicating that SLs play an important role in the physiological process in tomato [252].

Jasmonic acid

Phosphate deficiency is known to activate jasmonate biosynthesis and signalling in plants. Khan et al. (2016) reported higher levels of JA and its conjugate JA-isoleucine (JA-Ile) in both roots and leaves of wild-type Arabidopsis seedlings and the shoots of *pho1* mutant under Pi deficiency [253]. They also reported the induction of a low Pi marker gene, *IPS1*, and a JAZ gene, *JAZ10*, in both shoot and root tissues of Pi-deficient Arabidopsis plants. The activation predominantly occurs in green photosynthetic parts of plants and is less prominent in the roots [254]. Surprisingly, the same is not reflected in most transcriptomics studies examining the role of Pi-limitation in Arabidopsis and rice [131,166,183,255–257], which failed to capture the conspicuous changes in the transcript levels of the JA biosynthetic genes [253]. One of the characteristic features of low Pi-grown roots in Arabidopsis is inhibited primary root growth due to exhaustion of root apical meristem. To investigate the molecular signatures under such a response, Chacón-López et al. (2011) compared the root tip transcriptomes of WT and a low P insensitive mutant 4 [258]. The mutant seedlings do not exhibit the atypical inhibited primary root response under low Pi. This analysis revealed the downregulation of several JA-regulated genes in the mutant and implicated JA in primary root elongation under Pi deficiency. Similarly, Pi deficiency has also reported differential expression of JA pathway genes in leguminous crops like common bean and white lupin [144,145,233]. While the role of JA in inhibiting primary root length is known, its role in controlling low Pi-induced RH elongation is unknown. However, in a new study by Han et al. (2020) where different JA mutants such as *coi1* and *jaz* were used, authors revealed that the application of JA promotes root hair elongation under normal conditions [259]. Authors found that JA regulates such RH elongation by activating the expression of *RHD6, RSL1* and their transcriptional targets. The *coi1* mutant seedlings exhibited shorter root hairs whereas simultaneous mutation in JAZ proteins, co-receptors which act as repressors, promoted root hair elongation, implicating JA in this developmental process. Further investigation showed that over expression of *RHD6* reverted the root hair phenotype of *coi1* mutant and restored the root hair elongation. Authors finally concluded that Arabidopsis JAZ proteins by interacting and suppressing RHD6 transcription factor control jasmonate-stimulated root hair development. It is noteworthy to mention that RHD6 expression is up-regulated under P deprivation, also by ethylene, hence it will be interesting to relook at the root hair elongation events under P deprivation in the light of the recently emerged evidence, especially for JA-ethylene crosstalk [259].

Cytokinin

The first study of cytokinin involvement in a nutrient deficiency context was suggested in [260,261]. In this study, authors reported reduced cytokinin levels in plants under Pi or nitrate starvation, which was further explored by Martín et al. (2000) and revealed that exogenous cytokinin treatment inhibits the induction of numerous Pi starvation-responsive genes [262]. Cytokinins have also been reported to suppress lateral root initiation in Pi-starved plants López-Bucio, J. et al. (2002), higher shoot/root growth similar to low Pi, and reduced exogenous cytokinin concentration [262,263]. The exogenous treatment also decreases the low Pi responsive INDUCED BY PHOSPHATE STARVATION1 (AtIPS1), establishing its crucial role in manipulating root architecture and exhibiting its potentiality towards being a central regulator of Pi starvation.

Gibberellic acid

Gibberellic acid plays an important role in regulating the PSRs gene in Arabidopsi*s* and is involved in RSA modulation and anthocyanins accumulation through GA-DELLA signaling. The exogenous GA and mutants showed reduced primary root length, LR density, root hairs elongation, and root-to-shoot ratio under low Pi-grown plants (Jiang et al. 2007). Another study demonstrated that PSI transcription factor MYB62 regulates GA biosynthesis and P homeostasis in Arabidopsis [264].

Abscisic acid

The direct relation between ABA and PSRs has not been demonstrated in Pi-deficient plants. The ABA-insensitive *abi2-1* and ABA-deficient *aba-1* mutants behaved normally concerning inhibited plant growth, unchanged acid phosphatase production, and enhanced root-to-shoot ratio compared to WT plants. However, the total anthocyanins accumulation was reduced in *aba-1* mutant plants under Pi-depleted conditions [265]. At the molecular level, ABA also suppressed the expression of *AtPHO1, AtPHT1, At4, AtPHO1;H1,* and *AtIPS1* under Pi-deprived conditions [266,267]. While accumulated data indicate some relation between ABA and PSR, these studies are not enough to support a strong relationship between ABA and PSR in low Pi-grown plants.

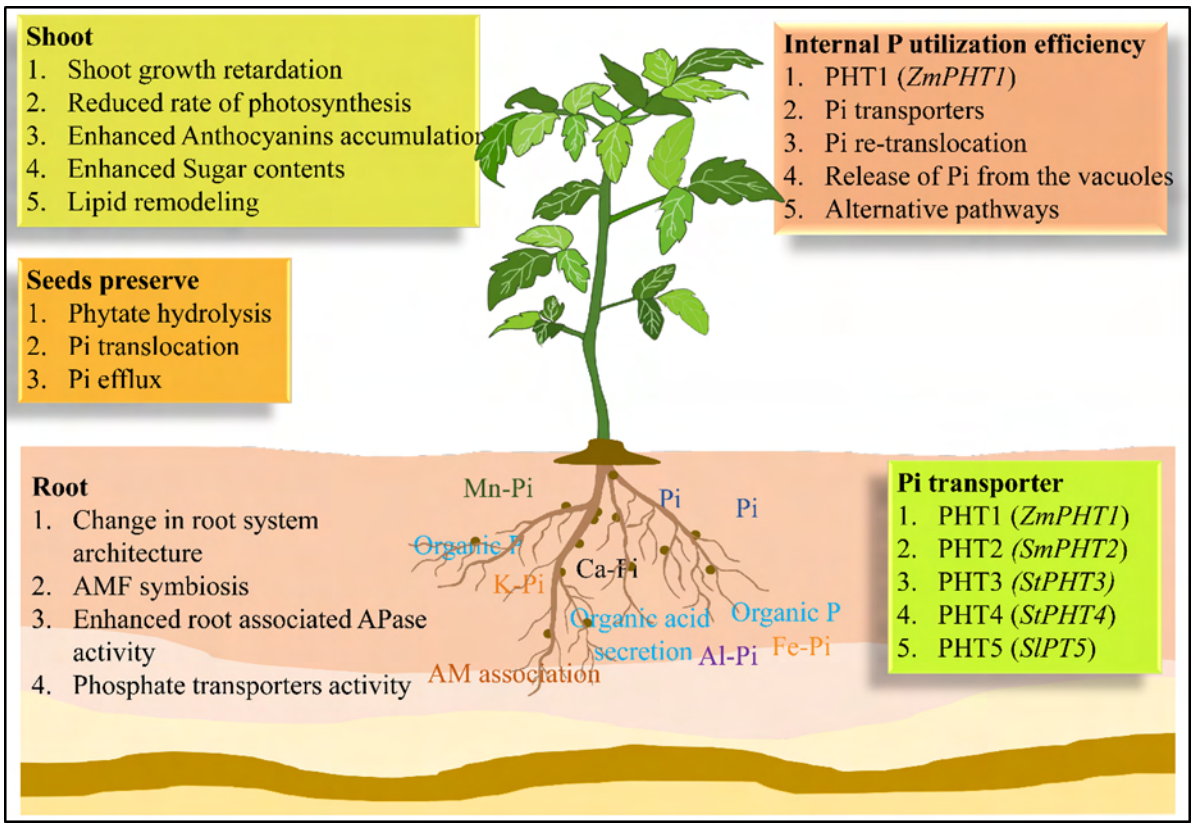

Fig. 4: Schematic representation of PSR and adaptive mechanisms in plants to optimize P remobilization and growth under Pi deficiency.

1.4. *Reactive oxygen species and P starvation responses*

Low Pi availability in plants generally results in altered RSA, including more lateral roots and RHs. ROS plays a vital role in mediating such changes in RSA. Plant primary roots have two areas of ROS formation: the elongation zone and quiescent center (QC). The oxidative condition of the plant QC is important in controlling the low cell division rate. ROS production in the elongation zone promotes cell wall extensibility within this part of the root [268,269]. Inside plant cells, the major organelle of ROS formation are mitochondria, chloroplast, peroxisomes, and apoplastic region. The enzyme complexes involved in ROS production belong to class III peroxidases, oxalate oxidases, amine oxidases, lipoxygenases, quinone reductases, and plant NADPH oxidases (NOXs) [270,271]. Under multiple stress conditions, these enzymes generate a huge amount of ROS and change the oxidative landscape of the cell. This redox homeostasis is maintained by complex antioxidant machinery in plants [270,272]. NADPH oxidases (also known as respiratory burst oxidases homologs, Rbohs) enzymes are responsible for synthesizing apoplastic ROS. NADPH oxi-

dase (NOXs/Rbohs) enzymes are an integral plasma membrane-bound protein with six transmembrane domains with C-terminal FAD, NADPH hydrophilic, two heme groups, and two calcium-binding domains [273,274]. The NADPH oxidase (NOX) genes belong to a small gene family in plants. It consists of ten members each in Arabidopsis and grapes, eight in tomato, and nine in rice [273]. These genes play diverse functions during plant growth and development. Based on the regulation of NOX genes, these proteins have been suggested to be better candidates for modifying ROS formation in terms of amplitude, period, and location [270,275]. In plants, apoplastic ROS (apROS) are mainly generated by plasma membrane-located NADPH oxidases, amine oxidases, and also cell wall peroxidases in minimal quantity. ApROS plays an important role in signal transduction from extracellular spaces and may directly eradicate the attacking pathogens. Apoplastic ROS also controls cell division, cell elongation, and whole plant growth [272,276–278].

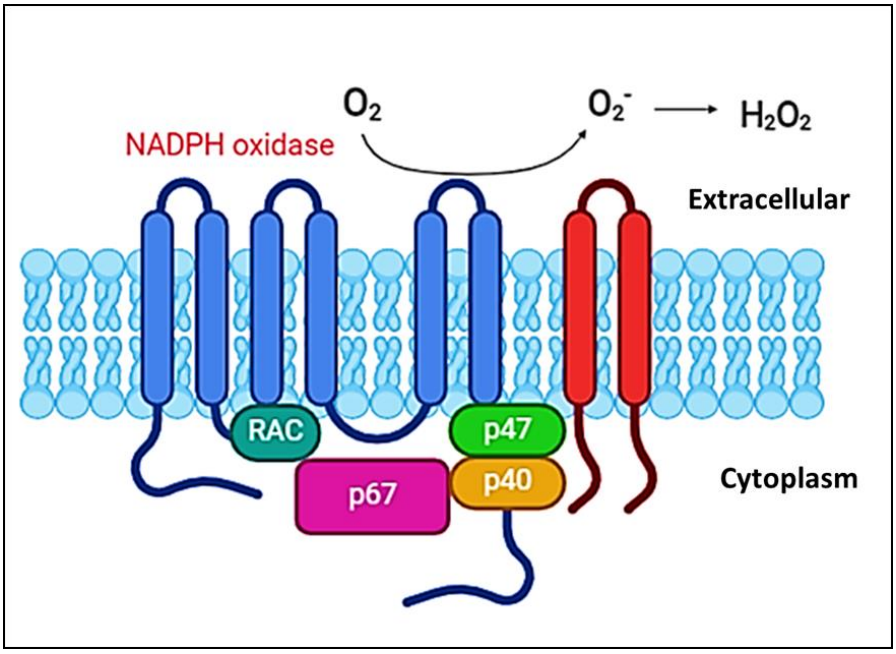

Fig. 5: Schematic diagram of a NADPH oxidase, the membrane-bound enzyme complex with six transmembrane domains.

1.4.1. Abiotic stress-responsive RBOHs

Plant ROS signaling induces adaptive response during different abiotic environmental stress conditions such as temperature, salinity, mechanical, and drought [276]. In *Arabidopsis thaliana*, *AtRbohD* plays an important role in ROS generation under wound stress conditions. Such ROS successively gather outside the plasma membrane (extracellular space) at the site of the initial

wound, suggesting that *AtRbohD*-generated ROS propagates through the whole plant [279]. *AtRbohD* is down-regulated by MAPK8 and stimulated by phosphorylation and binding of calmodulins in a calcium-dependent manner [280]. Recent evidence also suggests systemically acquired acclimation effects of the biomechanical wounding on freezing tolerance in wheat by Rboh genes [281]. The generation of H_2O_2 by NADPH oxidase in the apoplastic region of plant cells plays a significant role during cold acclimation-induced chilling tolerance [282]. *Citrus sinensis RbohD* (*CsRbohD*) was reported to play an important role during cold stress [283]. During osmotic stress, phytohormones are produced to enhance the mRNA level of *AtRbohD* and *AtrbohF* in guard cells. Arabidopsis double mutant plants *Atrbohd/Atrbohf* exhibit reduced ABA-induced stomatal closure [282]. Furthermore, a recent report indicates that the formation of ROS and expression level of *AtRbohD* are increased by mild salt stress. There is very low ROS production in *Atrbohd* mutant under low salt stress, revealing the pivotal role of *AtRbohD* in this aspect. *AtRbohD*-produced ROS was common under ABA and salinity stress [284]. Plant hormones like methyl jasmonate, salicylic acid (SA), and pathogen-derived coronatine also enhance AtRbohD-dependent ROS formation in the presence of beta-aminobutyric acid [285,286]. Further, *OsRbohA* also enhances salinity tolerance through K+ homeostasis in rice [287]. Ethylene response factor ERF74 controls the *AtRbohD*-dependent mechanism under different stresses and maintains H_2O_2 homeostasis in Arabidopsis [288]. The transcript level of *AtRbohI* is reduced by the exogenous application of ABA. In contrast, its expression is enhanced by mannitol. The transcript level of the *AtRbohI* gene was found to be significantly high in Arabidopsis seeds and roots. The mutant lines of *Atrbohi* were more sensitive to mannitol and ABA stress during seed germination. In addition, significantly hampered lateral root growth in mannitol-treated seedlings, yet improved drought tolerance in the complemented Arabidopsis *Atrbohi* mutant plants suggests its involvement in drought-stress tolerance [289]. *AtRbohI* also contributes to H_2O_2 formation during NaCl or mannitol stress to enhance proline content in plants. Another Rboh member, *RbohF* plays an important role in protecting the shoot cells from the extra accumulation of Na^+ ions. This gene also participates in lignin acquisition during Casparian strip development in the endodermis. This dispersion barricade directs the water and solutes through the soil to the water-leading tissues [272]. Silencing of *G. hirsutum RbohD* (*GhRbohD*) caused impairment in the lignin deposition in *V. dahliae*-infected plants, indicating the role of these genes in lignin accumulation in plants [290].

1.4.2. Interaction between RBOHs and symbiotic organisms

Rbohs are not only involved in root growth and plant pathogenic relations, but these genes play a significant role in plant-microorganisms symbiotic associations. For example, Rboh-dependent ROS formation has promoted plant-bacterial association in legumes. Diphenyleneiodonium chloride (DPI), an inhibitor of Rbohs activity, treated plants showed inhibition in the nodule formation [291,292], emphasizing the significant role of Rboh genes during the symbiosis process. The importance of Rbohs for their role during symbiotic interaction between the barrel medic (*Medicago truncatula*) and *Sinorhizobium meliloti* has also been reported and demonstrated [271]. The transcripts level of *MtRbohA* was found to be lower in root nodules and showed more sensitivity of ROS to leghemoglobin [293]. Furthermore, a lower level of *MtRbohA* led to declined nitrogen fixation and decreased expression of nitrogenase protein complex [271]. These results suggest that *MtRbohA* plays a significant role in signaling to facilitate interaction between plants and the symbiont. ROP9-GTPase, which is responsible for regulating *MtRbohE/3* at the transcript level, hindered the rhizobial infection thread of plant root hair cells in *Medicaga truncatula* [294]. Moreover, Belmondo et al. (2016) reported that root cortex colonization, promoted by activation of *MtRbohE* in symbiont cells, was not exaggerated in *MtRbohE* RNAi mutants [295]. Silencing of another gene of this family, i.e., *RbohB,* led to sequestering the infection thread synthesis and nodule formation [296]. In contrast, overexpression of *RbohB* enhanced the infection events and number of nodules and increased nitrogen fixation in *Phaseolus vulgaris* roots [297,298]. All these studies suggested that Rboh-dependent ROS is important for effective rhizobial infection threads, nodule development, and function. It is noteworthy that each member of Rbohs may have been suggested to have different roles in similar biological processes [299–301].

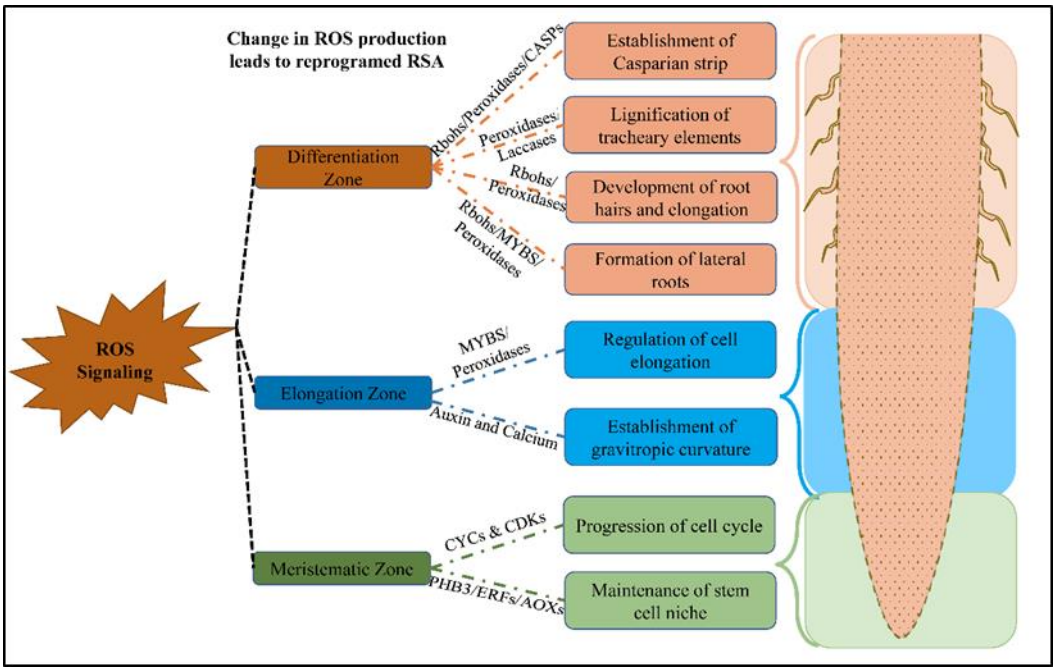

Fig. 6: ROS signaling by different genes in different root developmental zones, meristematic zone, elongation zone, and differentiation zone. The PRX=Peroxidases, UPB1= Transcription factor UPBEAT1 (Basic helix-loop-helix protein 151), Rbohs= Respiratory burst oxidase homologs, CYCs= Cyclins, CDKs=Cyclin dependent kinases, AOXs= Alternative oxidases, HB3= Prohibitin3, ERFs= Ethylene Response Factors [417].

1.4.3. Plant growth and development responsive RBOHs

Rbohs are evolved to play diverse developmental roles in different plant organs and tissues. For example, Rbohs are involved in root growth and polarized growth of trichome cells, pollen tube, and root hairs [302]. Cell wall softening and loosening are mediated by Rboh-generated ROS. Extracellular ROS generated by plasmalemma localized Rbohs is important for plant growth and cell elongation. Several studies have suggested that pollen tube, root hair tip, and *Fucus serratus* zygote growth are due to ROS produced by Rbohs [303,304]. Rboh isoform, i.e., *RHD2/AtRbohC* is particularly important for ROS production during root hair development as *rhd2* mutant plants exhibit reduced root hair elongation because of the imperfect ROS formation and calcium ion uptake [304]. *AtRbohH* and *AtRbohJ* also show their expression in pollen and stamens [305]. These two genes are involved in pollen growth and affect root hair growth and development [225]. Moreover, Rbohs-dependent ROS participate in growth like cell wall softening at the time of seed germination, root elongation, fruit softening, and hypocotyl elongation [306–308]. In DPI-treated Arabidopsis and cress *(Lepidium sativum)* plants, the possible function of Rbohs in

apoplastic ROS was demonstrated at the time of seed sprouting. In contrast, *atrbohb* mutant plants seed germination is altered [307]. *SlWfi* and *Lerboh1* tomato mutants' plants showed inhibited leaf growth and fruit development [309]. Further, a plant steroid hormone, brassinosteroid (BRs), which is involved in plant growth, enhances the transcripts level of Rbohs in cucumber and maize [309] [310]. Arabidopsis *AtRbohD,* which showed significantly high expression levels in different tissue/stages, has been suggested to perform a putative housekeeping function in plant growth and development [273]. Either increase or decrease in the level of ROS leads to many unfavorable phenotypes, like delaying nuclear envelope breakdown, preventing the formation of preprophase band, and loss of spindle bipolarity by the time of cell cycles [311]. Different plant species showed variable phenotypes concerning primary roots under low Pi conditions [13,122,263,312–314]. ROS levels and ROS mobilization occur during Pi starvation conditions in the root [315–317]. The roots QC center and the elongation zone are the most critical regions for cell division, cell wall extension, and elongation activity [268,269]. It has been shown that limited Pi-grown plants have higher ROS levels in the QC center, elongation zone, and root tips of the root [258,317]. During Pi starvation, the ROS localization in the root differs from the pattern seen in potassium and nitrogen-deficient plants. Hence, the production of ROS can be considered a measure of the nutrient-deficient plant root response [316].

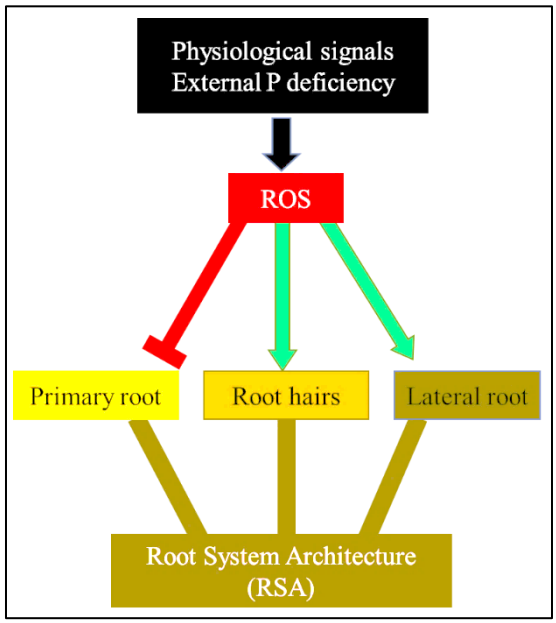

Fig. 7: Simple flow chart presenting the effect of ROS signaling to changed RSA under the low Pi condition in *Arabidopsis thaliana*.

1.5. Role of F-box protein in plants

Protein turnover is an essential regulatory mechanism underlying the regulation of many cellular processes such as cell cycle, cell lineage specification, embryogenesis, circadian rhythms, fruit development, stress responses, and several signaling pathways. The ubiquitin-proteasome route is the principal regulatory circuit that degrades selective intracellular proteins [318]. This pathway mainly operates in three main steps: (i) activation of ubiquitin (Ub) moiety by Ub-activating enzyme (E1), (ii) relocation of activated Ub to Ub-conjugating enzyme (E2), and (iii) transfer of Ub to the target proteins, followed by their degradation by Ub-protein ligase (E3) complex. F-box proteins constitute one of the Skp1-cullin-F-box (SCF) E3-ligase complex subunits and confer their specificity for appropriate substrates [319].

The characteristic feature of these proteins is the presence of a highly conserved, approximately 60 amino acids long N-terminally located F-box domain. In contrast, the C-terminal end of these proteins is less conserved and may possess one or more variable protein-protein interaction domains such as leucine-rich repeats (LRR), kelch repeat, tetratricopeptide repeat (TPR), and WD40 repeats [320]. F-box genes have been identified in various organisms after their initial discovery in humans [320,321]. Numerous studies have shown that more F-box genes are present in plant genomes than in any other organism. For example, in contrast to the 18 F-box genes available in yeast (*Schizosaccharomyces pombe*) and 33 genes in *Drosophila melanogaster*, 694 and 687 genes have been identified in Arabidopsis and rice, respectively [322–324].

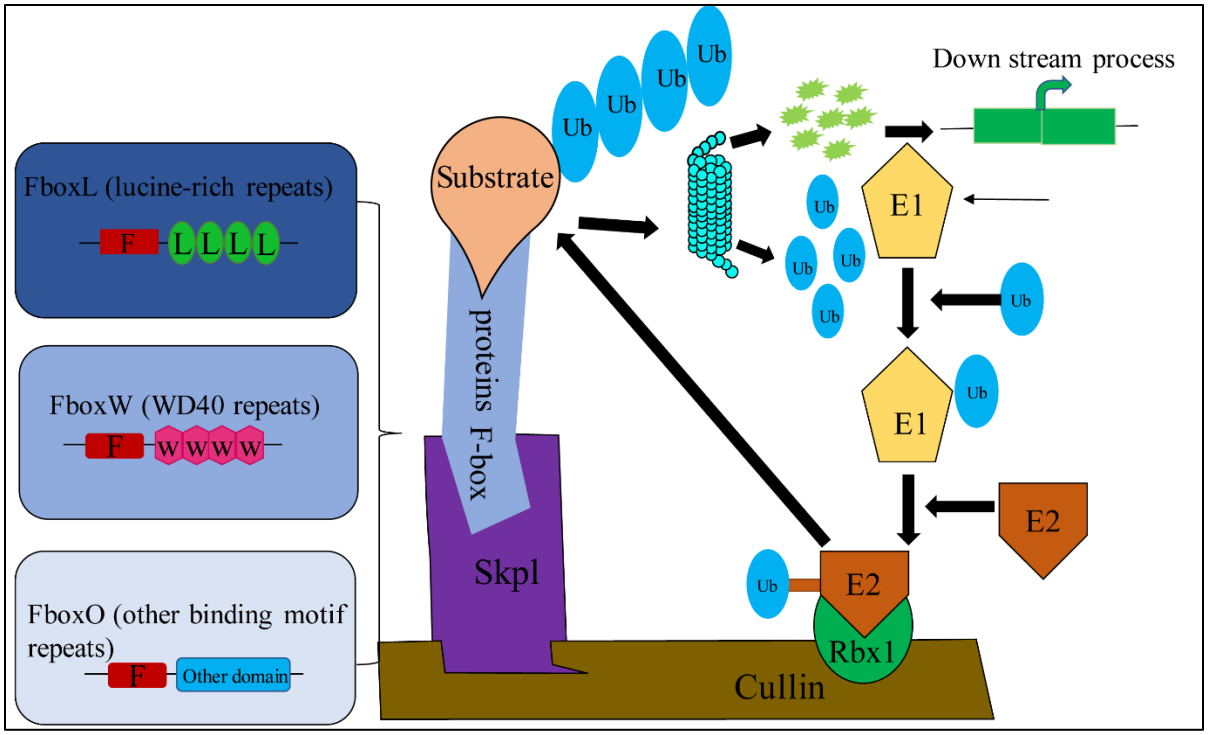

Fig. 8: The general mechanism of ubiquitination pathway. First, ubiquitin is activated by the ubiquitin-activating enzyme (E1), further ubiquitin is forwarded to another enzyme, the ubiquitin-conjugating enzyme (E2), and next delivered to substrates via ubiquitin ligases (E3). The ubiquitin proteins are recognized and then degraded by 26 proteasomes to several small peptides.

F-box genes regulate various developmental processes, secondary metabolism, senescence, hormonal responses, and in response to biotic and abiotic stresses [325]. For instance, UNUSUAL FLORAL ORGANS (UFO) regulates floral stem identity and organ development [326–328], whereas LOV kelch protein 1 (LKP1)/ ZEITLUPE (ZTL), LOV kelch protein 2 (LKP2)/ FKF1-like (FKL), and flavin-binding, kelch repeat, F-box (FKF1) proteins play regulatory roles in photomorphogenesis, circadian clock, and flowering time [329–332]. Further, a member of the F-box gene family known as *Solanum lycopersicum GA-INSENSITIVE DWARF2* (*SlGID2)* showed intense green leaves and a small plant in RNAi silenced line [333]. OsFBX1, a kelch-repeat domain-containing E3 Ligase subunit, is implicated in the development of rice anthers. It also regulates root lignification by controlling a Cinnamoyl-CoA reductase enzyme's turnover in rice [334]. In Arabidopsis, F-box proteins have also been implicated in phenylpropanoid biosynthesis regulation [335], the repressor of leaf growth [336], and streamlining seedling's response to aluminum toxicity by monitoring the levels of a C2H2 transcription factor sensitive to proton rhizotoxicity 1

(STOP1) [337]. Evidence suggests that F-box proteins are also involved in the regulation of plant metabolism. For example, manipulating a kelch-repeat containing gene, OsFBK12, expression either by RNAi or overexpression leads to enhanced leaf senescence, delayed seed germination, or increased grain size of rice in OsFBK12-Ox lines [338]. Further, Borah et al. (2022) presented SCF OsFBK1 E3 responsible for jasmonic acid mediation, leading to control lignification and rice anthers [339]. Recently, a phloem protein-related F-box member, AtPP2-B11, was reported to modulate abscisic acid (ABA) signaling and the abiotic stress response in Arabidopsis [340,341]. F-box genes also play a pivotal role in regulating hormone reception or signaling pathways in plants. The auxin receptor protein, TRANSPORT INHIBITOR RESPONSE 1 (TIR1), which governs the stability of Auxin/Indole-3-Acetic Acid (Aux/IAA) proteins and controls auxin responses, remains one of the best-studied F-box genes [342–344]. Other F-box proteins, such as EIN2-binding F-box factors (EBF1 and EBF2), act as negative regulators of ethylene signaling [345]. The jasmonic acid receptor CORONATINE INSENSTIVE1 (COI1) is also an F-box protein [346,347]. Another F-box gene, MORE AXILLARY BRANCHES2 (MAX2), is a crucial component of the strigolactone signaling pathway and imparts plant resistance against bacterial pathogen infection [348,349]. SLEEPY1 (SLY1) is a component of gibberellin signaling. It regulates the stability of DELLA family proteins in plants [350,351].

Several F-box genes have been directly implicated in the plant responses under Pi starvation. For instance, TIR1 alters lateral root development by modulating auxin sensitivity under Pi deficiency in Arabidopsis [122]. Another F-box protein, AtFBX2, negatively regulates Pi starvation responses in Arabidopsis [352]. While initial knowledge of the ubiquitin-mediated degradation of many proteins involved in Pi homeostasis in plants has been obtained, the identity of SCF-E3 ligases engaged in this process is still lacking. One of the outstanding questions in this context is which E3 is involved in PHO2-mediated PHO1 degradation.

The large numbers of F-box genes observed in plant genomes might correlate with enormously diverse SCF complexes to regulate various biological processes, including PSRs, distinctively recognizing a wide array of target proteins. The full complement of F-box genes has been identified in many crop species such as rice, pear, apple, chickpea, soybean, Medicago, maize, cotton, potato, and Poplar [353–362] (Given that these genes are constituted by a large gene family generally containing hundreds of members, assigning biological functions to each member of such a large gene family remains a monumental task in plants. One of the primary aims of this study is to

identify novel F-box genes that might be involved in Pi starvation responses in tomato. Although the role of several F-box proteins, such as TIR1 and EBFs, have emerged during fruit development and ripening, however, the available information on the structure and function of the entire set of F-box genes largely remains elusive in tomato.

2-Materials and Methods

2.1. Plant growth conditions, phosphate deficiency, and sucrose treatment

Tomato plants (*Solanum lycopersicum* cv Pusa Ruby) were grown in a culture room maintained at 24 ± 3 ˚C with a 16 h day/8 h night photoperiod regime, 200 µmol m^{-2} s^{-1} light intensity, and 60–70 % relative humidity (RH), as described earlier [363]. Ethylene treatment was given to two-week-old tomato seedlings, as described previously [364]. For Pi starvation experiments, tomato seeds were surface sterilized and kept on modified manually prepared ½ x MS medium for three days in a culture room at 24 ± 3 ˚C in the dark. On the 4th day, the germinated seeds with the same length (approximately 1 cm) radicles were transferred in Phyta Jars (500 mL capacity, Himedia, India) containing ½ MS media supplemented with either high phosphate (1.25 mM phosphate) or low phosphate (5 µM phosphate) [439, 440]. KH_2PO_4 was used as the main phosphate source in the media. The low phosphate media was supplemented with an equimolar concentration of KCl to compensate for potassium. The seedlings were cultivated and harvested after 8-DAT and 15-DAT of Pi starvation treatment.

Whereas for the sucrose treatment, 5th day, the germinated seedlings were transferred on HP/LP ½ MS agar media with 2 % sucrose and without sucrose (+P+S, +P-S, -P+S, -P-S) and allowed to grow for 8-DAT and 15-DAT after transferring. The seedlings were allowed to grow for the next eight and fifteen days on the respective media. After the completion of experiments, samples were harvested and snap-frozen in liquid N_2. The frozen samples were stored at -80 ˚C for further experiments. All experiments were repeated at least twice with ≥ 15 seedlings per treatment. °C

2.2. Plant growth in greenhouse

Tomato seeds were sterilized and germinated, as discussed earlier in section 1. Germinated seedlings or transgenic lines were transferred in small pots containing moisture soil rite rich in nutrients and allowed to grow for 15-to-20 days in a plant culture room as the condition described earlier section. All the seedlings with pots were moved into the greenhouse and incubated for three days for acclimatization. Finally, the plants were transferred to larger pots containing fertile soils with growth conditions, as mentioned in section 1.

2.3. Root morphological analysis

Before harvesting, seedlings' images were captured by a Canon PowerShot camera. Further, seedlings were removed gently without disrupting the roots and kept in double disitilled water (DDW) for root architecture study. For Root length and lateral root density, all the seedlings were with scale by HP LaserJet 1536dnf MFP printer. Root and Shoot length was measured by the Image J software tool. However, for the root hair number and length study, we first fixed the roots on 0.8 % agar and then scanned in Leica M105FC light microscope and counted the number of root hairs from the primary root tip, whereas root hairs lengths were measured as described previously [365].

$$Lateral\ root\ density = number\ of\ lateral\ root\ number\ /\ Prianry\ root\ length$$

$$Root\ hairs\ density = number\ of\ root\ hairs\ /\ mm\ primary\ root\ length\ from\ the\ tip$$

Table-1

Recipe for modified ½ Murashige and Skoog (MS) nutrient components, pH 5.8	
Macro-nutrients	**Required vol for ½ MS medium, pH-5.8 Conc.mg/L**
KH_2PO_4	170.1
$MgSO_4$-$7H_2O$	90.345
$CaCl_2.2H_2O$	166.1
KCl	70
NH_4NO_3	825
Micro-nutrients	
H_3BO_3	3.1
$MnSO_4.H_2O$	8.45
$ZnSO_4.7H_2O$,	4.3
$Na_2MoO_4.2H_2O$	18.65
$CuSO_4.5H_2O$	0.012
$CoCl_2.6H_2O$	3.125
$FeSO_4.7H_2O$	13.9
Na-EDTA	18.65

Myo-inositol	50
Sucrose	2 %

Table-2

Recipe for Hoagland's complete nutrient solution pH 5.8		
Ingredients **Macronutrients stock**	**Required vol for ½ x/L High Phosphate (HP)**	**Required vol for ½ x/L Low Phosphate (LP)**
1M KH_2PO_4	1.25 mL (1.25 mM)	5 µL (5 µM)
1M KNO_3	3 mL (6 mM)	3 mL (6 mM)
1M $Ca(NO_3)_2$-$4H_2O$	2 mL (2 mM)	2 mL (4 mM)
1M $MgSO_4$-$7H_2O$	1 mL (1 mM)	1 mL (1 mM)
Micronutrients stock	**Conc. g/L for stock solution**	**1000x micronutrient**
H_3BO_3	2.86	Combined all following components in total vol of 1 ltr of water and used 0.5 mL of this stock for ½ x/ltr working Hoagland solution
$MnSO_4.H_2O$	1.81	
$ZnSO_4.7H_2O$	0.22	
$Na_2MoO_4.2H_2O$	0.12	
$CuSO_4.5H_2O$	0.08	
Iron stock	**Conc. g/L for stock solution**	
Na-EDTA	26.1 in water containing 19 g of KOH	The pH rises to about 7.1 and the solution is wine red and very little precipitation occurs. Make to 1-liter final volume and store in a bottle covered with foil (dark). From stock 0.5 mL used for ½ x/ltr working Hoagland solution
$FeSO_4.7H_2O$	24.9 g dissolved in 500 mL of water and slowly added in KOH-NaEDTA solution and aerate this solution overnight with stirring.	

2.4. Quantification of total soluble Pi and P

Total soluble inorganic phosphate (Pi) of Pi-sufficient and Pi-deficient plant tissues was quantified using a phosphomolybdate spectrophotometric-based assay, as described by Ames (1966) [366]. The fresh plant tissue was powdered in a prechilled pestle and mortar. 30 mg of ground tissue was taken in a 1.5 mL microcentrifuge tube (MCT) and thoroughly mixed by vertexing with 250 µL of

1 % glacial acetic acid. Samples were subjected to liquid N_2 for about 30 sec and allowed to thaw at room temperature (RT). Thawed samples were centrifuged at 14000xg for 5 min. The 50 μL supernatant was taken in new MCT, and 600 mL of 0.42 % acidic ammonium molybdate was added. Along with 100 μL of 10 % ascorbic acid, mixed it properly and incubated at 45˚C for 30 min. Further, from each tube, 200 μL samples were taken and read OD_{820} nm to quantify the soluble Pi as described by Ames (1966) [366]. Each experiment was independently repeated at least three times, with ten or more tomato seedlings per repeat.

For total P estimation, first, we dried the whole plant at 65˚C in a hot air oven for 24 h. The next day, the whole dried plant was ground in fine tissue powder, and 50 mg of powdered tissues were taken in a 100 mL boiling tube. Further, 1 mL of concentrated sulfuric acid was added and incubation for O/N at RT. The next day, all tubes were again incubated at 120˚C for 2 h. Afterward, 1 mL of 30 % H2O2 is added to each hot tube, allowing them to become colorless solutions. The 10 μL solution from each was taken in new MCTs and added 600 μL of 0.42 % acidic ammonium molybdate, along with 100 μL of 10 % ascorbic acid, mixed it properly, and incubated at 45˚C for 30 min. Further, 200 μL samples were taken from each tube, read O.D. at 820 nm, and quantified the total P was using the P standard curve. Each experiment was independently repeated at least three times, with ten or more tomato seedlings per repeat.

2.5. H2DCFDA histochemical staining for H_2O_2 detection

For histochemical staining and detection of H_2O_2 in roots, we have used 2′,7′-Dichlorofluorescin diacetate (H2DCFDA- Sigma-Aldrich, cataloge number: 4091-99-0) with slight modification. HP and LP roots were taken from the media, washed gently with DDW, and incubated in 10 μM H2DCFDA solution for 30 min. Further roots were cleaned with DDW, and roots were used for imaging with a confocal microscope where 488nm wavelength was used for emission, and 522 nm wavelength was used for light detection [367].

2.6. Estimation of total anthocyanins

Total anthocyanins pigments of Pi-sufficient and Pi-deficient seedlings were quantified of the same node leaves in the two sets of plants. 150 mg of leaf tissue was ground in 10 mL of acidic methanol (methanol: water: HCl, 79:20:1, v/v/v) and incubated the samples in dark for 2 h. After incubation, samples were centrifuged at 5000xg at RT for 10 min. The absorbance of the supernatant was measured at 530 nm and 657 nm, as described previously [368]. The experiment was

independently performed three times. Total anthocyanins content was measured using the following formula: $\{A530 - (\frac{A657}{3})\}/gm\ FW$ where A_{530} and A_{657} are absorbance in nm of the extracted pigments solution.

2.7. Quantification of total carbohydrates

The total carbohydrates were quantified using Phenol Sulfuric acid method (HiPer Carbohydrates Estimation Teaching Kit-Himedia). First, we plotted the Glucose standard curve with the standard glucose Himedia-GRM016 (1mg/mL). Plant tissue was ground in liquid N_2, and 10 mg of powdered tissue was transferred to 2 mL MCTs. Afterward, 0.2 mL of 0.5 % phenol solution was added to all the MCTs, followed by gentle mixing. Then, 1 mL of concentrated Sulphuric acid was added to each tube, mixed well, and incubated for 10 min at RT, followed by a second incubation at 30 °C for 20 min. Finally, the O.D. was recorded at a wavelength of 490 nm. Sugar concentration was calculated by using the glucose standard curve.

2.8. Determination of root-secreted acid phosphatase activity

For secretory acid phosphatase (SAP) activity, roots from Pi-sufficient and Pi-deficient tomato seedlings were purged and submerged in a reaction buffer (10 mM pNPP, 10 mM $MgCl_2$, 50 mM NaOAc, pH 4.9) for 4h at 37 °C. After incubation, the reaction mixture was terminated by adding 100 µL of 0.4 N NaOH solution. The roots were then removed from the reaction buffer, and the absorbance of the solution was recorded at 410 nm. SAP activity was expressed in A_{410nm}/plant/h. For root-surface associated APase activity, roots of Pi-sufficient and Pi-deficient tomato seedlings were cut and washed with DDW. These roots were arranged vertically on the 24 cm^2 plates and kept wet with the help of DDW. These roots were then temporarily fixed by pouring 0.5 % agar solution containing 100 µM BCIP and the setup was incubated at RT for 24 h [369]. Images of all the roots were taken by scanning with an HP LaserJet 1536dnf MFP printer.

2.9. Pi kinetic and recovery experiments

Seeds were germinated on blotting paper, as mentioned in section 1. Further, these seedlings were transferred on standard 1/2x Hoagland media. After seven days of germination, phosphate starvation was given for the next 15 days. Samples were collected from the first the of starvation in a time-dependent manner till 15 days (15min, 4h, 12h, 24h, 48h, 7-day, and 15-day). Further, starved

seedlings were recovered by changing low P media to high P, and samples were collected hourly. All the samples were instant fridges by Liq. N_2 and stored in a -80 °C deep freezer.

2.10. Minerals nutrients stress

For nutrient stress, geminated seedlings were grown for seven days on normal media and then transferred to different stress media (-P, -K, -Mg, -N, and -Ca). For K depletion, we have replaced the KH_2PO_4 with H_3PO_4, for -Mg; $MgSO_4$ with NH_4SO_4, for -Ca; $CaCl_2$ with KCl, for -N; $CaNO_3$ with $CaCl_2$ for 15 days. After that, samples were collected and stored instantly at -80 °C. Further RNA was isolated from all the samples as described above section.

2.11. Non-targeted metabolite profiling

For GC-MS-based profiling of metabolites, 8-DAT and 15-DAT Pi-sufficient and Pi-deficient tomato seedlings were frozen and powdered in liquid N_2. 150 mg of each frozen pulverized sample was extracted in 1400 µL of 100 % MeOH solution. The extraction of the frozen samples and further processing were done as described previously by Bodanapu et al. (2016) [370]. Ribitol (0.2 mg ribitol/mL water) was used as an internal standard. Gas chromatography was performed using a hybrid quadrupole time-of-flight instrument (Leco Corporation, USA). ChromaTOF and Met-Align packages (Lommen et al. 2012) were used for processing and initial analysis of the raw data [445]. The mass signals present in at least three samples were used for further Research. The NIST (National Institute of Standards and Technology) GC/MS Metabolomics library software (NIST/EPA/NIH Mass Spectral Library 14, v 2.2, USA) was used to identify the metabolites. Statistical analysis was done using MetaboAnalyst 4.0 (https://www.metaboanalyst.ca/). Pearson's correlation was set as a default setting. PCA and partial least squares discriminant analysis PLS–DA) were performed in MetaboAnalyst 4.0 [371].

2.12. Histochemical analysis and quantification of ROS levels

Detection of H_2O_2 and O_2^- was done as described by https://bio-protocol.org/e1108#biaoti5025. Harvested leaf and root tissues were washed with DDW to remove extraneous materials. Root and leaves were placed in a 6-well tissue culture plate (Tarson, catalog number: 980010). For the H_2O_2 detection, the samples were immersed with 1 mg/mL 3, 3'diaminobenzidine (DAB). O_2^- detection

was done by immersing samples in 2 % NBT solution in 50 mM sodium phosphate buffer. In both cases, the plate was wrapped with aluminum foil and incubated overnight in the dark at room temperature. The next day solution was drained off the plate. Stained samples were bleached in acetic acid-glycerol-methanol (1:1:3) (v/v/v) by boiling the solution at 100 ^{o}C for 5 min. Finally, the samples were stored in glycerol-methanol (1:4) (v/v) solution until the photograph was taken. H_2O_2 was visualized as a brown color due to DAB polymerization.

Estimation of ROS (H_2O_2) levels was done as published previously [148]. In this protocol, 100 mg of fresh plant tissue (shoot/root) was ground in liquid N_2. The powder was transferred to 1.5 mL MCT with 100 µL of 0.1 % TCA. The samples were mixed well by vertexing, followed by a centrifugation step at 12000xg for 15 min 500 µL of supernatant was transferred to a new MCT and mixed with 500 µL of potassium phosphate buffer (pH 7.0), and 1 mL of 1M KI followed by gentle mixing of the reaction mix. The optical density of the mixture was recorded at 390 nm. The H_2O_2 content was determined by using an H_2O_2 standard. The NBT-stained root was used to determine O_2^- production through NBT precipitation. In short, NBT-stained tissues were homogenized in 2 M KOH-DMSO (1/1.16,v/v) and were centrifuged at 12,000xg for 10 min. OD_{630} of the supernatant was taken instantaneously. Superoxide ions were quantified using a standard prepared with the known concentrations of NBT.

2.13. Plasma membrane (PM) protein extraction by PVPP method for NADPH oxidase assay

First, 5 % 0.25mg PVPP (110 µm size) was mixed with DW and kept at 4 °C overnight. Next day, the protein extraction buffer is prepared with the below-mentioned composition:

Table 3: Composition of Protein Extraction Buffer (50 mL)	
0.25 mM Sucrose	4.278mg
50 mM HEPES	595.75mg
3.6 mM L-Cysteine	21.807mg
0.6 % PVP	300 mg
2mM EDTA	300µL from 0.5M stock

The PVPP was centrifuged at 2000xg for 5 min at room temperature, and the supernatant was discarded. PVPP is then equilibrated by adding extraction buffer, mixed by vertexing, and left on ice for 2h. After incubation, PVPP was again centrifuged at 2000xg for 5 min. After discarding the supernatant, 1.5 mL extraction buffer containing 1mM PMSF was added to PVPP, and vertexing was done to mix the components. We used 0.05g PVPP (Dry Weight)/gram of plant tissue (Fresh Weight). One-gram shoot and root tissues were powdered in liquid N_2, followed by adding 5 mL PVPP solution with extraction buffer. The solution was vortexed and maintained on ice until its centrifugation at 600xg for 5 min at 4 °C. The upper layer was transferred to a new 15 mL falcon tube. This step was repeated by adding ½ volume of the extraction buffer used for the first time. Then the supernatant was centrifuged at 10000xg for 5 min. The supernatant was transferred in an Ultracentrifuge tube (Beckman Coulter, cataloge number: 331374) and nonstop centrifuged at 220000xg for 2 h at 4 °C. Subsequently, the supernatant was discarded, and pellets were dissolved in 500 µL of 50 mM Trish-HCl buffer with pH 7.5. Protein concentration was measured at 594 nm using the Bradford method, and the final concentration of protein was calculated by BSA standard, as discussed earlier.

2.14. Determination of NADPH oxidase activity

The NADPH oxidase activity in the root and shoot tissues of Pi-sufficient and Pi-deficient seedlings was performed from the isolated PM proteins. First, the reaction buffer (50 mM Tris-HCL pH 7.5, 0.5 mM XTT, 100 µM NADPH) was prepared. The reaction was initiated by mixing 50 g membrane protein in 1 mL reaction buffer. The reduction of XTT was determined at 470 nm for 5 min with an interval of 30 sec. The extinction coefficient of 2.16 x 10^4 $M^{-1}cm^{-1}$ was used in the calculations [372].

2.15. H_2O_2 and DPI treatment in tomato seedlings

Sterilized tomato seeds (as described earlier) germinated on moist filter paper for four days under dark conditions. The germinated seeds were transferred to the half-strength Hoagland's nutrient solution (Hoagland & Arnon, 1950), as mentioned in **Table 2** [448]. Nutrient solutions were prepared with different concentrations of diphenyleneiodonium chloride (DPI) and H_2O_2. Plants were

grown with and without DPI and H_2O_2 for the next ten days in a growth culture room set at 22 ± 1°C, 50–70 % RH, and light intensity of 150-200 μmol m^{-2} s^{-1} under 16 h/8 h light/dark photo-period cycle.

2.16. RNA preparation, RNA-sequencing, and quantitative real-time PCR (qPCR)

Total RNA from different treatments, root, shoot, and fruits tissues were extracted using a Favor-Prep™ Plant Total RNA Mini Kit (sample size: up to 100 mg of plant tissue, fruit or seed, cat#FAPRK 001 Favorgen make, Taiwan). High-quality RNA samples were outsourced to Bionivid (https://www.bionivid.com/) for RNA sequencing. Four libraries were sequenced using with Illumina HiSEQ 4000 platform. The following parameters were used during RNA sequencing: 150 bp paired-end sequencing and ≥ 25 million reads per library. Stringent quality control of Paired End sequence reads of all the samples was done using the NGSQC Tool kit. Paired-end sequence reads with a Phred score >Q30 were taken for further analysis. Solanum *lycopersicum* Transcriptome from SGN was used for the reads alignment. Kallisto quant was used for alignment, and the DESeq R package was used for differential expression analysis with default parameters. In the treated samples, transcripts with log_2 fold change with a cut-off value of 1 and p-value <=0.05 were considered differentially expressed genes against their nontreated sample signal values (data unpublished). Unsupervised hierarchical clustering of differentially expressed genes was done using Cluster 3.0 and visualized using Java Tree View v1.1.6. Heatmaps were generated using online software called Heatmapper (http://www.heatmapper.ca/). For annotation, all the transcript sequences were used for BLASTN against the Refseq Plant database to get Gene Ontology (GO) and KEGG Pathways for Complete data. Gene ontology (Biological processes, Cellular components, and Molecular Functions) for significantly differentially expressed genes were fetched from Ensemble Plant Biomart (SL3.0) (Bionivid IT complements Research).

Quantitative real-time PCR (qPCR) specific primers were made using PRIMER EXPRESS version 2.0 (PE Applied Biosystems, USA). The qPCR reactions were performed in 96-well optical reaction plates using the Bio-Rad CFX96 Touch Real-Time PCR and Agilent Mx3000P QPCR system. Normalization of the qPCR expression data was done using the tomato *GAPDH* gene. qPCR-based expression analysis was performed using at least two biological samples with three technical replicates per sample. The $\Delta\Delta C_T$ method was selected to calculate the relative gene expression level of all the genes [373].

Table-4

Vector name	Type of vector	Cloned gene	Purpose
pCAMBIA1391	Promoter binary vector	1kb SlRbohH promoter	Promoter activity
pCAMBIA2302	35S overexpression binary vector	1.63kb *SlFBX2L1* CDS	Complement/ subcellular localization studies in plants
pTRV2	Tobacco rattle virus vector 2	35-409 bp VIGS fragments *SlRbohH*, *SlFBX2L1*, and *SlPDS*	Transient gene silencing studies in plants
pTRV1	Tobacco rattle virus vector1	N/A	Helper vector for mobilization of *pTRV2* plasmid in plants
pFASTRK-AtCas9-AtU6	Plant CRISPR vector	*SlFBX2L1* gRNA seq	For the generation of a stable knockout line

2.17. Construction of pSlRbohH::GUS transcriptional fusion construct

Further, the 1-kb upstream promoter region of SlRbohH harboring multiple P1BS (GNATATNC) elements was amplified by PCR using tomato genomic DNA as a template. The PCR product was purified by PCR/Gel elution kit (Favorgen Biotech, Taiwan). The purified amplicon was double digested with fast-digest FDPstI and FDBamHI (Thermo-Fisher Scientific, cataloge numbers: FD0614 and FD0054) restriction enzymes (Thermo-Fisher Scientific, Scientific USA). The binary vector pCAMBIA1391z was also digested with the same restriction enzymes. The digested products were purified again, as discussed previously, and concentrations of the eluted products were estimated using BioSpectrometer (Eppendorf Pvt. Ltd., Germany). Next, the vector and insert were taken in a 1:6 ratio for ligation reactions. T4 DNA Ligase (Invitrogen Life Technologies, USA, cataloge number: 5224017) was used in the ligation reaction, and MCT carrying the reaction mixture was incubated at 16 °C overnight. Afterward, the ligated reaction mixture was transformed into *E. coli DH5α* competent cells using a heat shock method. The transformed cells were first revived and then spread on LB-Agar plates supplemented with 50 mg/L Kanamycin (Himedia,

cataloge number: 25389-94-0). The plates were incubated at 37 °C in an incubator for 16 h. The next day, colony PCR was performed on the grown colonies on the selection plate with promoter-specific primers. The confirmed colonies were grown for plasmid isolation and further validation. FD PstI and FD BamHI restriction enzymes were used in double digestion, and the reaction was performed as described earlier. Agarose gel electrophoresis was used to visualize the released insert from the vector backbone on 0.8 % agarose gel. Final confirmation of the cloning of the *SlRbohH* promoter was done by Sanger sequencing. The cloned product was transformed in *Agrobacterium tumefaciens strain LB4404* and confirmed by colony PCR and double digestion with the same restriction enzymes. The single confirmed colony was inoculated in 5 mL of YEM media with respective antibiotics and then grown for 24 h. After 24 h, 10 mL of YEM media was used for secondary where 1 % inoculum from the primary culture was added with antibiotics for 16 h. Further, 187 mL of 80 % glycerol stock was added in 10 mL culture, gently mixed, and 1.5 mL mixed culture and stored in a deep freezer at -80 °Cfor further experiments.

2.18. Construction of *SlFBX2L1*-overexpression vector for gene complementation study

For the gene complement study, the *SlFBX2L1* coding sequence (CDS) was retrieved from SGN (https://solgenomics.net/tools/blast/), and primers were designed by adding NcoI and SpeI restriction sites. Full-length CDS was amplified using iProof™ High-Fidelity DNA Polymerase enzyme from (Bio-Rad USA)). The amplified product and pCAMBIA1302GFP binary vector were double digested by NcoI and BucI (SpeI) restriction enzymes and purified as described in section 16. Further, the ligation reaction mixture was performed as discussed previously. Next, Transformation, colony PCR, plasmid isolation, double digestion, Sanger sequencing, and glycerol stock preparation were performed as described previously. Additionally, the cloned product was transformed in *Agrobacterium tumefaciens strain LB4404*, confirmed by colony PCR and double digestion with the same restriction enzymes.

2.19. Generation of *pTRV2* plasmid constructs of *SlRbohH, SlFBX2L1,* and *SlPDS* for transient gene silencing

The complete coding sequence of *SlRbohH, SlFBX2L1* and *SlPDS* was used as a query sequence SGN VIGS tool (https://vigs.solgenomics.net/) to select the best VIG*S* fragment for these genes.

Using gene-specific VIGS primers, 350, 300, and 409 bp fragments of all three genes coding sequences were PCR amplified from tomato seedlings cDNA. The amplified PCR products were cloned into the tobacco rattle virus vector (*pTRV2)* using *Xba*I-*Bam*HI restriction sites. Cloning of the fragment was performed as described earlier section. The putative transformants were confirmed by colony PCR and restriction digestion. The verified plasmids were used to transform in *Agrobacterium tumefaciens GV3101* competent cells for VIGS experiments.

2.20. Generation of single guide RNA (gRNA) construction of the *SlFBX2L1* gene for generation of CRISPR/Cas9 knockout (KO) lines

The *SlFBX2L1* gene data were examined in the Sol Genomics Network (SGN) database using the Solyc06g073650 gene ID, and the coding and genomic sequences were extracted from the SGN database ITAG 3.20. Individual exons were submitted to the CRISPR-P 2.0 database (http://crispr.hzau.edu.cn/CRISPR2/) to find candidate guide sequences. Parameters like NGG-PAM, U6 snoRNA promoter, *Solanum lycopersicum* target genome, and exon sequence were decisive. Guides were examined from the provided list, and preference was given to guide RNA (gRNA) with a free 5' end in the secondary structure, high on-target potential, and a low off-target value. For designing the gRNA primers, restriction enzyme site BsaI, AtU6-26 promoter sequence or its scaffold sequence present in the template plasmid pEN-2xAtU6 was added to the chosen guide sequence. (https://gatewayvectors.vib.be/collection/pen-2xatu6-template), and the amplified sequence was purified as mentioned in previous section 16. Destination vector pFASTRK-AtCas9-AtU6 (https://gatewayvectors.vib.be/collection/pfastrk-atcas9-atu6-scaffold) and PCR purified fragments were digested using BsaI restriction digestion enzyme. Further, ligation, transformation colony PCR, plasmid isolation, and restriction digestion with FDEcoRI and FDPstI enzymes. The final plasmid was confirmed by Sanger sequencing. Verified plasmids were immobilized into Agrobacterium AGL1 cells. The successful mobilization was confirmed using colony PCR. Plasmids from positive colonies were used for generating gene-editing KO tomato lines.

2.21. Screening and validation of homozygous *Atfbx2* mutant (SALK_003143C)

Seeds of SALK *Atfbx2* mutant (SALK_003143C) were obtained from TAIR (http://signal.salk.edu/cgi-bin/tdnaexpress). The surface sterilization of seeds was done using 70 % ethanol for two min followed by 4 %-hypochlorite treatment. Seeds were washed with autoclaved double

distilled water and spread on ½ MS-Agar plate using 200 µL micro tips. The plate was incubated for three days in the dark at 4 °C. Later, the ½ MS-Agar containing seeds were transferred to the culture room and maintained a 16/8h light-dark cycle at 22 °C with light intensity 150 µmol/m^2/s^{-1}. After 3-4 weeks, the Dellaporta method was used to isolate genomic DNA [447]. To screen the homozygous mutant lines, Polymerase Chain Reaction was performed by using specific primers (Left primer, Right primer, LB3.1 primer, **Table-7**) made from the T-DNA primer designer tool (http://signal.salk.edu/tdnaprimers.2.html). After the screening of homozygous mutant lines, plants were allowed to grow, and seeds were harvested and stored at -20 °C. Arabidopsis *Atfbx2* mutant and Col-0 seeds were germinated on a plate with normal ½ MS-Agar media, transferred on HP/LP ½ MS-Agar plate, and kept vertically. Images were taken with Leica M105FC light microscope. Soluble Pi, total P, and anthocyanins were estimated as described previously.

2.22. Stable transformation of *Atfbx2* mutant plants with *pCAMBIA2302:SlFBX2L1* construct by floral dip

The *Arabidopsis thaliana Atfbx2* homozygous mutant seeds were grown under normal conditions with a 16/8 light-dark cycle at 22 °C. In the meantime, bacterial culture was prepared for *Agrobacterium tumefaciens* strain *AGL-1* harboring the expression vector (pCAMBIA1302GFP-*SlFBX2L1*:OX). For this, a fresh colony was inoculated into 5 mL LB broth medium with suitable antibiotics, and the culture was grown at 28 °C for 2-days. Sub-culturing was done by adding 1 % of the primary culture to 200 mL liquid LB with the appropriate antibiotics. The secondary culture was grown to a stationary phase until OD_{600} reached 1.5 at 28 °C. Later, cells were harvested by centrifugation at 5,000xg for 15 min at room temperature (RT). Pellet was suspended in a 5 % (w/v) sucrose solution. Sliwet L-77 was supplemented to a concentration of 0.03 % (vol/vol) and mixed well before dipping. The transformation solution was poured into was in 250 mL glass beaker. Next, plants were inverted and dipped whole aerial parts of the plant in *Agrobacterium* solution for 2 to 3 sec with gentle shaking. The pipette was used for dripping some bacterial suspension onto small axillary floral buds, which are enabled to immerse into the solution. A big transparent plastic bag enclosed the dipped plants for 24 h to maintain high RH. Care was taken to avoid the exposure of plants to excessive sunlight. The next day, the cover was removed, and the treated plants were kept back to normal condition 16/8 h light-dark cycle at 22°C. T_1 seeds were collected for further screening.

2.23. Screening of putative complemented lines on Hygromycin antibiotics

T_1 seeds were sterilized as described in section 20, spread on the 15 µg/mL HygR containing ½ MS solid agar plates, and incubated in the dark for three days at 4 °C. After 3rd incubation, plates were exposed to light for 6 h and further incubation in darkness for 24 h. Further, plates were transferred back in the light. After the 24 h incubation of plates, positive seedlings with long hypocotyls were allowed to grow for one week and then transferred on soil rite for further growth. Then homozygous lines were confirmed by PCR base methods using gDNA as a template of all positive lines where gene-specific primers to amplify the transformant DNA segment. Final homozygous line confirmation was done by checking the gene expression level of *SlFBX2L1* by qPCR. Homozygous *Atfbx2*:35S-*SlFBX2L1* complemented lines were used for further characterization.

2.24. Histochemical analysis of stable pSlRbohH:GUS Arabidopsis lines

Arabidopsis homozygous *SlRbohH* stable promoter line and WT Col-0 seeds were surface sterilized by using 70 % ethanol for 2 min, followed by 4 % hypochlorite treatment for 10 min in laminar airflow. These seeds were washed with autoclaved DDW and spread on ½ MS-agar plate using 200 µL micro tips. The ½MS plates with spread seeds were incubated at 4 °C in the dark for the next three days. Later, these plates were transferred to the culture room, maintained at 22 °C with 16/8 h light-dark cycle with light intensity 120-150 µmol/m^2/s^{-1}. After three days, the seedlings were transferred to ½ MS-Agar plates supplemented with either HP or LP and grown for the next 15 days. Seedlings were removed carefully without damaging the roots. For histochemical staining, the DDW washed seedlings were immersed in GUS solution {50 mM phosphate buffer pH 7.2, 5 mM $K_3Fe(CN)_6$, 5 mM $K_4Fe(CN)_6$, 0.2 % (v/v) Triton X-100, and 2 mM X-Gluc (5-bromo-4-chloro-3-indoxyl-beta-D-glucuronide cyclohexyl ammonium salt)} and incubated overnight at 37ºC with gentle shaking. Stained leaves and roots were submerged in 70 % and then 95 % ethanol solutions to bleach the chlorophyll and clear the tissues. Seedlings images were taken using Leica light microscope.

2.25. Transcriptional activation of *pCAMBIA1391z:SlRbohH* with *pCABIA2302:PHRL1/L2* in *N. benthamiana*

Prepared recombinant agrobacteria were used for infiltration using a procedure of K. Norkunas et al. (2018). In short, a single colony for each vector was inoculated into liquid Yeast Mannitol media (YEM) containing kanamycin (50 mg/L) and rifampicin (30 mg/L) at 28 °C for 24 h. The next day, the secondary culture was inoculated in 10 mL YEM with kanamycin (50 mg/L), rifampicin (30 mg/L), and 200 μM acetosyringone for 24 h at 28 °C. The bacterial cultures were centrifuged, the supernatant discarded, and pellets were resuspended in MMA (10 mM MES pH 5.6, 10 mM $MgCl_2$, 200 μM acetosyringone) with final OD_{600} 1. The resuspended cultures were incubated at room temperature for 2 h for the revival of cells. For the infiltration, recombinant bacteria containing different plasmids were mixed with 1:1:1 ratio (*pCAMBIA1391z-SlRbohH:GUS::pCAMBIA2302:PHRL1/L2:p19*) or (*pCAMBIA1391z-GUS::pCAMBIA2302:PHRL1/L2:p19*) just before infiltration. The top leaves of 6–8 weeks old plants were infiltrated with either blank vector or vector combination and kept in the dark for 24 h. Later, the infiltrated plants were kept for the next 72 h in a culture room maintained at 22 °C with RH-65, light intensity 200 μmol/m^2/s^{-1} with 16/8 h photoperiodic cycle. The histochemical staining of the *Agrobacterium* infiltrated leaves was performed, as mentioned previously.

2.26. Virus-induced gene silencing method (VIGS)

The germinated tomato seeds were transferred to the half-strength Hoagland's nutrient solution, as mentioned in the above sections, for seven days. To silence the candidate genes such as *SlRbohH* or *SlFBX2L1* genes, the VIGS protocol was followed, as prescribed by M. Senthil-Kumar et al. (2013) [446]. In brief, the primary culture of all VIGS constructs was initiated in YEM broth media with Rif 30 mg/L and Kan 50 mg/L at 28 °C overnight. The next day, the secondary culture was inoculated in Induction Media (IM) containing 50 mg/L Kan, 30 mg/L Rif with 200 μM acetosyringone for 24 h at 28 °C. The cells were harvested by centrifuging for 10 min at 3000xg and resuspended by the gentle shake in the same volume that the original culture medium (10 mM $MgCl_2$, 10 mM MES pH 5.5). Again, centrifugation was done for 10 min at 3000xg, and the cells were resuspended in 1/2 volume of the original culture in MES-$MgCl_2$ (10 mM $MgCl_2$, 10 mM MES pH 5.5). The cultures *pTRV1* and *pTRV2-SlRbohH/SlFBX2L1*, *pTRV1* and *pTRV2*, positive control *pTRV1* and *pTRV2-SlPDS* were mixed in separate 5 mL culture tubes with 1:1 ratio with

final equal bacterial density $O.D._{600}$ of 0.15. Bacterial resuspensions were infiltrated to both cotyledons and the first true leaves in 1 mL syringe. These seedlings were allowed to recover and grow for the next seven days in a culture room maintained at 22 °C, RH-65, light intensity 200 µmol/ m^2/s^{-1} with 16/8 h photoperiodic cycle. On the 8^{th} day after infiltration, seedlings were divided into two batches and grown in non-limiting phosphate (1.25 mM, HP) and limiting phosphate (5 µM, LP) conditions in a hydroponic system and grown for the next 15 days. The experiment was terminated after 15 days. Putative VIGS-plants were confirmed for the presence of a *pTRV2* vector by isolating the gDNA from each plant and performing a normal PCR reaction using viral coat-protein gene-specific primers. All the positive plants were used for RNA isolation and physiology. All the biochemical experiments, such as screening of roots, estimation of soluble Pi, total P, total anthocyanins, total carbohydrates, cDNA preparation, and other experiments, were performed as described earlier.

2.27. Identification and sequence analyses of F-box genes

We employed HMM profiling approach for data mining and identification of F-box genes in tomato. HMM profiles of F-box (PF00646), F-box like (PF12937), FBAs (PF04300, PF07734 and PF07735), and FBD (PF08387) were downloaded from Pfam database (http://pfam.xfam.org/). The HMM profiles were searched against the annotated proteins of tomato (ITAG release 3.20), and protein sequences for entries with e-value ≤ e-1 were retrieved. These sequences were examined for the presence of the F-box domain using a batch search tool at the Pfam database with a cutoff of less than 1.0 (http://pfam.xfam.org/). Sequence entries without a specific F-box domain were discarded. The tomato genome gff3 file (ITAG3.2_gene_models.gff3) was used to retrieve information on the chromosome locations and gene structure. Information on the length of coding sequences and the intron-exon organization was also retrieved from the tomato genome database (https://solgenomics.net/). WOLF-pSORT software was used to predict subcellular localization (www.genscript.com/wolf-psort.html). Gene Ontology (GO) classification of the identified F-box genes was performed using PANTHER (http://www.pantherdb.org/) at the Gene Ontology Consortium webpage (http://geneontology.org/page/go-enrichment-analysis). Enrichment analysis was done using Fisher's exact test in 'R'. Putative protein interacting partners were identified using STRING software (http://string-db.org/). For this purpose, the amino acid sequence of the selected F-box gene was used as a query sequence in the search option "protein by sequence". The output

figure was exported as a vector graphic (SVG) and manually curated for gene names of the interacting protein partners.

2.28. Chromosomal location map, gene duplication, and syntenic analyses

The chromosomal positions of F-box genes were retrieved from the ITAG3.2_gene_models.gff3 file of tomato and were used to generate a chromosomal map using MAPchart [374]. SynMap tool (https://genomevolution.org/CoGe/SynMap.pl) was used to identify syntenic regions within tomato genomes, and F-box genes falling in these regions were considered segmentally duplicated genes. The examination of segmental and tandem duplication events in the expansion of this superfamily was examined using the already defined parameters described previously [354,375]. For tandem duplications, the parameters used are: not more than ten genes should separate them, and duplicated genes should show ≥ 50 % similarity at the protein level. Similarly, syntenic analyses between tomato and other Solanaceae species, including *S. pennellii*, potato and capsicum, and the non-Solanaceous plant Arabidopsis, were carried out. The retrieved lists were searched for syntelog pairs for all F-box genes. The information was used to create ideograms in Circos [376].

2.29. Phylogenetic analysis

The multiple alignment of F-box protein sequences was done using ClustalW in MEGA7 [377]. Because the phylogeny was studied among the tomato F-box members only, Neighbor-joining (NJ) phylogenetic tree method was preferred over Maximum Likelihood (ML) method. Some of the short amino acid sequences were excluded from the analysis. The alignment 'MAS' file was imported in MEGA7, and an unrooted Neighbor-joining (NJ) phylogenetic tree was constructed using the bootstrap method with 1000 iterations. The evolutionary distances were computed using the Poisson correction method and are in the units of the number of amino acid substitutions per site. All ambiguous positions were removed for each sequence pair (pairwise deletion option). Finally, the generated tree was viewed in Tree Explorer, and the branch style was selected as a circle. The Poisson method with uniform rates and pairwise deletion was used.

2.30. Digital gene expression analysis

In-house Affymetrix GeneChip tomato genome microarray data (GSE20720) was explored to analyze the expression profiles of F-box genes during fruit ripening in the cultivated tomato cultivar Pusa Ruby and a homozygous line for the rin mutation (LA1795), as described earlier (Kumar et al., 2012). Differential expression between different stages of wild-type and rin mutant fruits were carried out, and Benjamini Hochberg correction for FDR was applied. Further, RNA-seq expression data from tomato was mined to retrieve expression values for the identified F-box genes [378]. These values were used to study their expression patterns at the RNA level in various organs/tissues/stages of tomato development. The final heatmaps were generated on log_2 transformed values using 'gplots' package in 'R'. Expression profiles of the selected F-box genes in Never-ripe mutant fruits and ethylene treatment were studied by employing the quantitative real-time PCR (qPCR) [379]. To investigate the expression profiles of F-box genes under Pi starvation, the online available RNA-seq data [134], was mined to retrieve the relative expression (treatment vs control). The final heatmap was generated on log10 transformed fold change values using MORPHEUS (https://software.broadinstitute.org/morpheus/).

2.31. Generation of single gRNA-mediated CRISPR/Cas9 knockout lines using tissue culture

A single colony of the transformed AGL1 with the desired clone was cultured in YEM broth and incubated for 24 h at 28 °C with 180 rpm. Inoculum (1 %) of primary culture was used to inoculate 15 mL of YEM broth and incubated for 18 h at 28 °C 180 rpm until the OD_{600} reached 0.5. Cells were then harvested by centrifugation (8,000xg for 10 min at 20 °C) and resuspended in 2 % MSO (4.3 g/L MS salts, 100 mg/L myo-inositol, 0.4 mg/L thiamine, and 20 g/L sucrose). The number of cells per mL was finally adjusted to $1x10^8$ cells/mL. Seeds of tomato cultivar Pusa Ruby were thoroughly washed with 4 % Sodium hypochlorite (NaOCl) for 10 minutes and rinsed 8-10 times with ADDW. Finally, washed seeds were inoculated on ½ MS-agar medium (Murashige and Skoog medium) and grown for five days (2-day dark incubation and transferred to light on the 3rd day). The cotyledons of germinated seeds were used for the explants preparation and incubated them on KCMS (Potassium containing MS) preculture plates (4.3 g/L MS salts, 100 mg/L myo-inositol, 1.3 mg/L thiamine, 0.2 mg/L, 2, 4-dichloro phenoxy acetic acid, 200 mg/L KH_2PO_4, 0.1 mg/L zeatin, 30 g/L sucrose, 0.8 % Agar, pH 6.0) at 25 °C in the dark for two days. After two days of incubation, explants were infected with AGL1 resuspension culture (volume of culture which contains $1x10^8$ cells/mL) for 10 min and transferred to a sterile tissue paper to remove the excess

suspension from explants. The explants were then transferred on KCMS/co-cultivation agar plates with the adaxial side down and incubated in the dark at 28 °C for 48 h. Further, explants were shifted on plant regeneration selective medium 2-ZKC (4.3 g/L MS salts, 100 mg/L myo-inositol, 1 mL/l Nitsch vitamins (1000X), 20 g/L sucrose, 2 mg/L zeatin, 100 mg/L kanamycin, 500mg/L cefotaxime, and 0.8 % agar) with adaxial side facing up. Healthy explants were subcultured to 2ZKC plates every week for three consecutive weeks and later to 1-ZKC plates (containing 1mg/L zeatin, 100 mg/L kanamycin, 500mg/L cefotaxime) biweekly. Subculturing into selection plates was done until shoots emerged from the callus and contained at least one internode. Leaf samples were taken from emerging calli to screen for the integration of the Cas9 cassette. Shoots of the Cas9-positive plantlets were cut-off from the callus and transferred to rooting medium (4.3 g/L MS salts, 1 mL/l Nitsch vitamins (1000X), 30 g/L sucrose, pH 6.0, and 0.8 % agar). After the emergence of roots, plantlets were transferred to peat in small pots for two weeks for hardening. After that, the first generation (T_0) lines were shifted to big pots in the greenhouse and grown until fruits were harvested.

2.32. Screening of KO lines for the integration of Cas9 cassette and presence of insertion/deletion (indels)

The gDNA was extracted from the leaves emerging from the calli and shoots using the Dellaporta method. Isolated gDNA was used as a DNA template for PCR reaction to screen for Cas9-positive lines. Gene-specific primers were designed using the Primer3Plus online tool to amplify the target region within the gene. The amplified fragment was sent for Sanger sequencing to confirm the presence of any Insertions/deletions (INDELS). Individual first-generation (T_0) lines confirmed for INDELS were transferred to pots in the greenhouse and maintained for harvesting T_1 seeds.

2.33. Screening of plants obtained in T_0 and T_1 for the presence of indels in *SlFBX2L1*

Using the Dellaporta method, the gDNA was isolated from the emerging leaves of the calli in T_0 generation. Isolated gDNA was used as a DNA template, and a Polymerase Chain Reaction (PCR) was performed to screen for Cas9-positive lines. Gene-specific primers were designed using the Primer3Plus online tool (Primer3Plus - Pick Primers) to amplify the target region within the gene in these lines. Region from wild-type (WT) Pusa Ruby plant was also amplified for reference sequence. The amplified fragments were cleaned up by using Favorgen Gel/PCR purification kit and

sent for Sanger sequencing to confirm the presence of any insertions/deletions (INDELS). Sequenced samples were screened for indels by alignment of sequence against reference target sequence using CLC Genomics Workbench software and ICE online tool (Synthego - CRISPR Performance Analysis). Simultaneously, lines were transferred to pots in the greenhouse and maintained for harvesting T_1 generation seeds. The independent lines T_1 seeds were grown on ½ MS Kanamycin (100 mg/L) agar bottles. Wild-type Pusa Ruby seeds were used as a negative control. After four weeks, gDNA was isolated from the leaves of the plantlets and transferred to coconut peat, followed by their transfer to the greenhouse after another week. Further, gDNA isolation and detection of indels were done as mentioned above.

2.34. Morphological, biochemical, and molecular analysis of KO lines

Plants of T_0 KO lines were observed for changes in the morphology of leaves, flowers, and fruits. Biochemical and molecular analyses of fruits were done in T_1 lines for *Slfbx2l1* edited lines. Fruits were tagged on the day of fruiting (DOF), 3-4 days after anthesis, when the petals withered off, and the fruit was visible. Both WT and T_1 plants were tagged and marked on the day of the breaker. Thereafter, pictures of individual fruits were taken regularly for phenotypic analyses. Data from at least two plants were used for calculating days to reach the breaker stage. For molecular and biochemical studies, fruits were harvested on two developmental stages, breaker + 3 (Br + 3) and B+10 days. Fruit size was measured in terms of the diameter of the fruit using ImageJ software. Harvested fruits of B+3 and B+10 stages were used for measurement of ethylene, fruit fresh weight and size, and total soluble contents. Thereafter mesocarp of harvested fruits was snap-frozen in liq. N_2 and stored at -80 °C. These samples were used for the quantification of pigments, determination of endogenous indole 3-acetic acid levels, and gene expression analysis. And small pieces of fruits were also stored in 2.5 % glutaraldehyde for transmission electron microscope (TEM) study.

2.35. Ethylene measurement

Tomato fruits at different developmental stages were gently harvested and immediately stored in a sealed container of known volume for 3 h. Further, 1 mL of headspace gas was used for the

detection of ethylene gas by gas chromatography (Analytical Technologies Limited, cataloge number: GC Optima-3007). Four fruits per ripening stage were evaluated to calculate ethylene production in nanoliters per gram of fruit per hour (nL/g/h).

2.36. Determination of fruit pigments

The extraction of total fruit pigments was done as described previously [370]. Briefly, frozen fruit mesocarp tissues (~150 mg) were crushed into a fine powder using a mortar and pestle. 1.5mL of chloroform: dichloromethane (2:1 v/v) was added to the homogenate and mixed at 1000xg at 4 °C for 20 min using Eppendorf Thermomixer. 0.5 mL of 1 M NaCl was added and mixed by gentle inversion. The mix was centrifuged at 5000xg for 10 min for phase separation. After that, the lower-colored organic phase was carefully collected into a new collection tube. The aqueous phase was again extracted by 0.75 mL of chloroform: dichloromethane and the organic phase was re-collected. The organic phase was dried under a speed vacuum evaporator at 45 °C for 2 h. For HPLC, dried samples were re-dissolved in 25:75 (red ripe tissues) or 60:40 (green tissues) v/v of methanol/Methyl Tert-Butyl ether (MTBE). Further, 10 µL of the sample was injected into the HPLC machine for the peak analysis.

2.37. Preparation of standards for HPLC

Pigment standards for lycopene (Sigma-Aldrich, SMB00706) and β-carotene (Sigma-Aldrich, C4582) were dissolved in chloroform and hexane, respectively, to make 1 mg/mL stock solutions. Aliquots of 100 µL were prepared, dried using nitrogen gas, and stored at -80 °C for long-term storage. For HPLC, individual standards were re-dissolved in methanol/MTBE in 60/40 v/v to obtain a final concentration of 0.5 mg/mL. Serial dilution was done to prepare working stocks of 100 ng/mL, 75 ng/mL, 50 ng/mL, 25 ng/mL, and 10 ng/mL for both pigments. 10µL of each working stock was injected into the HPLC system, and a graph was plotted to obtain the standard curve.

2.38. HPLC-PDA analysis of carotenoids

Carotenoids were analyzed by reversed-phase HPLC. Carotenoids were separated on a reverse-phase C18, 5 µm column (4.6 x 250mm). The mobile phases consisted of (A) methanol/water (98:2, v/v) and (B) MTBE. The gradient elution for the column was as follows: 80 % A and 20 % B for 0.1 min, followed by a linear gradient to 60 % A and 40 % B for 4 min. The gradient was

changed to 100 % B till 16 min, changing to 60 % A, 40 % B till 23 min. A re-equilibration with 80 % A and 20 % B was done for 26 min. Column temperature of 20 °C was maintained. The eluting peaks were scanned from the range of 250-700 nm wavelength using PDA. The total area of the peaks was obtained, and quantification was done using the standard curve. Peaks and retention time of the standards were used for the identification of the respective peaks in the sample. The concentration of carotenoids was calculated from the calibration curve of the standard curve using linear regression $y = mx + c$, where y = concentration and x = area of the standard curve. The regression was obtained using Microsoft excel 2019.

2.39. Study of plastid ultrastructure

To study the plastid ultrastructure of the *Slfbx2l1* KO and WT fruits, sections were excised into approximately 1 mm^3 pieces and reserved in 2.5 % glutaraldehyde until further use. The fruit sample was fixed in 2.5 - 3 % glutaraldehyde in 0.1 M phosphate buffer (pH 7.2) for 24 h at 4 °C. Further, 2 % aqueous osmium tetroxide in 0.1 M phosphate buffer (pH 7.2) was used for 2 h for the post-fixing of the samples. Afterward, the samples were dehydrated in a series of graded ethyl alcohols, penetrated, and embedded in Araldite 6005 resin or spur resin [444]. Ultra-thin (60nm) sections were made with a glass knife using an ultramicrotome (Leica Ultra cut UCT-GA-D/E-1/00), then mounted on copper grids and stained with saturated aqueous uranyl acetate and counter-stained with Reynolds lead citrate. Imaging was done by JEOL JEM-F200 cold field emission gun (FEG) transmission electron microscope (TEM) at 200 kV [380].

2.40. Metal elements analysis by using inductively coupled plasma-mass spectroscopy (ICP-MS)

Tomato seeds were surface sterilized and kept in the dark for germination for three days. The germinated seedlings were transferred to normal Hoagland media for 7 days, then subjected to Pi starvation for the next 15 days. Next, root and shoot tissues were washed, separated, and kept in a hot air oven at 65°C for complete drying. Elements study was performed as described by Kaur G. et al., (2019) [381].

Results

Objective-1

1.1 To study tomato seedlings' response under Pi deficiency and identification of Pi starvation inducible genes

In this objective, we first cataloged tomato seedlings' response to low Pi conditions at morpho-physiological and biochemical levels in an Indian tomato cultivar Pusa Ruby. For this, tomato seedlings were first grown under high P nutritional regimes. Subsequently, these seedlings were divided into two batches. One of the batches was transferred again to high-P conditions, whereas the second set of seedlings was subjected to Pi starvation experiments for 8- and 15-days. The end measurements were performed at both time points.

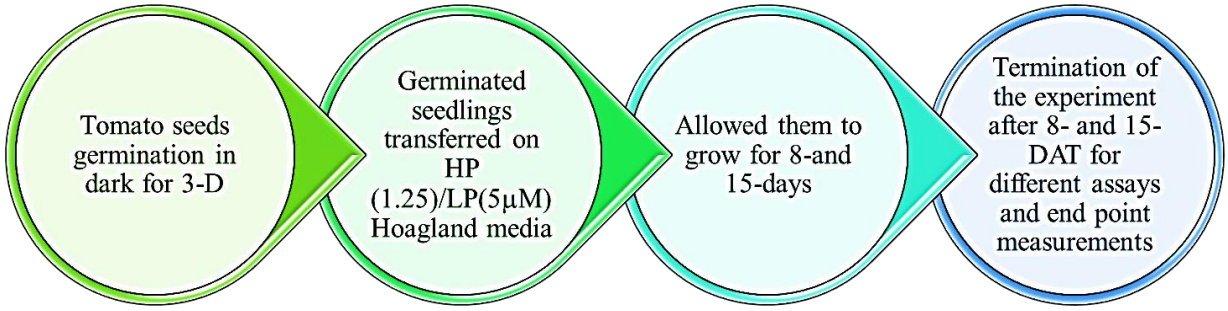

Fig. 9: Overview of the experimental plan to induce Pi starvation in tomato seedlings.

1.2. Morphometric characterization of tomato seedlings under Pi starvation

Morpho-physiological analyses of tomato seedlings grown at insufficient levels of Pi for 8-day (8-D) and 15-day (15-D) time points clearly showed longer primary roots in the LP-grown conditions. The average root length in these seedlings was 22 % and 38 % longer at 8-D and 15-D time points, respectively. The number of lateral roots was also high in Pi-deficient plants, which increased by 32 % and 33 % at 8-D and 15-D time point, respectively, over the same age HP-grown seedlings **(Fig. 10-Aand B and Fig. 11-A, B).**

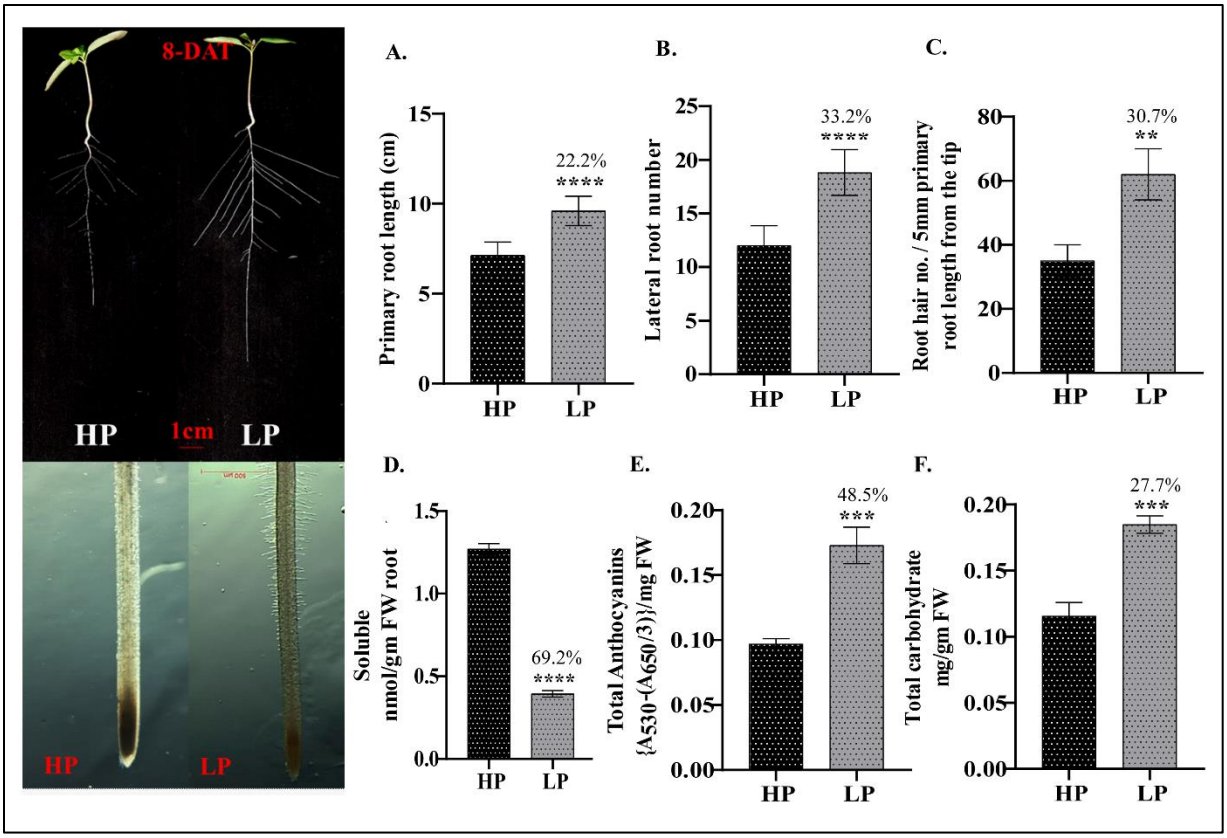

Fig. 10: Physio-biochemical characterization of tomato seedlings grown for 8-DAT in ½ MS agar media containing HP (1.25mM) and LP (5µM) concentration. (A, B and C) Primary root length, lateral root number and root hairs number per unit length of the root. **(D)** Total soluble phosphate (Pi) content. **(E and F)** Total carbohydrates and anthocyanins content. The experiment was performed with three independent biological replicates and repeated twice. HP, high phosphate; LP, low phosphate. Bar denotes 1 cm. Unpaired student's t-test was performed for statistical analysis, p-value ****=<0.05.

Pi-deficient seedlings also exhibited significantly more root hairs at both time points **(Fig. 10-C and Fig. 11-C).** The estimation of total soluble Pi at both time points showed severely reduced Pi levels in Pi-deficient seedlings than their Pi-sufficient controls **(Fig. 1-D, Fig. 2-D).** The Pi-deficient seedlings also accumulated 48 % and 55 % higher total anthocyanins levels and showed 27 % and 56 % higher total carbohydrates at both 8-D and 15-D time points, respectively, than Pi-sufficient seedlings. Overall, we noticed an exacerbated Pi starvation response, all the parameters studied, in Pi-deficient seedlings at 15-DAT time point than the 8-DAT time point, indicating a progressive increase in severity of plant response with the prolonged duration of Pi starvation **(Fig. 10-E, F and Fig. 11-E, F).**

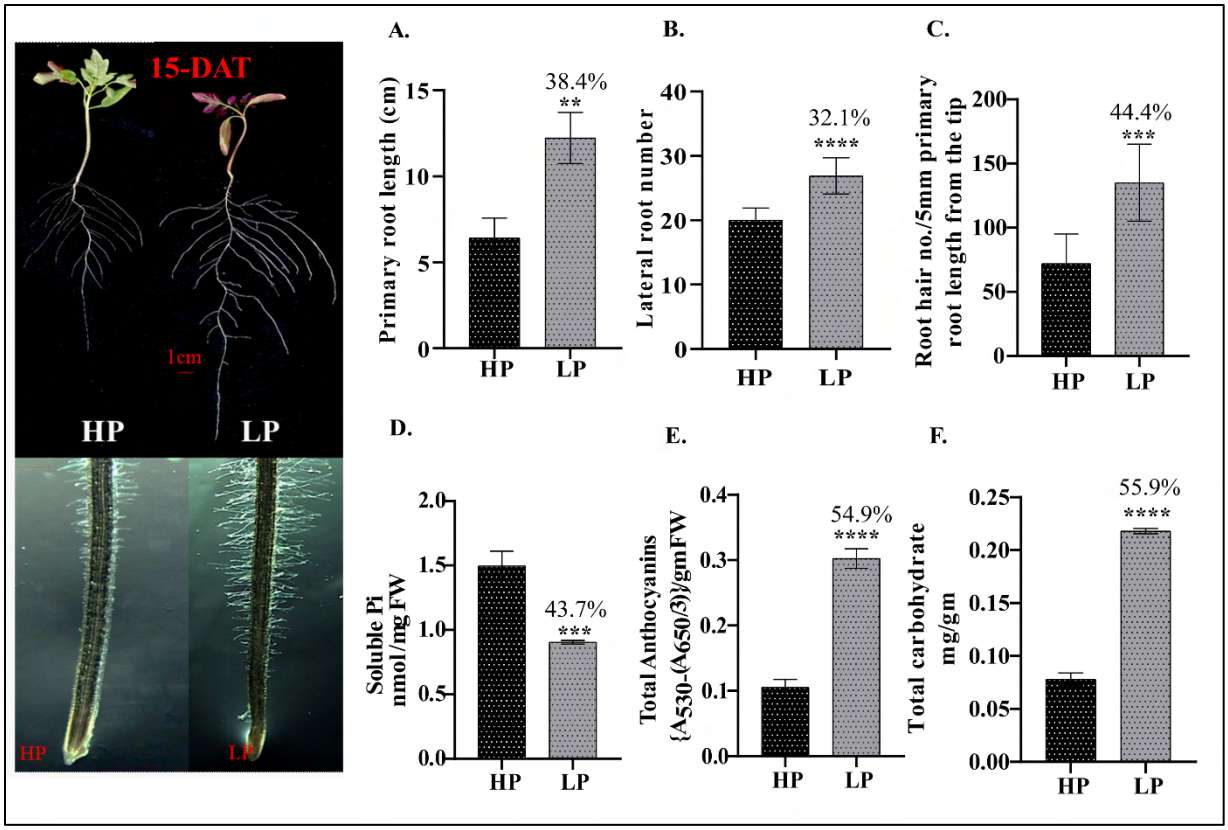

Fig. 11: Physio-biochemical characterization of tomato seedlings grown for 15-DAT in ½ MS agar media containing HP (1.25mM) and LP (5µM) concentration. (A, B and C) Primary root length, lateral root number and root hairs number per unit length of the root. **(D)** Total soluble phosphate (Pi) content. **(E and F)** Total carbohydrates and anthocyanins content. The experiment was performed in three independent biological replicates and repeated twice. HP, high phosphate; LP, low phosphate. Bar denotes 1 cm. Unpaired student's t-test was performed for statistical analysis, p-value ****=<0.05.

1.3. Pi starvation alters metabolites more strongly under long-term Pi deficiency

In total, 56 primary metabolites were detected in both HP- and LP-grown tomato seedlings **(Fig. 12-A).** Many of these metabolites accumulate differentially in the LP-grown tomato seedlings compared to their HP-grown seedlings. The principal component analysis (PCA) and correlation variance explained by the three principal components showed four distinct clusters. The correlation variances explained by PC1, PC2, and PC3 components are 61.2 %, 18.8 %, and 2.5 %, respectively, for the 3-D score plot **(Fig. 12-B, C).** Altogether, this analysis placed two clusters of HP-grown seedlings in proximity **(Fig. 12-B).** The 8-D LP-grown seedlings form a different group. Tomato seedlings grown under Pi deficiency for 15 days formed the most diverged cluster. This analysis revealed that the two sets created by LP-grown seedlings are significantly different to

each other concerning their metabolite accumulation. Many metabolites, such as isoleucine, aspartic acid, and asparagine, showed a transient reduction at 8-D; however, they remained unchanged under prolonged starvation **(Fig. 12-A).** The level of β-alanine and phosphonic acid was reduced gradually under Pi-deficiency from 8-D to 15-D. In contrast, several metabolites such as glycine, o-ethyl hydroxylamine, quinic acid, stearic acid, and linoleic acid showed a gradual increase under long-term Pi deficiency. In contrast, fumaric acid, malic acid, α-ketoglutaric acid, pyroglutamic acid, and threonic acid showed a more prominent enhancement in their accumulation only under long-term treatment **(Fig. 12-B).** Long-term Pi deprivation also augmented the synthesis of several sugar metabolites such as sucrose, glucopyranose, fructopyranose, D-psicofuranose, and myoinositol in tomato seedlings **(Fig. 12-D).**

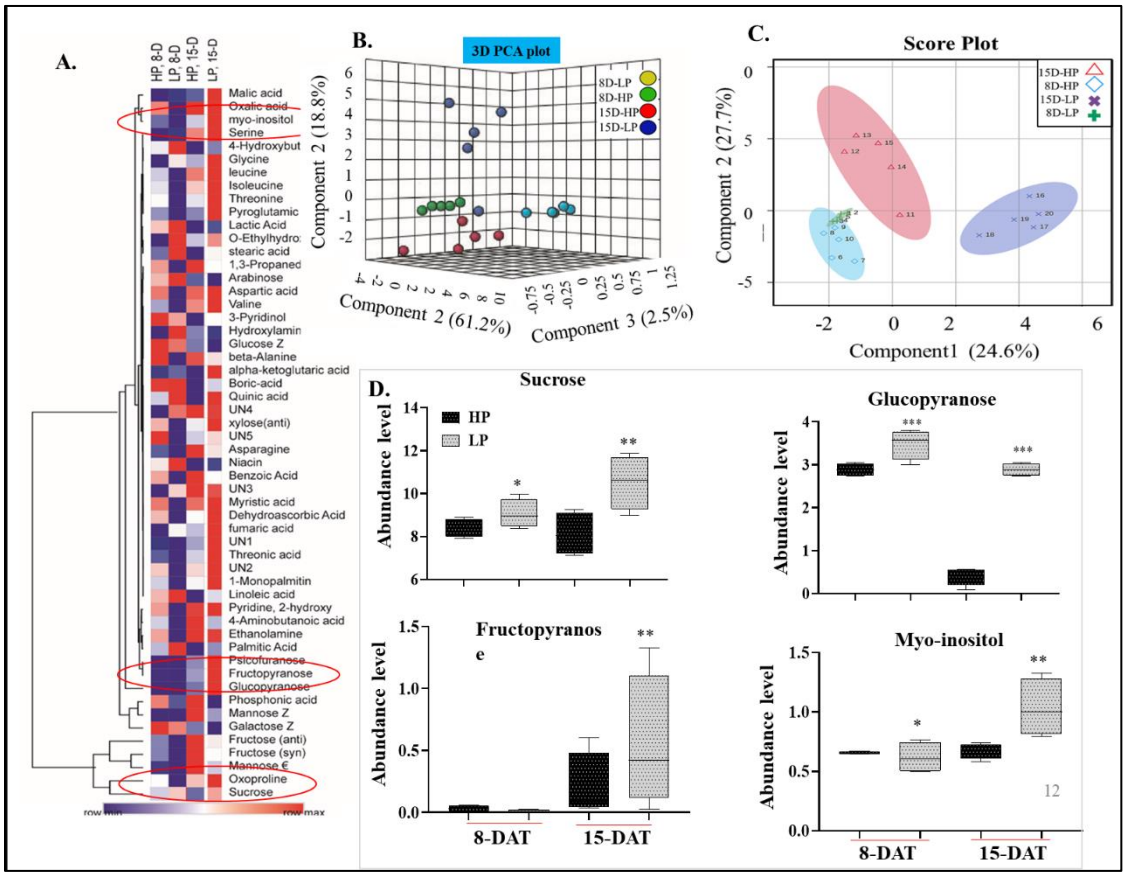

Fig. 12: Metabolite profiling of tomato seedlings grown for 8-D and 15-D under low (LP) and high phosphate (HP) conditions. (A) Heat map of the abundance of metabolome on 8-DAT and 15-DAT LP seedlings. **(B and C)** 3D PCA plot and 2D PCA plot of detected metabolites in both stages of tomato seedlings under LP condition. **(D)** Selected sugar metabolites at both stages on HP/LP condition.

1.4. Sucrose promotes phosphorus starvation response in tomato seedlings

In metabolite profiles, since we observed enrichment of sugars in Pi-deficient seedlings on 8-D and 15-D time points, we next examined the role of sucrose on P starvation response. For this, the germinated seedlings were transferred on HP/LP MS medium with and without sucrose for 8-D/15-D, and again morphometric analyses and end point measurements were performed. From this study, it became clear that the longer primary root length of Pi-deficient (-P+S) seedlings at 8-D/15-D was due to the presence of sucrose in the growth medium, as -P-S seedlings did not exhibit any increase in this root traits and remained similar to the Pi sufficient seedlings **(Fig. 13-A, 14-A and 13-B, 14-B).**

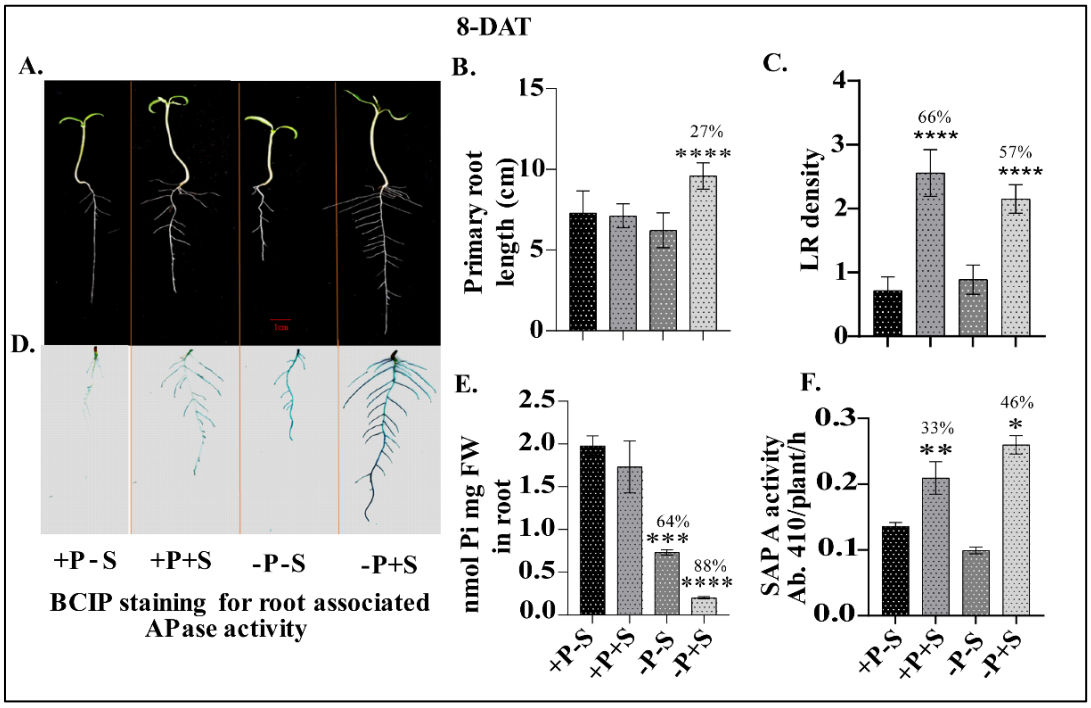

Fig. 13: Physio-biochemical characterization of tomato seedlings grown for 8-D in ½ MS agar media containing HP (1.25 mM) and LP (5 µM) concentration with and without sucrose. (A, B and C) Phenotypes of 8-day-old seedlings, primary root length, lateral root density. **(D, E and F)** BCIP staining for root-associated APase activity, Total soluble phosphate (Pi) and **t**otal carbohydrates content, respectively, at 8-DAT. The experiment was subjected to three independent biological replicates and repeated twice. HP, high phosphate; LP, low phosphate. Bar denotes 1 cm. Unpaired student's t-test was performed for statistical analysis, p-value <0.05=****.

A similar observation was made about increased lateral root number in –P+S seedlings at both time points **(Fig. 13-C and 14-C).** Interestingly, -P+S seedlings exhibited the lowest total soluble

Pi levels, even lower than the –P–S seedlings. Whereas soluble Pi content was significantly decreased by 64 % and 72 % in –P–S seedlings, a more severe reduction (88 % and 79 %) was observed in -P+S seedlings at both time points, respectively, as compared to +P–S or +P+S seedlings **(Fig. 13-E and 14-E).**

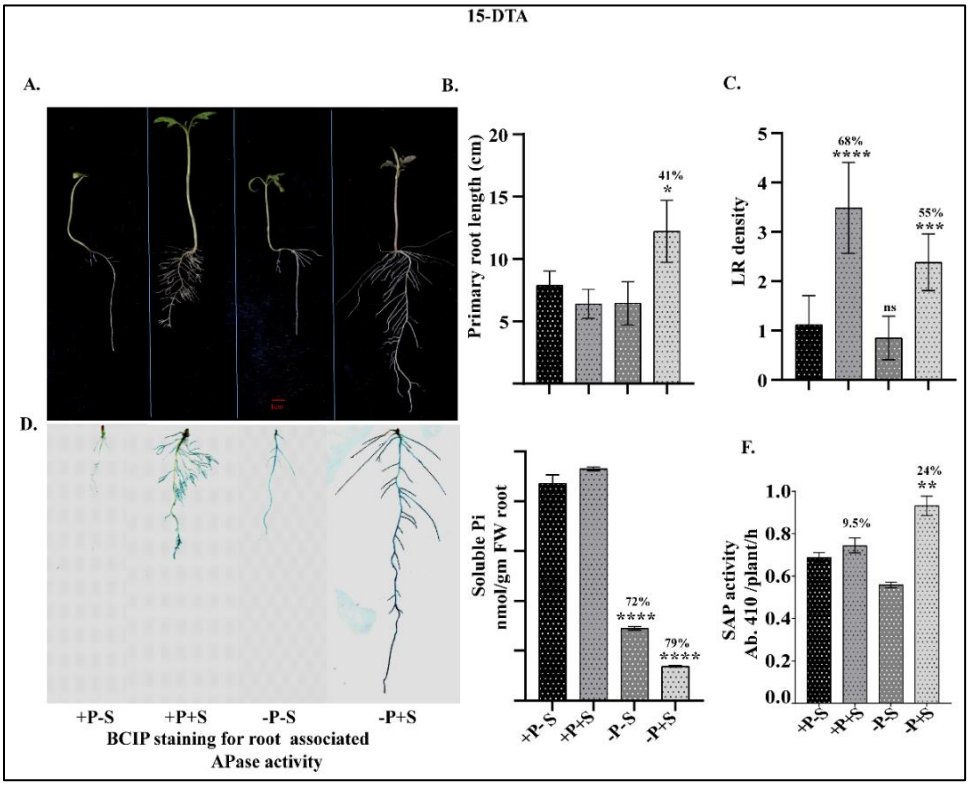

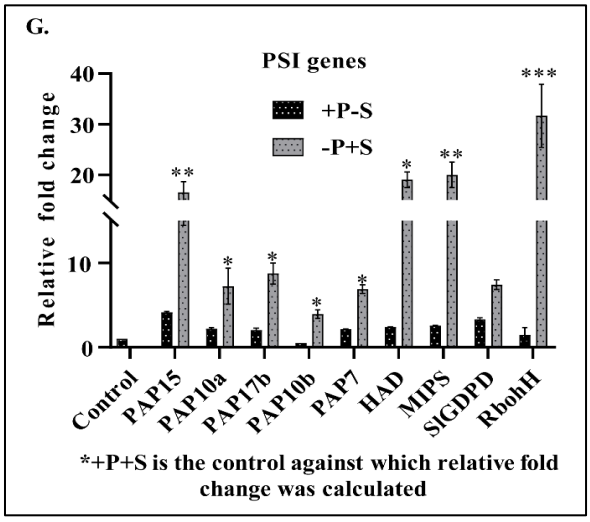

Fig. 14: Physio-biochemical characterization of tomato seedlings grown for 15-D in ½ MS agar media containing HP (1.25mM) and LP (5µM) concentration with and without sucrose. (A, B and C) The phenotype of 15-day-old seedlings, primary root length, lateral roots density.

(D, E and F) BCIP staining for root-associated APase activity, total soluble phosphate (Pi) and total carbohydrates content, respectively, at 15-DAT. **(G)** Expression profiling of the different PSI genes in Pi-deficient seedlings grown with and without sucrose on 15-DAT. HP, high phosphate; LP, low phosphate. HAD= Haloacid acid dehalogenase, MIPS= Myo-inositol-3-phosphate synthase, PAP =Purple acid phosphatases, SlRbohH= Respiratory burst oxidase homolog H. The experiment was subjected to three independent biological replicates and repeated twice. Bar denotes 1 cm. Unpaired student's t-test was performed for statistical analysis, p-value <0.05=****

Next, we noticed higher APase activity and SAP activity in sucrose-supplied +P+S and –P+S seedlings at both time points as compared to +P–S as well –P–S seedlings. Enhanced sugar remobilization from shoot to root is key to reprogramming root system architecture (RSA). Such enhanced carbon repartitioning also increases root-associated secretory acid phosphatase activity (SAP) to improve Pi acquisition efficiency (PAE) in Pi-deficient plants. External sucrose supply was found to promote SAP activity, even under Pi-sufficient conditions at both time points. We next studied the pivotal role of sucrose in PSR by analyzing the transcript profiling of selected PSI genes, including purple acid phosphatases, haloacid dehalogenase, glycerodiester phosphodiesterases, and *SlRbohH*. Our analysis indicated a more robust upregulation of most of these genes in an external supply of sucrose, revealing their sugar-dependent expression of many PSI genes **(Fig. 14-G).**

1.5. Transcriptome study of Pi starved seedlings at 8-D and 15-D time points

Next, we studied transcriptomes of tomato seedlings to identify phosphorous starvation inducible (PSI) genes on a global scale. For this purpose, four RNA sequencing libraries were sequenced on an Illumina HiSeq 4000 platform with 150 bp read length and paired-end sequencing approach. Approximately 30 million high-quality reads (>= 30 Phred score) were obtained for each library, and over 25 million reads each were aligned successfully to the reference tomato genome. An excellent alignment percentage of over 90 % was observed for each library **(Table. 5).** To provide a framework for understanding how tomato genes respond to Pi starvation, we compared mRNA populations from 8-D and 15-D HP-grown seedlings transcriptome with that of 8-D and 15-D LP-grown seedlings, respectively. Genes that were altered by at least 2-fold ($\log_2$=1) at p-value ≤0.05 in their mRNA levels in the DESeq analysis were considered as the differentially expressed genes (DEGs) for respective time points.

Table 5: Summary of RNA-sequencing and reads alignment

Sample	HQ Reads	Aligned Reads	Alignment %	Unaligned Reads
8-D HP	3,14,78,766	2,89,48,356	92	25,30,410
8-D LP	3,75,14,532	3,44,02,110	91.7	31,12,422
15-D HP	2,95,24,532	2,71,77,488	92.1	23,47,044
15-D LP	2,92,86,358	2,68,26,118	91.6	24,60,240

The differential analysis identified 1246 and 1201 transcripts as DEGs at 8-D and 15-D, respectively. Overall, Pi starvation led to the activation of more genes than the down-regulated genes. In comparison to the 669 upregulated transcripts at 8-D, mRNA levels of 922 genes were elevated at 15-D **(Fig. 15-A and B).** In contrast, only 577 and 279 transcripts were down-regulated at the two time-points, respectively **(Fig. 15-A and B).** Next, we focused on the common DEGs at both the time-points. This examination showed that 316 upregulated genes, representing 24.8 % of total upregulated genes, are shared between 8-D and 15-D. Likewise, 84 common DEGs (constituting only 10.9 % of total suppressed genes) were down-regulated at both 8-D and 15-D (**Fig. 15-A and B).**

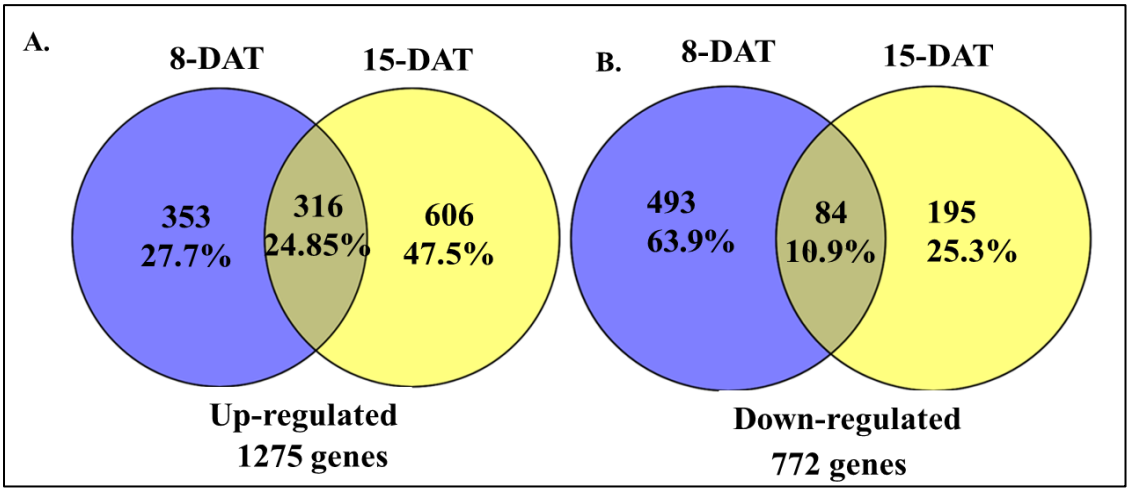

Fig. 15: Venn diagram representing the common as well as unique DEGs at 8-DAT and 15-DAT with LP condition. (A-B) Comparative genomics approach using RNA-seq from 8-DAT and 15-DAT old tomato seedlings grown in low and high P media identified a combined 1275 genes upregulated (FC ≥ 2; p-value ≤ 0.05) and 772 genes down regulated (FC ≥ 2; p-value ≤ 0.05) under low phosphate conditions. A total of 316 genes were found to be commonly upregulated

under low P. On the contrary, only 84 genes were found to be commonly down regulated in both 8-DAT and 15-DAT tomato seedlings.

1.6. Significant biology analysis of the differentially expressed genes

The Gene Ontology (GO) analysis of DEGs identified different categories of genes involved in Pi-starvation responses. Enriched GO categories for biological processes and cellular components are presented in Fig.16. The KEGG pathways analysis revealed an enrichment of several groups, including 'metabolic pathways', 'biosynthesis of secondary metabolites', 'phenylpropanoid biosynthesis', 'glycerolipid metabolism', and amino acid metabolism-related processes at both 8-DAT and 15-DAT **(Fig. 16-A).** A similar analysis of DEGs for their molecular function revealed enrichment of 'metal ion binding', 'heme-binding', 'iron ion binding', 'phosphatase activity', 'oxidoreductase activity', and 'transporter activity', functions at both time points **(Fig. 16-B).** However, the genes with 'hydrolase activity' were enriched only at 15-DAT. Concerning the cellular component category, Pi starvation seemed to affect cytosolic components only at 8-DAT, whereas vacuole and endoplasmic reticulum-related functions were exclusively affected under the long-term phosphate stress at the 15-DAT time point **(Fig. 16-B).** In this analysis, the most common affected cellular components were found to be the extracellular region, cytosol, apoplast, membrane, and cell wall **(Fig. 16-C).**

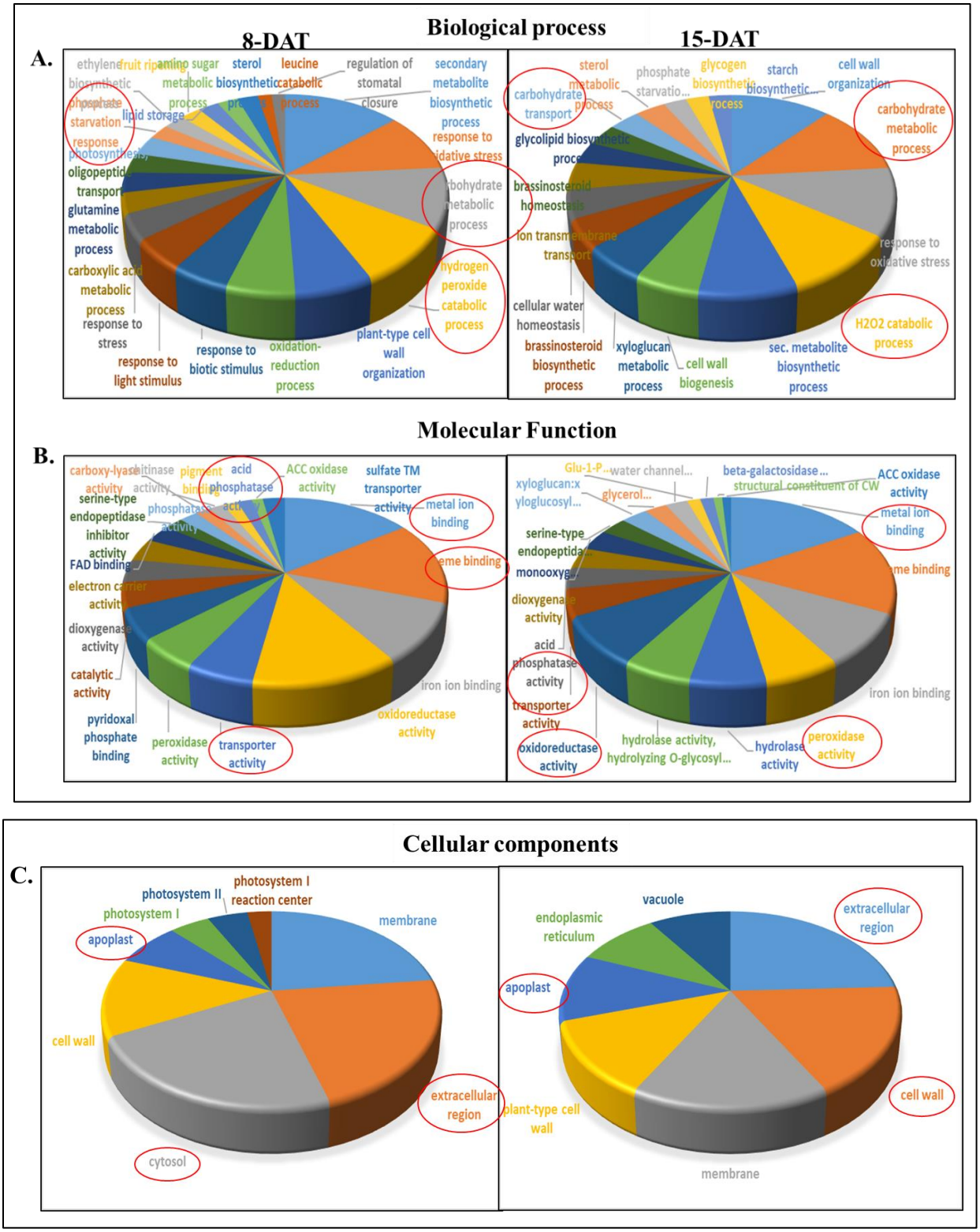

Fig. 16: Significant biology analysis of the differentially expressed genes. (A, B and C) Different biological processes, different molecular functions and different cellular components at 8-DAT and 15-DAT in LP seedlings.

1.7. Pi starvation activates the transcription of several sugar metabolism-related genes, including sugar transporters

Scrutiny of the GO and KEGG pathways revealed differential regulation of many genes which are responsible for sugar metabolism and transporter activity. Therefore, we next studied the transcript accumulation of these two major classes of genes in detail. In total, 17 transcripts involved in sugar metabolism were identified as DEGs, at least at one of the time points. Among these, 10 genes are commonly present in both 8-D and 15-D DEGs lists and published Pfaff et al. (2020) [134]. The majority of these genes are upregulated upon Pi-starvation **(Fig. 17-A).** The most prominent categories among the differentially expressed sugar metabolism genes such as sucrose biosynthetic process, sucrose-phosphate synthase, UDP-glucose metabolic process, UDP-glucose glucosyltransferase, UDP-sugar pyrophosphorylase, starch biosynthesis process, glycogen synthase, 1,4-alfa-glucan branching enzyme II and glucose-6-phosphate 1-epimerase activity are commonly upregulated. UDP-glucose 4-epimerase activity and UDP-glucose 4-epimerase were found to be 8-D specific, whereas glucose-1-phosphate adenylyltransferase, carbonyl reductase 1, glucose dehydrogenase, and UDP-glucose glucosyltransferase were upregulated only at 15-DAT **(Fig. 17-A).** Additionally, nine sugar transporter genes were differentially regulated in Pi-deficient seedlings at both time points. Among these, seven genes, including two genes of carbohydrate transporter, glucose transporter 8, glucose-6-phosphate translocator 2, myoinositol transporter, and glucose-6-phosphate translocator, are commonly upregulated in Pi-deficient seedlings at both the time points, whereas hexose transporter gene and another carbohydrate transporter gene were found to upregulated at only 8-DAT and 15-DAT, respectively **(Fig. 17-B).**

1.7. Genes belonging to glycerolipid remodeling and primary metabolism are also differentially regulated in Pi-deficient seedlings

In the DEGs list, genes belonging to different metabolic pathways and enzymatic activity are predominantly present **(Table 6).** Transcripts belonging to glycerolipid remodeling genes such as Phospholipase D (Solyc01g100020), GDPD2 (Solyc02g094400), and digalactosyldiacylglycerol synthase 2 (Solyc10g017580) are highly activated at both time points under Pi deprivation **(Table 6).** Multiple PEP carboxylase encoding genes such as Solyc04g006970, Solyc07g055060, Solyc04g009900, and Solyc06g053620, and myoinositol-1-phosphate synthase (Solyc04g054740)

are also differentially regulated in Pi-deficient seedlings. Similarly, genes encoding critical bypass enzymes, such as pyrophosphate-dependent phosphofructokinase (Solyc04g014270, and

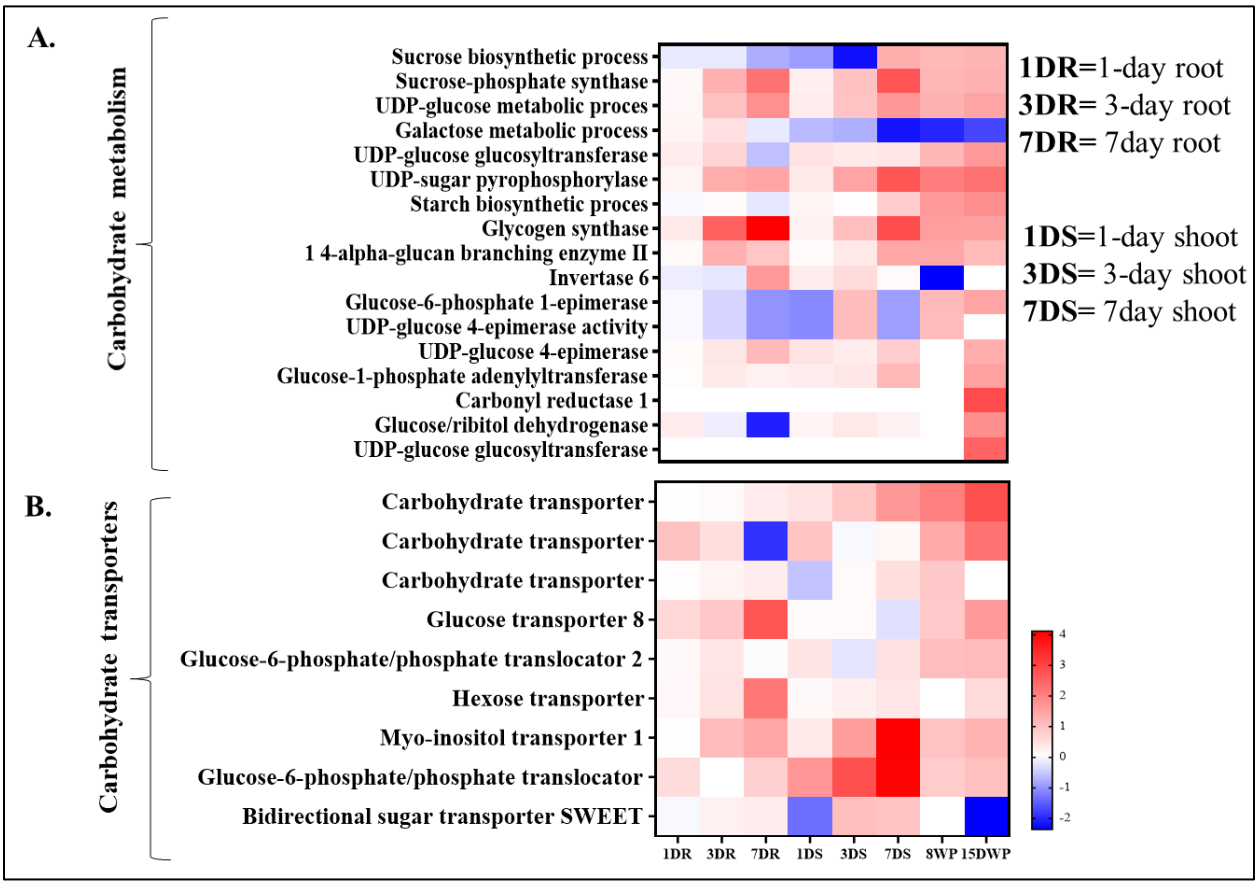

Fig. 17: Transcriptome analysis of carbohydrate metabolism and transporters genes at different stages/tissues in Pi-deficient seedlings. (**A and B)** Expression pattern of different sugar metabolism and transporters related genes at 1-DR and 1-DS, 3-DR and 3-DS, 7-DR and 7-DS, 8-WP and 15-WP seedlings under LP condition. DR=day-old-root, DS= day-old-shoot, WP=whole plants.

(Solyc07g045160), pyruvate phosphate dikinase (Solyc01g080460), and UDP-sugar pyrophosphorylase (Solyc06g051080) of the glycolytic pathway are also induced upon Pi deficiency **(Table 6).**

1.8. Pi starvation causes alterations in the expression of hormone-related and general stress-related genes

Several hormone-related genes belonging to the common DEGs include carotenoid cleavage dioxygenase 8 (Solyc08g066650; strigolactone), AP2-like ethylene-responsive transcription factor

(Solyc02g092050; ethylene), SlERB1B (ethylene), and methyl jasmonate esterase (Solyc02g065280; jasmonic acid) are also differentially expressed in Pi-deficient seedlings **(Table 6).** Pi deficiency is known to affect the expression of many genes controlling reactive oxygen species (ROS) (Mission et al., 2005). Transcripts corresponding to enzymes such as NADPH oxidase, glutathione peroxidase (GPX), and superoxide dismutase are also upregulated at both time points under Pi deprivation **(Table 6).**

1.9. Pi starvation alters the expression of many transcription factors

A manual search for the identification of AtPHR1 homologs revealed the presence of four close members (Solyc06g008200, Solyc09g072830, Solyc05g055940, and Solyc04g050070) in tomato. Among these, Solyc04g050070 encoded transcripts could not be detected in the complete RNA-seq data. The most prominent categories in this set of genes belonged to 'MYB', 'AP2/ERF', 'Zinc finger family', and basic helix-loop-helix (bHLH). To narrow down the list of putative candidate genes, we further focused on the TFs present in the common list of DEGs. This analysis retrieved 26 TFs with differential mRNA accumulation at both time points **(Fig. 18).** Some of the important differentially regulated MYB TFs included in the list are Solyc05g055030 (SlMYB10, down-regulated), Solyc06g083900 (SlMYB13, up-regulated), Solyc10g086250 (SlMYB90, up-regulated), Solyc10g086270 (SlMYB113, up-regulated). Similarly, transcripts of Solyc04g014530 (SlERB.1B), SlbHLH136 (Solyc06g062460), SlbHLH066 (Solyc10g079650), and Solyc08g067340 (SlWRKY46) are upregulated at both time points (**Fig. 18).**

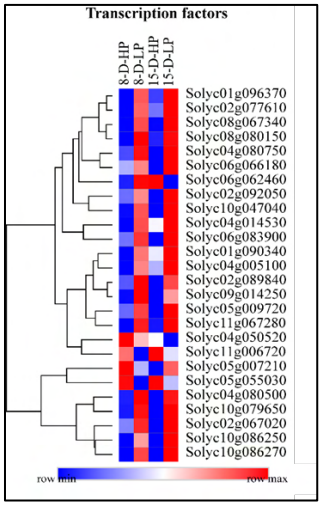

Fig. 18: Expression pattern of differentially expressed transcription factors in Pi-deficient tomato seedlings. Heat map was created on Log2 FC values using Morpheus online tool.

1.10. Validation of transcriptome data by qPCR using 8-D and 15-D LP-grown seedlings

qPCR was used to verify the accuracy of RNA-sequencing data and the credibility of the identified DEGs. For this purpose, we selected 18 genes belonging to various categories such as "phosphatase', 'transporter', 'transcription factor and gene regulation', 'enzymatic activity' and 'lipid remodeling'. In this analysis, we profiled genes that showed up-regulation of transcript levels or remained unaltered under Pi-starvation in the RNA-seq data. The log_2 fold change values obtained for each gene in the two datasets were plotted against each other. This analysis was done separately for the two time-points taken in the study. A good correlation was observed between the RNA-sequencing and qPCR data, as at least 14 genes each exhibited similar trends in both datasets at 8-D and 15-D **(Fig. 20).** Most upregulated genes showed a matching trend in the two datasets. Albeit, the degree of up-regulation in the two datasets varied. Only transcripts encoded by Solyc08g007800 showed opposite profiles in RNA-seq and qPCR at both time-points. The transcript levels of the genes unaffected by Pi starvation showed little variations in the two data sets and did not change much. Overall, this analysis supported the differential gene analysis results observed in our RNA-sequencing data.

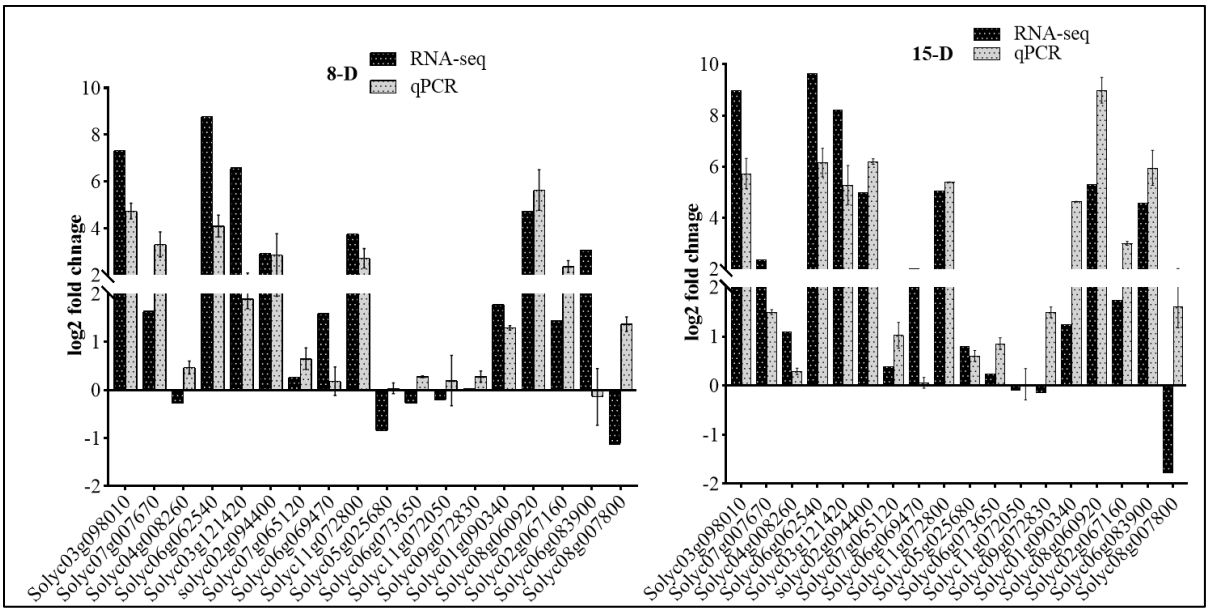

Fig. 19: Validation of RNA-seq results by the qPCR approach of selected candidate genes. (A-B) 8-DAT and 15-DAT, respectively, under low phosphate conditions. *GAPDH* was used as an internal control.

1.11. Pi starvation leads to enhanced manganese and zinc levels in tomato seedlings

In the DEGs list, we observed that many metal transport-related genes are differentially regulated in our transcriptome data as well as those published by Pfaff et al. (2020) [134]. Out of ten metal transport-related genes, eight encoded metal transporters, including iron transporter, molybdate transporter, zinc transporter, potassium transporter, myo-inositol transporter, sulfate transporter, phosphate transporter, and peptides transporter, are commonly upregulated in 8-DAT and 15-DAT LP seedlings. In contrast, a copper transporter and an amino acid transporter gene are down regulated at both time points **(Fig 20-A).** Inorganic elements and basic earth metals like K, Na, Mg, and Ca transition metals e.g., Mn, Co, Fe, Cu, and Zn, which are very important for the many biological functions in the cellular context. Many of these elements influence cell signaling, maintain protein structure and regulate many enzymes catalytic centers. Carbohydrate metabolism and transport were also significantly affected in the Pi-deficient seedlings. Following the upregulation of several metal transporters, ICP-MS analysis further confirmed elevated levels of Zn and Mn in both root and shoot tissues. At the same time, Fe accumulation exhibited opposite profiles in the two tissues, higher in shoots but lower in root tissues of Pi-deficient seedlings at the 15-DAT time point **(Fig. 20-B).**

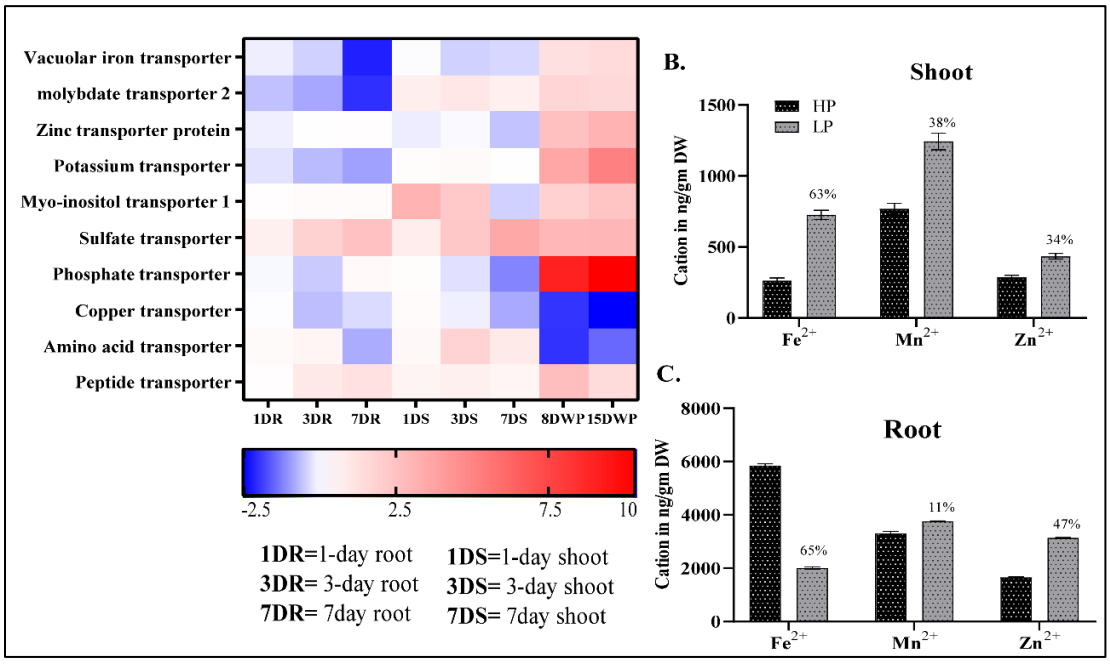

Fig. 20: (A) Transcript profiles of important metal transporters related genes in-house and published transcriptome data by Pfaff et al. (2020) [134]. **(B and C)** ICP-MS analysis of shoot and root tissues Pi-deficient seedlings for the content of the metals at 15-DAT.

Altogether, we profiled tomato seedlings' response to prolonged Pi deficiency and found an important role of sucrose in influencing the amplitude of PSR in Pi-deficient seedlings. These seedlings were found to reprogram their RSA and alter their transcriptome to activate PSI genes as PSR.

1.11. Summary

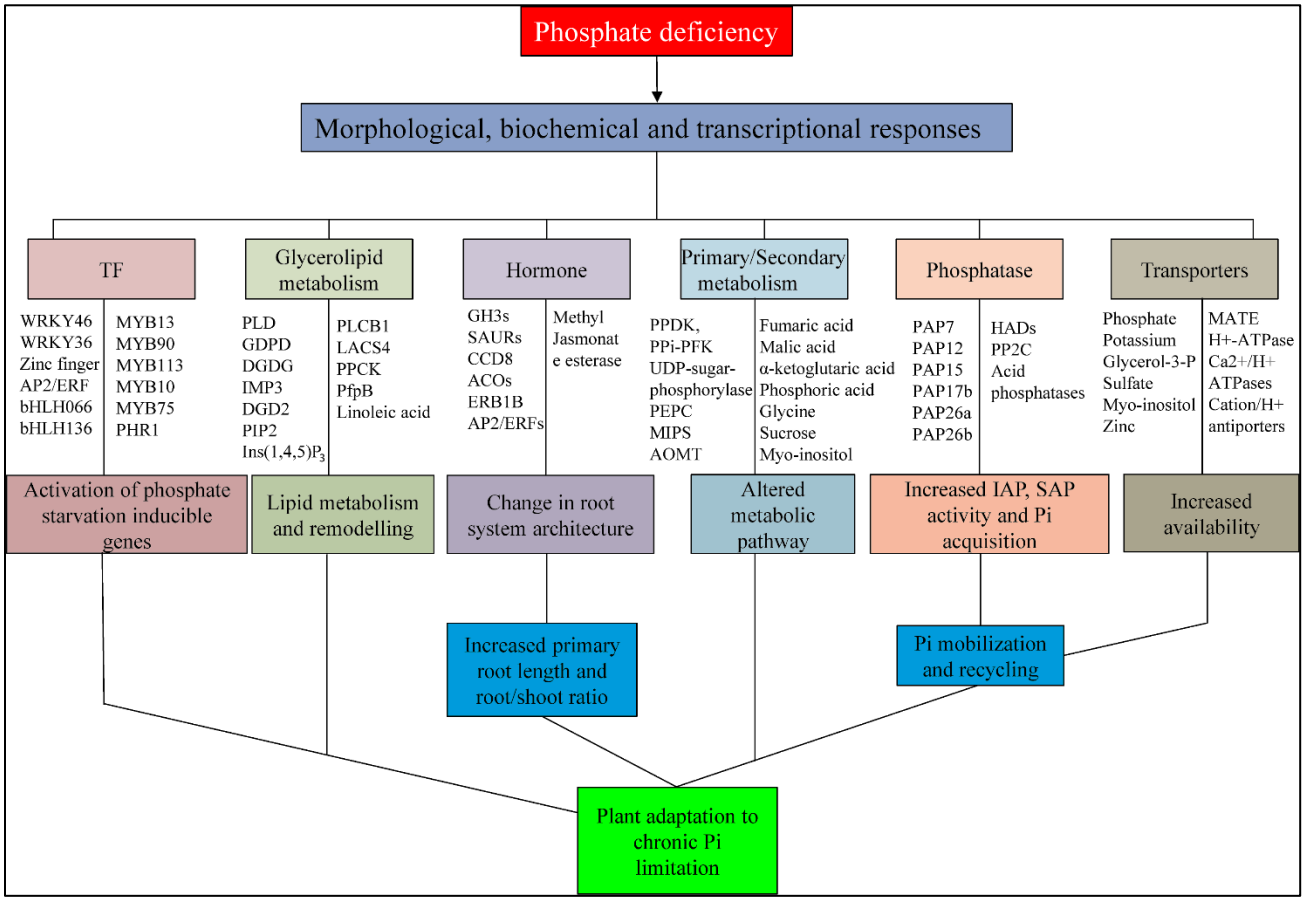

Fig. 21: Summary of differentially expressed genes in tomato seedlings under Pi starvation. Upon its deficiency, Pi-deficient seedlings deploy a battery of transcription factors belonging to various groups to control the expression of genes belonging to lipid remodeling, altered root structure, Pi-dependent metabolic pathways, Pi transporters and acid phosphatases. The induction of PSI genes leads to the activation of Pi starvation adaptive mechanisms, such as modified RSA for better root surface area or mechanisms promoting better Pi uptake or its internal recycling to combat chronic Pi unavailability.

Objective-2

To understand the effect of reactive oxygen species and functional elucidation of a Respiratory burst oxidase homolog *SlRbohH* gene on phosphorus starvation response in tomato seedlings.

2.1 ROS levels and NADPH oxidase activity are enhanced in shoot and root tissues of Pi-deficient seedlings.

ROS is important for pathogenesis and plant growth and development. ROS levels were higher in K^+, Na^+, and Pi-limited plant roots [158, 316]. In this study, NBT and DAB staining and subsequent quantification analysis showed an enhanced level of O_2^- and H_2O_2 in leaves and root tissues of Pi-deficient plants compared to their Pi-sufficient counterparts at both 8-D and 15-DAT time points. Between the two time points, 15-DAT Pi-deficient seedlings accumulated even higher ROS levels than 8-DAT Pi-deficient seedlings **(Fig. 22-A, B and C).**

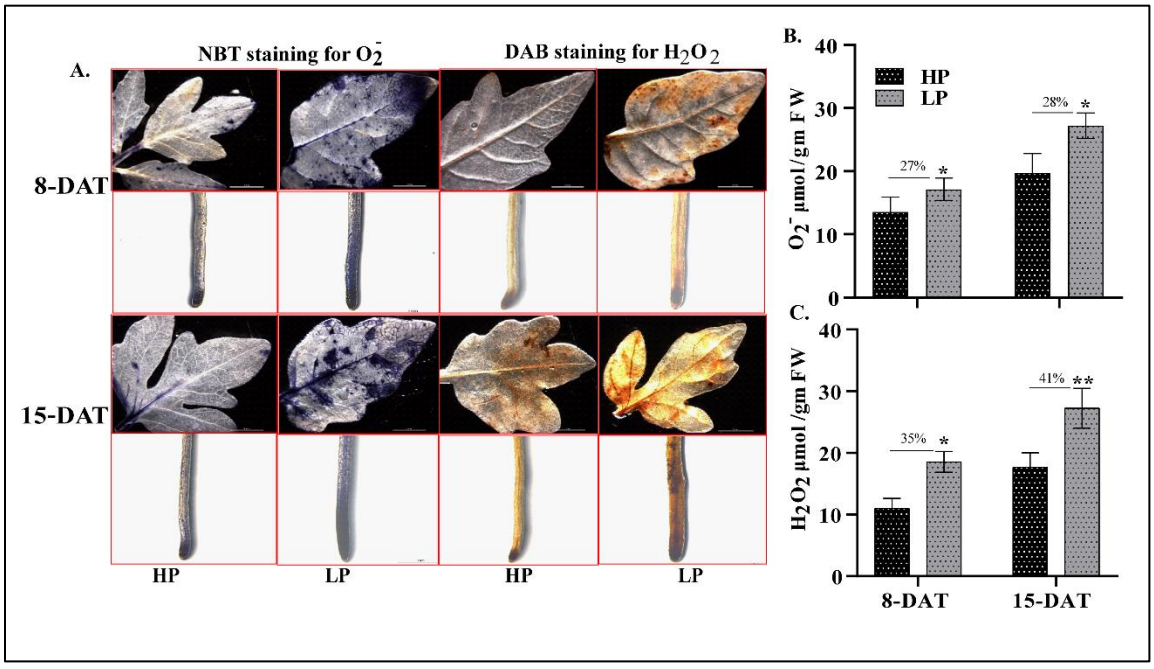

Fig. 22: ROS levels in tomato seedlings under HP and LP conditions. (A) Histochemical staining of leaves and roots with NBT and DAB staining for O^{2-} and H_2O_2 detection. (B and C) Spectrophotometer-based quantification of O^{2-} and H_2O_2 at 8-DAT and 15-DAT, respectively, in Pi-deficient seedlings. The error bar show the standard deviation. Two-way INOVA was performed for statistical analysis, and **** represents P-value <0.05

Further, H2DCFDA staining of the roots of LP-grown seedlings and subsequent live imaging confocal microscopy showed higher fluorescence in Pi-deficient roots validating the higher ROS levels in Pi-deficient seedlings at 8-D and 15-D time points **(Fig. 23-A)**. Further examination of the apoplastic ROS responsive NADPH oxidase enzyme activity from shoot/root crude membrane proteins confirmed the enhanced NADPH oxidase activity in Pi deficient seedlings than their control counter parts at both time points. However, we could not establish a significant difference in shoot NADPH oxidase activity at 8-D in Pi-deficient seedlings **(Fig. 23-B).** In contrast, root tissues showed significantly increased NADPH oxidase activity at 8-D and 15-D seedlings under low Pi conditions **(Fig. 23-C).**

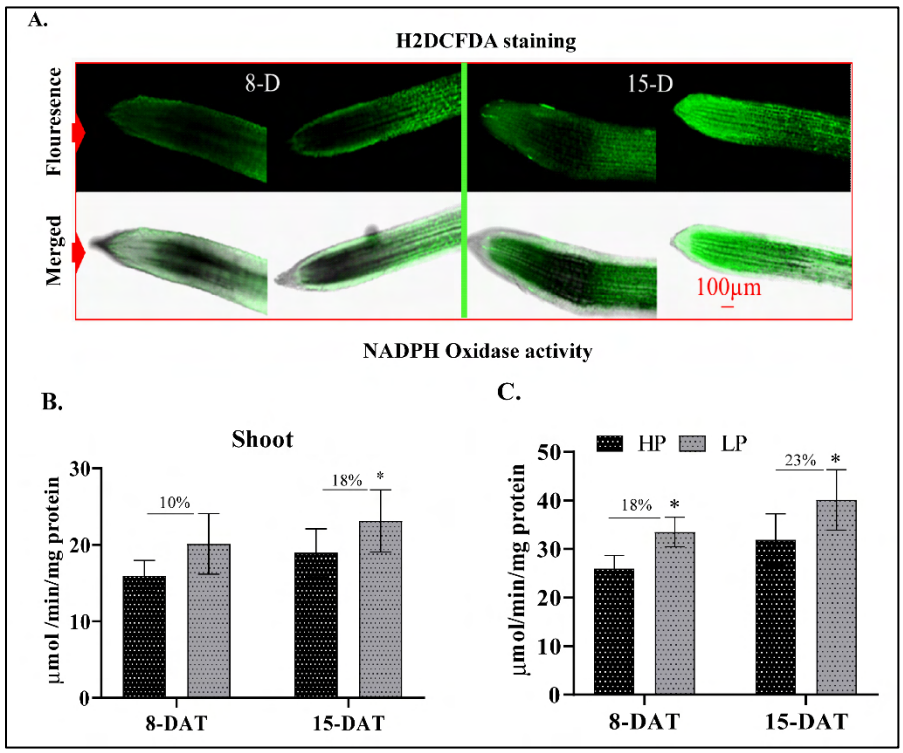

Fig. 23: (A) Histochemical staining of 8-D and 15-D HP/LP roots with H2DCFDA dye for H_2O_2 visualization. **(B and C)** NADPH oxidase activity in the shoot and root of HP/LP seedlings at both stages. The error bar shows the standard deviation. Two-way INOVA was performed for statistical analysis and **** represents P-value <0.05.

2.2. External supply of NADPH oxidase inhibitor diphenyleneiodonium (DPI) and ROS donor H_2O_2 influence Pi levels in tomato seedlings

To understand how enhanced ROS affect RSA and PSR under LP conditions, we first used DPI, an NADPH oxidase inhibitor, to check the effect of inhibited ROS on plants' growth and Pi accumulation. First, we treated 4-day-old hydroponically grown seedlings with three different concentrations (10nM, 100nM and 500nM) of DPI for 8 days. DPI treatment was found to cause a significant reduction in plant growth, including primary root length in all the treated groups of seedlings as compared to control buffer-treated seedlings **(Fig. 24-A and B).** We observed that H_2O_2 content was gradually decreased with increased concentration of DPI in the treated seedlings with respect to control **(Fig. 24-C).**

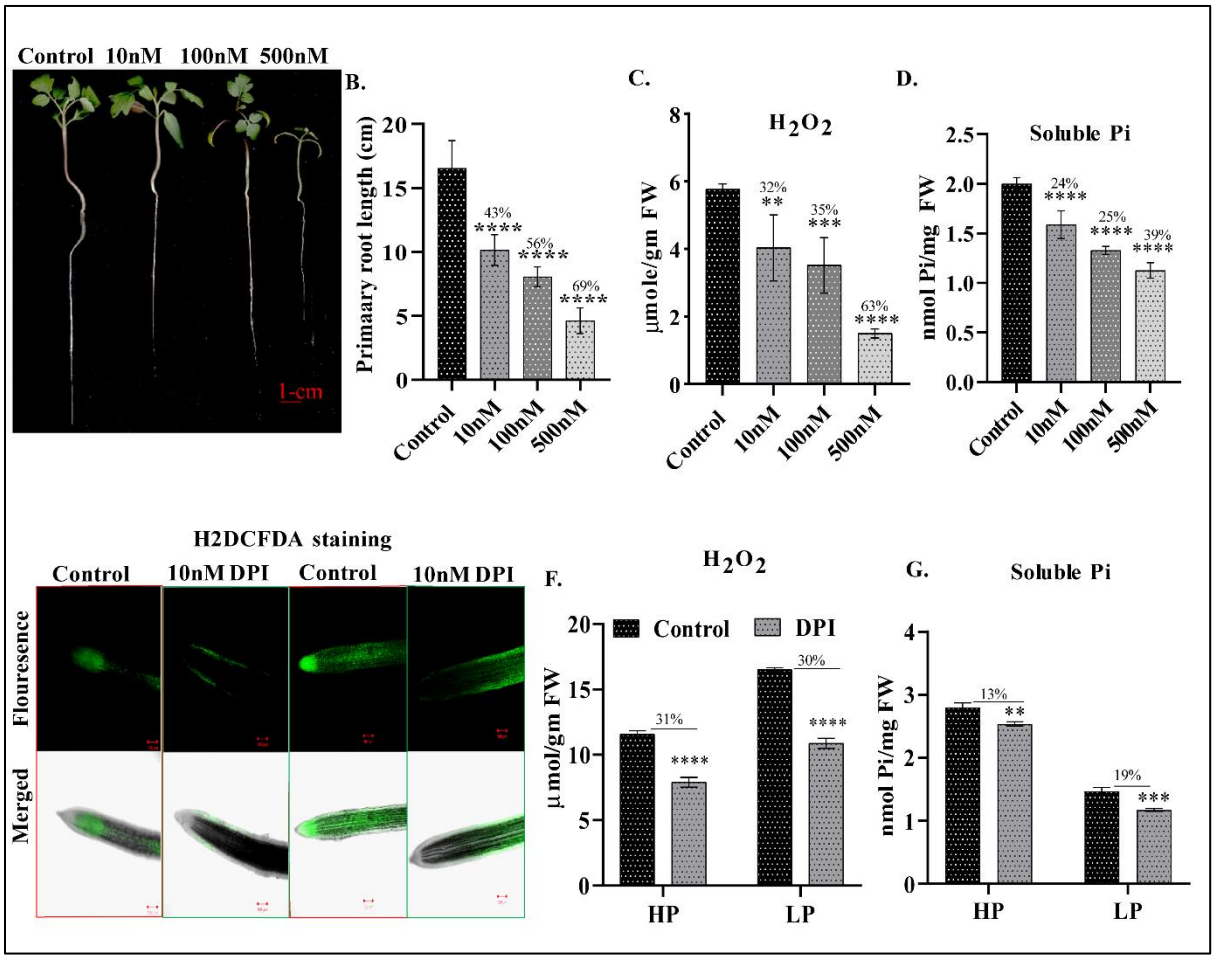

Fig 24. Effect of NADPH oxidase inhibitor diphenyleneiodonium (DPI) treatment on tomato seedlings. (A and B) Images of 10-day-old seedlings and primary root length of DPI-treated seedlings, respectively. **(C and D)** H_2O_2 accumulation and total soluble Pi content in DPI treated seedlings. **(E, F and G)** H2DCFDA staining for H_2O_2 detection, quantification of H_2O_2 and soluble Pi

level in HP/LP seedlings with and without 10nM DPI treatment, respectively. The error bar shows standard deviation. An unpaired t-test was performed. For statistical analysis. **** represents P-value <0.05.

Interestingly, soluble Pi content was also found to follow the same trend as that of H_2O_2 with increasing DPI concentrations **(Fig. 24-D).** We performed subsequent experiments with 10nM DPI concentration and found lower H_2O_2 accumulation, as evident by lower fluorescence of H2DCFDA observed in these treated roots **(Fig. 24-E)**. Further spectrophotometric quantification also suggested a drop in the level of H_2O_2 by 31 % in HP and 30 % in LP-grown seedlings with respect to their respective buffer-treated control seedlings **(Fig. 24-F).** Interestingly, total soluble Pi content also significantly decreased by 13 % in HP and 19 % in LP-treated seedlings compared to their respective control **(Fig. 24-G).**

Next, we examined the effect of exogenously supplied H_2O_2 on seedlings grown under LP conditions. First, we performed a dosage experiment where different concentrations of H_2O_2 (100, 200, 400, 600, 800 and 1000µM) were used for treating the 4-day-old tomato seedlings, which were then allowed to grow for the next eight days. As anticipated, we obtained the opposite results in H_2O_2-treated seedlings compared to DPI-treated seedlings.

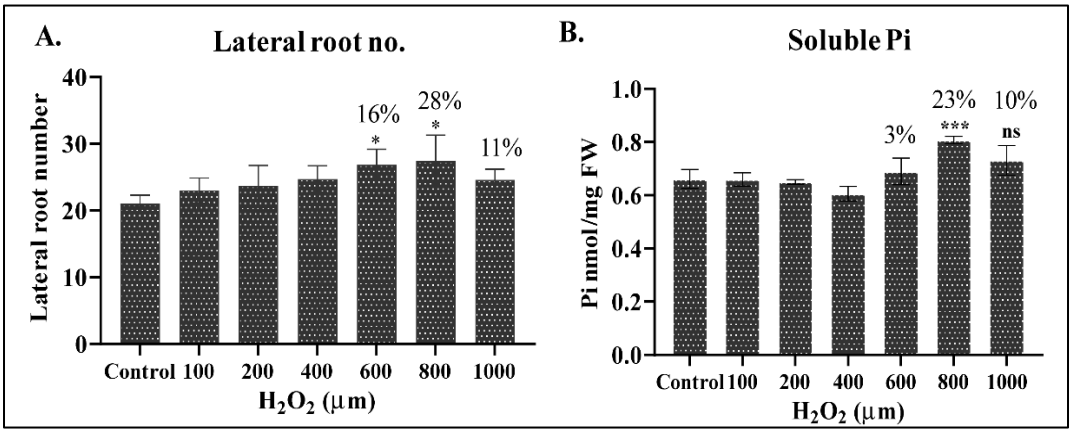

Fig. 25: Exogenous H_2O_2 treatment to tomato seedlings under LP conditions. (A and B) Lateral root number and total soluble Pi content at different concentrations of H_2O_2 treated seedlings, respectively.

The H_2O_2 treated seedlings showed growth promotion with higher lateral root numbers, which increased (16 % at 600µM, 28 % at 800µM and 11 % at 1000µM) in H_2O_2 treated seedlings as compared to control on the 8th day **(Fig. 25-A).** The total soluble Pi content also increased (3 % at 600µM, 23 % at 800µM and 10 % at 1000µM) in H_2O_2-treated seedlings compared to their control counterparts **(Fig. 25-B).**

Given the most optimum growth promotion, 800 µM H_2O_2 was further used to treat Pi-sufficient and Pi-deficient seedlings for eight days. The treated Pi-sufficient and Pi-deficient seedlings showed 23 % and 24 % increases in primary root length and 28 % and 35 % increases in lateral root number, respectively, as compared to buffer-treated control seedlings **(Fig. 26-A, B, C and D).**

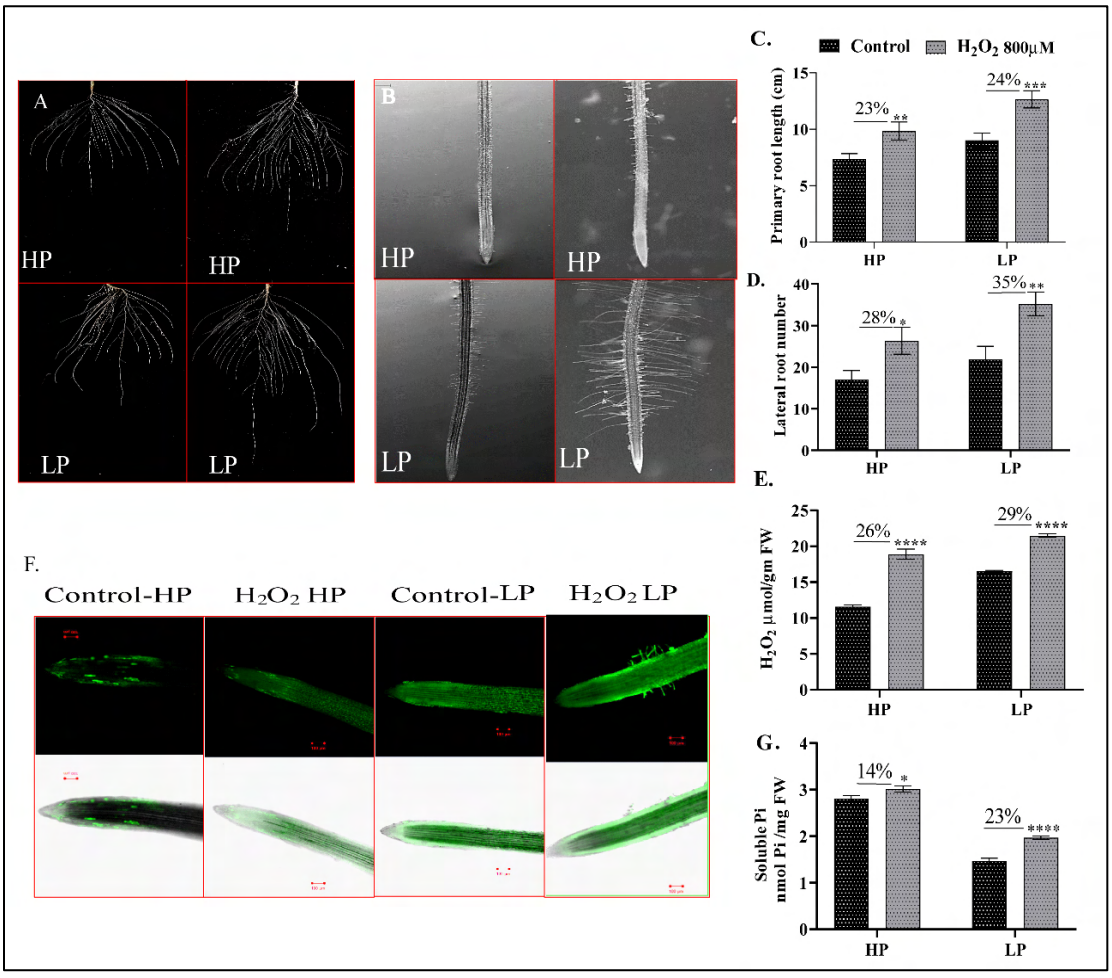

Fig. 26: Effect of H_2O_2 treatment on tomato seedlings under HP/LP conditions. (A-C and D) Primary root length and lateral root numbers in HP/LP seedlings with and without 800µM H_2O_2.

(E and F) Quantification of H_2O_2 and H2DCFDA staining for H_2O_2 detection by confocal microscopy. **(G)** Total soluble Pi levels in HP/LP seedlings with and without 800µM H_2O_2, respectively. Unpaired Two-way ANOVA was performed. For statistical analysis. **** represents P-value <0.05.

The treated Pi-sufficient and Pi-deficient seedlings also exhibited more root hairs with increased length with respect to control seedlings. As expected, 800 µM H_2O_2 supplied seedlings exhibited higher H_2O_2 accumulation, which increased by 26 % in Pi-sufficient and 29 % in Pi-deficient seedlings compared to their respective control seedlings **(Fig 26-E and F).** The enhanced ROS accumulation was further validated by H2DCFDA histochemical staining, followed by spectrophotometric-based quantification of H_2O_2. As observed earlier, the Pi levels increased by 14 % in Pi-sufficient and 23 % in Pi-deficient seedlings compared to their respective controls **(Fig. 27-G).** Altogether, the experiments revealed that ROS levels influence Pi accumulation or acquisition in low Pi-grown tomato seedlings.

2.3. Eight SlRboh genes are present in the tomato genome

NADPH oxidases (NOX or Rboh) genes are enzymes involved in ROS production in plants. We also observed an enhanced NADPH oxidase activity in Pi-deficient seedlings. Gene identification analysis identified eight SlRboh members in tomato. Analysis of RNA sequencing data shows that seven genes, including *SlRbohA, B, C, E, F, G,* and *H* are preferentially expressed in roots. *SlRbohD* was found to be a fruit-preferential NADPH oxidase **(Fig. 27-A).** Investigations on their expression profiling under Pi deficiency revealed upregulation of *SlRbohB, SlRbohD, SlRbohF,* and *SlRbohH* in roots of Pi deficient seedlings. Among all, *SlRbohH* remained the only gene with increased mRNA abundance in shoot and root tissues under Pi-starved conditions at both 8- and 15-days **(Fig. 27-B)**. The upregulation of *SlRbohH* gene was also validated by qPCR analysis, projecting it as one of the important potential candidates to be checked for its role during PSR in tomato seedlings **(Fig. 19)**.

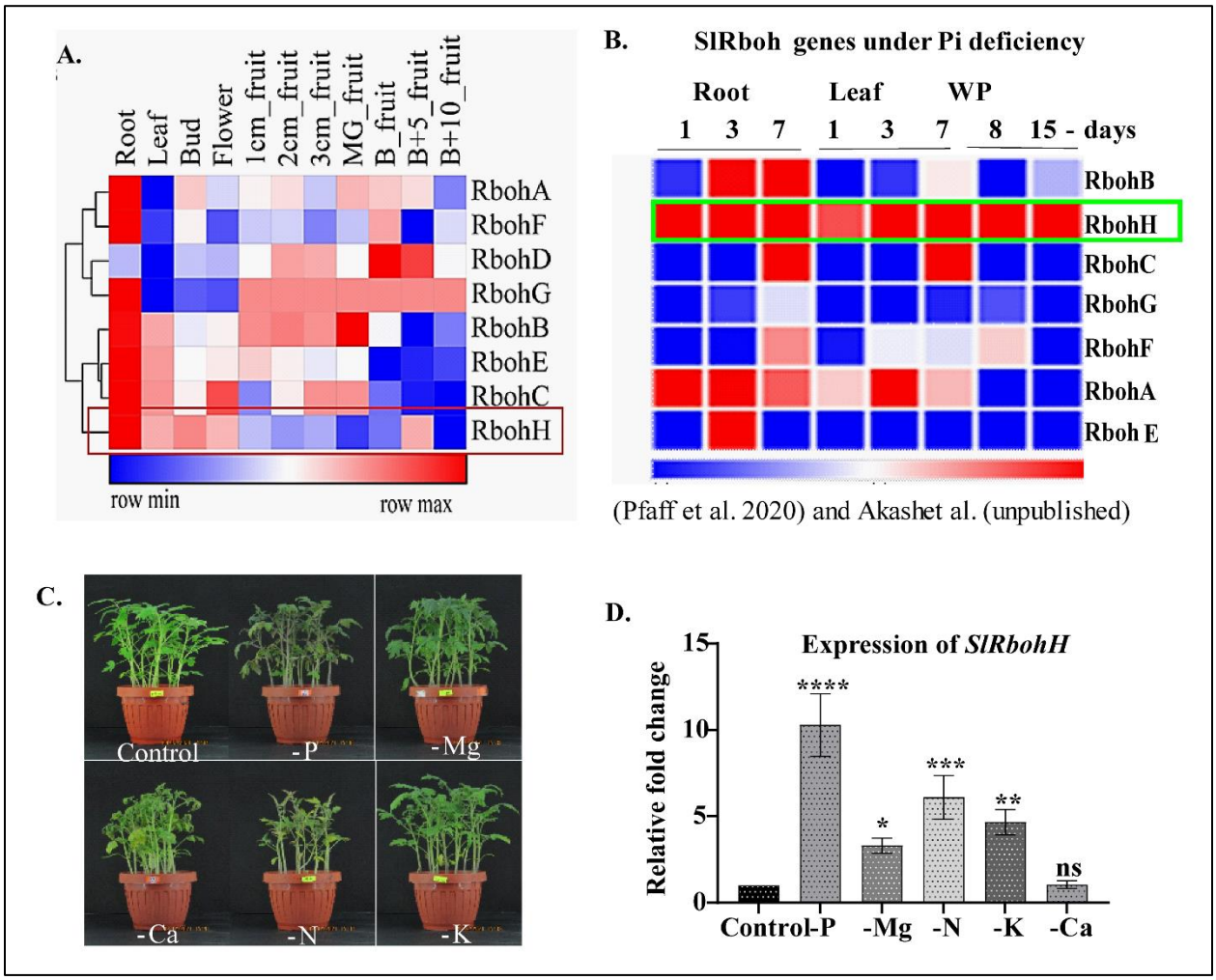

Fig 27. Expression profiling of Rboh genes. (A) Heat map representation of eight Rbohs genes at different development stages in tomato (TGC, 2012). **(B)** Transcriptome analysis of Rboh genes under Pi starvation. 1, 3, 7, 8, and 15-day-old seedlings, WP= whole plant. (MG= Mature green, B-Breaker). **(C and D)** Expression profile of a selected *SlRbohH* candidate gene in different minerals stresses. -P= without phosphate, -Mg= without magnesium, -Ca= without calcium, -N=without nitrogen and –K= without potassium. Error bar shows standard deviation. Two-way INOVA was performed for statistical analysis and **** represents P-value <0.05

Next, *SlRbohH* showed a higher expression pattern in roots as compared to other tissues by using *Multi-Plant eFP Browser 2.0 – BAR tool* (http://bar.utoronto.ca/efp2/) and In house qPCR data of different development stages of tomato cDNA **(Fig. 28-A and B).** We also checked the kinetics of the *SlRbohH* mRNA accumulation at different time points of Pi starvation and Pi recovery. The

resulting data showed significant upregulation of *SlRbohH* on 7-DAT and 15-DAT after Pi starvation. During the recovery experiment, ~ 95 % of the transcripts declined within 15 min of Pi recovery **(Fig. 28-C)**. Further, this gene was found to be upregulated by external sucrose supply low Pi condition **(Fig. 28-D).** Altogether, *SlRbohH* appears to be a late-responsive gene of Pi starvation.

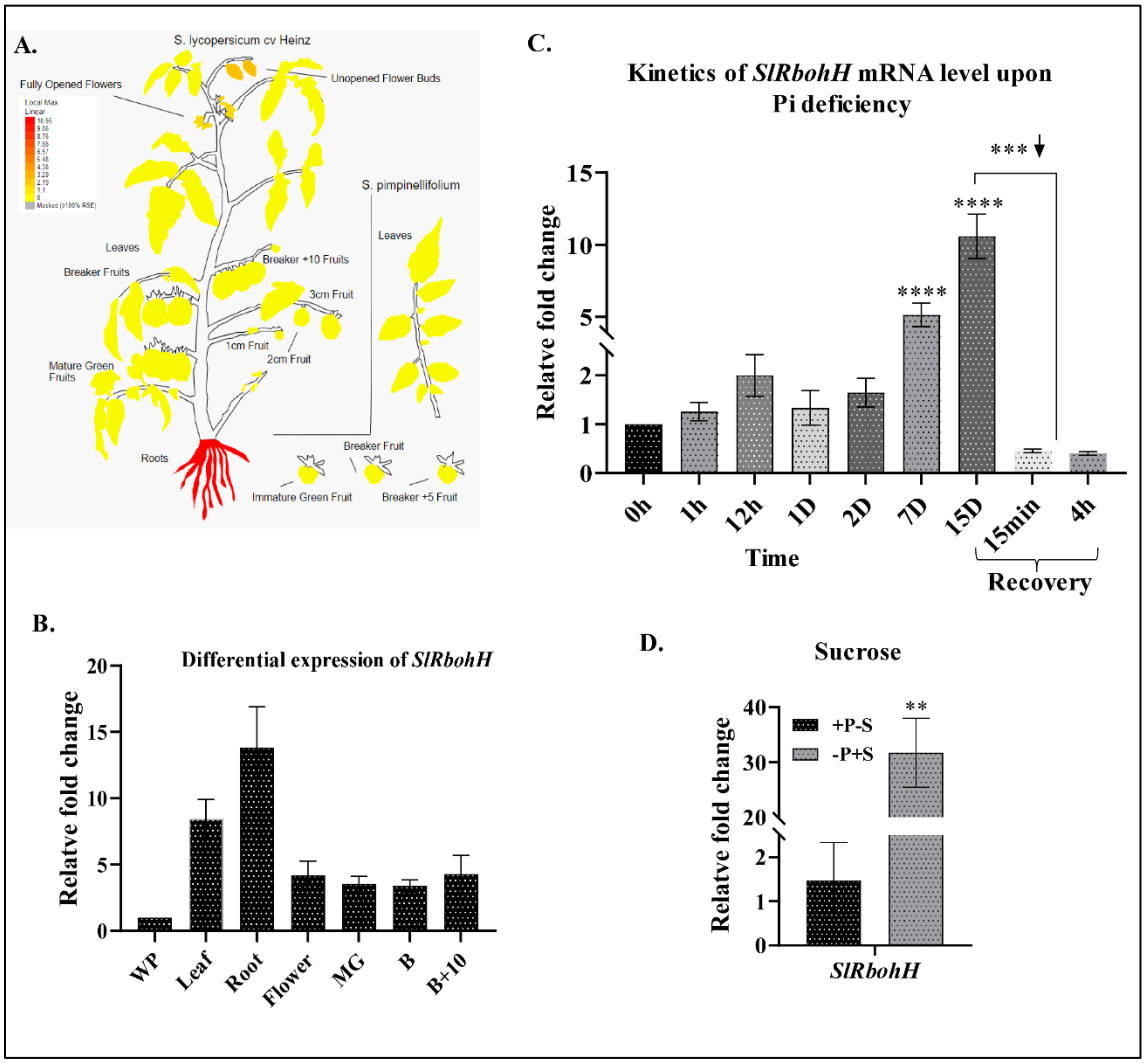

Fig. 28: Expression dynamics of *SlRbohH* gene. (A and B) Expression profile of *SlRbohH* during tomato growth and development. **(C)** Kinetics of its mRNA accumulation upon Pi deficiency/Pi recovery. **(D)** The expression level of *SlRbohH* upon low Pi with and without sucrose supply. Unpaired Two-way ANOVA was performed. For statistical analysis. **** represents P-value <0.05.

2.4. Characterization of pSlRbohH::GUS transcriptional reporter stable Arabidopsis lines

After confirming the PSI nature of the *SlRbohH* gene, we cloned its 1-kb upstream promoter sequence, harboring two P1BS elements, in the pCAMBIA1391Z vector **(Fig. 29-A, B and C)** and generated the stable transcriptional reporter lines deriving the expression of *gus* (pSlRbohH::GUS) in *Arabidopsis thaliana* Col-0 background **(Fig. 30-A).**

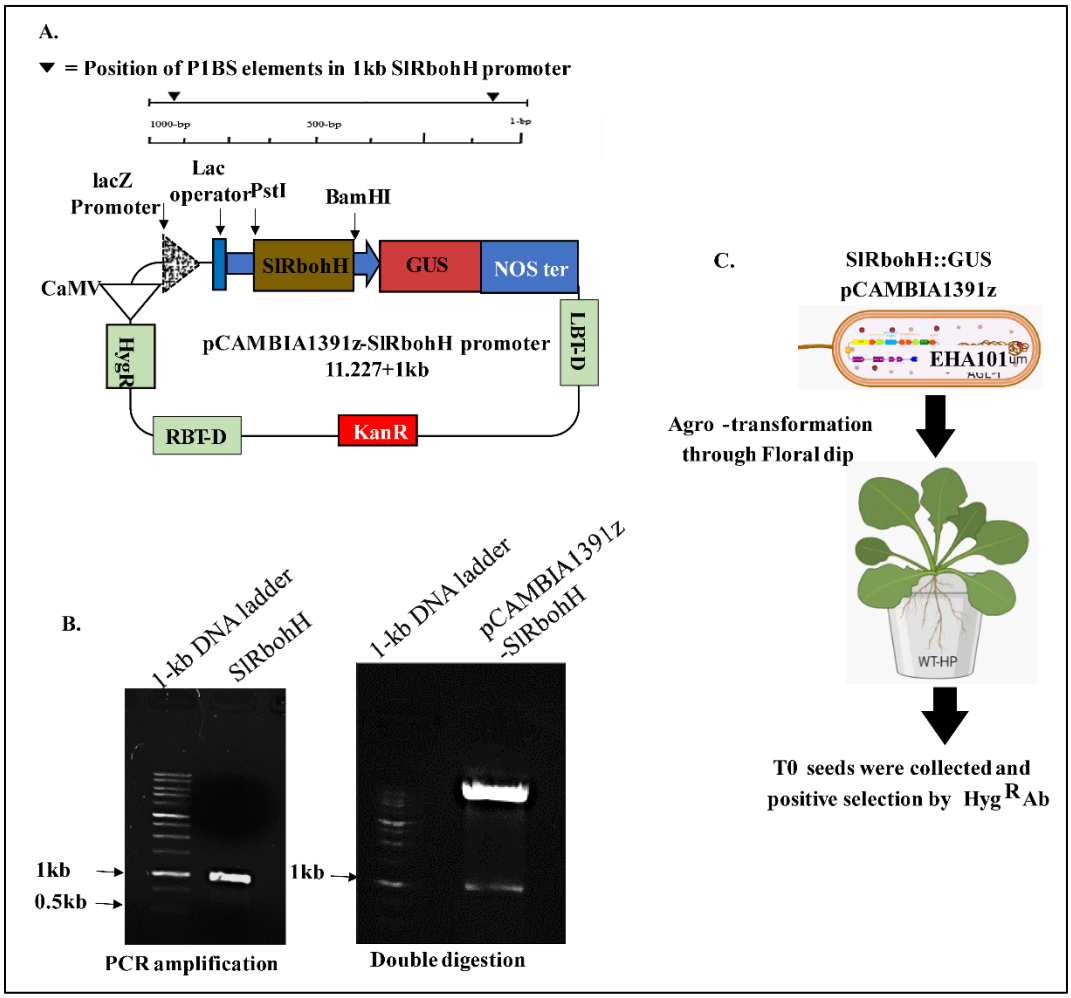

Fig. 29: Cloning of *SlRbohH* promoter in pCAMBIA1391Z:GUS binary vector. (A) Schematic diagram of 1-kb promoter with P1BS elements. **(B)** Amplification of *SlRbohH* promoter fragment and confirmation of cloning by double digestion with respective restriction enzymes (XbaI and SacI). **(C)** Agro-transformation of Arabidopsis plants with pCAMBIA1391Z:pSlRbohH:GUS vector through Floral dip methods.

The root preferential mRNA abundance of *SlRbohH* was further confirmed by analyzing its promoter activity using GUS histochemical staining. The activity was found to be more in roots than

shoot tissue in the pSlRbohH::GUS transcriptional reporter Arabidopsis lines. Since this promoter harbored two P1BS elements, and its transcript levels were induced in Pi-deficient seedlings, more intense GUS staining of the roots of these lines under Pi deficiency supported the gene expression data. It confirmed the PSI nature of this promoter. **(Fig. 30-B).**

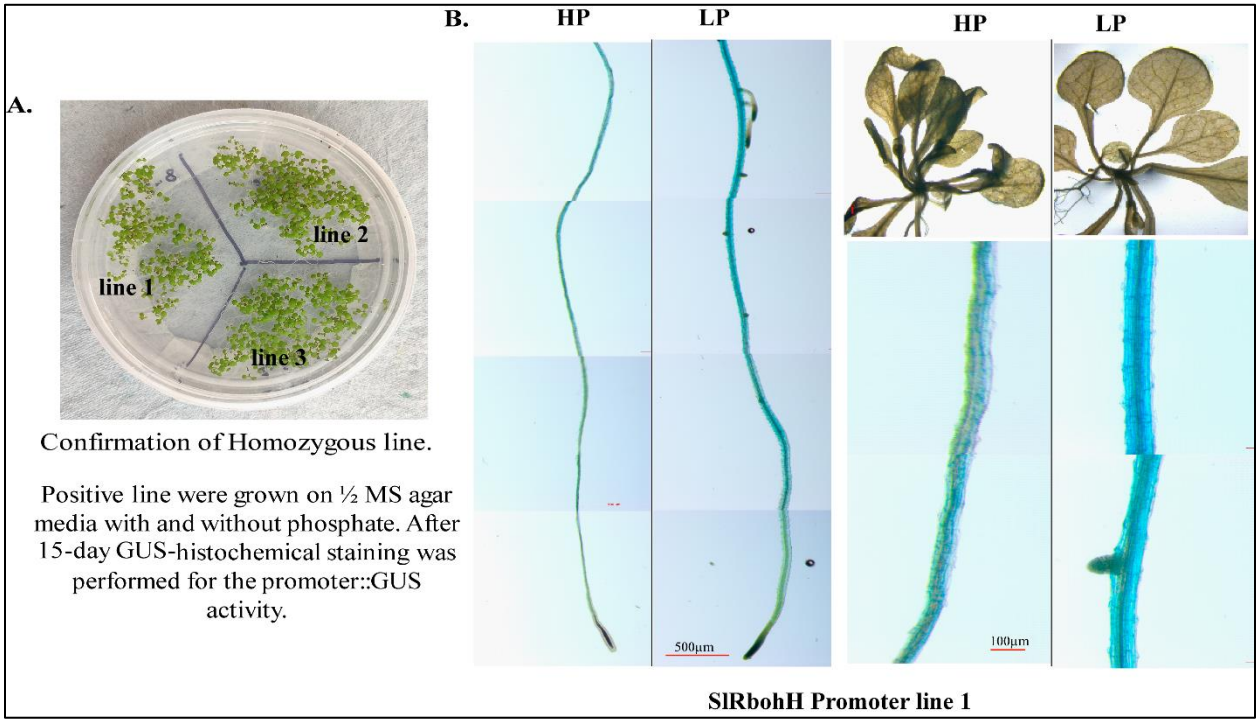

Fig. 30: Promoter activity in the stable *SlRbohH:GUS* promoter line. (A) Homozygous stable *SlRbohH:GUS* promoter lines on the selection medium supplemented with hygromycin antibiotics (15 µg/ml). **(B)** *SlRbohH* promoter activity in 15-day-old grown promoter:GUS transgenic line on HP/LP ½ MS solid media.

2.5. SlRbohH promoter is a direct target of SlPHRL1/L2

Because the promoter of SlRbohH harbored two P1BS elements, it is a likely target of the master regulators of PSR, PHRL1/L2 transcription factors. Next, we checked the transcriptional activation of the SlRbohH promoter by PHRL1/L2 in *N. benthamiana*. GUS assay was performed for the SlRbohH promoter activity with and without PHRL1/L2. The enhanced GUS activity of the SlRbohH promoter in the presence of PHRL1/L2 suggested the activation of this promoter by binding two TFs at the P1BS elements. Stronger activation of SlRbohH promoter activity was observed with PHRL2 compared to PHRL1, indicating a more prominent role of this TF in activating the *SlRbohH* gene in Pi-deficient seedlings **(Fig. 31).**

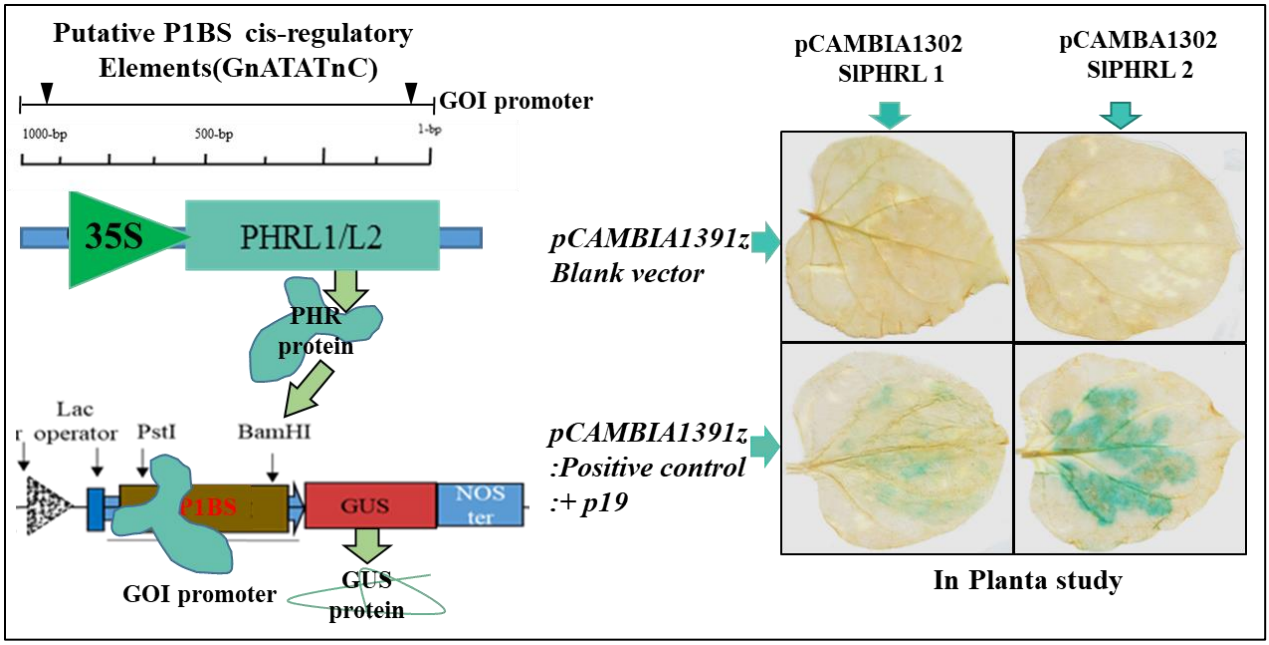

Fig 31: Transient transcriptional activation of pSlRbohH:GUS promoter reporter activation by SlPHRL1/L2 in *N. benthamiana*. GUS assay for SlRbohH promoter activity was performed with SlPHRL1 and SlPHRL2 homologs.

2.6. Characterization of *SlRbohH* using Virus Induced Gene Silencing (VIGS)

To get primary insight into the function of *SlRbohH* during PSR, we decided to transiently silent this gene using Virus Induced Gene Silencing (VIGS) approach. Using standard and lab-optimized VIGS protocols by (Senthil Kumar et al., 2011, Akash et al., 2022) [449,450], we used *pTRV2-SlRbohH* construct to induce silencing of this gene in tomato plants. The silencing of *SlRbohH* was confirmed by quantitative real-time PCR (qPCR) analysis using gene-specific primers **(Fig. 32-D).** As a positive control for the VIGS experiments, we also silenced *Phytoene Desaturase* (PDS) genes and scored the characteristic bleaching leaf phenotype in the transiently silenced tomato seedlings **(Fig. 32-C).** Overall, an excellent silencing effect (over 80 %) in the repeated VIGS experiments was observed. The silencing of this gene was found to modulate plant response to Pi starvation at morpho-physiological, biochemical, and molecular levels indicating perturbed PSR in tomato seedlings.

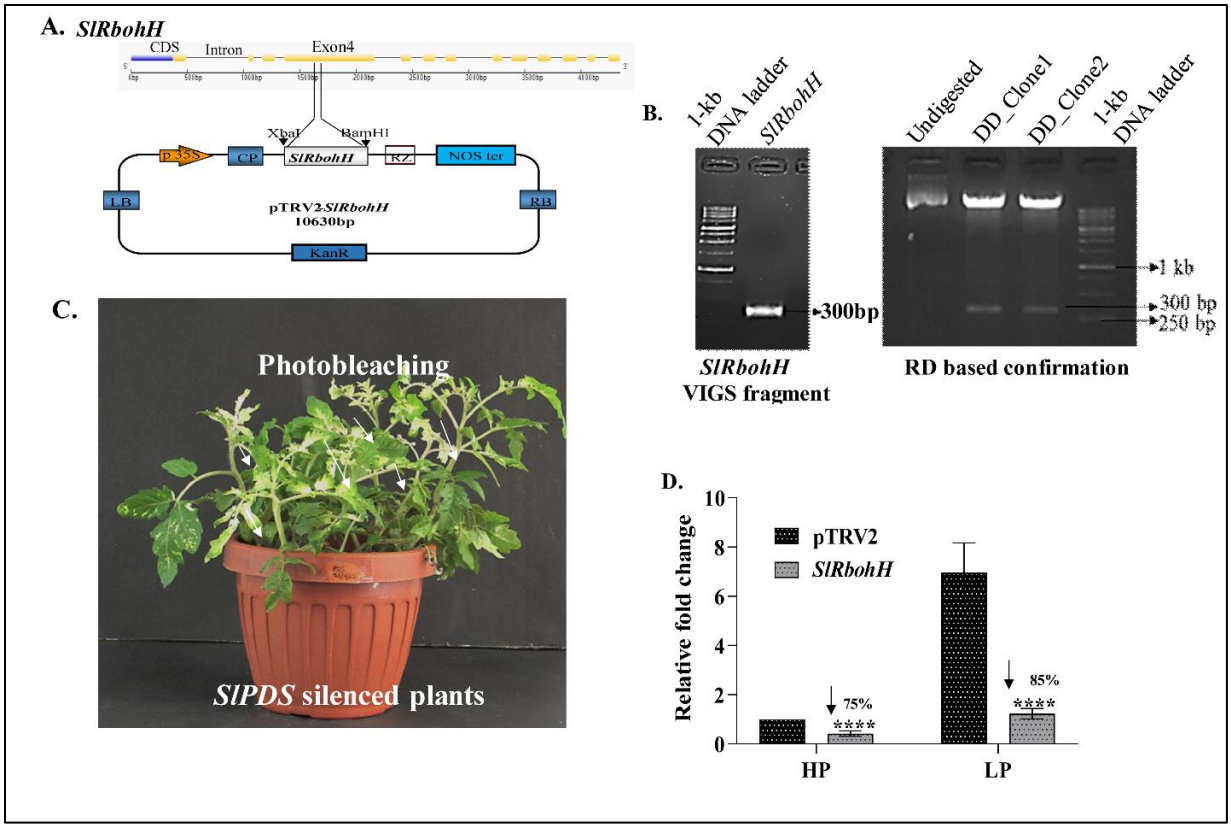

Fig. 32: VIGS-based functional characterization of *SlRbohH* in tomato seedlings. (A) Details of the VIGS vectors. (B) PCR amplification of *SlRbohH* VIGS fragment and the confirmation of its cloning in pTRV2 vector. **(C)** *SlPDS* acted as a positive control of VIGS experiments as the photobleaching phenotype was scored upon the silencing of this gene to determine the efficiency of gene silencing in these experiments. **(D)** qPCR-based confirmation of the relative expression of *SlRbohH* in transiently silenced plants.

2.6. *SlRbohH* silencing leads to lower ROS generation in both Pi-sufficient and Pi-deficient seedlings

In the transiently silenced lines of *SlRbohH*, we first noticed a lower amount of ROS generation in both Pi-sufficient and Pi-deficient seedlings than in the non-silenced control plants. The H2DCFDA staining also confirmed the lower ROS levels in the roots of both Pi-sufficient and Pi-deficient plants **(Fig. 33-A).** This was further confirmed by the quantification of ROS levels in these silenced plants. Significantly reduced levels of ROS were detected in the *SlRbohH* silenced plants than in the empty vector infiltrated control seedlings **(Fig. 33-B and C).**

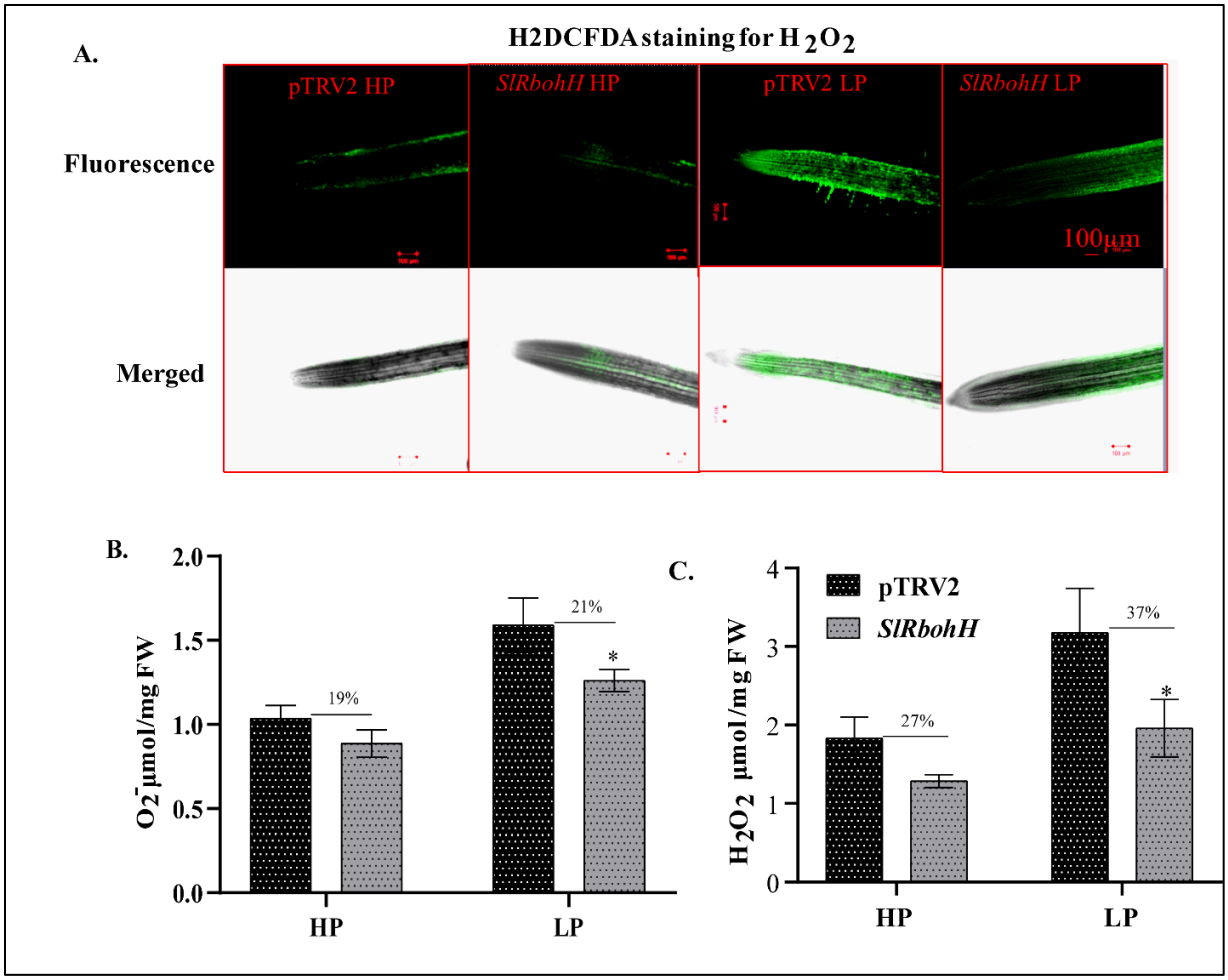

Fig 21: Comparison of ROS levels between WT and *SlRbohH-VIGS* tomato plants. **(A)** H2DCFDA staining of the roots of silenced and vector control seedlings**. (B and C).** Quantification of H_2O_2 and superoxide radicals in the roots of silenced and vector control seedlings HP and LP conditions.

2.7. *SlRbohH* silencing leads to reduced total NADPH oxidase activity and inhibited Pi accumulation under both HP and LP conditions

Once the low levels of H_2O_2 were confirmed in the silenced plants, we next quantified the NADPH oxidase activity in these seedlings and compared that with the WT plants under both HP and LP conditions. The transiently silenced plants showed suppressed NADPH oxidase activity compared to the non-silenced controls under both HP and LP conditions. The activity was found to be inhibited by 31 % and 39 % in the roots of the silenced plants under HP and LP conditions, respectively **(Fig. 34-A).** We then quantified the total P and soluble Pi levels in the *SlRbohH*-silenced plants and found lower Pi accumulation in the roots compared to the non-silenced control counterparts.

The silenced plants accumulated approximately 23 % and 39 % lesser soluble Pi under HP and LP conditions, respectively **(Fig. 34-B).** Total P levels followed a similar trend, as evident by the reduction of total P levels by 27 % and 30 % in the silenced seedlings compared to the non-silenced plants under HP and LP conditions, respectively **(Fig. 34-C).**

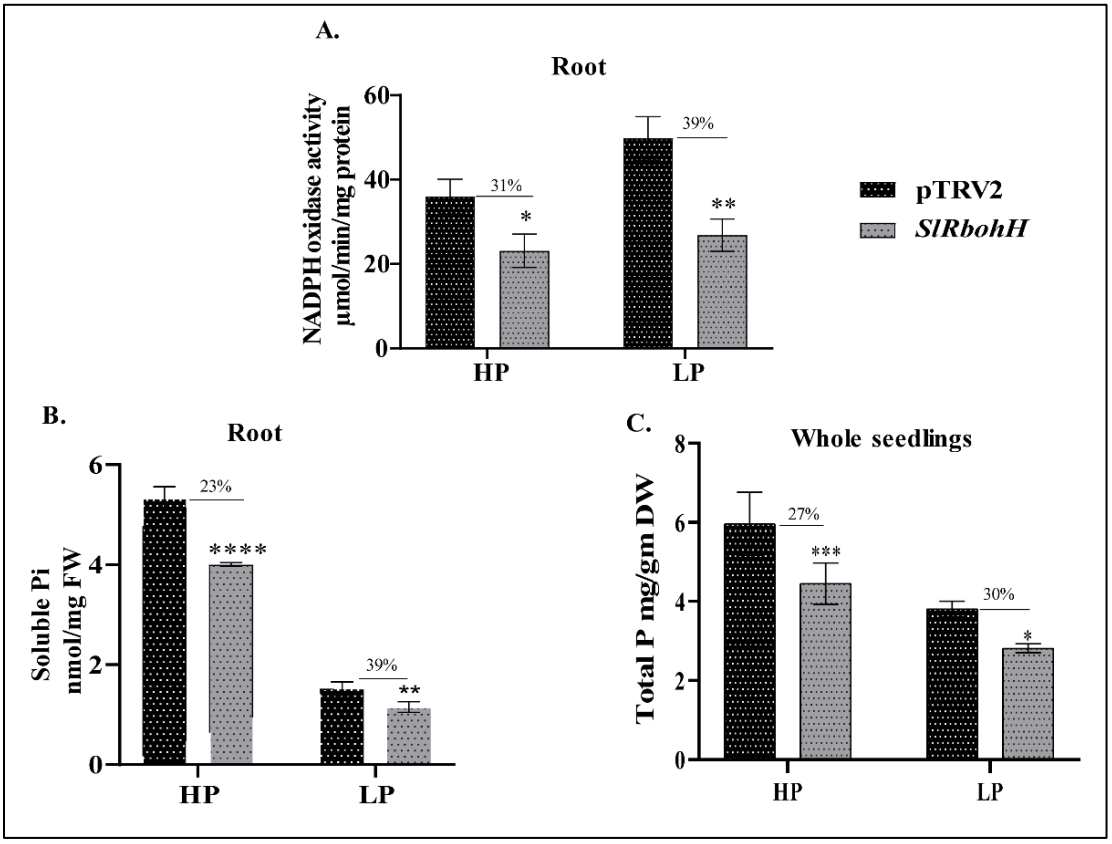

Fig. 34: (A) Comparison of NADPH oxidase activity in WT and VIGS *SlRbohH* seedlings in tomato. **(B and C)** Total **s**oluble Pi and total P content in *SlRbohH* silenced and non-silenced HP/LP seedlings. Two-way ANOVA was performed for statistical analysis, and **** represents P-value <0.05.

2.8. Silencing of *SlRbohH* leads to altered RSA in both Pi-sufficient and Pi-deficient seedlings

We further investigated the phenotypic repercussions of *SlRbohH* silencing in the roots of *SlRbohH* silenced plants and observed altered RSA in both Pi-sufficient and deficient conditions **(Fig. 35-A and B).** Primary root length, root hair number, and average root hair length were all significantly reduced in the silenced plants compared to their control counterparts. On average, the primary root length was found to be reduced by 29 % and 42 % in the *SlRbohH*-silenced plants under HP and LP conditions, respectively **(Fig. 35-C).** Similarly, the number of root hairs decreased by approximately 57 %, whereas the length of root hairs decreased by about 32 % in the silenced plants

under LP conditions **(Fig. 35-D and E).** Since RSA was altered in the silenced lines, we next checked the relative expression of genes involved in root hair formation in the silenced plants. There was an approximate 50 % reduction in the relative expression levels of *Root Hair Defective-Six Like2* (*RSL2*) in the silenced plants in both HP and LP conditions. Similarly, *RSL4* was reduced by approximately 46 % and 52 % in these plants under HP and LP conditions, respectively **(Fig. 35-F).**

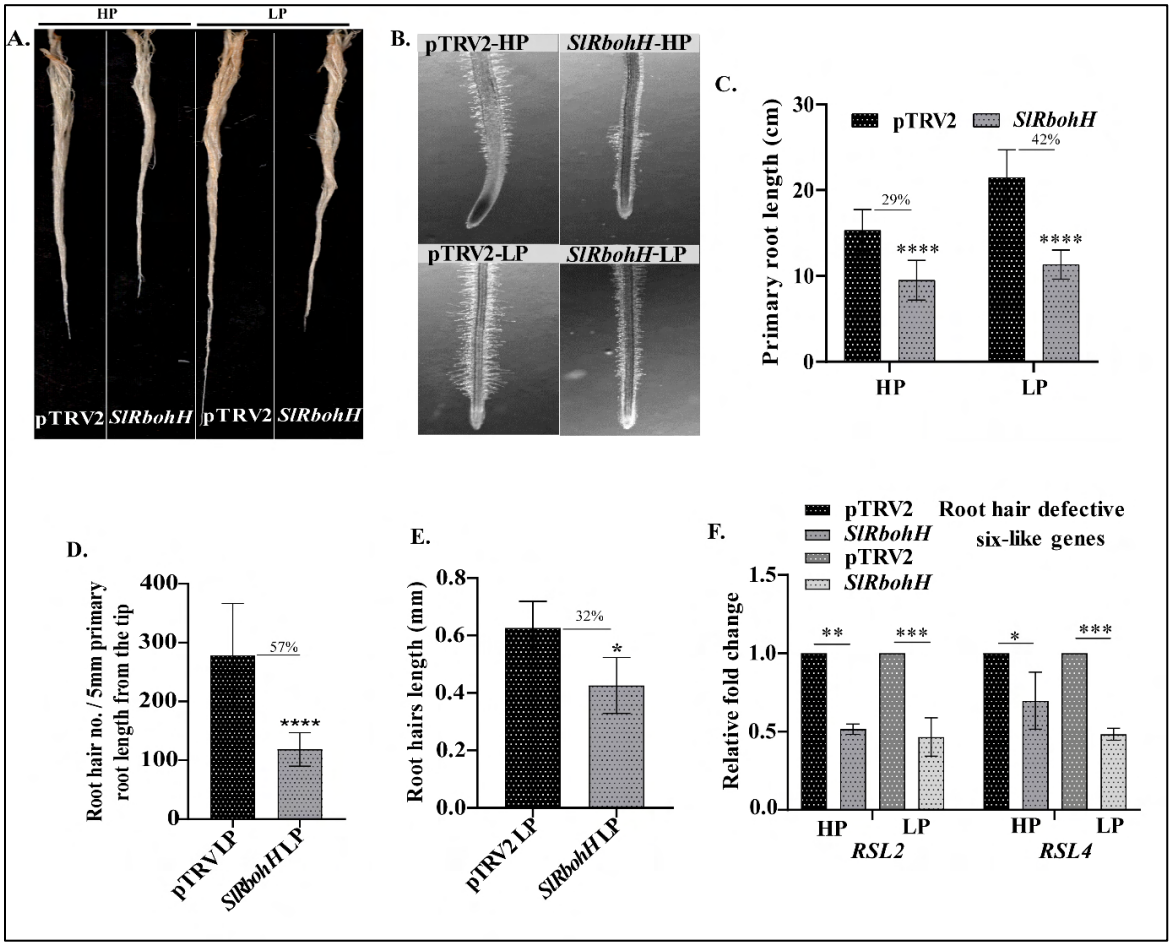

Fig. 35: RSA is modified in the *SlRbohH*-silenced VIGS plants. (A and B) Root images of control and silenced seedlings under HP and LP conditions. **(B)** Measurement of primary root length of control and silenced seedlings under HP and LP conditions. **(C)** An average number of root hairs in WT and silenced seedlings under LP conditions. **(D)** The average root hair length of control and silenced seedlings under LP conditions. **(E)** Relative expression levels of Root Hair Defective-Six Like (RSL) genes in control and silenced seedlings under HP and LP conditions. An unpaired t-test was performed for statistical analysis. **** represents P-value <0.05.

2.9. *SlRbohH* silencing also affects total anthocyanins and total carbohydrates content in Pi-sufficient and Pi-deficient seedlings

We further investigated shoot phenotype in the *SlRbohH*-silenced tomato seedlings. The leaves of these plants were purplish in appearance, which indicated a higher accumulation of total anthocyanins. This observation was substantiated by spectrophotometric quantification of total anthocyanins in both control and transiently silenced *SlRbohH* seedlings. We observed 13 % and 40 % higher total anthocyanins levels in the *SlRbohH*-silenced seedlings compared to the control plants under HP and LP conditions, respectively **(Fig. 36-A and B).**

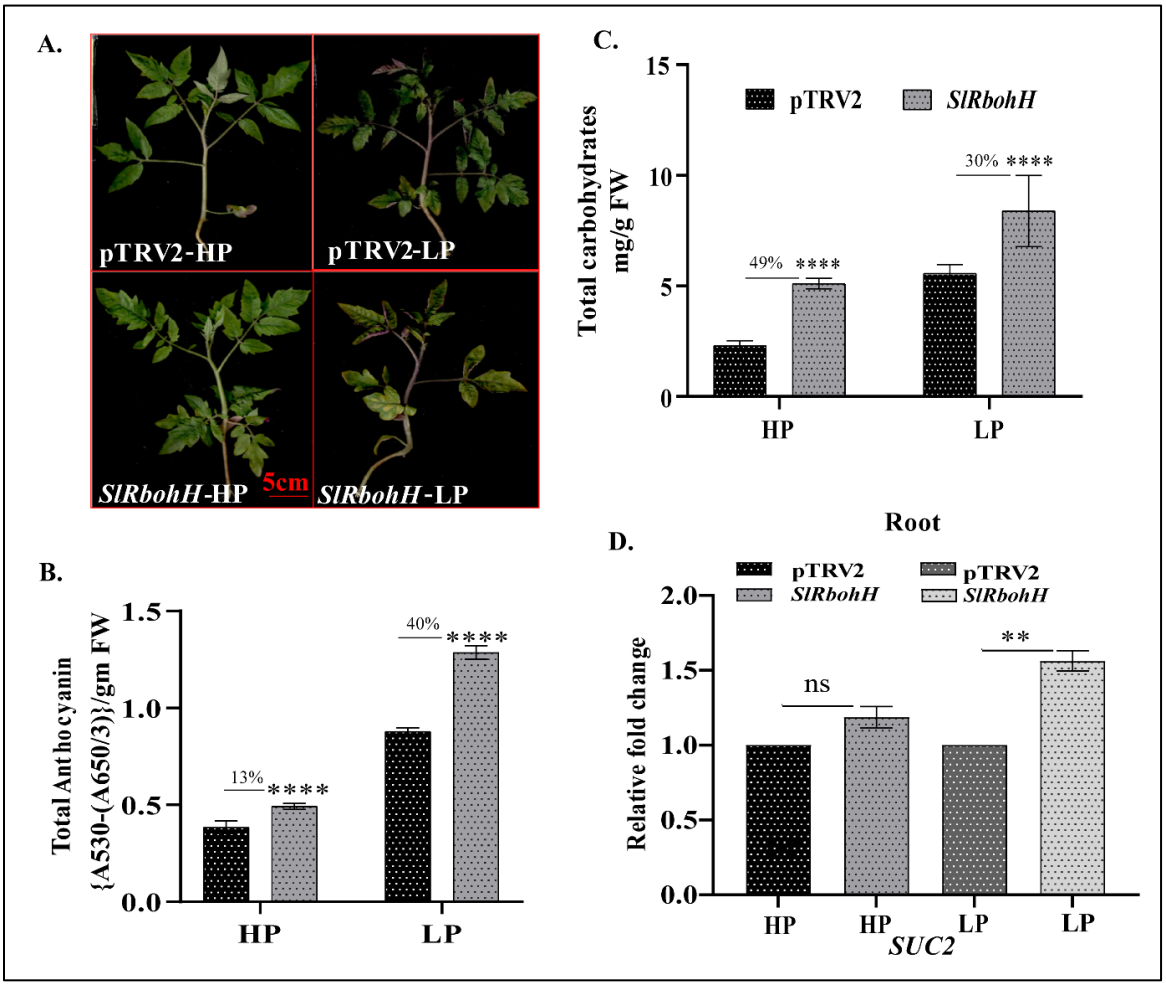

Fig. 36: Shoot phenotype in *SlRbohH* silenced and non-silenced tomato seedlings under HP/LP conditions. (A, B) Total anthocyanins levels in non-silenced and transiently silenced *SlRbohH* plants under HP and LP conditions. **(C)** Total carbohydrate levels in silenced and WT plants under HP and LP conditions. **(D)** Relative expression of *SUC2* in the silenced and control seedlings

under HP and LP conditions. Error bar shows standard deviation. Two-way ANOVA was performed for statistical analysis, and **** represents P-value <0.05.We also quantified the total carbohydrate levels in these seedlings and recorded 49 % and 30 % higher carbohydrate levels in the silenced plants under HP and LP conditions, respectively **(Fig. 36-C).** In the silenced plants under LP, we also found a significant difference in the relative expression levels of *SUC2*, a gene responsible for sucrose transport into the cell/phloem loading. There was a 33 % increase in the relative expression of *SUC2* in the silenced plants, possibly linked to the variability of total carbohydrate levels and altered RSA in these plants **(Fig. 36-D).**

2.10. *SlRbohH* silenced seedlings appear to experience exacerbated P starvation response

For further confirmation of PSR, we subjected the roots of *SlRbohH* silenced tomato seedlings to APase activity and total secretory acid phosphatase (SAP) activity experiments.

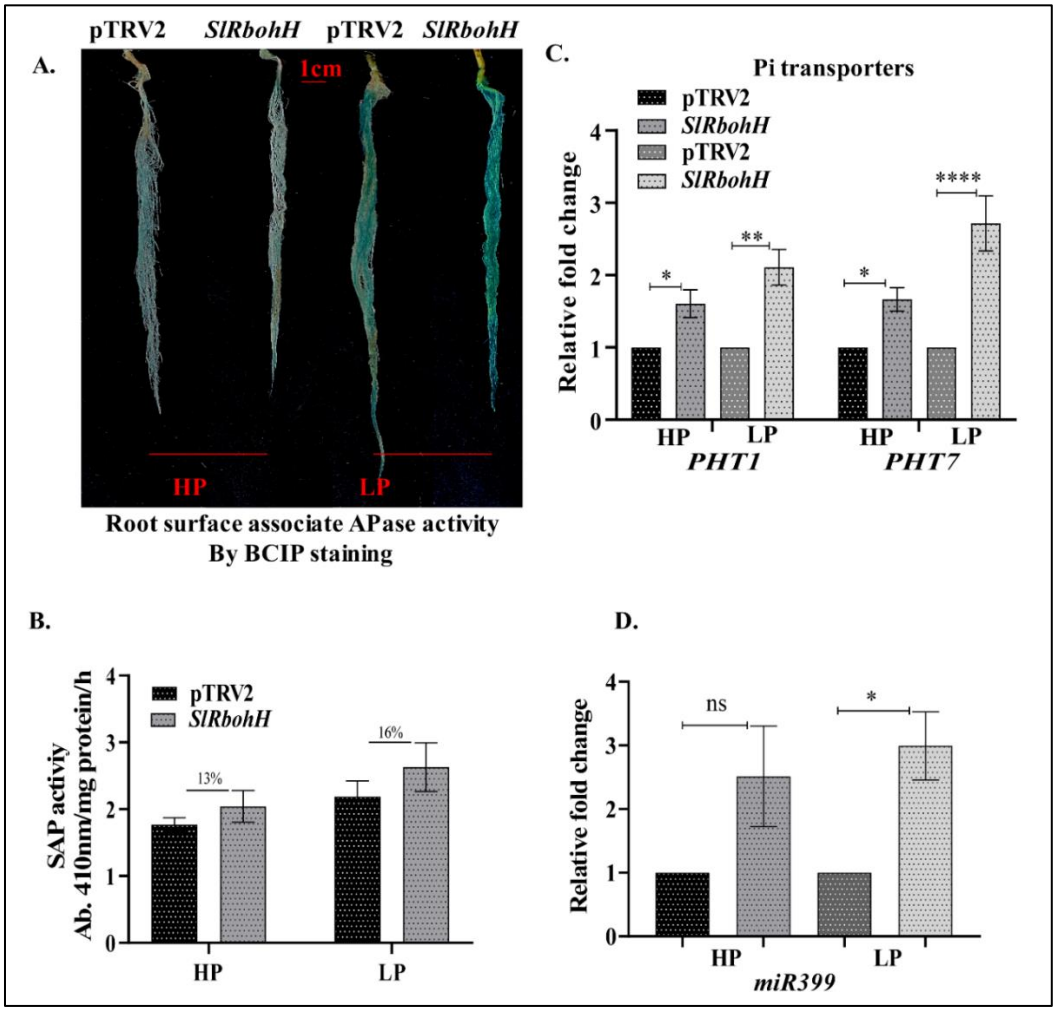

Fig 37. (A and B) Estimation of root surface-associated APase activity by BCIP staining and the secretary APase activity (SAP) in the roots of both *SlRbohH*-silenced and non-silenced seedlings under HP/LP conditions, respectively. **(C, D and E)** Expression profiling of PSR genes, including phosphate transporters, *miR399*, and purple acid phosphatase (*PAP15*) in the roots of *SlRbohH*-silenced and non-silenced seedlings under HP/LP conditions, respectively. The error bar shows the standard deviation. Two-way ANOVA was performed for statistical analysis, and **** represents P-value <0.05.

First, we conducted the NBT-BCIP staining to detect the alkaline phosphatase activity (APase) in the roots of these silenced plants. The APase activity was found to be higher in the *SlRbohH* silenced seedlings, especially under LP conditions, indicating a significant role of *SlRbohH* in PSR. Similarly, the SAP activity increased by 16 % in the silenced plants to their control counterparts **(Fig. 37-A and B).** After observing the activated PSR symptoms in the *SlRbohH* silenced seedlings, we profiled the expression of typical PSI genes, including different Pi transporters (*PHT1*, *PHT7*), *miR399*, and purple acid phosphatase15 (*PAP15*). We observed significant increases in the relative expression of all these genes under LP conditions in the silenced plants compared with the non-silenced plants **(Fig. 37-C, D, and E).**

Summary of the objective 2.

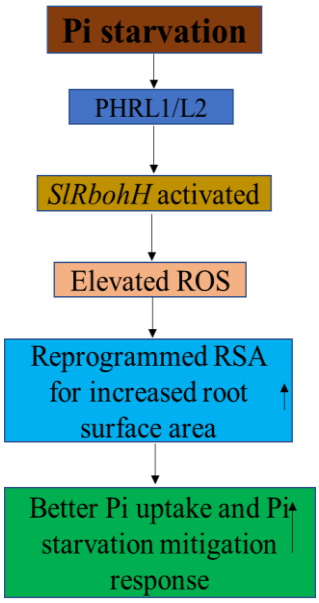

Fig. 38: Overview of the role of *SlRbohH*-mediated ROS production in PSR in tomato seedlings.

Objective-3

To Investigate the role of a F-box domain containing *SlFBX2L1* gene in phosphorus starvation response and fruit ripening

F-box genes are an integral component of SCF-mediated protein degradation, a process important for the turnover of proteins in a cell. The primary function of F-box genes is in substrate selection. Because several components of plants' PSR are subjected to ubiquitin-mediated proteasomal degradation, we were interested in looking into this aspect of PSR in tomato seedlings. Since F-box gene family was not characterized in tomato, we first identified and characterized the members of this family for their role in PSR and fruit ripening.

3.1. Total 410 members constitute the full complement of tomato F-box genes

The rigorous data mining performed using HMM profiling initially identified 463 putative F-box genes in tomato. Among these, 53 putative F-box proteins lacked a specific F-box domain (https://pfam.xfam.org/search); therefore, those entries were removed from the final list. This analysis resulted in the identification of 410 F-box proteins. F-box proteins contain diverse C-terminal domains, which often facilitate protein-protein interactions. Based on the presence of these additional C-terminal domains, the identified tomato F-box proteins were classified into ten subfamilies, as described previously (Gupta et al., 2015) **(Fig. 39).** Among these, F-Box proteins containing leucine-rich repeat domain (108 genes) constituted the most abundant subfamily. The second-largest category was formed by 91 F-box proteins lacking any additional C-terminal domain. The remaining F-box members contained either one or more other domains at their C-terminals. These were accordingly named as FBA (68) with F-box associated domain, FBD (23) with FBD domain, FBDUF (22) with a domain of the unknown function, FBK (35) with kelch repeat domain, FBT (10) having TUB domain, FBW (6) with WD40 domain, FBP (22) constituted by proteins with PP2 domain and FBO (25) containing other domains such as Actin, Cupin, FIST, HERPES, PAS_9, Sel1, SnoaL_3, G-alpha and SWIM **(Fig. 39).**

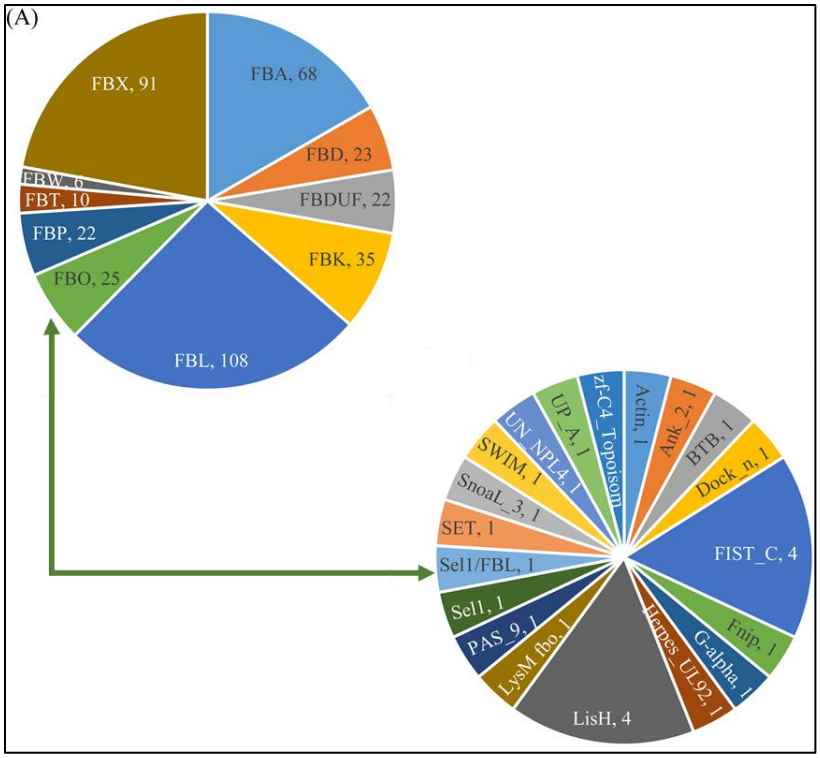

Fig. 39: **Classification of tomato F-box proteins. (A)** Based on the additional C-terminal domains, the identified F-box members are grouped into ten categories, FBL being the largest among these**. (B)** 25 F-box genes harboring other domains (FBO) such as Actin, Cupin, FIST, HERPES, PAS_9, Sel1, SnoaL_3, G-alpha, and SWIM are further classified into 19 subcategories. The value presented in each category and subcategory represents the number of F-box genes in that group.

3.2. Structural organization and evolutionary relatedness of F-box genes

The compiled information of their genomic locus IDs, length of mRNAs, domain architecture, predicted subcellular localization, and intron-exon organization of the identified 410 F-box genes is listed. The length of their coding sequences displayed a wide range and varied from 174 base pairs (bp) (*Solyc06g008470*) to 15379 bp (*Solyc04g017610*). Further, an unrooted NJ-phylogenetic tree was constructed using protein sequences of the identified tomato F-box members. The phylogenetic tree revealed the clustering of proteins belonging to the same subfamily in one cluster **(Fig. 40)**. FBK, FBA, FBL, FBDUF, FBT, and FBP members formed separate groups in the phylogenetic tree. However, a few members of FBL, FBX, FBK, FBA, and FBD subfamilies were also present in more than one cluster in the phylogram, revealing contamination of specific groups by members of the other subfamilies **(Fig. 40).**

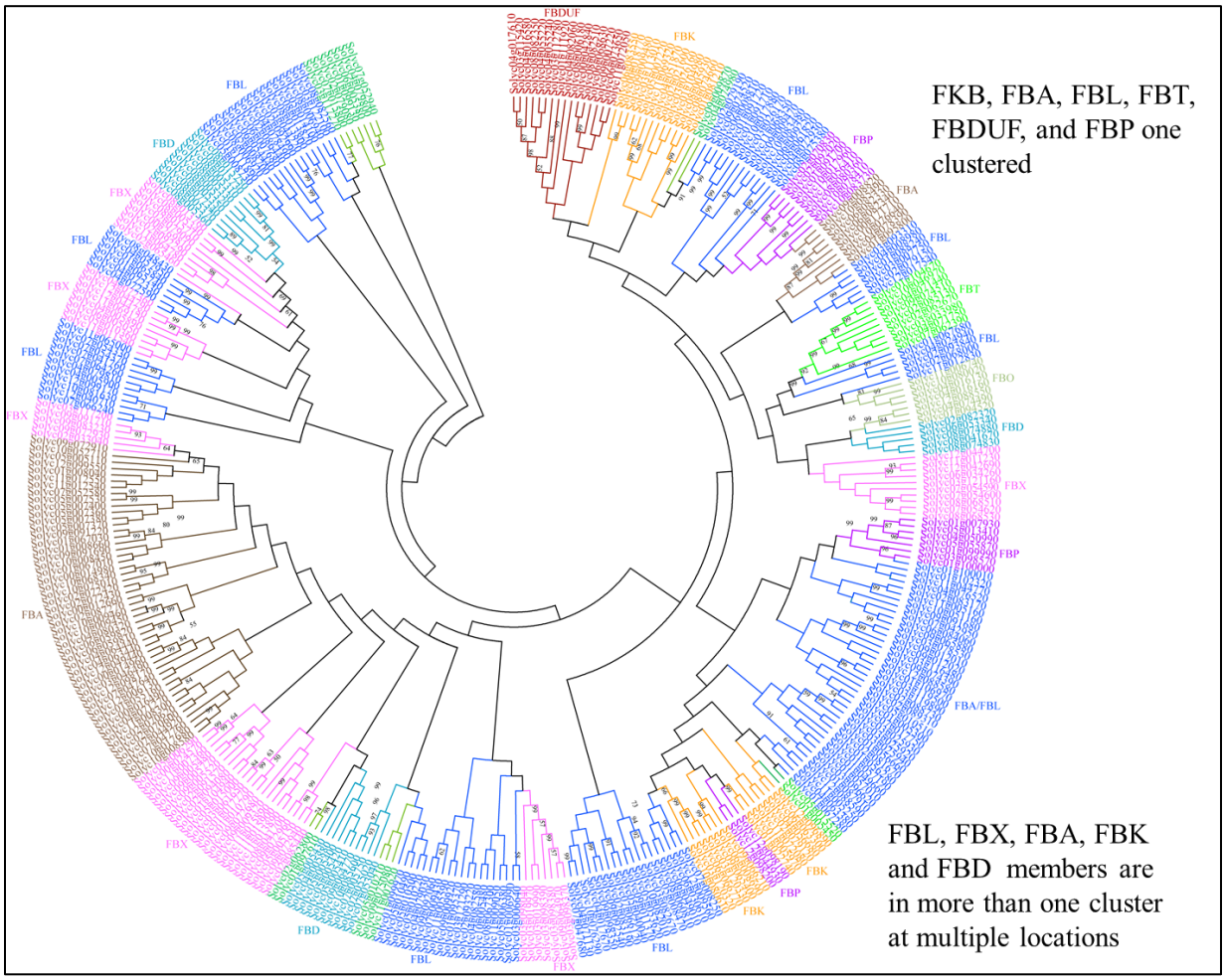

Fig. 40: **Phylogenetic analysis of F-box genes in tomato.** The complete amino acid sequences of 371 F-box proteins were aligned using ClustalW. Short or divergent amino acid sequences were excluded from this analysis. A Neighbor-joining (NJ) tree was constructed using MEGA7. The following parameters, such as the bootstrap method with 1000 iterations, the Poisson method with uniform rates, and pairwise deletion, were used to build the tree. Values with >50 % supporting the node are indicated. Members of different F-box subfamilies are represented in a different color, and the name of the respective subfamily is mentioned next to it.

3.3. Chromosomal distribution and gene duplication of F-box genes

Members of the F-box gene family showed a non-uniform distribution on 12 chromosomes of tomato. We noticed the highest and the lowest gene densities of F-box genes on chromosomes 2 and 12, respectively **(Fig. 41).** This analysis assigned at least 44 F-box genes (22 pairs) to the segmental duplication blocks on all chromosomes except 11. Similarly, 148 tandemly duplicated F-box genes, present in 51 groups, were also identified. Interestingly, 18 F-box genes, including

Solyc01g091700, *Solyc01g091710*, *Solyc03g120330*, *Solyc04g005890*, *Solyc05g010360*, *Solyc07g054620*, *Solyc09g091710*, and *Solyc12g098190*, are present in both tandem and segmentally duplicated blocks **(Fig. 41).** The tandem duplicates that exhibited high sequence similarity were mostly placed in the same cluster in the phylogenetic tree **(Figs. 40 and 41).** Further, the duplication events were prevalent within FBL, FBX, and FBA subfamilies. The majority of the identified duplicated gene pairs belonged to the same subfamily **(Figs. 40 and 41).**

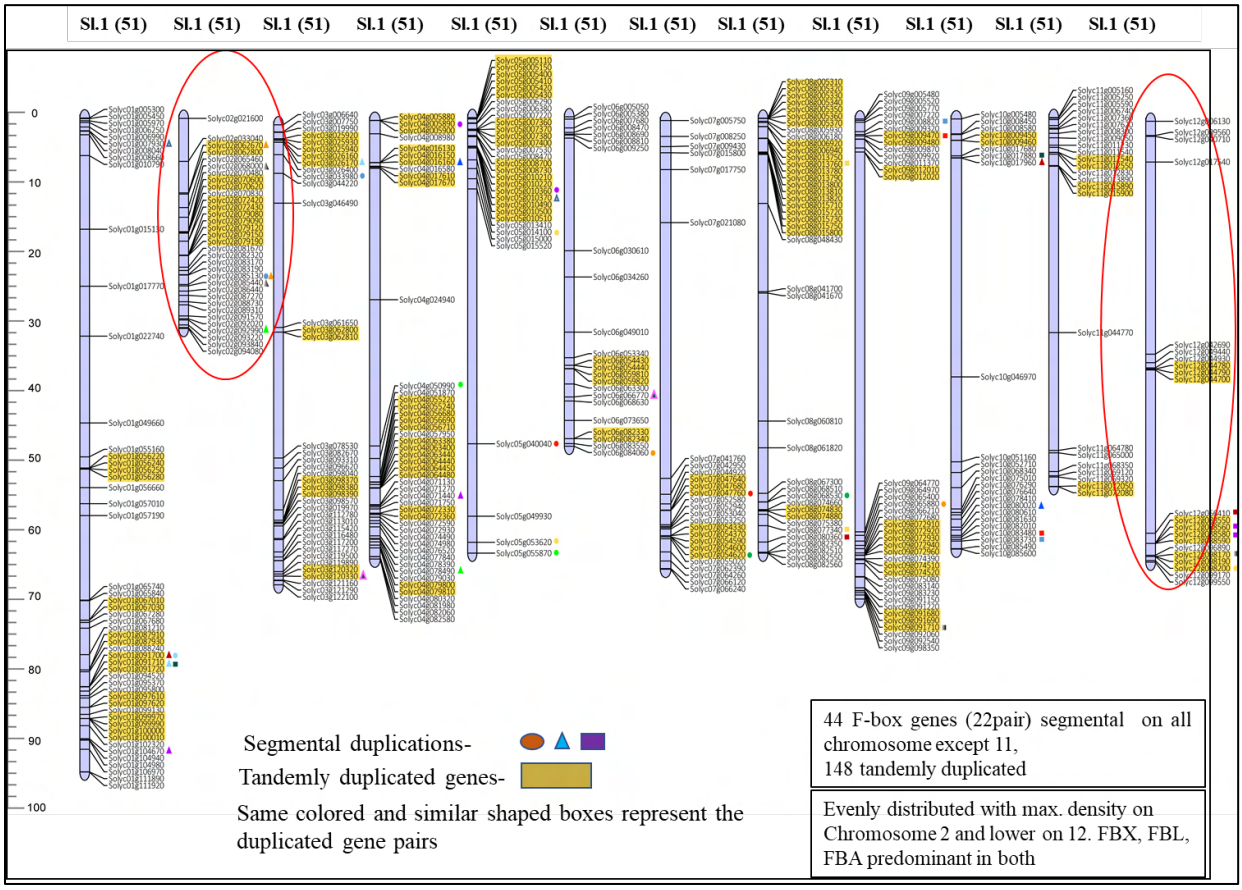

Fig. 41: Chromosomal distributions and gene duplication events. The chromosome number is indicated at the top of the respective bar. Values in parentheses, next to each chromosome name, show the number of F-box genes located on the chromosome. The scale on the left is in megabases (Mb). Tandem duplicated genes are highlighted in yellow color. Segmental duplication events are shown in colored blocks placed next to each such gene. The same colored and shaped boxes (squares or triangles) present on single or different chromosomes correspond to the segmentally duplicated gene pairs.

3.4. Duplicated F-box genes broadly show dissimilar transcript profiles

We next examined the duplicated members' transcript profiles using the publicly available RNA-seq data (Sato et al., 2012). Expression data for the majority of the identified F-box genes are available in the form of a heatmap. Of the 44 segmentally duplicated F-box genes, barring members of three gene pairs, including *Solyc07g054620*:*Solyc08g068530*, *Solyc09g009470*:*Solyc10g083480*, and *Solyc05g053620*:*Solyc12g098200*, the remaining duplicates showed different expression profiles to each other within a gene pair **(Fig. 42-A).** For instance, transcripts of *Solyc03g062800* remained undetected, whereas its duplicated partner, *Solyc02g085440*, was found to have flower-specific mRNA abundance.

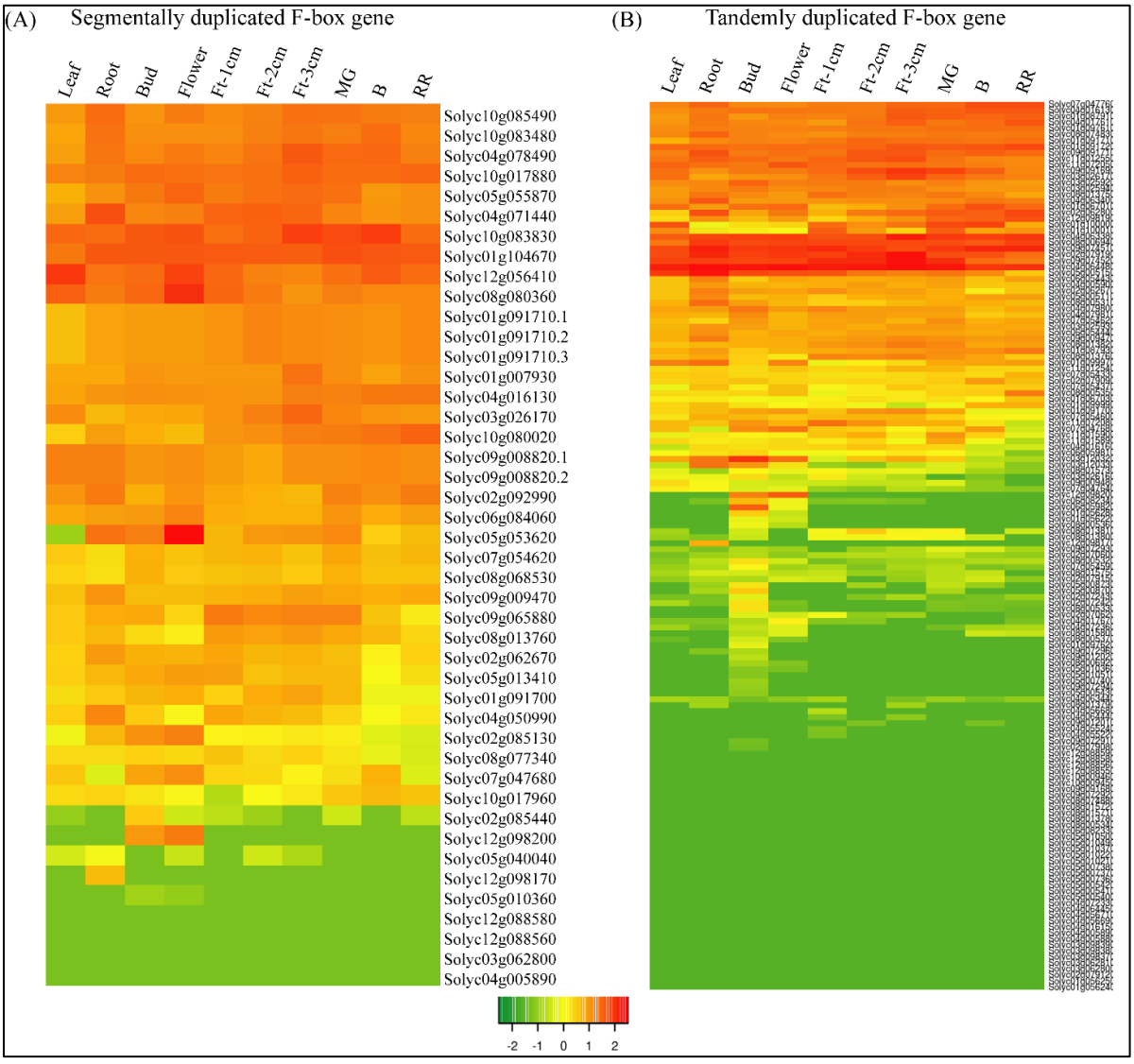

Fig. 42: **Expression profiles of segmental and tandem duplicate F-box genes.** (A and B) Heatmap is constructed using log2 reads per kilo per million mapped reads (RKPM) values obtained from the RNA-seq data published along with sequenced tomato genome (Sato et al., 2012) using 'gplots' package in 'R'. Corresponding gene locus IDs are mentioned on the right side of each row. Ft-1, -2, and -3 represent young fruits of 1-cm, 2-cm, or 3-cm diameter, respectively; MG, mature green fruit; B, breaker stage fruit; RR, red-ripe stage fruit.

Likewise, excluding a few tandem duplicates, such as *Solyc04g079800:Solyc04g079810*, *Solyc05g008700:Solyc05g008730*, and *Solyc11g072050:Solyc11g072080*, most of the remaining genes located in other tandemly duplicated blocks exhibited different expression profiles to each other. A few tandemly duplicated blocks also contained genes with both similar and dissimilar expression profiles within that block. For instance, tandemly duplicated blocks such as *Solyc02g079080:Solyc02g079190* on chromosome 2, *Solyc04g063380:Solyc04g064480* on chromosome 4, *Solyc08g005310:Solyc08g005370*, and *Solyc08g013750:Solyc08g013820* on chromosome 8 contained duplicated genes with both similar and distinct expression profiles **(Fig. 42-A and B).**

3.5. Pi deficiency and sucrose unavailability influence the transcription of several F-box genes

The AtFBX2 gene is known to regulate PSR in Arabidopsis [352]. To identify tomato F-box genes affected by Pi deficiency, we next checked their mRNA levels at multiple time-points and in different tissues using *in-house* 8-DAT and 15-DAT RNA-seq data (unpublished) along with the recently published RNA-seq data by (Pfaff et al., 2020) [134]. Together, we were able to retrieve and analyzed expression profiles of 207 genes in the two data-sets. This analysis identified 55 F-box genes as differentially expressed (≥2-fold change, p-value ≤0.05) at least one of the time points/tissues in the two data-sets **(Fig. 42A)**. Similar to Arabidopsis, transcript levels of the two close tomato homologs of *AtFBX2*, *SlFBX2L1* (*Solyc06g073650*) and *SlFBX2L2* (*Solyc11g072050*), remained unchanged in the tomato seedlings grown under Pi starvation **(Fig. 43-A).** Based on the activation and inhibition upon Pi starvation, the differentially expressed genes fell into three groups: downregulated (I), upregulated (II), and genes with mixed regulation, including both down or upregulation at different stages/tissues (III**) (Fig. 43-B).** Further scrutiny revealed a clear enrichment of FBL subfamily genes (14) among these differentially regulated genes. The other prominent subfamilies featured in the 55 differentially expressed genes were FBD

(9 genes), FBX and FBK (8 genes each), and FBP (6 genes). The pronounced activation of eight F-box transcripts, including *Solyc02g079150*, *Solyc09g065400* (*Galactose oxidase homolog*), *Solyc04g008980* (*RNI-like superfamily protein homolog*), *Solyc07g062390* (*Tubby like protein 7 homolog; SlTLP7*), *Solyc10g076290* (*RNI-like superfamily protein homolog*), *Solyc05g055870* (*MATERNAL EFFECT EMBRYO ARREST 66* homolog*; SlMEE66*), *Solyc01g100010* (PP2-B15 homolog; SlPP2-B15), and *Solyc05g040040* (*SLEEPY1 homolog; SlSLY1*) was observed at multiple time-points in the root, shoot, or seedling, in at least two data-sets, under Pi deficiency **(Fig. 43-B).**

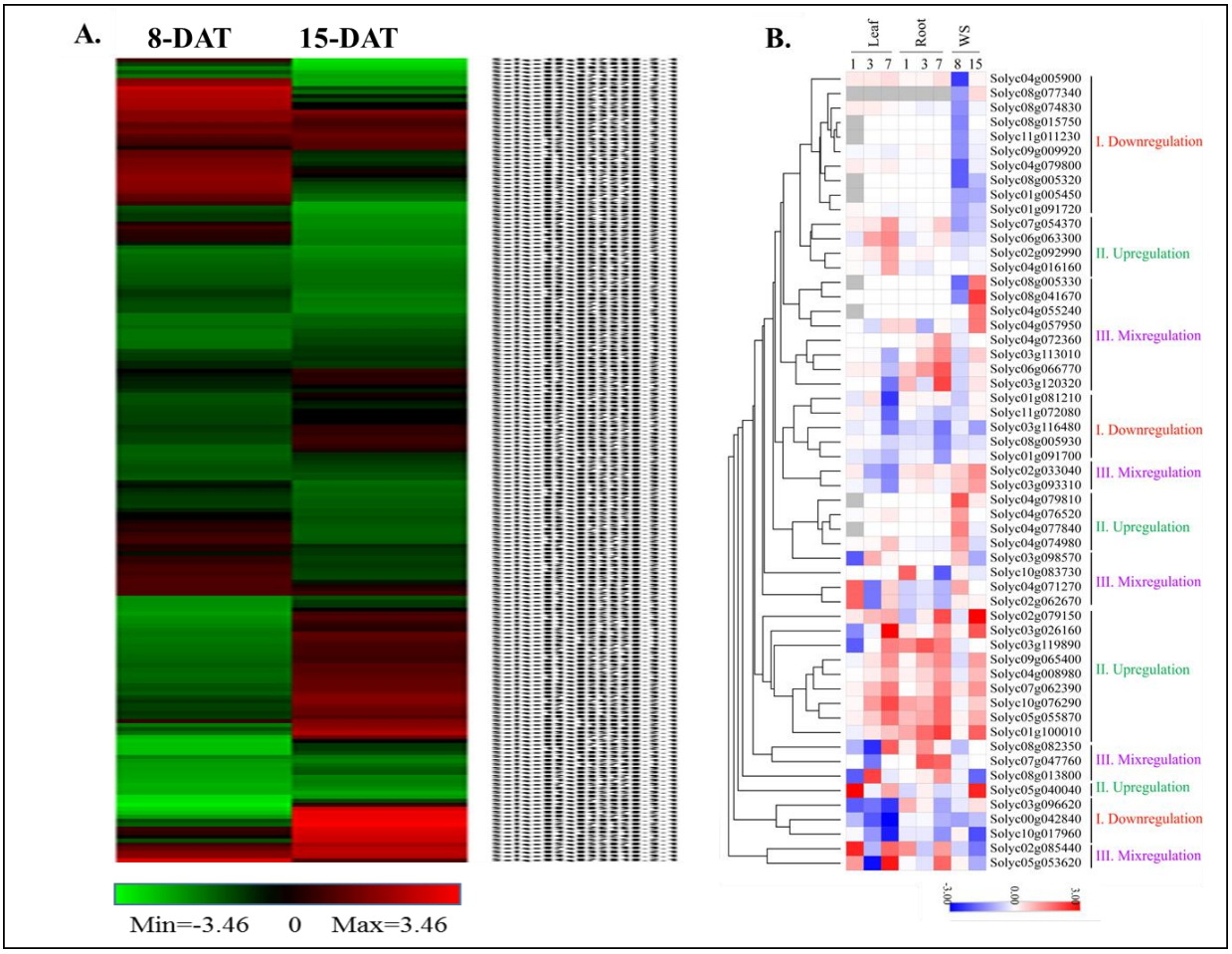

Fig. 43: The differentially expressed F-box genes in Pi-deficient tomato seedlings. (A) Heat map of 206 differentially expressed F-box genes at 8-DAT and 15-DAT in tomato seedlings. **(B)** Heat map of 55 F-box genes which are differentially expressed *In-house* and publically available RNA-seq data [134]. Heatmap was generated by taking the $\log_2$ fold change of transcripts per million (TPM) values (treatment vs. control) for each gene using MORPHEUS (https://software.broadinstitute.org/morpheus/). 1, 3, 7 represent the respective number of days of Pi starvation

treatment. WS, whole seedling. The color bar at the side indicates the minimum and maximum values of gene expression.

3.6. SlFBX2L1 interacts with SlTIR1 and SlEBF2

STRING-based *in-silico* scrutiny of protein-protein interactions predicted robust interaction activity of Solyc06g073650 (SlFBX2L1**)** with many putative proteins. TIR-like and EBF2-like proteins among the interacting partners showed strong protein-protein interaction potential with SlFBX2L1 **(Fig. 44 A)**. The Yeast-2-Hybrid assay confirmed the protein-protein interaction of SlFBX2L1 with TIR1 and EBF2, indicating that this gene might regulate both auxin and ethylene signaling in tomato plants **(Fig. 44-B)**

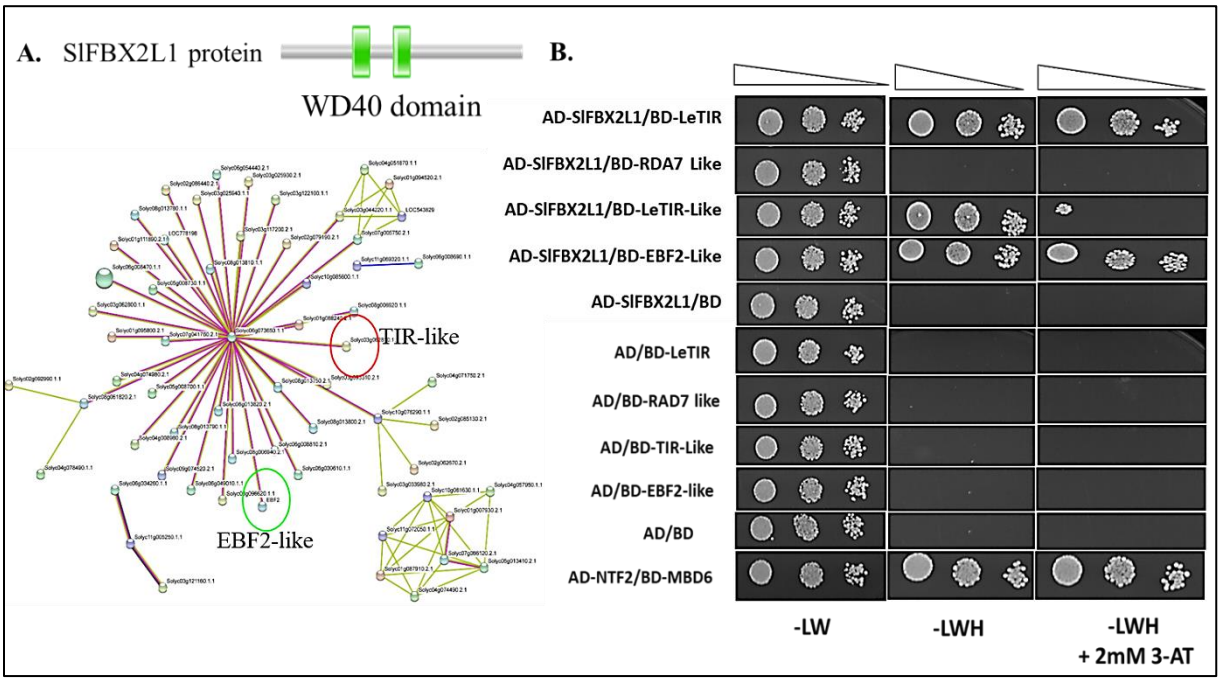

Fig. 44: (A) In-silico prediction of putative protein interacting partners of SlFBX2L1 using STRING (http://string-db.org/). **(B)** Y2H-based validation of SlFBX2L1 with TIR-like1 and EBF2-like proteins.

3.7. SlFBX2L1 is a cytosolic protein with the highest expression in roots and red-ripe fruits

SlFBX2L1 is a close homolog with Arabidopsis *AtFBX2* **(Fig. 45-A).** In the RNA-seq data, this gene was found to have root and fruit-specific expression **(Fig. 45-B).** To validate its expression, we checked its mRNA abundance using qPCR and found that *SlFBX2L1* shows maximum transcripts in root and fruit tissues **(Fig. 45-C**).

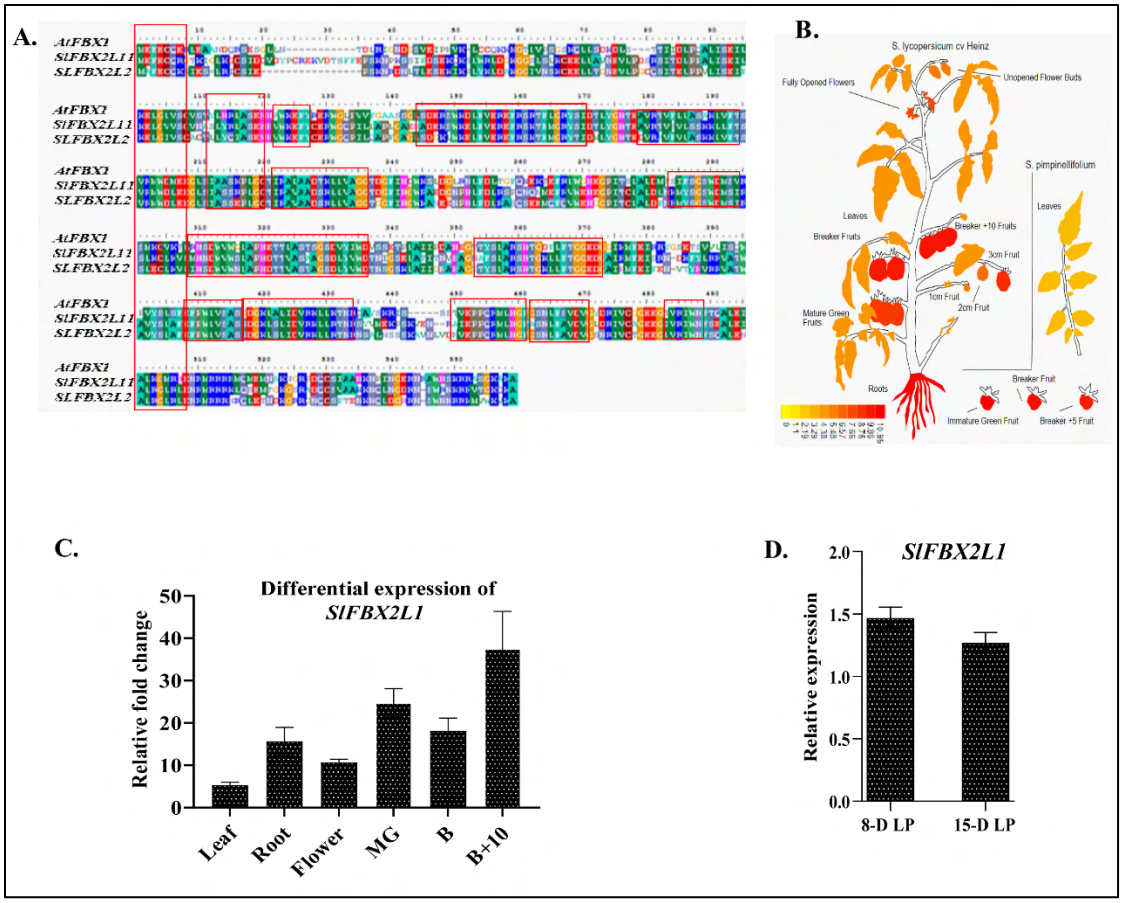

Fig. 45: (A) *SlFBX2L1* tomato and Arabidopsis homologs protein sequences were alignment using the BioEdit tool. The three genes showed a high level of homology **(B and C).** Expression analysis of *SlBX2L1* gene at different development stages using Multi-Plant eFP Browser 2.0 – BAR tool and qPCR. **(D)** *SlFBX2L1* is mildly induced under low Pi.

Expression profiling in Pi-deficient seedlings revealed approximately 50 % increase in transcript levels of SlFBX2L1 on the 15th day of starvation than their control counterparts **(Fig. 45-D).** To confirm its subcellular localization, the *SlFBX2L1* CDS was fused with N-terminal GFP in the pCAMBIA1302 binary vector **(Fig. 46-A, B and C).** The expression vector was infiltrated in *N. benthamiana* leaves. The confocal laser scanning microscopy revealed that SlFBX2L1 is a cyto-solic protein **(Fig. 46-D).** The same was confirmed in the roots of *SlFBX2L1* complemented *Atfbx1* mutant stable Arabidopsis lines.

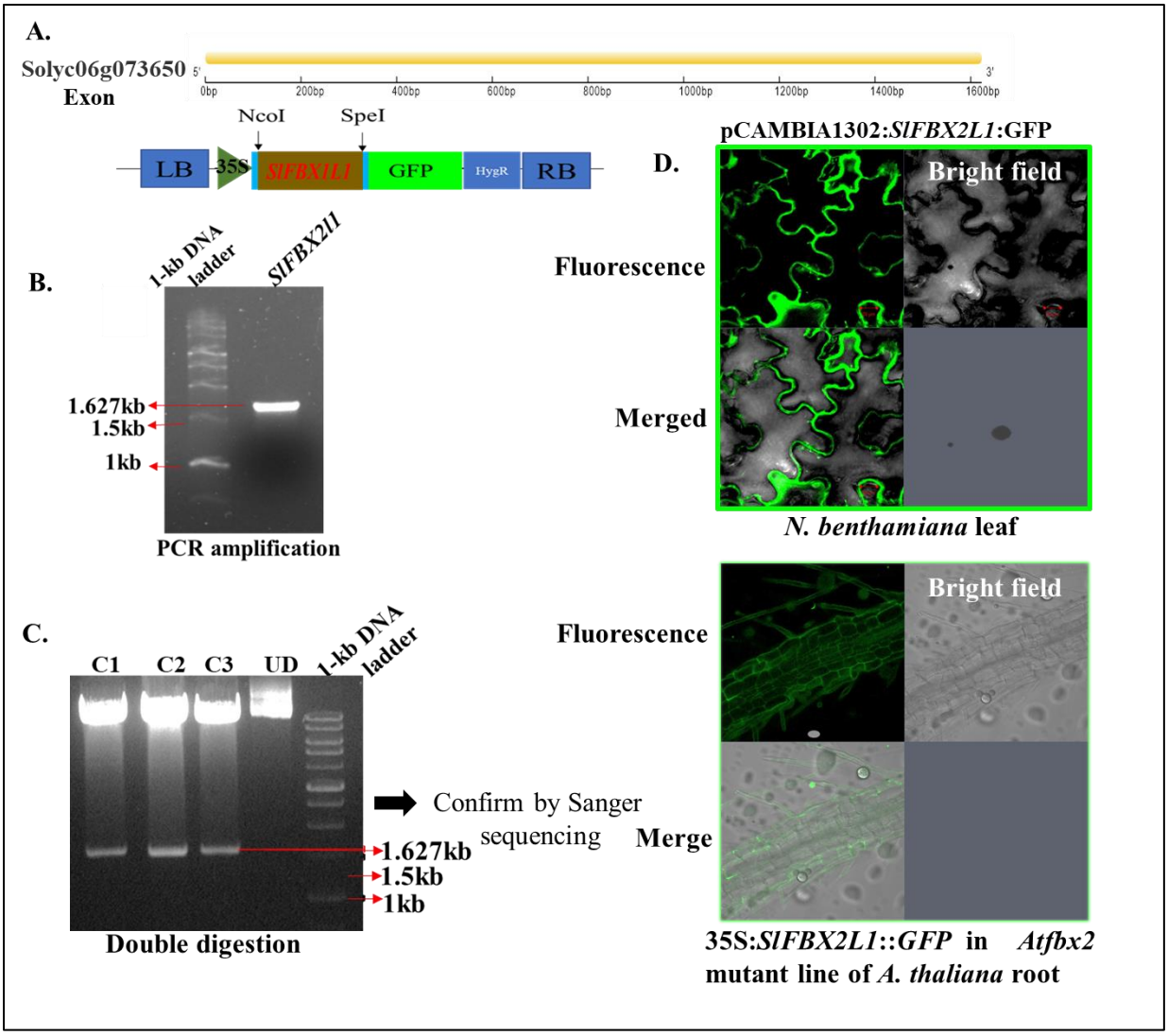

Fig 46: **Molecular cloning and subcellular localization of SlFBX2L1 protein. (A)** Gene structure and orientation of *SlFBX2L1* gene in binary vector pCAMBIA1302 with N-terminal fused GFP. **(B and C)** PCR amplification of 1.6 kb *SlFBX2L1* CDS on agarose gel electrophoresis. Double digestion-based confirmation of plasmids with NcoI and BucI restriction enzymes**. (D)** Subcellular localization of SlFBX2L1 protein in *Nicotiana benthamiana* and 35S:*SlFBX2L1*::GFP stable complemented line in *Atfbx2* mutant background.

3.8. Screening of *Atfbx2* homozygous mutants under Pi deficiency

To check if *SlFBX2L1* has a conserved function in PSR, as previously described in Arabidopsis, we screened *Atfbx2* SALK mutant seeds for homozygosity by PCR with specific primers along with LB3.1 primer (**Fig. 47-D)**.

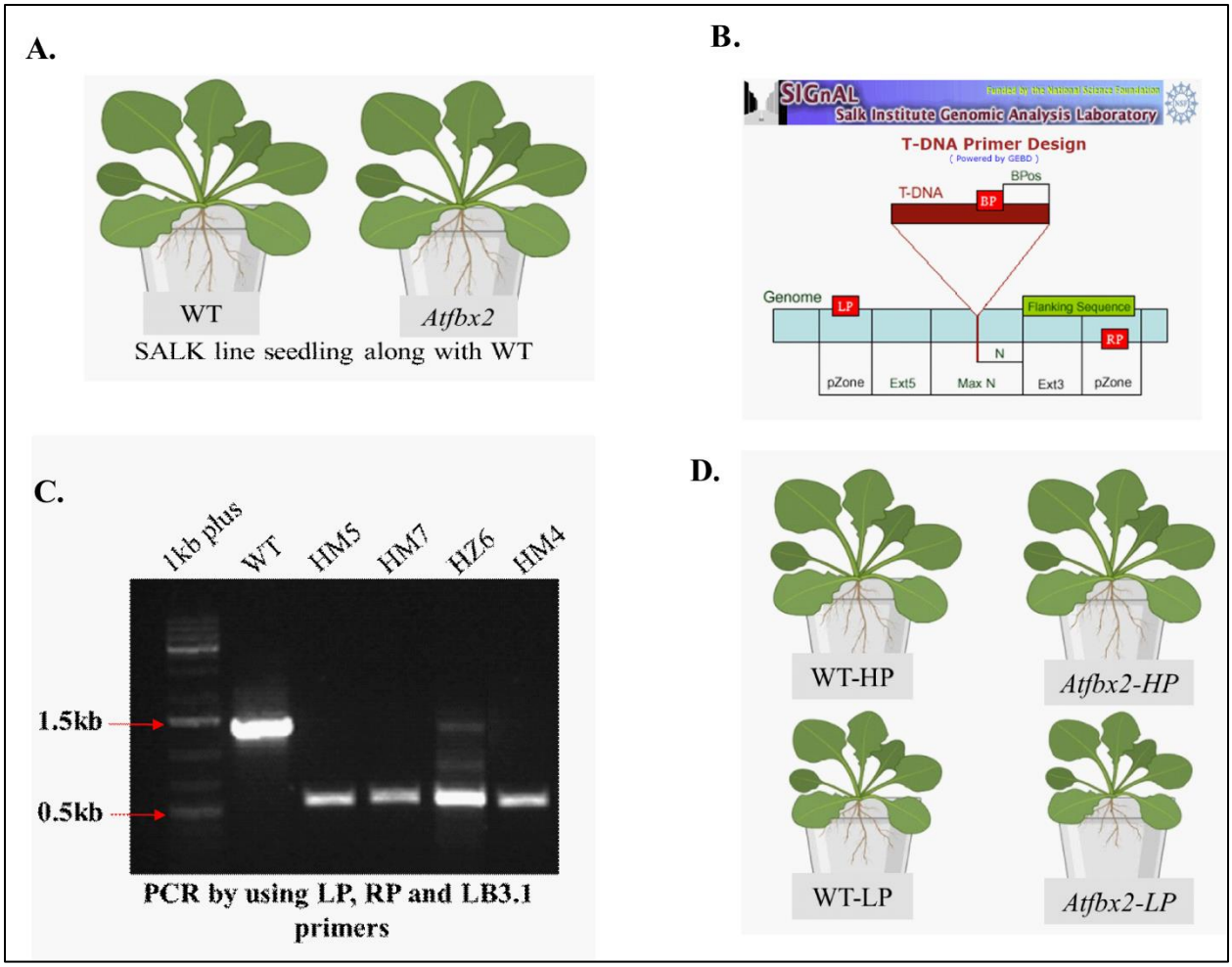

Fig. 37: Screening of *Atfbx2* homozygous mutant (HM) lines. (A) Representative images of the T-DNA insertion mutant seedlings of *Atfbx2* and Col-0 on soilrite under 16/8 day/night cycle at 22ºC. **(B and C)** Confirmation of homozygous *Atfbx2* mutant lines by PCR amplification with left, right and LB3.1 primers. **(D)** Screening of *Atfbx2* homozygous mutant lines with Col-0 on solid ½ MS media under HP and LP conditions.

Next, Arabidopsis homozygous *Atfbx2* mutant and Col-0 seeds were germinated and transferred on ½ MS medium with and without Pi. The plates were kept vertically for 16/8h light-dark cycle at 22^{0}C for seven days. *Atfbx2* mutants showed enhanced root hair density compared to Col-0 control under both HP and LP conditions **(Fig. 48-B and C).** *Atfbx2* mutant seedlings also accumulated higher soluble Pi, which increased by 15 % and 50 % in these seedlings compared to Col-0 in both high and low Pi conditions (**Fig. 48-D)**.

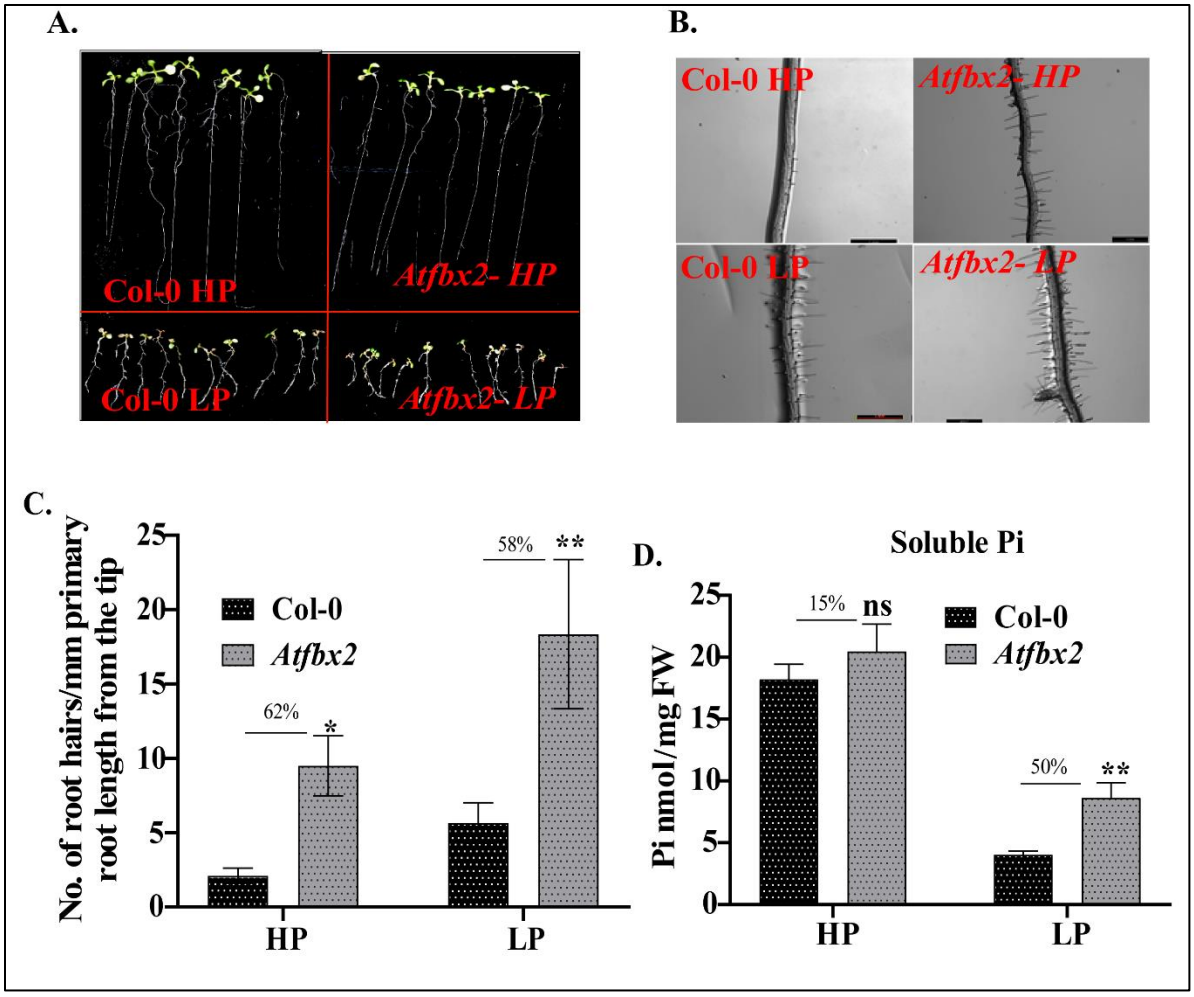

Fig. 48: *Atfbx2* homozygous mutant and WT Col-0 seedlings grown on ½ MS agar media HP/LP conditions. (B and C) Root hairs phenotype and number in mutant line and Col-0 during HP/LP conditions. **(D)** Soluble Pi content in *Atfbx2* mutant and WT Col-0 seedlings under HP/LP conditions. One-way ANOVA was used for statistical analysis. ** denotes P-value ≤0.01.

3.9. *SlFBX2L1* complements *Atfbx2* mutant for PSR

To explore the function of *SlFBX2L1* gene in PSR, its transgenic overexpression lines were generated in *Atfbx2* mutant background. For this purpose, *SlFBX2L1* CDS was cloned in pCAMBIA1302GFP binary vector (pCAMBIA1302GFP::*SlFBX2L1*-OX) and used for transformation in the mutant background. These putative transgenic lines were confirmed for their Hyg^R resistance and by PCR using gene-specific primers. The level of overexpression of this gene in the mutant background was established by qPCR using *SlFBX2L1* specific primers **(Fig. 49-B, C and D).**

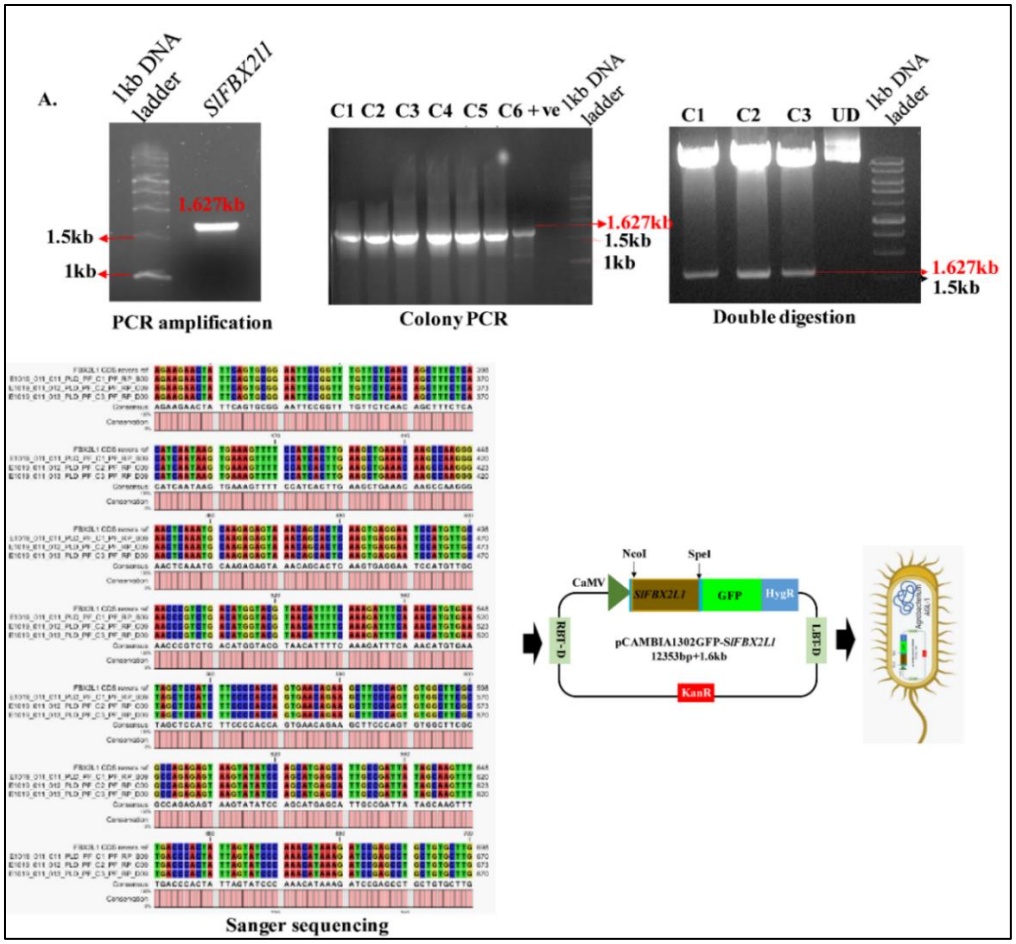

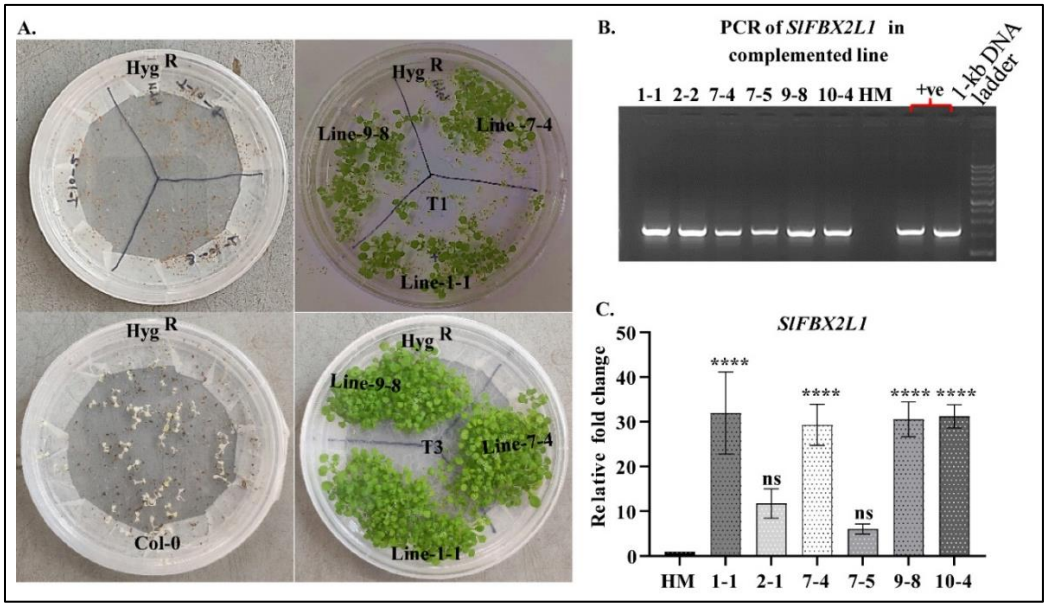

Fig. 49: **Screening of *SlFBX2L1* complemented transgenic lines. (A)** Cloning of *SlFBX2L1* CDS in *pCAMBIA1302* expression vector. **(B)** Hygromycin-based screening of T1 lines for iden-

tifying homozygous lines. **(C)** PCR-based screening of *SlFBX2L1* positive lines using gene-specific primers. **(D)** Expression profiling of *SlFBX2L1* gene in the complementation lines using qPCR. Error bar shows standard deviation. Two-way ANOVA was performed for statistical analysis, and **** represents P-value <0.05.

Further, we have screened the complemented lines on ½ MS agar in HL/LP conditions. The seedlings showed 55 % and 59 % lower root hairs number in the complemented seedlings under HP and LP conditions, respectively, with respect to *Atfbx2* mutant plants **(Fig. 50 & 51 A and B).** We didn't find much difference in the primary root length in all the complemented lines compared to the mutant plants **(Fig. 51-C).** Soluble Pi content in the complemented lines also decreased significantly to the mutant and WT plants **(Fig. 51-D).**

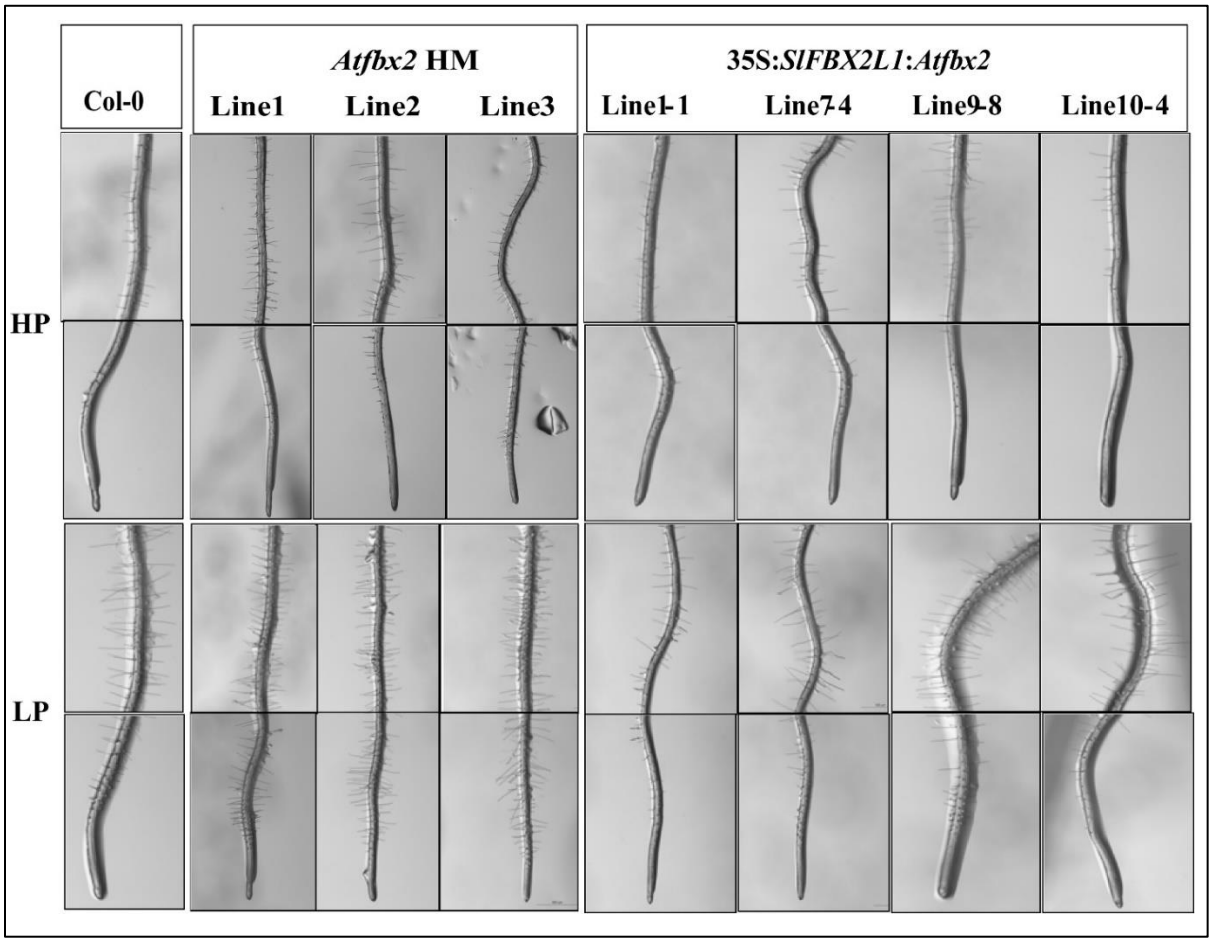

Fig. 50: Screening of *SlFBX2L1:Atfbx2* complemented stable Arabidopsis lines under HP/LP conditions.

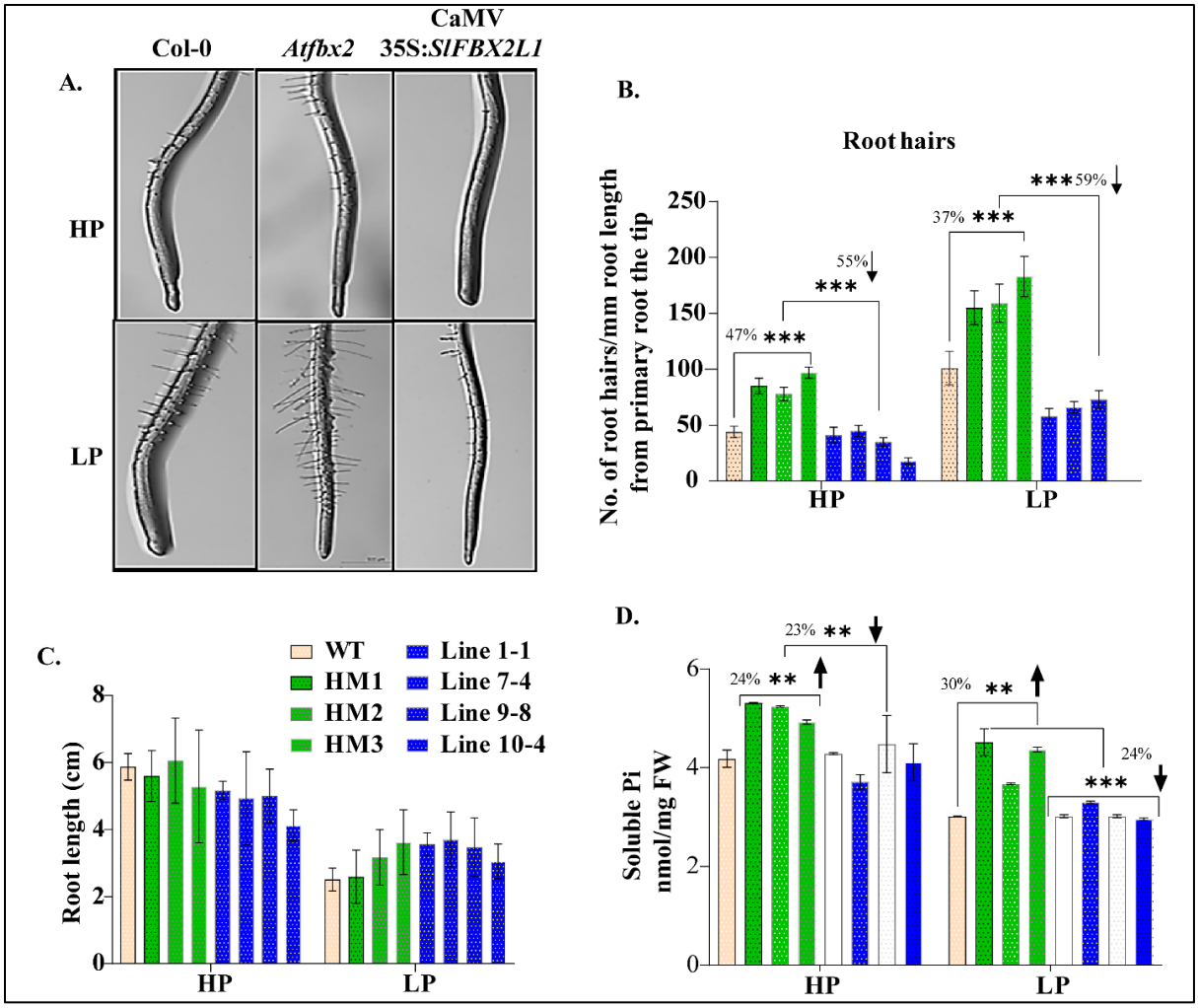

Fig. 51: Screening of stable *SlFBX2L1:Atfbx2* complemented lines under HP/LP conditions. (A, B and C) Root hairs phenotype, root hairs number and primary root length of Col-0, *Atfbx2* HM mutant and *SlFBX2L1:Atfbx2* complemented lines under HP/LP conditions. **(D)** Soluble Pi contents of Col-0, *Atfbx2* HM mutant, and *SlFBX2L1* complemented lines under HP/LP conditions. The error bar shows the standard deviation. Two-way ANOVA was performed for statistical analysis, and **** represents P-value <0.05.

3.10. *SlFBX2L1* silencing increases root hairs formation and enhance Pi accumulation in both Pi-sufficient and Pi-deficient seedlings

Next, *SlFBX2L1* was transiently silenced using VIGS, and the infiltrated plants were confirmed as described previously for *SlRbohH*. *SlPDS* gene was used as a positive control in the VIGS experiments. Photobleaching of leaves was observed in all *SlPDS* silenced plants, indicating an excellent gene silencing efficiency **(Fig. 52).**

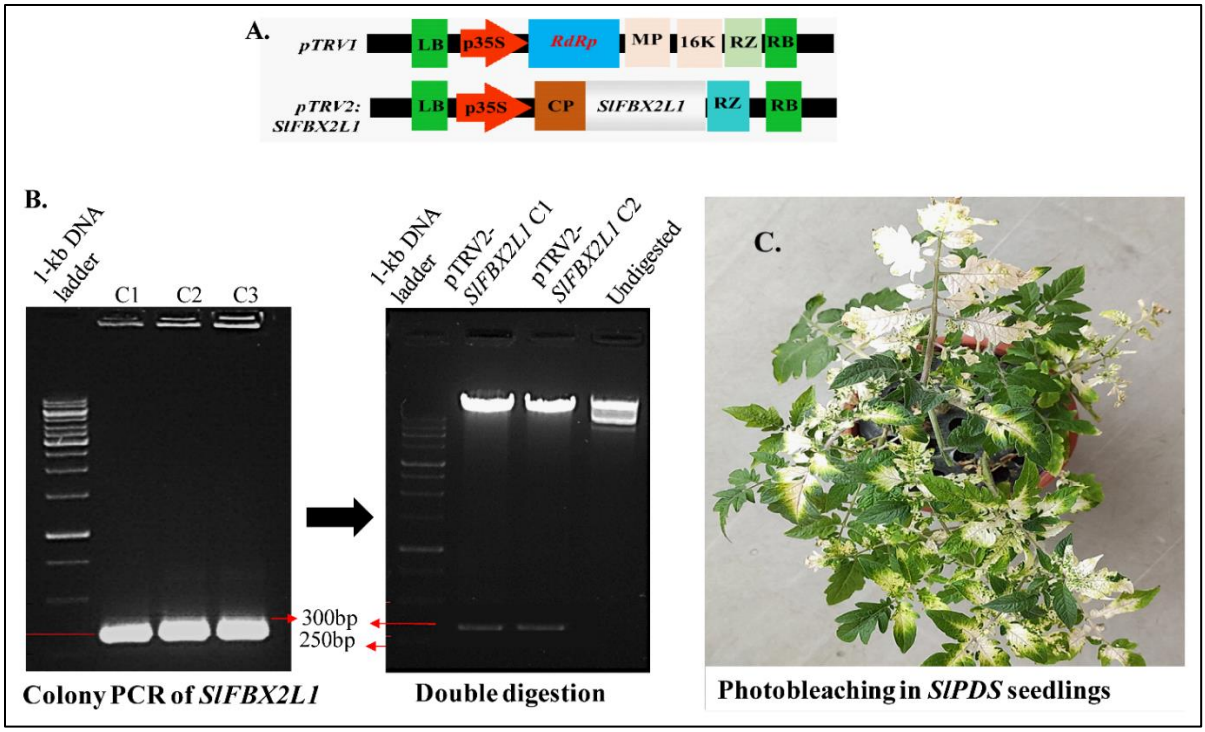

Fig. 52: (A) *SlFBX2L1* VIGS fragment was cloned in between duplicated *CaMV35S* promoter (*2X35S*) and nopaline synthase terminator (NOSt) in a T-DNA vector. RdRp, RNA dependent RNA polymerase; 16K, 16 kDa cysteine-rich protein; MP, movement protein; CP, coat protein; LB and RB, left and right borders of T-DNA; Rz, self-cleaving ribozyme; MCS, multiple cloning sites. **(B)** PCR amplification of 300 bp *SlFBX2L1* CDS and release of the same band after double digestion for cloning confirmation in *pTRV2* vector (**C**). Photobleaching phenotype of VIGS PDS seedlings on the 15th day after the infection.

The infection of TRV vectors was confirmed by PCR analysis using coat protein–specific gene primers. The coat protein gene was found to be present in all the inoculated plants but not in the wild-type control plant **(Fig. 53-A).** The qPCR analysis confirmed the silencing of *SlFBX2L1* gene in both Pi-sufficient and Pi-deficient plants compared to their respective blank pTRV1/2 inoculated plants. While *SlFBX2L1* transcripts were downregulated by 50 % in the Pi-sufficient plants, a more robust silencing of this gene was observed (76 % inhibition) in Pi-deficient plants compared to non-silenced control seedlings **(Fig. 53-B).** Under LP condition, silencing of *SlFBX2L1* resulted in a significant increase in root hair density, which increased by 28 %, compared to non-silenced plants. Under HP condition, the increase in root hair density of *SlFBX2L1* silenced plant was found to be non-significant **(Fig. 53-C and D).** Along with root hairs density, which was calculated as the number of root hair/mm root length, the root hairs length was also analyzed. It was found that

the average length of root hairs in *SlFBX2L1* silenced plants increased by 33 % over their non-silenced plants under Pi deficient conditions. No significant increase in root hair length was observed in silenced plants when subjected to Pi sufficient condition **(Fig. 53-E).**

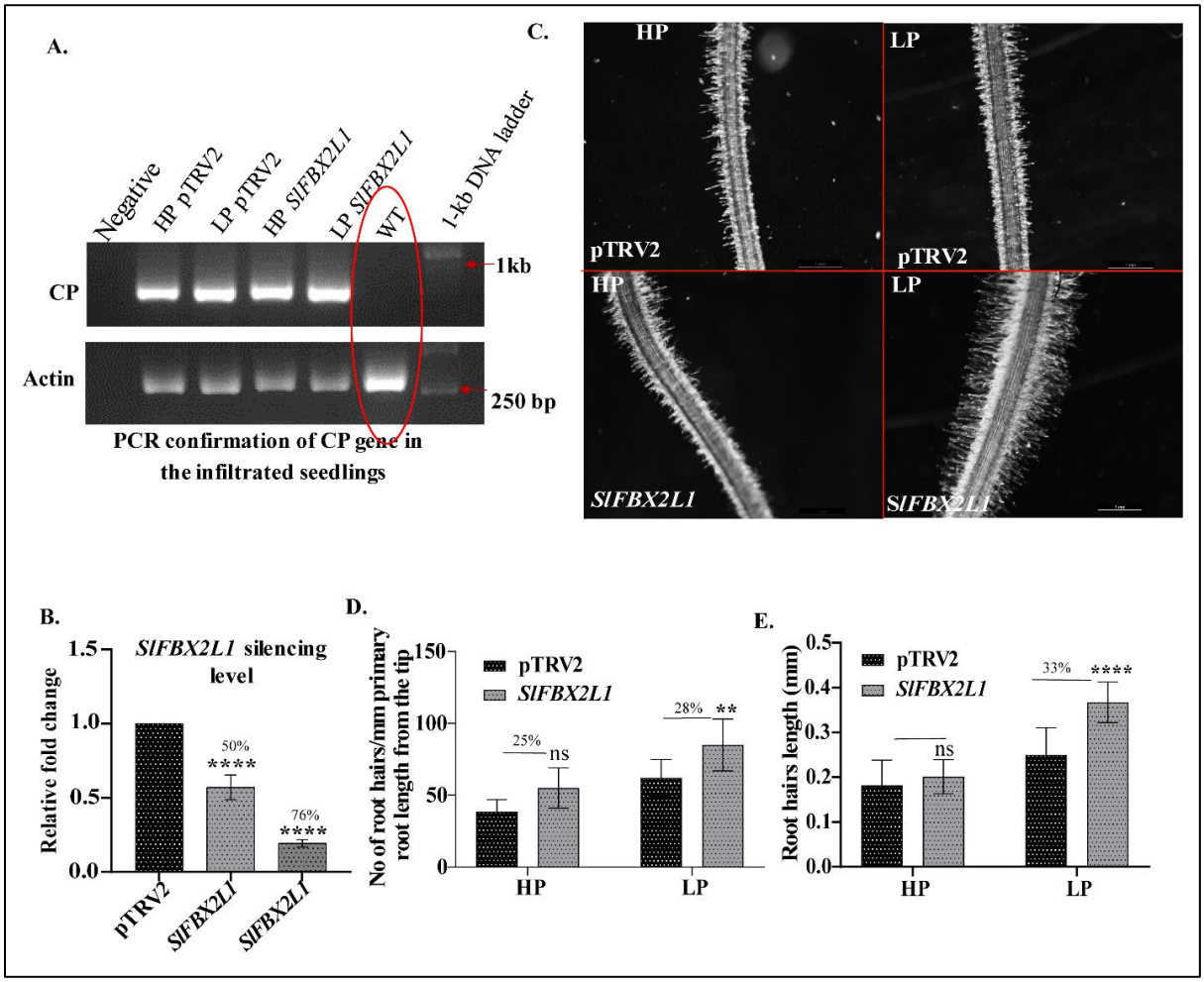

Fig. 53: Silencing effect of *SlFBX2L1* genes in the VIGS tomato plants. (A) The infiltration efficiency in the seedlings was confirmed by PCR using pTRV2 coat protein (CP) specific gene primers. Tomato *Actin* gene expression from the *pTRV2*-infiltrated and control seedlings cDNA acted as a control. **(B)** qPCR of *SlFBX2L1* transcript levels in *pTRV2* control and *pTRV2-SlFBX2L1* silenced plants. The *GAPDH* gene was used as an internal control. **(C and D)** The average number length of the silenced and non-silenced seedlings in HP/LP conditions. Error bar shows standard deviation. One-way ANOVA was used for statistical analysis. **** shows P-value <0.05.

Biochemically, silencing of *SlFBX2L1* led to elevated levels of soluble Pi in plants, showing an increase of up to 25 % in HP condition and up to 28 % in LP condition compared to their respective

non-silenced control plants **(Fig. 54-A).** *SlFBX2L1* silenced plants also showed a significant increase of 22 % in SAP activity under LP conditions, but no significant change in SAP activity in silenced Pi-sufficient plants was recorded **(Fig. 54-B).** This increase in soluble Pi accumulation and SAP activity was further investigated by qPCR analysis of selected PSI phosphate transporter (PHT) and acid phosphatase (PAP) genes. *PHT1* and *PHT7* transcripts showed an increase of 48 % and 72 % in the silenced plants under LP conditions, respectively. *PHT1* and *PHT7* transcripts showed a comparatively modest increase of 9 % and 25 % in HP conditions, respectively **(Fig. 54-D).**

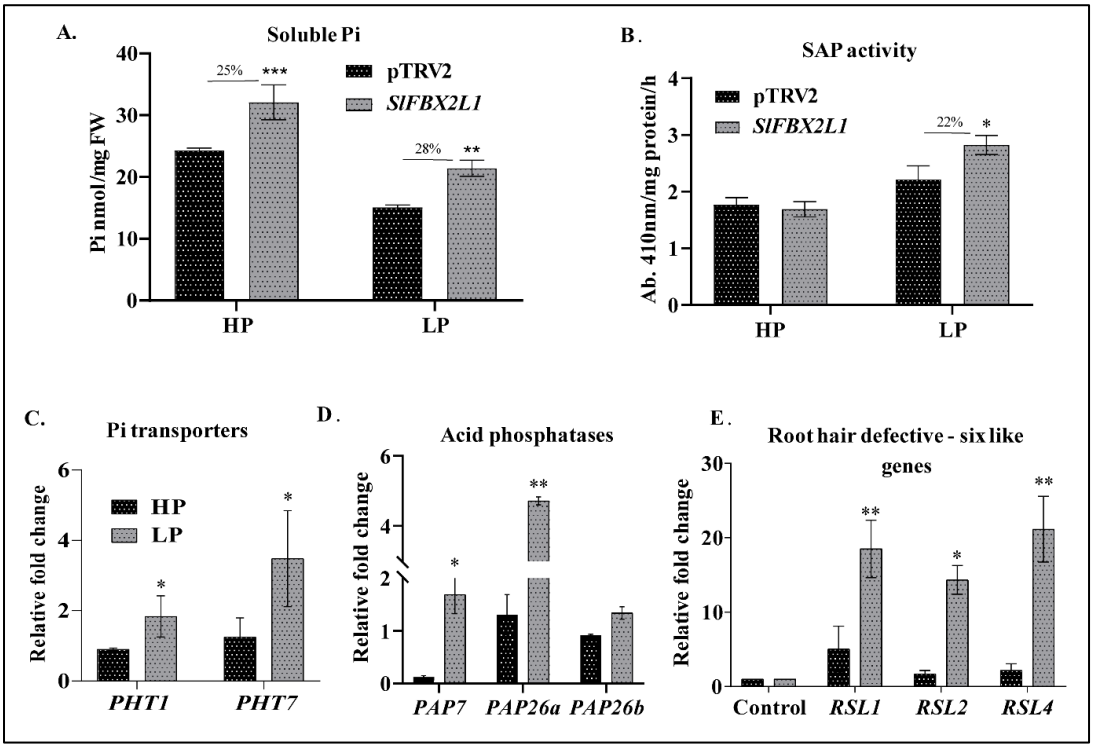

Fig. 54: Biochemical and molecular characterization of *SlFBX2L1* silenced plants. (A and B) Total soluble Pi content and SAP activity in the silenced and non-silenced seedlings under HP/LP conditions. **(C, D and E)** Transcript levels of Pi transporters, acid phosphatases, and Root hair defective-six-like (RSL) genes in *SlFBX2L1* silenced and non-silenced seedlings. The error bar depicts the standard deviation. One-way ANOVA was used for statistical analysis. **** shows P-value <0.05.

A similar trend in the transcript levels of *PAP7*, *PAP26a*, and *PAP26b* genes was observed in *SlFBX2L1* silenced plants, which showed an increase of 45 %, 77 %, and 80 %, respectively, for these genes in the LP condition. In the HP condition, *PAP7* transcript levels remained unchanged, *PAP26a* transcript levels were increased by 17 %, and *PAP26b* transcripts by 25 % in the silenced

plants compared to non-silenced plants **(Fig. 54-D).** The increased root hair length and root hair density in *SlFBX2L1* silenced plants was further validated by the upregulation of *RSL1*, *RSL2*, and *RSL4* genes in the silenced plants under HP and LP conditions. *RSL1*, *RSL2*, and *RSL4* transcripts were found to be considerably increased in the silenced plants than in non-silenced plants under LP and HP conditions **(Fig. 54-E).**

3.11. Functional characterization of *Slfbx2l1* knockout line under the low Pi availability

We next generated CRISPR/Cas9-based gene-edited knockout (KO) stable mutant tomato lines of *SlFBX2L1* gene. In total, six lines were generated. Out of these, four KO lines showed deletion of 2-base pairs, which disrupted the conserved motifs such as the WD domain in this protein. The loss of conserved domains suggested a severely altered function of the mutated protein in the KO background **(Fig. 55).**

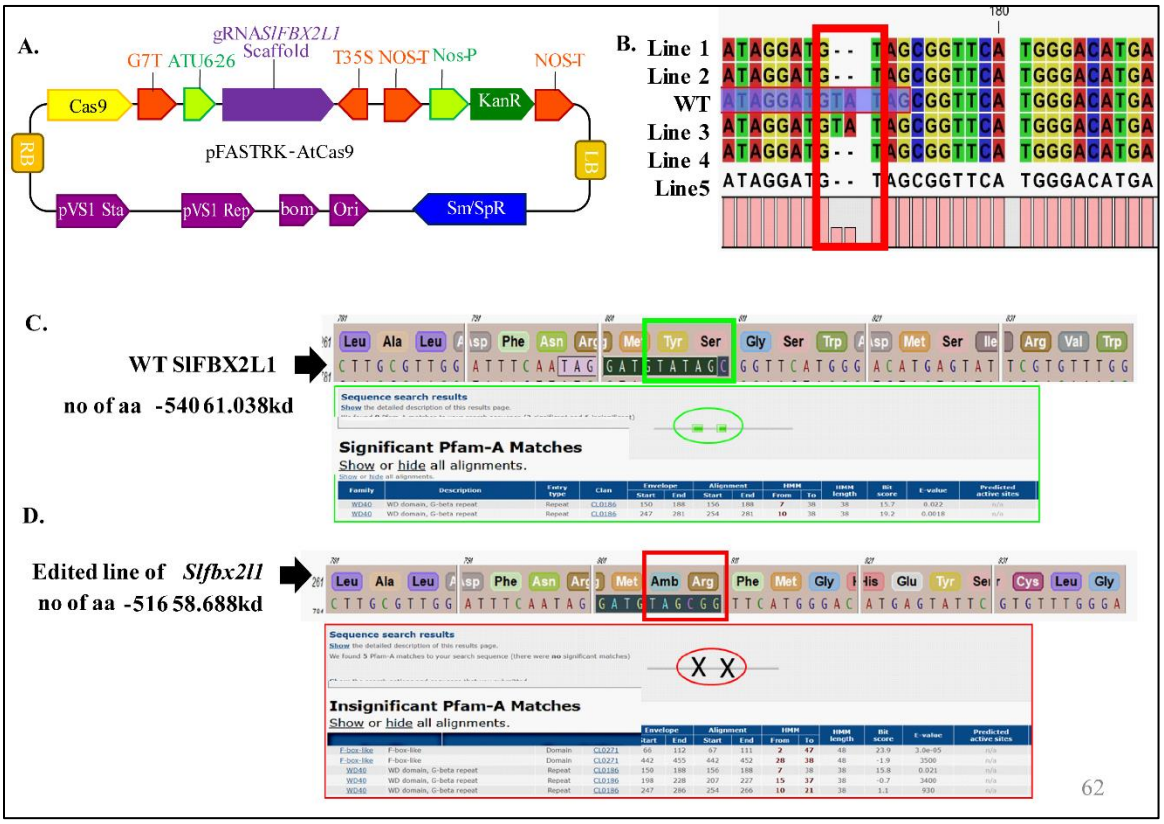

Fig. 55. Generation of *SlFBX2L1* CRISPR/Cas9 knockout tomato lines. Two base pairs deletion in the *SlFBX2L1* coding sequence disturbed the conserved domains in this protein. **(A and B)** Vector map of *pFASTRK-AtCas9-AtU6* and two base pairs deletion observed in the CRISPR edited KO lines in Pusa Ruby. **(C and D)** Domain structures of SlFBX2L1 protein sequences in WT and the edited KO lines.

Similar to VIGS plants, *Slfbx2l1* knockout lines showed more root hairs in 15-day-old seedlings compared to their respective control seedlings under HP and LP conditions (**Fig. 56-B and C**). The changed RSA, especially for root hairs, in the KO lines seedlings was further confirmed by the reduced transcript levels of two Root Hair Defective-Six Like genes (*RSL2* and *RSL4*) under HP and LP conditions **(Fig. 56-C).** Regarding biochemical attributes, the total P and soluble Pi levels significantly increased, with 41 % and 67 % enhancement in KO lines under HP and LP conditions **(Fig. 57-C).** After observing these PSR symptoms in the knockout lines, we checked the transcript levels of typical PSR marker genes to understand their behavior in the KO lines during LP conditions. The relative mRNA abundance of Pi transporters (*PHT2, PHT3, PHT5* and *PHT7*), phosphatases *(PAP10a, PAP26a*, and *PAP26b*) was significantly increased in the roots of the KO line plants compared with the WT counterparts under LP conditions (**Fig. 57-C and D)**.

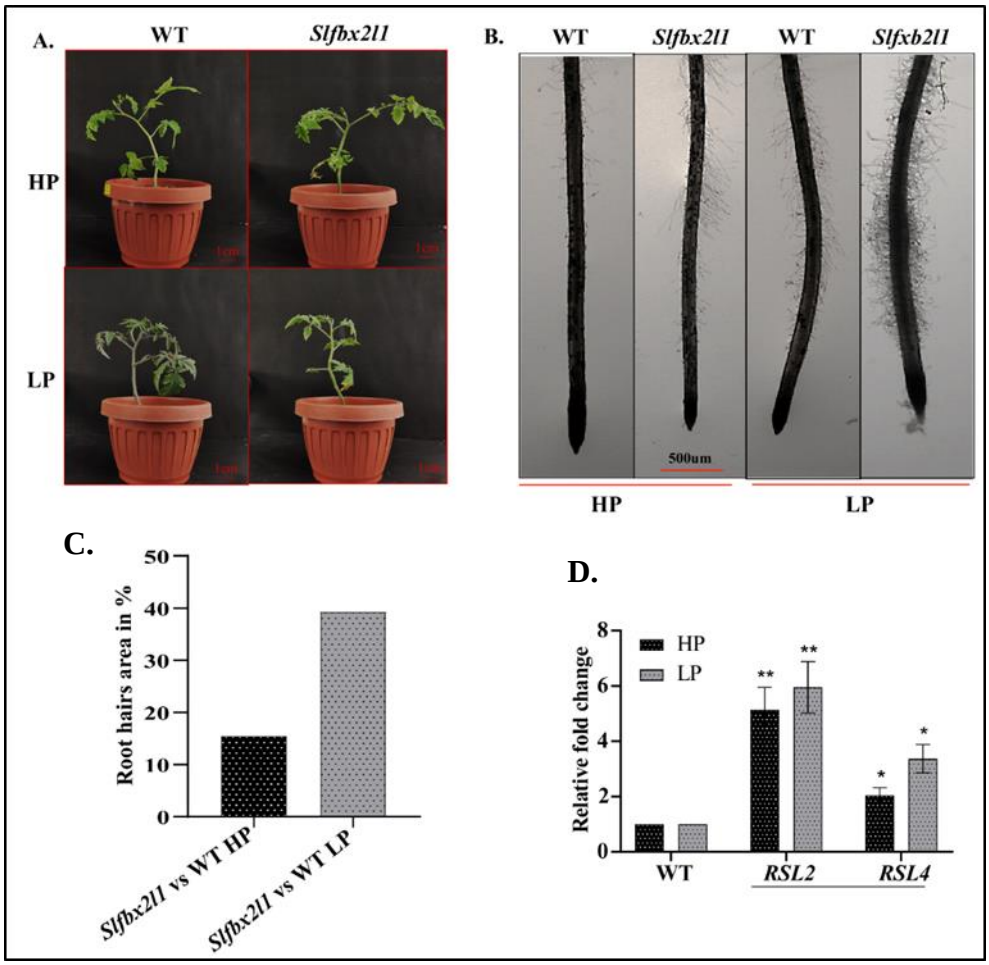

Fig. 56: RSA is altered in the *Slfbx2l1* KO lines. (A) The phenotype of KO lines and WT seedlings on HP and LP media. **(B and C)** Root hairs phenotype of KO line and WT seedlings on HP and LP media. **(D)** Transcript profiling of RSL genes in WT and KO line seedlings under HP/LP

conditions. Error bar shows standard deviation. One-way ANOVA was used for statistical analysis. **** depcits P-value <0.05.

Further, the KO line seedlings accumulated 39 % lesser total anthocyanins than WT seedlings under LP conditions. We did not find any such significant change in the knockout plants under HP condition **(Fig. 58-A and B).**

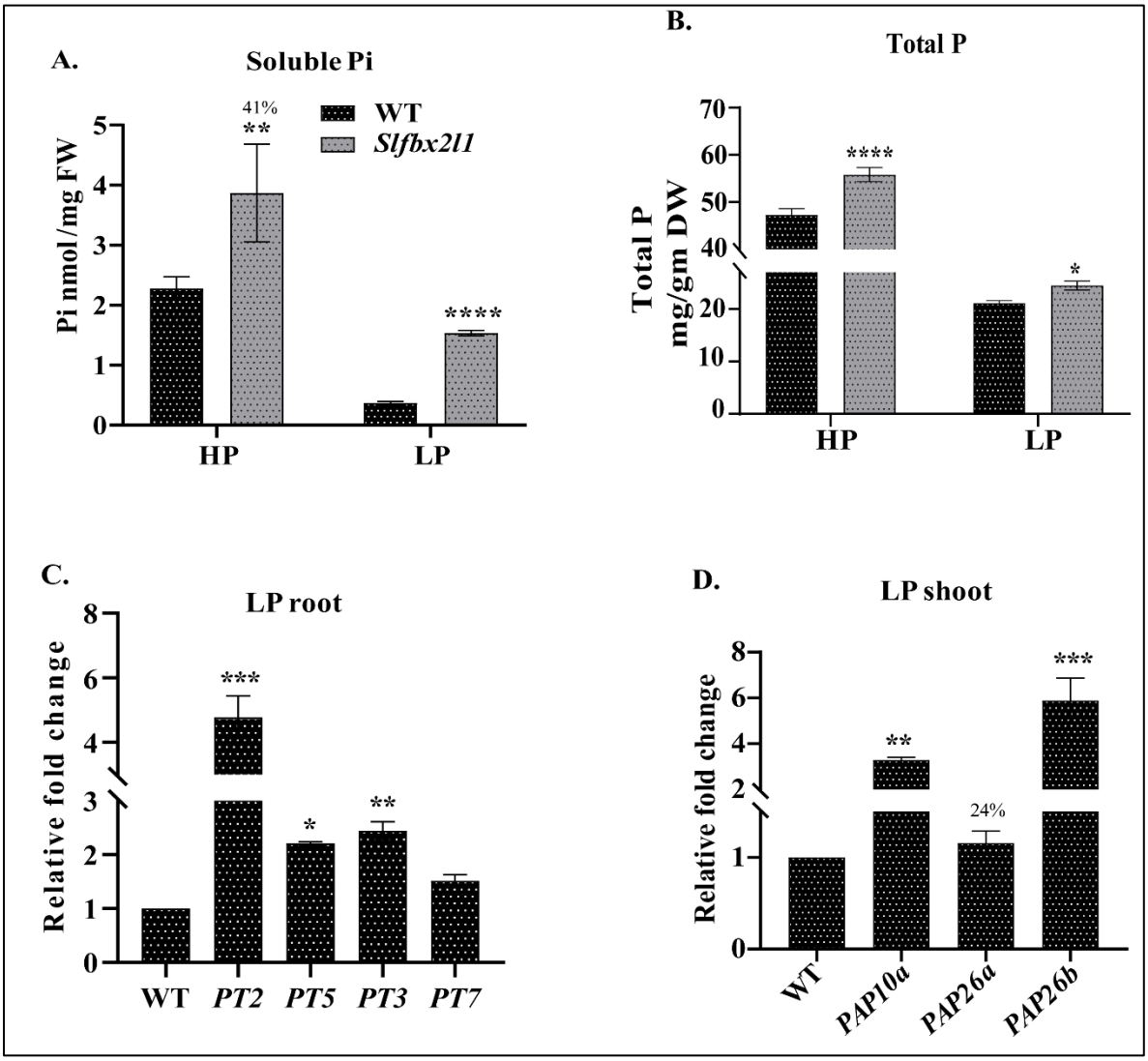

Fig. 57: *Slfbx2l1* KO line seedlings accumulate higher soluble Pi levels. (A) Total soluble Pi and total P accumulation in KO line and WT seedlings under HP and LP conditions. **(B and C)** Transcript profiling of Pi transporters (PHTs) and acid phosphatases in both the conditions in KO and WT seedlings by qPCR. Error bar shows standard deviation. One-way ANOVA was used for statistical analysis. **** depicts P-value <0.05.

Further, expression profiling confirmed the downregulation of regulators of anthocyanins biosynthesis pathway in KO line seedlings under HP and LP conditions. While *SlMYB28* transcript levels were reduced by 75 % and 82 %, a downregulation of 34 % and 54 % was observed in *SlMYB75* mRNA levels in the KO lines with respect to WT seedlings under HP and LP conditions, respectively **(Fig. 58-C).** Similarly, transcripts of the key genes of anthocyanins biosynthesis, such as *Dihydroflavonol 4-reductase* (*DFR*), is reduced by 73 % and 74 %, and *Flavanone 3-hydroxylase* (*F3H*) by 47 % and 75 % in the KO plants under HP and LP conditions, respectively **(Fig. 58-D).**

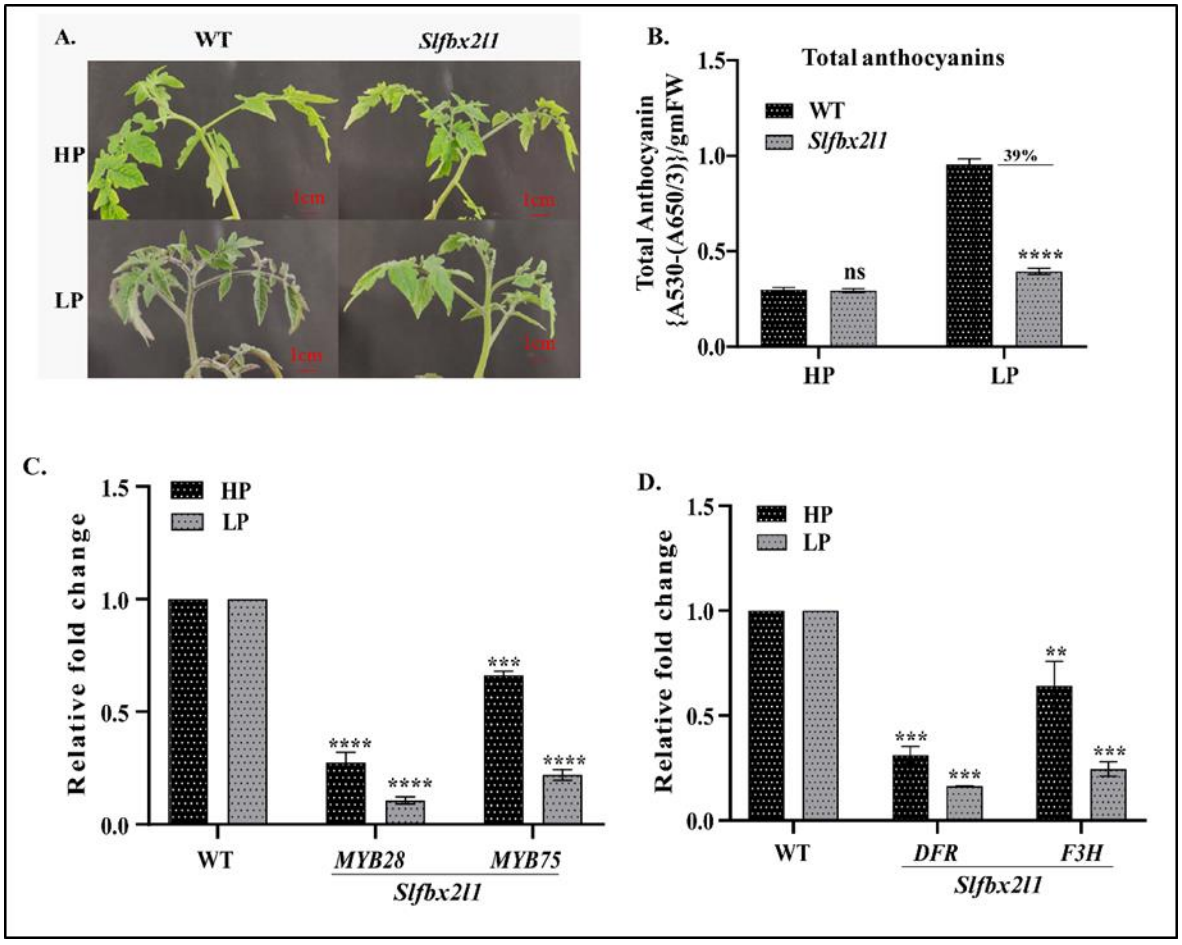

Fig. 58: *Slfbx2l1* KO plants accumulate higher anthocyanins levels. (A and B) Total anthocyanins estimation of *Slfbx2l1* KO line and WT seedlings grown on HP/LP media. **(C and D)** qPCR analysis of anthocyanins biosynthesis related gene for their expression in the WT and KO mutant backgrounds. DFR= Dihydroflavonol 4-reductase, F3H= Flavanone 3-hydroxylase. Error bar shows standard deviation. One-way ANOVA was used for statistical analysis. **** indicates P-value <0.05.

3.12. *Slfbx2l1* knockout affects fruit ripening

3.12.1. *Slfbx2l1* KO fruits show higher respiration and develop intense red coloration during ripening

Investigations of KO lines during fruit development showed that *SlFBX2L1* also plays a prominent role during ripening. In *Slfbx2l1* KO mutants, fruit ripening was altered as the fruits of these lines displayed accelerated transition from greenish-yellow (breaker stage) to orange color at 3-days post breaker (B+3) stage **(Fig. 59-A).** Surprisingly, these fruits produced only a few seeds compared to the WT fruits **(Fig. 59-B).** Since respiration is one of the important factors for climacteric fruit ripening in fleshy fruits, we checked the respiration rate in both WT and KO line fruits at B+3 and B+10. We observed a significantly higher respiration rate, which increased by 18 % and 45 % at B+3 and B+10 stages, respectively, in the KO fruits compared to WT fruits **(Fig. 59-C).**

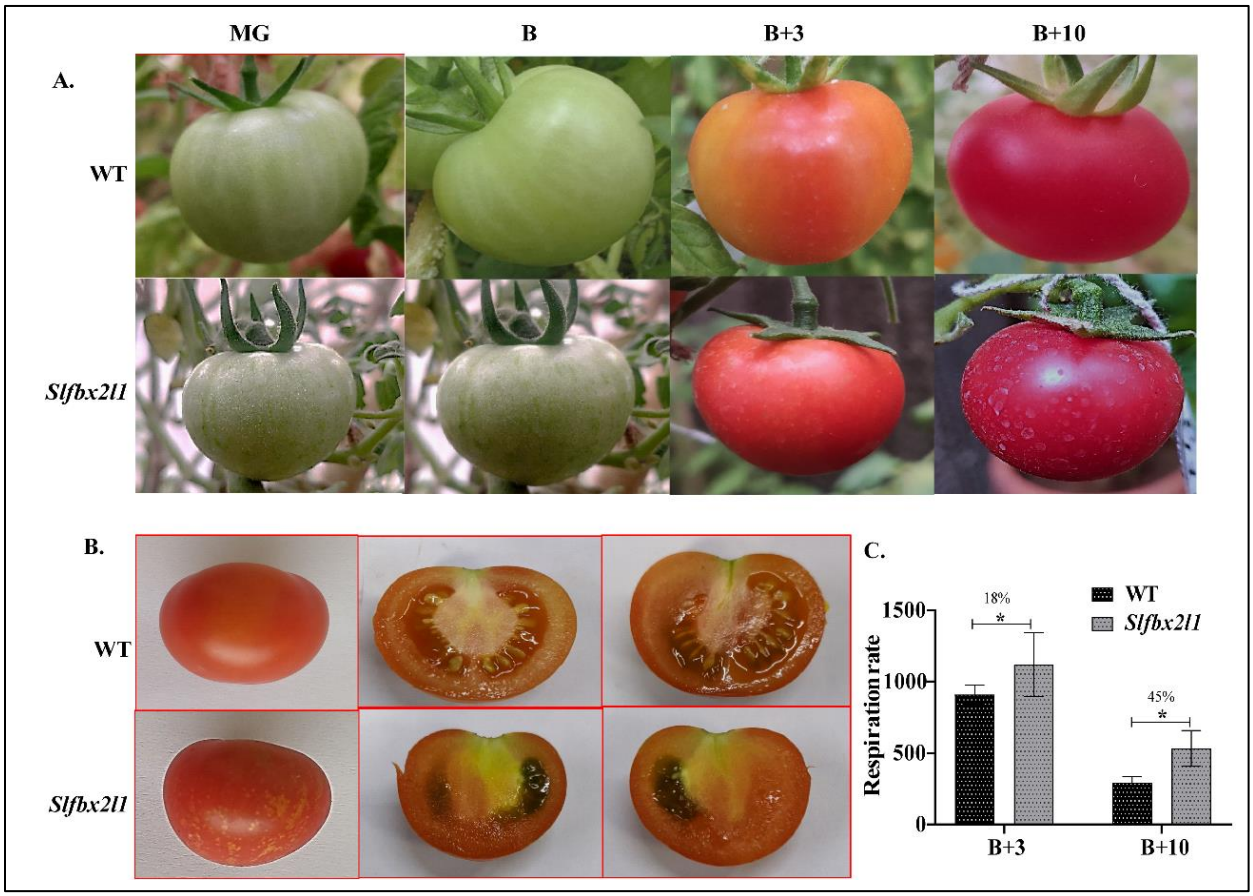

Fig. 59: Ripening phenotype of WT and *Slfbx2l1* KO line fruits. (A) Fruits shape, size and color of KO lines and WT. **(B)** Locules development. **(C)** Quantification of respiration rate by portable CO_2 gas analyzer in KO and WT fruits at breaker+3 (B+3) and B+10 stages. Error bar shows standard deviation. One-way ANOVA was used for statistical analysis. **** depicts P-value <0.05.

3.12.2. *Slfbx2l1* KO line fruits exhibit enhanced ethylene biosynthesis and signaling during ripening

Since the *Slfbx2l1* KO fruits exhibited accelerated ripening phenotype, we next investigated the ethylene levels in these fruits. Ethylene level was also enhanced by 20 % and 32 % at B+3 and B+10 stages, respectively, in the KO line fruits with respect to WT counterparts **(Fig. 61).**

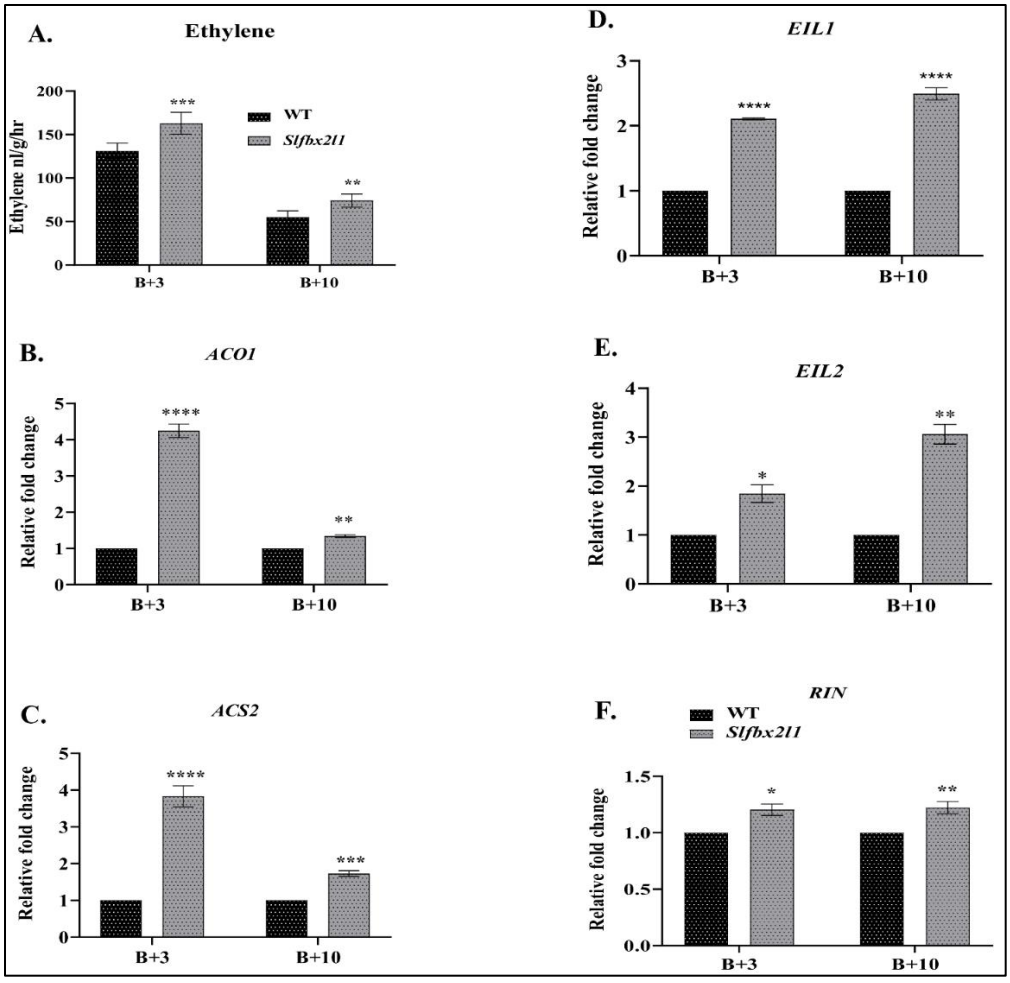

Fig. 60: Ethylene biosynthesis and signalling are perturbed in the *Slfbx2l1* mutant fruits. (A) Analysis of ethylene level by GC analyzer. **(B, C, D, E and F)** Expression levels of ethylene biosynthesis and signaling genes at B+3 and B+10 stages in WT and KO line fruits. ACO; Amino-cyclopropanecarboxylate oxidase, EIL; Ethylene insensitive like, and RIN; Ripening inhibitor. Error bar shows standard deviation. One-way ANOVA was used for statistical analysis. **** depicts P-value <0.05.

The quantitative real-time expression profiling of ethylene biosynthesis genes such as *ACS2* (*ACC Synthase2*) and *ACO1* (*ACC Oxidase1*) further supported enhanced ethylene biosynthesis in the KO fruits. These genes were found to be significantly upregulated in the *Slfbx2l1* knockout fruits at both the ripening stages **(Fig. 60-B and C).** Genes involved in the ethylene signaling pathway, like *Ethylene insensitive* (*EIL*) and ripening master regulator *Ripening Inhibitor* (*RIN*) were also found to be upregulated at B+3 and B+10 fruits stage as compared to WT fruits **(Fig. 60-D, E and F).**

3.12.3 *Slfbx2l1 KO* line fruits accumulate higher lycopene and β-carotene during ripening

Quantification of pigments using High-Performance Liquid Chromatography (HPLC) revealed that the *KO* mutant fruits accumulated significantly higher levels of lycopene at B+3 (increased by 68 %) and B+10 (increased by 22 %) stages than the WT fruits **(Fig. 61-A).** Interestingly, β-carotene was also increased in the *KO* fruits at both ripening stages, which increased by 79 % and 45 %, respectively, at B+3 and B+10 stages **(Fig. 61-B).**

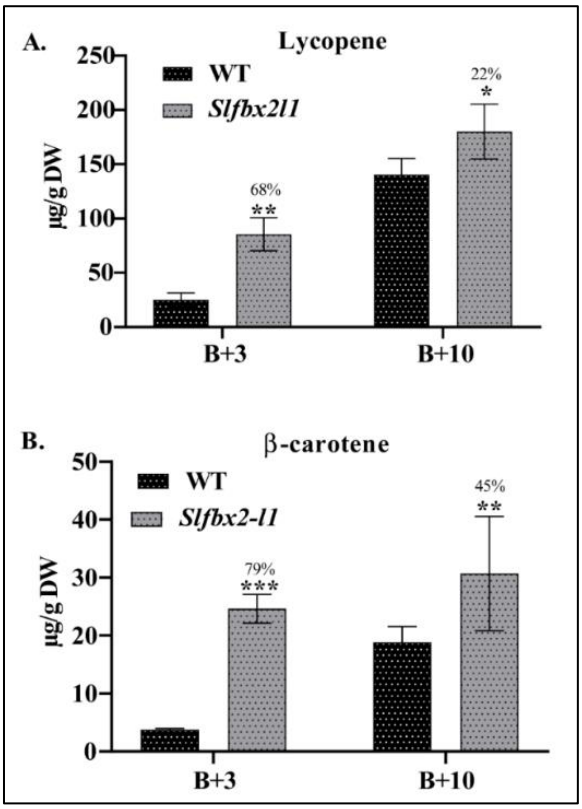

Fig. 61: HPLC-based estimation of fruit pigments. (A and B) Lycopene and β-carotene accumulation in WT and *KO* line fruits at B+3 and B+10 stages. Error bar shows standard deviation. One-way ANOVA was used for statistical analysis. **** shows P-value <0.05.

Since we observed the higher accumulation of lycopene and β -carotene levels in *KO* line fruits, we next performed TEM imaging of WT and KO line fruits at B+3 and B+10. This analysis confirmed the significantly increased accumulation of lycopene crystals in *KO* line fruits at B+3 and B+10 stages compared to WT fruits from the same stages **(Fig. 62).**

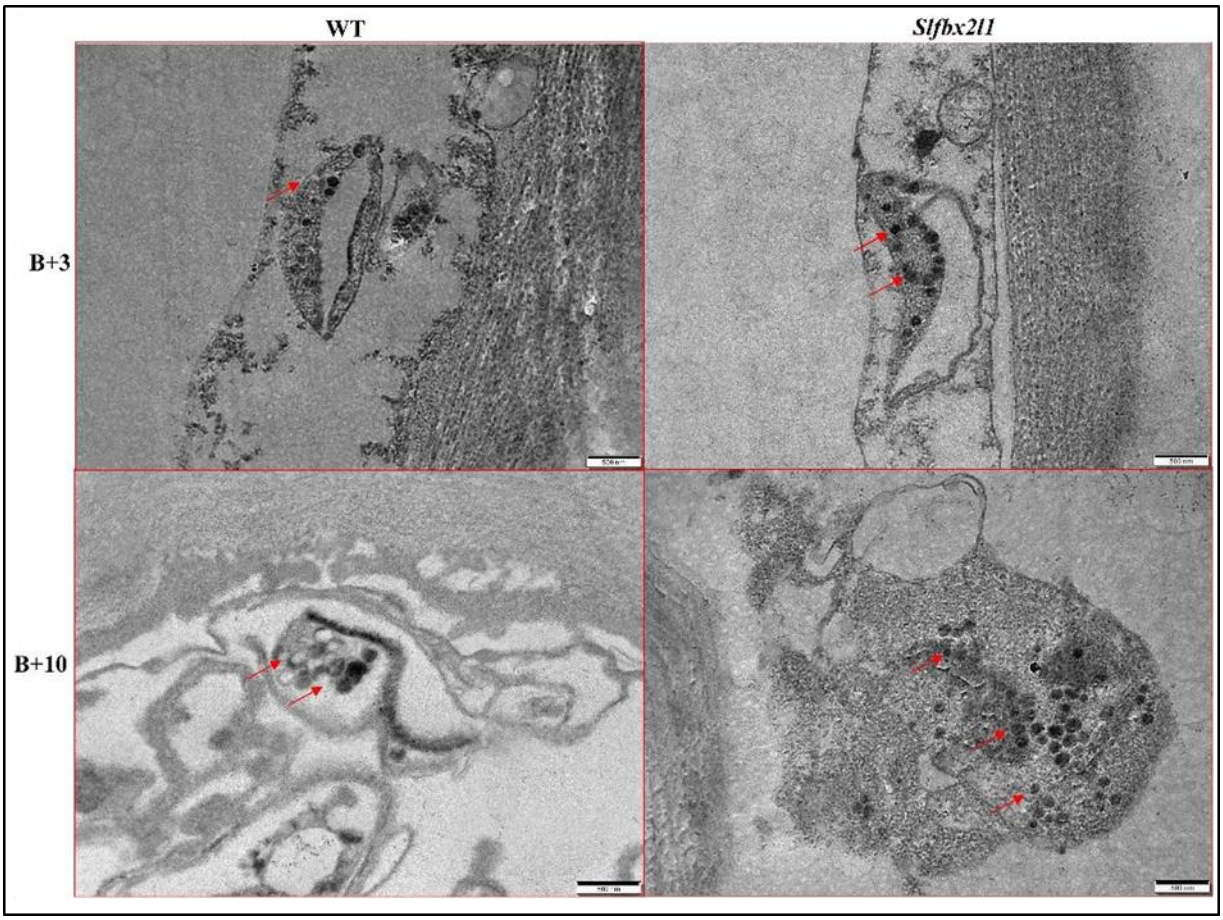

Fig. 62: Transmission electron microscopy of WT and KO line fruits at B+3 and B+10 fruits. Red arrow shows the lycopene crystals in the fruits.

Further, we confirmed the expression pattern of key genes of the carotenoid biosynthesis pathway. The transcript levels of *PSY1*, *PDS* and *ZDS* were found to be upregulated in the *KO* background fruits, supporting the increased lycopene biosynthesis **(Fig. 63-A, B and C).** Astonishingly, mRNA levels of β-carotene biosynthesis genes, such as *LCYB*, *LCYB1* and *LCYB2* were also increased in the *KO* fruits compared to their WT counterparts, substantiating the higher β-carotene levels observed in the HPLC data **(Fig. 63-D, E and F).**

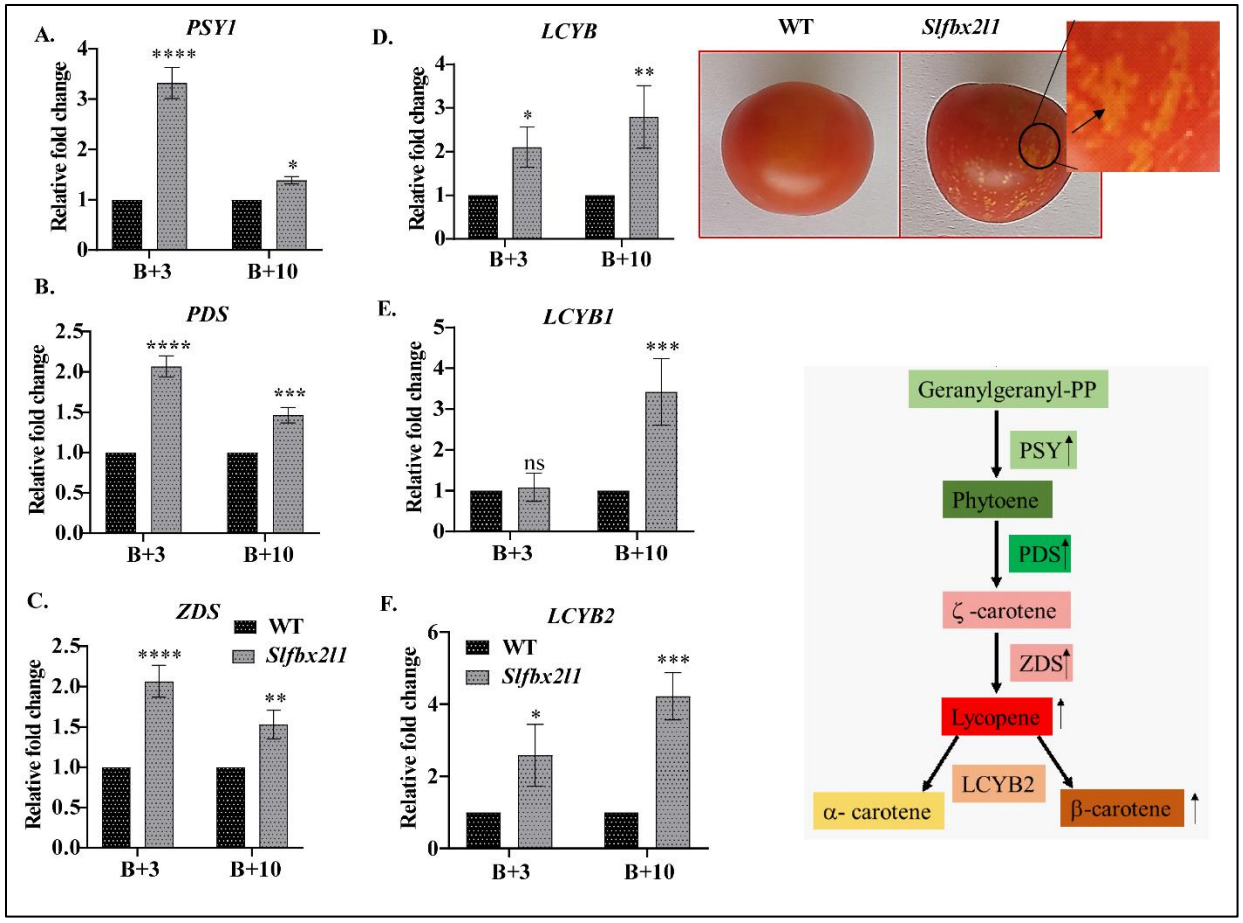

Fig. 63: Transcript levels of carotenoids biosynthesis pathway genes in WT and *Slfbx2l1* KO fruits during ripening. PSY1; Phytoene synthase 1, PDS; Phytoene desaturase, ZDS; Zeta-carotene desaturase, LCYB; Lycopene β-cyclase. The error bar shows standard deviation One-way ANOVA was used for statistical analysis. **** depicts P-value <0.05.

3.12.4. Genes encoding cell wall loosening enzymes are upregulated in *Slfbx2l1* KO fruits

Next, we checked the transcript levels of cell wall softening enzyme-related genes such *as Cellulose2* (*CEL2*), *Pectinesterase* (*PE*) and *Expansin1* (*EXP1*) and noticed upregulation in their expression at the B+10 stage in the knockout fruits compared to WT counterparts **(Fig. 64-A, B and C).**

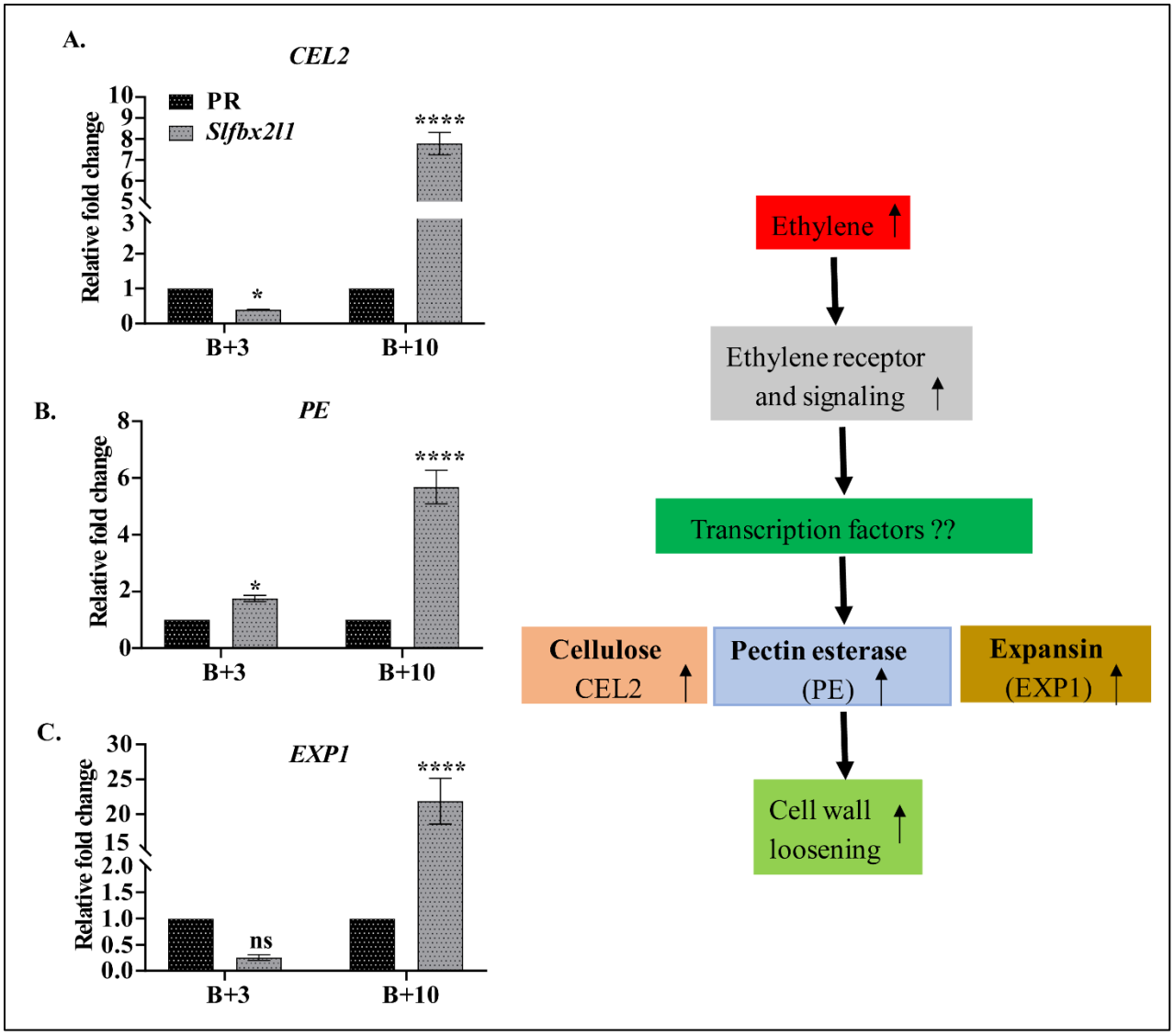

Fig. 64: Quantitative real-time PCR of cell wall loosening enzyme coding genes for their expression level in WT and *Slfbx2l1* KO fruits. CEL2; Cellulose2, PE; Pectinesterase and EXP1; Expansin1. Error bar shows standard deviation. One-way ANOVA was used for statistical analysis. **** shows P-value <0.05.

Discussion:

In this study, the Indian tomato cultivar Pusa Ruby has been used to catalog P starvation responses (PSR) and characterize the selected candidate genes functionally. The candidate PSI genes were identified using a transcriptomic approach in the Pi starvation condition. *Arabidopsis thaliana* has been used for the complementation study of the selected candidate *SlFBX2L1* gene and for the characterization of SlRbohH promoter activity. Besides the repeated use of the Virus-Induced Gene Silencing (VIGS) method, the CRISPR/Cas9 based gene-editing approach was also adopted for the characterization of the *SlFBX2L1* gene for its role in P starvation responses and fruit ripening. *Nicotiana benthamiana* was used for the transient gene expression studies for sub-cellular localization and promoter activity experiments with GUS as a marker protein.

Under most natural conditions, the concentration of available Pi in the soil is generally low and ranges between 0.65 μM to 2.5 mM [382]. Plants employ an array of well-coordinated morphological, physiological, biochemical, and molecular adaptations to orchestrate their response under chronic Pi limitation [115]. Transcriptional studies at the global scale in Arabidopsis have provided an in-depth insight into the molecular mechanisms underlying Pi starvation responses in plants [132,383,384]. However, these studies have primarily covered the transcriptional changes occurring within the first week of Pi starvation in mature seedlings. While PSR remains broadly conserved in plants, variations in plants' response to Pi-deficiency also exist between the model plant Arabidopsis and crop species. For example, in contrast to the characteristic shorter root phenotype in Arabidopsis, the primary roots of tomato seedlings tend to grow longer under Pi-deficiency [385,386]. Secondly, most genes belong to gene families, and BLAST search of Arabidopsis PSI genes against a crop's genomes often retrieves more than one close ortholog, making it difficult to choose the right candidate. Given these facts, precise information on the entire set of PSI genes in tomato was needed for the identification and subsequent functional characterization of candidate PSI genes.

To mimic the Pi deficient natural conditions, we germinated tomato seeds in the presence of 5 μM Pi and directly transferred them to either HP (High Pi/ Pi sufficient/non-limiting Pi) or LP (Low Pi/ Pi deficiency/ Pi limiting) conditions. The comprehensive morpho-physiological analysis revealed a more substantial effect of Pi starvation at 15-DAT compared to the 8-DAT time point. In contrast to the 8-DAT, prolonged Pi starvation led to longer primary roots, higher lateral root numbers, higher anthocyanins, and higher total carbohydrates. Besides the activation of high-

affinity Pi transporters, vacuolar Pi pools are utilized under chronic Pi limitation [387]. Physio-morphological analyses clearly showed that PSR in tomato seedlings becomes more robust under extended chronic Pi stress [385,388,389]. Accumulated literature also suggests higher levels of several sugars metabolites are essential for activating PSI genes under low Pi conditions [117,118]. In our metabolome study, we also observed a higher abundance of sugar metabolites, including sucrose, glucopyranose, fructopyranose, D-psicofuranose, and myoinositol with some other non-sugar metabolites in the Pi-deficient tomato seedlings than Pi sufficient plants at 8-DAT and 15-DAT. Therefore, we inspected the importance of sucrose on Pi starvation response by growing seedlings with and without sucrose. It became clear that sucrose supply enhances the robustness of PSR, as evident by the longer primary root length in seedlings, increased LR density, and higher SAP/APase activity of -P+S grown seedlings at 8-DAT/15-DAT. Along with these studies, we also witnessed higher induction of selected PSI genes in sucrose-supplied seedlings supporting the earlier observations [109,117,390]. The higher sucrose level in the metabolome data further signifies the importance of sucrose in PSR. The formation of two separate clusters by the Pi-starved seedlings at 8-DAT and 15-DAT in the PCA analysis suggests more robust metabolic alterations happening under extended Pi limitation. A more severe reduction in the phosphoric acid levels at 15-DAT might be required to maintain the intracellular Pi levels under chronic Pi limitation. The increased content of several amino acids under Pi stress in tomato seedlings is consistent with the previous findings [115]. Increased levels of malic acid and fumaric acid are compatible with the observation that these organic acids are profoundly synthesized and secreted in the rhizosphere, under extended chronic Pi limitation [15,115]

RNA-sequencing is a useful tool for profiling and quantifying transcripts in tomato [391]. Indeed, the activation of more transcripts at 15-DAT (922) than 8-DAT (669) in our RNA-seq data of Pi-starved seedlings reflects tomato seedlings experiencing severe stress at 15-DAT. A further decrease in the number of down-regulated genes at 15-DAT from 8-DAT provided additional support to the findings. Altogether, activating a larger set of genes than downregulated ones in Pi-starved seedlings at both time points reiterates the significance of gene activation over gene suppression in PSR [131,137–141,143,392]. The presence of 316 commonly upregulated transcripts at both time points implicates a broader role of these genes in Pi homeostasis in tomato. On the contrary, the time-point-specific DEGs indicate their temporally-regulated functions.

Gene ontology-based annotation of DEGs for ‘cellular component’ revealed that Pi starvation targets cell wall, membrane, and extracellular region function similarly at both time points. These findings are consistent with the earlier observations in wheat and soybean [393,394]. It further showed that while cytosolic components are enriched only at 8-DAT, vacuole and endoplasmic reticulum-related functions are affected more significantly upon extended starvation. Concerning the molecular function of the DEGs, genes with ‘metal ion binding, heme binding, iron ion binding, oxidoreductase activity, phosphatase activity, and transporter activity are equally affected at both time points. However, transcripts with ‘hydrolase activity’ seem to be activated only at 15-DAT. Under the ‘biological process’ category, the affected processes are broadly similar at both time points. Albeit, the glycolipid biosynthetic process only stimulates after prolonged Pi starvation. Enrichment of ‘metabolic pathways’, ‘phenylpropanoid pathways’, ‘glycerolipid metabolism’, and ‘secondary metabolite biosynthesis pathways’ in the KEGG analysis is consistent with the previous observations [134,383]. Differential regulation of many glycerolipid metabolism-related genes is consistent in Pi-starved seedlings and suggests that similar transcriptional changes underlie the rerouting of this metabolic process in different tissues of tomato [134].

Long-term Pi starvation-induced processes involve lineage-specific transcription factors (TFs) that play crucial roles in the regulation of gene expression [395]. No significant change in the transcripts of putative PHOSPHATE STARVATION RESPONSE1 (PHR1) homologs suggests that these genes are not responsive to Pi deficiency in tomato, unlike in Arabidopsis and rice [183,396]. The MYB transcription factors play pivotal roles in regulating the expression of PSI genes in plants [397–400]). Sharma et al. (2020) reported the identification of 127 MYB genes in the tomato genome. Differential regulation of other MYB transcription factor genes such as SlMYB13, SlMYB90, and SlMYB113 at both time points and in leaf and root tissues (Pfaff et al., 2020) [134] suggests that the three TFs play ubiquitous but perhaps overlapping roles during tomato PSR. Their direct involvement in regulating Pi-starvation-induced Anthocyanins accumulation cannot be ruled out. Upregulation of phenylpropanoid biosynthesis pathway genes, such as flavonol synthase (Solyc06g083910), flavanone 3-hydroxylase (Solyc02g083860), and Anthocyanins O-methyltransferase (Solyc09g082660) in the Pi starved seedlings not only corresponds to higher anthocyanins accumulation but also suggests that they may serve as the direct targets of these MYBs. The differential regulation of several other TFs belonging to AP2/ERF

(Solyc02g092050, Solyc01g090340) and bHLH (SlbHLH066, SlbHLH136) families indicates that together these TFs control transcriptional networks underlying PSR in tomato.

Differential regulation of several genes belonging to plant hormone biosynthesis and signaling pathways facilitate plant response to Pi deficiency [8,401]. In the DEGs list, ethylene response factors such as those encoded by Solyc02g092050, and SlERB.1B suggests their role in tomato PSR. Auxin is known to participate in Pi deficiency-induced root architectural changes in plants [21,122]. Down-regulation of several auxin signaling and metabolism-related genes such as SlGH3s (Solyc04g081250, Solyc01g107390, and Solyc01g107400), and SlSAURs (Solyc01g110560, Solyc06g072650) suggests that increased IAA levels probably mediate PSR in tomato by altering auxin signaling. Differential regulation of *SlGH3-2* (Solyc01g107390) is exciting because this gene is known to maintain IAA levels in tomato fruits during ripening [379]. Strong activation of carotenoid cleavage dioxygenase encoding gene (Solyc08g066650, SlCCD8) at both time points in the present study and the root-tissue provide strong evidence of the involvement of strigolactone as an endogenous signal of tomato PSR [134,402]. Similarly, down-regulation of an ethylene-forming gene, 1-aminocyclopropane-1-carboxylate oxidase (Solyc07g026650), in the common DEGs between root, leaf, and seedlings is in concordance with the previously published results in wheat and soybean [393,403].

Scrutiny of the GO and KEGG pathways revealed differential regulation of many genes responsible for sugar metabolism and transporter activity. Thus, we observed the transcript accumulation of sugar metabolism and its transporter-related genes in both 8-DAT and 15-DAT DEGs lists and in the data published by Pfaff et al. (2020) [134]. The majority of these genes showed upregulation of sugar metabolism genes such as sucrose biosynthetic process, sucrose-phosphate synthase, UDP-glucose metabolic process, UDP-glucose glucosyltransferase, UDP-sugar pyrophosphorylase, Starch biosynthesis process, Glycogen synthase, 1,4-alfa-glucan branching enzyme II and Glucose-6-phosphate 1-epimerase activity are commonly upregulated whereas, UDP-glucose 4-epimerase activity and UDP-glucose 4-epimerase 8-DAT specific and Glucose-1-phophate adenylyltransferase, Carbonyl reductase 1, Glucose dehydrogenase and UDP-glucose glucosyltransferase 15-DAT upregulated. Additionally, nine sugar transporter-related genes were differentially regulated at both time points. Among these, seven genes, including two genes of carbohydrate transporter, glucose transporter 8, glucose-6-phosphate translocator 2, myoinositol

transporter, and glucose-6-phosphate translocator, are commonly upregulated in both the LP tissues, whereas the hexose transporter gene and another carbohydrate transporter gene is upregulated at 8-DAT and 15-DAT time points, respectively.

In plants, activation of PAP genes and glycerol-3-phosphate permease (G3Pp) family genes regulate Pi homeostasis under Pi deficiency [84,404]. Up-regulation of many acid phosphatases and two G3Pp members in Pi-starved seedlings in this study suggests a broad set of phosphatases are involved in tomato PSR. This is also reflected by the enhanced root surface associated APase activity and SAP in LP-grown tomato seedlings, especially under prolonged treatment [405–407]. Previous studies have implicated four purple acid phosphatase genes in regulating enhanced PAP activity in tomato [98,407]. Identification of ten purple acid phosphatase genes, including *SlPAP1, SlPAP10b, SlPAP12, SlPAP15, SlPAP17b, SlPAP26a*, and *SlPAP26b*, in the 24 common DEGs in this category not only identifies the additional members of PSI PAPs in tomato but also highlights their vital contribution to SAP under different time-points of Pi starvation [84,407–410].

Organic acid excretion from roots into the rhizosphere includes two pathways: plasma membrane H+-ATPase for their efflux and channel-like transporters for passive efflux of their anions [411]. In the transcriptome, up-regulation of three aluminum-activated malate transporters (Solyc11g071350, Solyc05g009590, and Solyc08g006990), two cation/H^+ antiporter/transporters (Solyc08g081820, Solyc11g039980), and two Ca^{2+}/H^+ ATPase transporters (Solyc01g096190, Solyc02g092450) suggest their crucial role in Pi acquisition for the Pi-starved seedlings [393]. Enhanced production of organic acids is usually accompanied by elevated activity of PEP carboxylases, malate dehydrogenase, and citrate synthase enzymes in Pi-starved plants [412]. Five activated PEP carboxylase genes (Solyc04g006970, Solyc07g055060, Solyc04g009900, Solyc06g053620, and Solyc10g007290) in Pi-deficient seedlings at both 8-D and 15-D time points indicate enormously enhanced PEPC activity in tomato seedlings under Pi stress. More robust activation of the PEPC genes at 15-D than 8-D time points also reinforce the opinion that such activation increases gradually with the longer duration of stress treatment [178,383].

Pi levels are tightly associated with the intracellular levels of ATP, ADP, and related nucleoside Ps, and severe Pi stress is known to reduce their quantity [113,114]. Activation of inorganic pyrophosphate-dependent bypass enzymes is crucial for the metabolic adaptations of plants under depleted intracellular Pi [115]. Such changes facilitate the C flux for the enhanced synthesis

of organic acids in the glycolytic pathway under chronic Pi limitation and help plant survival under depleted ATP levels [115]. Activation of bypass enzymes such as pyrophosphate-dependent phosphofructokinase (Solyc04g014270, Solyc07g045160), pyruvate phosphate dikinase (Solyc01g080460), and UDP-sugar pyrophosphorylase (Solyc06g051080) under prolonged Pi stress suggests that similar transcriptional changes occur to ensure increased production of organic acids in the Pi starved tomato seedlings. Up-regulation of two alternative oxidases (Solyc08g005550 and Solyc08g075550) further contributes to such adaptation by maintaining the proper functioning of the mitochondrial citric acid cycle and electron transport chain with impaired ATP production, especially under long-term starvation [114,116]. Many genes involved in reactive oxygen species (ROS) production and scavenging are also differentially regulated in the Pi-starved tomato seedlings. ROS are recognized as critical players in plant stress signaling [413]. While the role of these genes in general stress responses is known, how these signals affect plant response to Pi deficiency warrants further studies.

Activation of several transporters, such as phosphate, glycerol-3-phosphate, sulfate, molybdate, zinc, and iron, show that a robust reprogramming of these genes is critical during PSR in tomato [178,383,393]. ICP-MS analysis also demonstrated the elevated levels of Zn and Mn in both root and shoot tissue, whereas Fe accumulation displayed reverse profiles in the two tissues, higher in shoots but lower in root tissues of Pi-deficient seedlings at 15-DAT. The relevance of the enhanced levels of these metal ions in Pi-deficient seedlings is still not clearly understood. However, decreased Zn levels are known to generate Pi toxicity due to higher accumulation and diminution of P regulation. At the same time, plants grown with a high concentration of Zn lead to Pi deficiency and enhanced APase activity [414]. Zn deficiency seedlings promote higher regulation of Pi transporter genes under high Pi and low Pi conditions in barley [415]. Thus, Zn maintains the P homeostasis in many plants but the role of enhanced levels of Zn in Pi-starved tomato seedlings is still not clear and warrants further investigations.

Reprogramming of root system architecture (RSA), generally to increase the surface area of roots, is a central response to almost all nutrient deficiencies [416]. Production of reactive oxygen species (ROS) such as superoxide anion (O_2^-) and hydrogen peroxide (H_2O_2) invariably underlies such reprogramming of RSA, indicating their critical role in altering root growth and development under mineral nutrient deficiencies [417]. The apoplastic reactive oxygen species are

generated mostly by NADPH oxidases (NOXs). NOXs are highly expressed in roots and are involved in the growth of root hairs, pollens, stomatal closure, nodule functioning, biotic response, and abiotic stress response. Our screening of tomato seedlings for RSA under Pi-deficient conditions revealed that primary root length, number of lateral roots, and root hairs significantly increased under low Pi at 8-DAT and 15-DAT. While more LR and denser and longer RHs under Pi starvation represents a conserved response in plants, the primary root length response varies in different plants, as evident from the longer primary roots of tomato and smaller roots in Arabidopsis under Pi starvation [13,263]. Further, Pi-limited medium-grown seedlings showed more intense staining near the root tip region than those grown in Pi-sufficient medium, indicating that O_2^- and H_2O_2 production is high compared to the control counterparts. H2DCFDA staining also suggests higher H_2O_2 accumulation in the root under low Pi conditions. Simultaneously, we also found higher NADPH oxidase activity in Pi-deficient roots. We also noticed more H_2O_2 and O_2^- production in the roots compared to shooting under Pi-starved conditions. Since cell growth is a fundamental process in all organisms, NOX genes have been implicated in polarized cell growth in plants. Rboh genes are apoplastic ROS-producing enzymes. Both ROS generation and polarized root growth are tightly associated with cell wall loosening and stiffening, which have been shown to be ROS and Rbohs-dependent. Jordan et al. (2019) reported that DPI inhibits ROS accumulation generated by Rbohs, and hampers plant growth [418]. Whereas H_2O_2-treated seedlings showed more root growth and improved K^+ retention in rice and sweet potato [419,420]. Further, we have also found inhibited root growth, low Pi accumulation, and lowering ROS production in 10nM DPI-treated seedlings under HP and LP conditions. Lateral root number and root hairs increased in the H_2O_2 (800μM) treated seedlings. These seedlings also accumulated higher Pi levels in both high and low Pi conditions. We expected a role of these genes in mediating enhanced root growth under Pi stress. In light of these facts, we studied the expression profiles of apoplastic ROS-generating genes at the mRNA level at multiple time points and in different tissues using in-house (unpublished) and recently published RNA-seq data [134]. In total, eight Rboh genes were identified in the tomato genome. Among these, a consistent induction in the transcripts of *SlRbohH* gene at all-time points and all three treated samples suggest a critical role of this candidate gene in the Pi starvation response in tomato. Further, online tools for gene expression profiling suggest that seven SlRboh genes are root preferential and only one Rboh gene is fruit-specific. The qPCR analysis of *SlRbohH* in different tomato tissues confirmed the root preferential expression of this gene

in tomato. Next, we studied the expression profile of *SlRbohH* gene in different minerals deficiency (-P, -Mg, -N, -K, and -Ca) and found the highest induction of this gene under Pi stress concerning others minerals nutrients. Therefore, we were curious whether the *SlRbohH* gene is an early or late-responsive during the low Pi condition. The transcript profiling showed its induction only at 8-DAT, which increased further to 15-DAT under low Pi conditions, ruling it out to be an early PSI gene. After 15 min and 4 h of Pi resupply, the instant recovery of its mRNA levels suggested the reversal of ROS levels caused by this gene under Pi-optimum conditions. We also found this gene as sucrose-dependent, as evidenced by the enhanced transcript level upon sucrose treatment under low Pi condition. P1BS conserved sequence (GNATATNC) is a *cis*-acting element that serves as the site for PHR1 homologs binding, hence regulating the mRNA abundance of many PSI genes under Pi deficiency [398]. Analysis of 1-kb upstream promoter region of this gene revealed the presence of two P1BS elements. The transactivation of *SlRbohH* was found to be under the direct control of PHR1 activity as this TF was found to bind to the pSlRbohH in our *in-planta* experiments. The results established SlPHR1L2 (SlPHL2) as the dominant regulator of PSR in tomato seedlings. Analysis of the promoter activity in stable Arabidopsis *SlRbohH:GUS* lines and higher GUS activity in the Pi-deficient roots only further validated the PSI nature of the *SlRbohH* gene. For functional characterization of the selected *SlRbohH* gene, it was cloned in a *pTRV2* vector for elucidating its role in PSR, especially reprogramming of RSA under Pi-stress through virus-induced gene silencing method. The photo-bleached leaves phenotype in the *pTRV2-PDS* silenced VIGS plants confirmed the effectiveness of the VIGS experiments. As expected, contrary to their *pTRV2* control (*SlRbohH* non-silenced) VIGS plants, the *pTRV2-SlRbohH* silenced plants showed strong suppression of this gene. The *SlRbohH* mRNA levels were significantly reduced by 75 % and 85 % in the silenced HP/LP seedlings, respectively. Morphological examination of the roots in non-limiting Pi conditions of *SlRbohH*-silenced plants showed reduced root length, root hairs and root hairs number compared to non-silenced plants. *SlRbohH*-silenced plants also accumulated less H_2O_2 as compared to non-silenced plants, as confirmed by H2DCFDA staining of the roots. At biochemical level, silenced plants accumulated reduced ROS levels (O_2^- and H_2O_2) compared to non-silenced seedlings. Decrease in the ROS levels was confirmed by performing NADPH oxidase enzyme activity in HP/LP non-silenced and silenced seedlings, respectively. Interestingly, *SlRbohH* silenced seedlings showed a significant reduction in the soluble Pi and total P content in both HP/LP seedlings, the magnitude of such decline was not severe in the pTRV2

control plants. Further, we found that there is moderate increase in root surface associated APase activity, as evident by BCIP staining, in *SlRbohH* silenced seedlings under low Pi availability. To explore the reason behind the elevated soluble Pi levels, especially under Pi-deficient condition, we studied the transcripts level of the selected PSI genes like phosphate transporter genes (*PHT1* and *PHT7*), PAPs, *miR399* and *SUC2*. We observed induction in these selected PSI genes transcripts upon 8-DAT and 15-DAT of Pi starvation in tomato seedlings in our RNA-seq data. These genes showed moderate induction in the *SlRbohH*-silenced seedlings than their pTRV2-control plants under Pi deficiency. Also, silencing of *SlRbohH* led to more Anthocyanins and carbohydrates accumulation under both condition (HP and LP) as compared to the non-silenced control seedlings. Altogether, VIGS based characterization of *SlRbohH* gene suggests its involvement in tomato PSR, including reprogramming of RSA and enhanced Pi-uptake efficiency for better survivability under Pi starvation condition in tomato seedlings.

The ubiquitin/proteasome protein degradation pathway regulates protein turnover in cellular processes [319]. F-box genes, an integral component of SCF-complexes of this pathway, belong to a large superfamily in plants. However, minimal information is available on these genes in tomato. The data mining of the tomato genome revealed at least 410 members constitute the F-box superfamily. Only 90 tomato members without any additional C-terminal domain (accounting for 22 % of the identified genes) and the remaining 78 % F-box with other motifs indicate that acquiring these new domains would be essential for the neofunctionalization of the duplicated genes during the evolution. Like many other plant species, except Arabidopsis, the absence of lectin-domain-related F-box genes in tomato is also intriguing [320,421]. The prevalence of LRR-containing F-box members in the identified tomato C-terminal domain containing members and the lowest number of WD40 repeat domain-containing F-box genes in tomato is in line with already reported FBD genes in Arabidopsis, rice, and chickpea [320,354,422].

The presence of 31.8 % F-box genes lacking any intron in tomato is exciting and indicates that intron-less genes' prevalence is ostensibly a unique feature of this superfamily [324]. Phylogenetic analysis grouped members of different subfamilies in separate clusters. However, the presence of FBL, FBX, FBK, FBA, and FBD members in more than one place in the phylogram and the contamination of specific groups by members of the other groups point towards a complex evolutionary ancestry of these genes. It further suggests that while it is easy to divide these genes,

based on their C-terminal domain, into different subfamilies, some members belonging to other subfamilies may have similar biological functions.

Gene duplication is an important phenomenon contributing to expanding genomes and functional diversification of gene families during evolution [421,423]. Among the identified 410 F-box genes, the presence of 192 (47 %) duplicated genes revealed that both segmental (11 %) and tandem (36 %) duplication events have contributed to the growth of this superfamily in tomato. These observations reiterate the significant role of tandem duplication events during the expansion of the F-box superfamily in plants [320,324,422]. It is anticipated that the amplification of these genes in such large numbers has probably matched with the increasing number of their putative substrate in plant genomes [354]. The overrepresentation of FBX, FBL, and FBA members in the duplicated blocks indicates that the frequency of duplication events may differ among different subfamilies within a superfamily. This conclusion supports the findings of a previous report where duplication events were suggested to occur in the form of waves, leading to a non-linear expansion of F-box subfamilies [424].

Sequence comparison of related sequences among close and distant taxa has augmented phylogenetic studies to construct the evolutionary lineage of a gene family [425]. The syntenic analyses of F-box genes in tomato and three other Solanaceae species, *S. pennellii* (70.5 %), potato (60.2 %), and pepper (37.3 %), revealed close evolutionary relationships of tomato F-box genes with its wild relative, followed by that of potato and pepper [364]. The most significant number of syntenic blocks within tomatoes and between tomato and potato is in the expected lines as tomato, *S. pennellii*, and potato belong to the same genus *Solanum*. Identification of only a few syntenic blocks (5.8 %) between tomato (asterids) and Arabidopsis (rosids) indicates that the two species are evolutionary distant and belong to different groups within eudicots. Due to the observed high sequence divergence between Arabidopsis and tomato F-box members, we cannot rule out the evolution of novel F-box genes for performing species-specific functions in the two genomes.

Previous studies have shown the involvement of F-box proteins in different aspects of plant development [332,334,336,426–431]. The undetected transcripts of 52 tandemly duplicated genes suggest that these genes might have very precise spatiotemporal mRNA accumulation, which is missing from the developmental stages undertaken in this study. The other possibility is that these genes are still evolving for novel functions and are yet to undergo transcription. Of the 192 dupli-

cated genes, different expression profiles for most duplicated gene pairs/blocks indicate their functional divergence. Altered expression of a few genes between wild-type and ripening mutants during fruit ripening directly implicates those members in the fruit ripening regulation. Three tomato EBF homologs (EBF1-3) are known to induce at the time of ripening induction. These genes also respond positively to exogenous ethylene treatment [431,432]. In the qPCR analysis, mostly unaltered transcript levels of the selected genes, except *Solyc04g074490*, revealed that, unlike tomato EBFs, ripening-associated expression of many F-box genes might remain independent of ethylene [433]. RNA-Seq is often employed to profile and quantify plant transcripts [391]. The differential expression of 55 tomato F-box genes in the RNA-seq data directly implicates them in Pi starvation responses. The consistent induction of eight PSI F-box genes, including *SlMEE66* and *SlPP2-B15,* in all three tissues, suggests a vital role of these proteins in Pi starvation response.

In Arabidopsis, a WD40 domain-containing F-box protein (AtFBOX2) regulates phosphate starvation responses; however, its mRNA levels remain unaffected under Pi deficiency [352]. We were intrigued by the extensive protein-protein interaction potential of AtFbx2 homolog Solyc06g073650 (SlFBX2L1) with other proteins, including TIR1 and EBF2, and hence decided to characterize it further for its potential roles in plant development. Transcriptional profiling demonstrated that this gene is moderately expressed throughout tomato development, though its maximum expression was observed in fruits and roots. Further, the SlFBX2L1 protein accumulates in the cytosol. Next, we have observed that in the *Atfbx2* mutant, root hair density is significantly increased compared to Col-0 in HP/LP condition. Also, in the *Atfbx2* mutant, the total Pi level is high with respect to Col-0 in both high and low Pi conditions. Upon expression of *35S*:*SlFBX2L1* gene in *Atfbx2* mutant plants, we observed the reversal of low Pi-induced root phenotypes and Pi levels in the *SlFBX2L1* complemented lines. These lines showed fewer root hairs with lower Pi levels than *Atfbx2* mutant plants. These results suggest a conserved function of *FBX2* homologs in plant development and during PSR in plants. Therefore, we investigated the role of *SlFBX2L1* in tomato and found a significant increase in the root hairs density, with the expression level of RSL genes, in both *SlFBX2L1* VIGS plants and *Slfbx2l1* KO lines in both HP/LP conditions. Additionally, the soluble Pi and total P levels were enhanced in the VIGS plants and *Slfbx2l1* KO lines in both HP/LP conditions. These observations found good support in changes observed at the molecular level, as confirmed by the higher expression of Pi transporters and PAPs genes in the

SlFBX2LI modulated plants. *Slfbx2l1* CRISPR knockout lines showed increased Pi acquisition efficiency and accumulated lower levels of anthocyanins, as evident by both spectrophotometric estimation and expression profiling of its biosynthesis-related genes, indicating that the higher Pi levels in the mutant plants alleviate the severity of PSR under low Pi availability.

Interestingly, the *Slfbx2l1* CRISPR knockout fruits displayed fastened ripening phenotype. Respiration, ethylene biosynthesis, and its signaling are important for the ripening program in climacteric fleshy fruits [434]. The significantly higher respiration rate and ethylene level at ripening stages (B+3 and B+10) in KO fruits as compared to WT fruits explains their overripening phenotype. Further, higher transcript accumulation of ethylene biosynthesis-related genes *ACO1*, *ACS2,* and its signalling pathway-related genes *EIL1, EIL2,* and master regulator, *RIN,* at both the stages of KO fruits suggested enhanced ethylene biosynthesis and signaling underlies the fast ripening response in KO fruits. Since KO fruits were intensely red with yellow spots on the fruits, compared to WT fruits, we found significant enhancement in the lycopene content in KO fruits than in wild-type counterparts. Increased transcript levels of carotenoid biosynthesis pathway genes such as PSY1, PDS, and ZDS further supported the higher lycopene level in KO fruits. The KO line fruits also showed small yellow dots, which were absent in WT fruits. HPLC analysis revealed significantly enhanced levels of β-carotene at the red-ripe stages in KO fruits than their WT counter parts. The enhanced transcript levels of *LCYB*, *LCY1,* and *LCYB2* genes in KO fruits at both ripening stages provided good support with the improved β-carotene in these fruits. Overall, the upregulation of carotenoid biosynthesis pathway genes and increased lycopene and carotene in KO line fruits support the previous observations [435–437]. Accumulation of a significantly higher number of lycopene crystals in the KO line fruits in electron microgram and upregulation of most MEP pathways genes further confirmed the HPLC data on overaccumulation of lycopene and β-carotene in edited fruits. Such over-ripening phenotype could be attributed to enhanced ethylene biosynthesis and signalling in KO fruits. We suspect the involvement of EBF2, an interacting partner of *SlFBX2L1* and a negative regulator of ethylene signaling, in influencing both root and fruit traits in *Slfbx2l1* KO lines.

Summary and Conclusion:

In summary, we first cataloged the Pi starvation response at morpho-physiological and biochemical levels in an Indian tomato cultivar Pusa Ruby. Global untargeted metabolites profiling indicated enhanced sugar levels in the Pi-deficient seedlings. Further characterization revealed that sugars, mainly sucrose, are a vital regulator of PSR as it is required for altered RSA, robust activation of many PSI genes, and enhanced secretion of APases. Transcriptome studies identified a list of candidate PSI genes, including sugar metabolism and transport, phosphatases, PHT1 transporters, metal ion transporters, transcription factors, etc., in Pi-deficient tomato seedlings. Increased Zn levels in the Pi-deficient seedlings are an interesting phenomenon and need further investigation to decipher the functional relevance of such increment. Overall, the transcriptome study captured the global-level changes in the transcripts and identified several candidate genes. One a such gene (*SlRbohH*) belongs to NADPH-oxidase gene family. NOX genes contribute to apoplastic ROS formation. The DPI and H_2O_2 treatment to tomato seedlings revealed that inhibited NOX activity and optimally enhanced ROS levels have opposite effects of RSA and Pi accumulation in tomato seedlings grown under HP or LP conditions, revealing a pivotal role of ROS in PSR. *SlRbohH* was consistently upregulated by Pi starvation throughout the plant, though it is a root preferential gene. VIGS based silencing of this gene was found to affect RSA and other Pi starvation responses, indicating its active involvement in Pi-stress mitigation in tomato seedlings. Manipulation of another candidate gene, *SlFBX2L1*, an F-box protein, using VIGS or CRISPR/Cas9-based gene-editing revealed the function of this gene in both RSA and fruit ripening. *SlFBX2L1* was identified as a negative regulator of root hair formation and Pi accumulation in plants under HP and LP conditions. Astonishingly, the *SlFBX2L1* KO lines also exhibited elevated fruit pigmentation, indicating a de-repression of the carotenoids biosynthesis pathway in tomato fruits. It is anticipated that such diverse functions of *SlFBX2L1* could emerge due to its physical interaction with two important proteins, TIR1 and EBF2, auxin and ethylene signaling pathway genes, in tomato. Overall, the study provides comprehensive details of PSR in tomato seedlings and identifies potential candidate genes regulating it. Functional characterization of *SlRbohH* and *SlFBX2L1* also reveals their involvement in plant development and PSR. However, further investigations are warranted to uncover the underlying molecular regulatory mechanisms of their diverse actions from root to fruit tissues.

Table 6: List of the selected most prominent upregulated genes in Pi-deficient tomato seedlings.

SGN ID	Gene description	FC (log2 mean signal values) 8-D LP/HP	pValue	FC (log2 mean signal values) 15-D LP/HP	pValue
Glycerolipid metabolism					
Solyc02g094400	Glycerophosphodiester phosphodiesterase (GDPD2)	2.93	2.28E-05	5.01	4.14E-07
Solyc11g012410	Inositol monophosphatase 3	1.67	0.0015	2.73	4.32E-06
Solyc08g007080	Inositol 1, 4, 5-trisphosphate 5-phosphatase	1.86	0.0005	1.37	0.0110
Solyc10g076710	Phospholipase C	1.58	0.0308	1.45	0.0325
Solyc01g100020	Phospholipase D	5.73	1.78E-18	7.03	3.16E-20
Solyc09g065180	UDP-glucose 4-epimerase	1.07	0.0381	0.47	0.5436
Solyc08g082440	UDP-galactose 4-epimerase	-0.89	0.0846	1.31	0.0219
Solyc08g063080	UDP-sulfoquinovose synthase	1.46	0.0061	1.52	0.0077
Solyc09g014300	UDP-sulfoquinovose:DAG sulfoquinovosyltransferase	2.61	5.06E-06	3.36	1.31E-06
Solyc10g085100	UDP-sulfoquinovose:DAG sulfoquinovosyltransferase	3.59	3.20E-10	4.25	1.64E-11
Solyc10g017580	Digalactosyldiacylglycerol (DGDG) synthase 2	1.70	0.0013	2.40	3.14E-05
Solyc08g006640	Monogalactosyldiacylglycerol (MGDG) synthase 1	0.39	0.4423	1.48	0.0068
Solyc07g007620	Monogalactosyldiacylglycerol (MGDG) synthase 2	5.51	1.37E-17	4.97	2.59E-12
Solyc12g009820	Monogalactosyldiacylglycerol (MGDG) synthase 3	0.48	0.3978	2.18	0.0060
Solyc10g007960	Allene oxide synthase 3	3.30	9.39E-06	1.90	0.0428
Metabolic activity and stress-related genes					
Solyc01g090660	Carotenoid cleavage dioxygenase	5.20	4.60E-05	4.98	1.99E-05

Solyc03g078500	Glycosyltransferase	7.86	1.71E-24	9.46	1.41E-26
Solyc04g009900	Phosphoenolpyruvate carboxylase kinase	3.60	3.40E-10	5.54	1.37E-15
Solyc07g045160	Pyrophosphate-dependent phosphofructokinase	2.45	7.57E-06	2.41	4.62E-05
Solyc01g080460	Pyruvate phosphate dikinase	1.36	0.009572	nd	Nd
Solyc06g051080	UDP-sugar pyrophosphorylase	2.08	8.87E-05	2.26	5.17E-05
Solyc08g005550	Alternative oxidase	nd	nd	2.26	0.005226
Solyc08g075550	Alternative oxidase1b			2.17	0.000468
Solyc04g006970	Phosphoenolpyruvate carboxylase	1.75	0.000941	3.00	1.87E-07
Solyc07g055060	Phosphoenolpyruvate carboxylase 1	2.15	0.000259	3.30	5.89E-06
Solyc06g053620	Phosphoenolpyruvate carboxylase 1	1.45	0.018348	2.44	0.000135
Solyc04g016490	Phosphohydrolase	2.91	0.0002	5.16	1.30E-08
Solyc04g054740	Myo-inositol-1-phosphate synthase	6.44	5.44E-17	4.10	3.76E-10
Solyc05g007950	Extracellular ribonuclease	5.22	7.55E-17	5.70	3.23E-15
Solyc05g009960	Taurine catabolism dioxygenase	3.26	0.0196	4.39	0.0022
Solyc06g071240	Glutamine-dependent NAD+ synthetase	5.26	3.26E-05	4.14	1.27E-06
Solyc08g080190	Choline dehydrogenase	3.16	0.0024	3.90	3.17E-05
Solyc10g054910	Peptidyl-prolyl cis-trans isomerase	6.83	8.42E-23	7.39	6.96E-17
Solyc10g085100	Glycosyltransferase	3.59	3.20E-10	4.25	1.64E-11
Solyc11g072800	NADPH oxidase (SlRboh)	3.76	9.99E-10	5.06	1.34E-14
Solyc11g066390	Superoxide dismutase (SOD)	2.02	0.0002	1.33	0.0271
Solyc10g076220	Peroxidase 1	1.42	0.0086	1.67	0.0048
Solyc03g080150	Peroxidase	1.43	0.0090	1.74	0.0041
Solyc05g006740	Glutathione S-transferase (GST)	1.12	0.0352	1.21	0.0346
Solyc09g007150	Glutathione S-transferase (GST)	2.34	0.0010	1.90	0.0011
Solyc02g065190	Cytochrome P450	1.63	0.0082	1.60	0.0135

Solyc08g079300	Cytochrome P450	5.07	9.23E-05	6.08	3.59E-05
Solyc02g082960	Chitinase	1.78	0.0175	4.47	5.27E-09
Solyc12g056240	Glutathione peroxidase (GPX)	1.27	0.0157	1.41	0.0092
Phenylpropanoid pathway					
Solyc00g282510	Phenylalanine ammonia-lyase	-1.90	0.0004	-1.28	0.019397
Solyc02g085020	Dihydroflavonol 4-reductase	1.84	0.3870	4.70	0.002143
Solyc05g053170	Chalcone synthase-A	2.36	0.0001	1.61	0.128255
Solyc02g067870	Putative chalcone isomerase	3	0.0005	-0.13	1
Solyc06g083910	Flavonol synthase	1.50	0.0251	2.88	5.03E-05
Solyc02g083860	Flavanone 3-hydroxylase	0.85	0.1219	1.98	0.0008
Solyc09g082660	Anthocyanins O-methyltrans-ferase	2.90	0.0473	5.58	0.0003
Proteins of un-known func-tions					
Solyc01g096400	Unknown Protein	3.20	1.45E-06	4.41	1.90E-11
Solyc01g109100	Unknown Protein	3.32	8.03E-08	3.60	1.98E-09
Solyc04g007730	Unknown Protein	3.91	1.38E-10	5.57	5.54E-11
Solyc04g015120	U-box domain protein	6.29	2.14E-19	7.07	4.47E-17
Solyc04g050820	Unknown protein	5.16	0.001399	4.27	0.0007
Solyc07g042400	Unknown Protein	8.12	3.09E-26	9.73	7.41E-26
Solyc07g053900	Unknown function	6.85	1.54E-22	8.78	1.07E-20
Solyc09g091060	Unknown Protein	3.28	4.56E-07	3.40	1.36E-08

Table 7: List of primers used in the study.

S.N.	Primers Sequences	FP/ RP	Sol ID	Name	Type
1	GGCTGCAATCAAGGAGGAA	FP	Solyc05g014470	GAPDH	qPCR
2	AAATCAATCACACGGGAACT	RP	Solyc05g014470	GAPDH	qPCR
3	TCTCAACCCTAAGGCCAACAGAGAG	FP	Solyc11g005330	Actin	qPCR
4	TCTCTCGGTGAGGATCTTCATCAGG	RP	Solyc11g005330	Actin	qPCR
16	TGGCGAACGATTTGCAAGTG	FP	Solyc09g090070	PT1	qPCR
17	ATGCCAGCAATCACAATCGC	RP	Solyc09g090070	PT1	qPCR
18	TGCTGCTGTTTTCGCTATGC	FP	Solyc09g066410	PT7	qPCR
19	TGCTTGAGGAACCGTTGAAC	RP	Solyc09g066410	PT7	qPCR
5	CGCATGAAAATGCCCGAAAC	FP	Solyc03g005555	PT2	qPCR
6	CCTCGCTTTCAATTTCCACCTG	RP	Solyc03g005555	PT2	qPCR
7	TTCGCGATGCAAGGATTTGG	FP	Solyc09g090080	PT3	qPCR
8	TCCATACGAAATCAGCCTCAGG	RP	Solyc09g090080	PT3	qPCR
9	TTGCCGGCCTTGTTTCAATG	FP	Solyc06g051860	PT5	qPCR
	AGACGATCCGCCAGACATAATC	RP	Solyc06g051860	PT5	qPCR
10	TCCAACTTTGCAGGACTCA	FP	Solyc02g078210	Pho2	qPCR
11	CTTTGAATACTCTTTCGCACA	RP	Solyc02g078210	Pho2	qPCR
12	ACACTCTATTGGCATGCAAC	FP	NR_108003	mir399	qPCR
13	GCAACTCTCCTTTGGCATT	RP	NR_108003	mir399	qPCR
20	TGCTTGAAGAGGCAGTTCAG	FP	Solyc10g049720	RSL2	qPCR
21	TAGGCAATGGGAGCATACATCC	RP	Solyc10g049720	RSL2	qPCR
22	CCAAAACAAGGGCAAGTAGAGG	FP	Solyc12g088380	RSL4	qPCR
23	TGTGCTTAAGTCAACCCTTGC	RP	Solyc12g088380	RSL4	qPCR
24	AGCCAAGAATCGTCGAGAAC	FP	Solyc02g091440	RSL6	qPCR
25	TTGCCAACACCTTCACTTGC	RP	Solyc02g091440	RSL6	qPCR
26	ATCAGCTTCTTCCTACCATGCC	FP	Solyc03g121420	HAD	qPCR
27	AACAACCCGAGGAATTGCAG	RP	Solyc03g121420	HAD	qPCR
28	ATGGAATCGGCGATTTCTGC	FP	Solyc06g062540	Phospho1	qPCR
29	TGGACCCCTGCTTTTACTAGTG	RP	Solyc06g062540	Phospho1	qPCR
36	ATTCTCGTCCTCGTTCTCATCC	FP	Solyc10g086250	*SlMYB75*	qPCR
37	TTGAGAAGTTCCGAGGTTGAGG	RP	Solyc10g086250	*SlMYB75*	qPCR

38	GGACTGAACAAGAAGATCTCCTC	FP	Solyc10g086270	*SlMYB28*	qPCR
39	TCAGACCAGCTCTTATGGGAAC	RP	Solyc10g086270	*SlMYB28*	qPCR
40	CCTGATGGGAATTGATGGAG	FP	Solyc02g094400	*SlGDPD2*	qPCR
41	TGAACCTTTTCCTCCCCTTC	RP	Solyc02g094400	*SlGDPD2*	qPCR
42	CTGCAGGGCATAATGAATAGATGTG-TATTTGAACTTAATT	FP	Solyc11g072800	*SlRbohH*	Promoter
43	CCTAGGTTTACACAAAATTCTCTTCTTCTTCTTCTTTATGT	RP	Solyc11g072800	*SlRbohH*	Promoter
14	CCTTTATCCCTCTCCCTGACG	FP	Coat protein seq	CP	PCR VIGS confirma-tion
15	CCATCAAGTCAGCAGGACCG	RP	Coat protein seq	CP	PCR VIGS confirma-tion
32	AGGCTGTTAGTGGCTGGGGGTA	FP	Solyc06g073650	*SlFBX2L1*	gene edit confirma-tion
33	AGATCCGAGCCTGCTGTGCT	RP	Solyc06g073650	*SlFBX2L1*	gene edit confirma-tion
30	TGATCTAGAATATCCCATAATCTT-GAAGGCTTCTCTC	FP	Solyc11g072800	*SlRbohH*	VIGS
31	AGAGGATCCCTGATCATTTAGGATA-TATTGAGATATGGC	RP	Solyc11g072800	*SlRbohH*	VIGS
34	ATCCATG GAC ATGGCATTTGAATG	FP	Solyc06g073650	*SlFBX2L1*	OX PCR
35	AGACTAGTGGCCTTCACCTTCCA	RP	Solyc06g073650	*SlFBX2L1*	OX PCR

Table.8. Differentially expressed genes in the RNA-seq transcriptome data

S.N.	Gene id	Expression status	S.N.	Gene id	Expression status	S.N.	Gene id	Expression status
1	Solyc03g114910	Up regulated	51	Solyc02g084850	Up regulated	101	Solyc09g090010	Up regulated
2	Solyc01g104400	Up regulated	52	Solyc10g006290	Up regulated	102	Solyc05g007950	Up regulated
3	Solyc03g114890	Up regulated	53	Solyc07g064600	Up regulated	103	Solyc11g045160	Down regulated
4	Solyc03g116700	Up regulated	54	Solyc01g095150	Up regulated	104	Solyc02g065740	Up regulated
5	Solyc07g008140	Up regulated	55	Solyc12g008510	Down regulated	105	Solyc03g114860	Up regulated
6	Solyc12g015690	Up regulated	56	Solyc02g079960	Down regulated	106	Solyc07g055730	Up regulated
7	Solyc02g088380	Up regulated	57	Solyc02g082850	Down regulated	107	Solyc01g060070	Up regulated
8	Solyc03g121180	Up regulated	58	Solyc03g025610	Down regulated	108	Solyc06g010010	Up regulated
9	Solyc09g083390	Down regulated	59	Solyc06g007180	Down regulated	109	Solyc11g045440	Up regulated
10	Solyc04g008230	Up regulated	60	Solyc08g079020	Down regulated	110	Solyc12g088420	Up regulated
11	Solyc05g044615	Down regulated	61	Solyc08g080570	Down regulated	111	Solyc05g005680	Up regulated
12	Solyc09g014300	Up regulated	62	Solyc10g054870	Down regulated	112	Solyc03g078500	Up regulated
13	Solyc10g085100	Up regulated	63	Solyc01g006630	Up regulated	113	Solyc08g006410	Down regulated
14	Solyc09g065155	Down regulated	64	Solyc01g018020	Up regulated	114	Solyc09g008060	Up regulated
15	Solyc10g017580	Up regulated	65	Solyc01g058720	Up regulated	115	Solyc01g105350	Up regulated
16	Solyc08g061480	Up regulated	66	Solyc01g098700	Up regulated	116	Solyc09g098080	Up regulated
17	Solyc09g009830	Up regulated	67	Solyc01g111900	Up regulated	117	Solyc12g005840	Up regulated
18	Solyc11g066950	Up regulated	68	Solyc04g006970	Up regulated	118	Solyc09g074930	Down regulated
19	Solyc02g085100	Up regulated	69	Solyc06g051080	Up regulated	119	Solyc01g096190	Up regulated
20	Solyc07g042830	Up regulated	70	Solyc07g014640	Up regulated	120	Solyc02g070450	Up regulated
21	Solyc08g005665	Up regulated	71	Solyc07g055060	Up regulated	121	Solyc04g080750	Up regulated
22	Solyc08g005720	Up regulated	72	Solyc07g062810	Up regulated	122	Solyc08g063090	Up regulated
23	Solyc08g066650	Up regulated	73	Solyc08g082440	Up regulated	123	Solyc04g081870	Up regulated
24	Solyc09g007190	Up regulated	74	Solyc09g010380	Up regulated	124	Solyc03g111570	Down regulated
25	Solyc11g008250	Up regulated	75	Solyc10g007290	Up regulated	125	Solyc04g074110	Up regulated
26	Solyc08g066720	Up regulated	76	Solyc10g085830	Up regulated	126	Solyc02g081050	Up regulated
27	Solyc04g078460	Down regulated	77	Solyc06g059990	Down regulated	127	Solyc01g103660	Up regulated
28	Solyc04g054740	Up regulated	78	Solyc04g007650	Down regulated	128	Solyc05g050980	Up regulated
29	Solyc06g062430	Up regulated	79	Solyc02g089350	Up regulated	129	Solyc08g005650	Up regulated
30	Solyc01g101180	Down regulated	80	Solyc11g011210	Up regulated	130	Solyc04g081300	Up regulated
31	Solyc04g014270	Up regulated	81	Solyc02g092120	Up regulated	131	Solyc05g007830	Up regulated
32	Solyc03g117590	Down regulated	82	Solyc07g049460	Down regulated	132	Solyc06g049050	Up regulated
33	Solyc08g078850	Up regulated	83	Solyc03g083840	Up regulated	133	Solyc02g088100	Up regulated
34	Solyc03g111140	Down regulated	84	Solyc08g069040	Up regulated	134	Solyc01g099650	Up regulated
35	Solyc11g011960	Up regulated	85	Solyc02g092110	Up regulated	135	Solyc03g097420	Up regulated
36	Solyc01g101170	Down regulated	86	Solyc02g091920	Up regulated	136	Solyc08g075240	Up regulated
37	Solyc02g067750	Down regulated	87	Solyc03g031800	Up regulated	137	Solyc02g014300	Down regulated
38	Solyc02g078860	Down regulated	88	Solyc05g046290	Down regulated	138	Solyc03g083360	Up regulated
39	Solyc01g103390	Up regulated	89	Solyc09g008320	Up regulated	139	Solyc01g015080	Down regulated
40	Solyc02g081340	Up regulated	90	Solyc12g098610	Down regulated	140	Solyc01g110280	Up regulated
41	Solyc05g051750	Up regulated	91	Solyc01g094970	Down regulated	141	Solyc02g069490	Up regulated
42	Solyc05g054590	Up regulated	92	Solyc01g102910	Down regulated	142	Solyc04g054730	Down regulated
43	Solyc06g083070	Up regulated	93	Solyc02g090470	Down regulated	143	Solyc06g075650	Up regulated
44	Solyc07g045160	Up regulated	94	Solyc01g005120	Up regulated	144	Solyc06g060760	Up regulated
45	Solyc07g049560	Up regulated	95	Solyc02g085120	Up regulated	145	Solyc03g019820	Down regulated
46	Solyc09g011590	Up regulated	96	Solyc05g007940	Up regulated	146	Solyc01g006360	Down regulated
47	Solyc10g078320	Up regulated	97	Solyc06g082420	Up regulated	147	Solyc01g080570	Down regulated
48	Solyc12g097080	Up regulated	98	Solyc07g006560	Up regulated	148	Solyc01g106820	Down regulated
49	Solyc04g050820	Up regulated	99	Solyc09g084460	Up regulated	149	Solyc02g062890	Down regulated
50	Solyc06g071240	Up regulated	100	Solyc10g076220	Up regulated	150	Solyc02g071090	Down regulated

S.N.	Gene id	Expression status	S.N.	Gene id	Expression status	S.N.	Gene id	Expression status
151	Solyc02g071350	Down regulated	201	Solyc03g122360	Up regulated	251	Solyc12g019480	Up regulated
152	Solyc02g082070	Down regulated	202	Solyc04g008250	Up regulated	252	Solyc12g043030	Up regulated
153	Solyc02g085745	Down regulated	203	Solyc04g008900	Up regulated	253	Solyc12g056760	Up regulated
154	Solyc02g088560	Down regulated	204	Solyc04g054990	Up regulated	254	Solyc12g056960	Up regulated
155	Solyc03g020060	Down regulated	205	Solyc04g074740	Up regulated	255	Solyc12g088920	Up regulated
156	Solyc03g094000	Down regulated	206	Solyc04g077420	Up regulated	256	Solyc01g009830	Up regulated
157	Solyc04g083140	Down regulated	207	Solyc04g078140	Up regulated	257	Solyc02g077550	Up regulated
158	Solyc07g009130	Down regulated	208	Solyc04g079300	Up regulated	258	Solyc03g118940	Up regulated
159	Solyc07g017610	Down regulated	209	Solyc04g079760	Up regulated	259	Solyc08g079300	Up regulated
160	Solyc08g014010	Down regulated	210	Solyc05g006020	Up regulated	260	Solyc11g011285	Up regulated
161	Solyc08g079310	Down regulated	211	Solyc05g008580	Up regulated	261	Solyc03g025730	Up regulated
162	Solyc09g005330	Down regulated	212	Solyc05g012700	Up regulated	262	Solyc02g087880	Up regulated
163	Solyc09g066400	Down regulated	213	Solyc05g047680	Up regulated	263	Solyc05g006550	Down regulated
164	Solyc09g092600	Down regulated	214	Solyc05g047710	Up regulated	264	Solyc11g010920	Up regulated
165	Solyc10g078280	Down regulated	215	Solyc05g055400	Up regulated	265	Solyc05g051400	Up regulated
166	Solyc10g081200	Down regulated	216	Solyc06g005560	Up regulated	266	Solyc01g058410	Up regulated
167	Solyc10g086570	Down regulated	217	Solyc06g005750	Up regulated	267	Solyc06g050870	Up regulated
168	Solyc11g056670	Down regulated	218	Solyc06g034290	Up regulated	268	Solyc10g048065	Up regulated
169	Solyc12g056160	Down regulated	219	Solyc06g064440	Up regulated	269	Solyc09g075210	Down regulated
170	Solyc12g096310	Down regulated	220	Solyc06g064570	Up regulated	270	Solyc02g089620	Up regulated
171	Solyc12g100250	Down regulated	221	Solyc06g072950	Up regulated	271	Solyc07g006500	Down regulated
172	Solyc10g079690	Down regulated	222	Solyc06g074090	Up regulated	272	Solyc04g015750	Down regulated
173	Solyc01g006640	Up regulated	223	Solyc06g084130	Up regulated	273	Solyc08g066120	Down regulated
174	Solyc01g010350	Up regulated	224	Solyc07g006850	Up regulated	274	Solyc02g089840	Up regulated
175	Solyc01g080680	Up regulated	225	Solyc07g021700	Up regulated	275	Solyc09g057950	Up regulated
176	Solyc01g087890	Up regulated	226	Solyc07g041500	Up regulated	276	Solyc11g007000	Up regulated
177	Solyc01g091320	Up regulated	227	Solyc07g042400	Up regulated	277	Solyc05g055110	Down regulated
178	Solyc01g095330	Up regulated	228	Solyc07g063930	Up regulated	278	Solyc02g093335	Up regulated
179	Solyc01g095980	Up regulated	229	Solyc08g074495	Up regulated	279	Solyc12g013880	Up regulated
180	Solyc01g111350	Up regulated	230	Solyc08g076670	Up regulated	280	Solyc01g106220	Down regulated
181	Solyc02g065190	Up regulated	231	Solyc08g078960	Up regulated	281	Solyc01g112010	Up regulated
182	Solyc02g069750	Up regulated	232	Solyc08g080430	Up regulated	282	Solyc03g113940	Up regulated
183	Solyc02g081040	Up regulated	233	Solyc09g007765	Up regulated	283	Solyc10g086250	Up regulated
184	Solyc02g081890	Up regulated	234	Solyc09g008910	Up regulated	284	Solyc04g009910	Up regulated
185	Solyc02g082170	Up regulated	235	Solyc09g011360	Up regulated	285	Solyc03g120380	Up regulated
186	Solyc02g084810	Up regulated	236	Solyc09g015170	Up regulated	286	Solyc08g021820	Down regulated
187	Solyc02g084930	Up regulated	237	Solyc09g060100	Up regulated	287	Solyc04g082840	Up regulated
188	Solyc02g086650	Up regulated	238	Solyc09g098190	Up regulated	288	Solyc10g082020	Up regulated
189	Solyc02g089890	Up regulated	239	Solyc10g005500	Up regulated	289	Solyc01g090760	Up regulated
190	Solyc02g091590	Up regulated	240	Solyc10g006150	Up regulated	290	Solyc08g066510	Up regulated
191	Solyc02g092230	Up regulated	241	Solyc10g009310	Up regulated	291	Solyc01g099410	Up regulated
192	Solyc02g093430	Up regulated	242	Solyc10g009590	Up regulated	292	Solyc07g062400	Down regulated
193	Solyc03g026130	Up regulated	243	Solyc10g055770	Up regulated	293	Solyc03g095510	Up regulated
194	Solyc03g031530	Up regulated	244	Solyc10g083880	Up regulated	294	Solyc08g075840	Down regulated
195	Solyc03g079980	Up regulated	245	Solyc11g008610	Up regulated	295	Solyc08g075760	Up regulated
196	Solyc03g083010	Up regulated	246	Solyc12g005590	Up regulated	296	Solyc09g015770	Up regulated
197	Solyc03g093140	Up regulated	247	Solyc12g005710	Up regulated	297	Solyc01g005390	Down regulated
198	Solyc03g097840	Up regulated	248	Solyc12g006460	Up regulated	298	Solyc01g087420	Down regulated
199	Solyc03g114940	Up regulated	249	Solyc12g008490	Up regulated	299	Solyc01g110180	Down regulated
200	Solyc03g120020	Up regulated	250	Solyc12g017880	Up regulated	300	Solyc03g045030	Down regulated

S.N.	Gene id	Expression status	S.N.	Gene id	Expression status	S.N.	Gene id	Expression status
301	Solyc03g111710	Down regulated	351	Solyc12g017860	Up regulated	401	Solyc08g048290	Up regulated
302	Solyc03g120910	Down regulated	352	Solyc12g055990	Up regulated	402	Solyc08g068850	Up regulated
303	Solyc04g050520	Down regulated	353	Solyc03g059270	Up regulated	403	Solyc09g091400	Up regulated
304	Solyc06g035940	Down regulated	354	Solyc01g079385	Down regulated	404	Solyc09g098310	Up regulated
305	Solyc06g053220	Down regulated	355	Solyc02g093190	Up regulated	405	Solyc10g049580	Up regulated
306	Solyc07g026675	Down regulated	356	Solyc02g038740	Down regulated	406	Solyc11g007780	Up regulated
307	Solyc09g009250	Down regulated	357	Solyc03g032020	Down regulated	407	Solyc11g069250	Up regulated
308	Solyc09g090970	Down regulated	358	Solyc10g007600	Down regulated	408	Solyc02g067190	Up regulated
309	Solyc09g091000	Down regulated	359	Solyc09g061840	Up regulated	409	Solyc08g062200	Up regulated
310	Solyc10g075030	Down regulated	360	Solyc04g008730	Up regulated	410	Solyc09g075820	Up regulated
311	Solyc10g075035	Down regulated	361	Solyc11g044910	Down regulated	411	Solyc02g083480	Up regulated
312	Solyc10g079380	Down regulated	362	Solyc04g072850	Up regulated	412	Solyc03g080150	Up regulated
313	Solyc11g006720	Down regulated	363	Solyc10g085225	Up regulated	413	Solyc04g081860	Up regulated
314	Solyc11g056650	Down regulated	364	Solyc12g019440	Up regulated	414	Solyc05g046020	Up regulated
315	Solyc11g069160	Down regulated	365	Solyc11g071350	Up regulated	415	Solyc05g055320	Up regulated
316	Solyc02g094270	Down regulated	366	Solyc01g104750	Up regulated	416	Solyc07g047740	Up regulated
317	Solyc01g096790	Up regulated	367	Solyc03g097580	Up regulated	417	Solyc07g049240	Up regulated
318	Solyc01g108610	Up regulated	368	Solyc04g064620	Up regulated	418	Solyc08g013930	Up regulated
319	Solyc02g070440	Up regulated	369	Solyc05g005960	Up regulated	419	Solyc08g075830	Up regulated
320	Solyc02g077610	Up regulated	370	Solyc07g014690	Up regulated	420	Solyc12g005370	Up regulated
321	Solyc02g087840	Up regulated	371	Solyc07g006900	Up regulated	421	Solyc01g009400	Down regulated
322	Solyc02g089210	Up regulated	372	Solyc01g099880	Down regulated	422	Solyc02g089260	Down regulated
323	Solyc02g091440	Up regulated	373	Solyc02g071520	Up regulated	423	Solyc12g013700	Down regulated
324	Solyc02g092050	Up regulated	374	Solyc04g064610	Down regulated	424	Solyc01g006320	Up regulated
325	Solyc02g092450	Up regulated	375	Solyc09g010200	Up regulated	425	Solyc02g080670	Up regulated
326	Solyc03g078630	Up regulated	376	Solyc01g100880	Up regulated	426	Solyc04g071900	Up regulated
327	Solyc04g005100	Up regulated	377	Solyc01g100920	Down regulated	427	Solyc04g082140	Up regulated
328	Solyc04g008820	Up regulated	378	Solyc11g012930	Down regulated	428	Solyc05g055910	Up regulated
329	Solyc04g077220	Up regulated	379	Solyc02g079440	Down regulated	429	Solyc07g052240	Up regulated
330	Solyc04g080500	Up regulated	380	Solyc03g013440	Down regulated	430	Solyc10g008440	Up regulated
331	Solyc05g009720	Up regulated	381	Solyc04g011340	Down regulated	431	Solyc09g065120	Down regulated
332	Solyc06g005310	Up regulated	382	Solyc04g071140	Down regulated	432	Solyc08g005680	Up regulated
333	Solyc06g063430	Up regulated	383	Solyc04g072760	Down regulated	433	Solyc09g008670	Up regulated
334	Solyc06g068930	Up regulated	384	Solyc06g005813	Down regulated	434	Solyc12g010025	Up regulated
335	Solyc06g074350	Up regulated	385	Solyc07g063700	Down regulated	435	Solyc01g079790	Up regulated
336	Solyc06g075510	Up regulated	386	Solyc08g075570	Down regulated	436	Solyc07g056140	Up regulated
337	Solyc06g083900	Up regulated	387	Solyc01g067510	Up regulated	437	Solyc01g109790	Up regulated
338	Solyc06g084090	Up regulated	388	Solyc01g107340	Up regulated	438	Solyc11g066390	Up regulated
339	Solyc07g052700	Up regulated	389	Solyc02g070210	Up regulated	439	Solyc07g062390	Up regulated
340	Solyc08g067340	Up regulated	390	Solyc02g081600	Up regulated	440	Solyc08g063080	Up regulated
341	Solyc08g067360	Up regulated	391	Solyc03g005960	Up regulated	441	Solyc11g044840	Up regulated
342	Solyc08g082070	Up regulated	392	Solyc03g006890	Up regulated	442	Solyc04g039820	Up regulated
343	Solyc09g007260	Up regulated	393	Solyc03g114750	Up regulated	443	Solyc09g091960	Up regulated
344	Solyc09g061280	Up regulated	394	Solyc04g025880	Up regulated	444	Solyc08g006470	Up regulated
345	Solyc10g074930	Up regulated	395	Solyc04g040210	Up regulated	445	Solyc07g056540	Down regulated
346	Solyc10g076370	Up regulated	396	Solyc04g063370	Up regulated	446	Solyc04g071610	Up regulated
347	Solyc11g008630	Up regulated	397	Solyc07g005110	Up regulated	447	Solyc04g049920	Up regulated
348	Solyc11g065190	Up regulated	398	Solyc07g014680	Up regulated	448	Solyc02g070560	Up regulated
349	Solyc11g067280	Up regulated	399	Solyc07g048085	Up regulated	449	Solyc07g040970	Up regulated
350	Solyc12g010800	Up regulated	400	Solyc07g052360	Up regulated	450	Solyc08g014560	Up regulated

S.N.	Gene id	Expression status	S.N.	Gene id	Expression status	S.N.	Gene id	Expression status
451	Solyc11g008540	Up regulated	501	Solyc10g076730	Up regulated	551	Solyc01g005590	Up regulated
452	Solyc08g066730	Down regulated	502	Solyc09g008760	Up regulated	552	Solyc04g007250	Up regulated
453	Solyc08g075940	Down regulated	503	Solyc02g090990	Up regulated	553	Solyc06g073220	Up regulated
454	Solyc01g067103	Down regulated	504	Solyc06g007580	Up regulated	554	Solyc10g018320	Up regulated
455	Solyc12g057030	Up regulated	505	Solyc02g090950	Up regulated	555	Solyc07g049530	Up regulated
456	Solyc01g086930	Up regulated	506	Solyc04g076190	Up regulated	556	Solyc10g007960	Up regulated
457	Solyc06g053760	Up regulated	507	Solyc12g010540	Up regulated	557	Solyc11g021060	Up regulated
458	Solyc03g063220	Down regulated	508	Solyc02g076830	Up regulated	558	Solyc11g067270	Up regulated
459	Solyc05g016120	Up regulated	509	Solyc01g091100	Up regulated	559	Solyc10g086500	Up regulated
460	Solyc11g039980	Up regulated	510	Solyc03g006250	Down regulated	560	Solyc11g066430	Up regulated
461	Solyc12g017250	Up regulated	511	Solyc01g091110	Up regulated	561	Solyc11g012410	Up regulated
462	Solyc04g081350	Up regulated	512	Solyc01g107710	Up regulated	562	Solyc06g062390	Up regulated
463	Solyc05g010060	Up regulated	513	Solyc02g067020	Up regulated	563	Solyc05g051880	Up regulated
464	Solyc08g075870	Up regulated	514	Solyc01g106510	Up regulated	564	Solyc02g088210	Up regulated
465	Solyc09g090360	Up regulated	515	Solyc03g119930	Up regulated	565	Solyc10g055780	Up regulated
466	Solyc06g083580	Up regulated	516	Solyc09g009810	Up regulated	566	Solyc07g009060	Down regulated
467	Solyc02g093700	Down regulated	517	Solyc02g070090	Down regulated	567	Solyc02g088390	Up regulated
468	Solyc03g120750	Up regulated	518	Solyc05g052680	Down regulated	568	Solyc05g046030	Up regulated
469	Solyc04g008060	Up regulated	519	Solyc09g075700	Up regulated	569	Solyc01g094270	Up regulated
470	Solyc06g073910	Up regulated	520	Solyc01g005320	Up regulated	570	Solyc06g083910	Up regulated
471	Solyc07g008410	Up regulated	521	Solyc07g066540	Up regulated	571	Solyc06g062560	Up regulated
472	Solyc08g079090	Up regulated	522	Solyc03g119820	Up regulated	572	Solyc02g086402	Up regulated
473	Solyc01g100020	Up regulated	523	Solyc01g091760	Up regulated	573	Solyc04g007760	Up regulated
474	Solyc02g078690	Up regulated	524	Solyc02g089920	Up regulated	574	Solyc09g082250	Up regulated
475	Solyc01g110000	Down regulated	525	Solyc03g119810	Up regulated	575	Solyc07g007620	Up regulated
476	Solyc12g008840	Down regulated	526	Solyc07g065530	Up regulated	576	Solyc07g026650	Down regulated
477	Solyc03g121540	Down regulated	527	Solyc03g098490	Up regulated	577	Solyc04g012020	Up regulated
478	Solyc01g094690	Up regulated	528	Solyc01g090340	Up regulated	578	Solyc09g082660	Up regulated
479	Solyc11g012360	Down regulated	529	Solyc07g007610	Up regulated	579	Solyc01g079480	Up regulated
480	Solyc01g087970	Up regulated	530	Solyc01g094130	Up regulated	580	Solyc08g077770	Up regulated
481	Solyc01g111660	Up regulated	531	Solyc05g014550	Up regulated	581	Solyc03g116910	Up regulated
482	Solyc06g069470	Up regulated	532	Solyc04g074400	Down regulated	582	Solyc11g006250	Up regulated
483	Solyc08g008050	Up regulated	533	Solyc05g008370	Up regulated	583	Solyc04g016430	Down regulated
484	Solyc04g080040	Down regulated	534	Solyc04g014520	Up regulated	584	Solyc10g079870	Up regulated
485	Solyc08g080620	Up regulated	535	Solyc10g080430	Up regulated	585	Solyc07g007750	Up regulated
486	Solyc01g095170	Up regulated	536	Solyc05g007210	Up regulated	586	Solyc01g059900	Up regulated
487	Solyc03g123400	Up regulated	537	Solyc02g069800	Up regulated	587	Solyc02g082740	Up regulated
488	Solyc01g110150	Up regulated	538	Solyc06g036110	Up regulated	588	Solyc08g081780	Up regulated
489	Solyc01g079670	Up regulated	539	Solyc03g113570	Up regulated	589	Solyc10g055230	Up regulated
490	Solyc03g098710	Up regulated	540	Solyc03g113580	Up regulated	590	Solyc02g078910	Up regulated
491	Solyc04g080480	Up regulated	541	Solyc10g081520	Up regulated	591	Solyc12g049070	Down regulated
492	Solyc04g080740	Up regulated	542	Solyc06g062950	Down regulated	592	Solyc02g090730	Up regulated
493	Solyc10g080840	Up regulated	543	Solyc09g065710	Up regulated	593	Solyc07g006800	Up regulated
494	Solyc10g050880	Down regulated	544	Solyc04g014530	Up regulated	594	Solyc07g043490	Up regulated
495	Solyc06g034370	Up regulated	545	Solyc05g009890	Up regulated	595	Solyc07g043500	Up regulated
496	Solyc03g112040	Down regulated	546	Solyc09g011540	Up regulated	596	Solyc01g079170	Up regulated
497	Solyc05g012490	Up regulated	547	Solyc03g032230	Up regulated	597	Solyc06g075800	Up regulated
498	Solyc03g083710	Up regulated	548	Solyc02g063510	Up regulated	598	Solyc01g086820	Up regulated
499	Solyc03g113850	Up regulated	549	Solyc05g056470	Up regulated	599	Solyc02g077480	Up regulated
500	Solyc03g019690	Down regulated	550	Solyc12g010940	Up regulated	600	Solyc10g008910	Up regulated

S.N.	Gene id	Expression status	S.N.	Gene id	Expression status	S.N.	Gene id	Expression status
601	Solyc11g07286	Up regulated	651	Solyc02g083280	Down regulated	701	Solyc07g052135	Down regulated
602	Solyc07g00725	Up regulated	652	Solyc02g087090	Down regulated	702	Solyc07g055470	Down regulated
603	Solyc04g05810	Up regulated	653	Solyc02g087620	Down regulated	703	Solyc07g065900	Down regulated
604	Solyc08g07869	Up regulated	654	Solyc02g092530	Down regulated	704	Solyc08g061490	Down regulated
605	Solyc10g07507	Up regulated	655	Solyc02g092820	Down regulated	705	Solyc08g065540	Down regulated
606	Solyc10g07510	Up regulated	656	Solyc03g007290	Down regulated	706	Solyc08g066570	Down regulated
607	Solyc09g01828	Up regulated	657	Solyc03g025585	Down regulated	707	Solyc08g067610	Down regulated
608	Solyc09g08310	Up regulated	658	Solyc03g043880	Down regulated	708	Solyc08g067690	Down regulated
609	Solyc11g06613	Up regulated	659	Solyc03g071590	Down regulated	709	Solyc08g067870	Down regulated
610	Solyc05g01400	Up regulated	660	Solyc03g080030	Down regulated	710	Solyc08g068085	Down regulated
611	Solyc01g08041	Down regulated	661	Solyc03g083490	Down regulated	711	Solyc09g005420	Down regulated
612	Solyc10g05491	Up regulated	662	Solyc03g098760	Down regulated	712	Solyc09g007010	Down regulated
613	Solyc09g06641	Up regulated	663	Solyc03g111550	Down regulated	713	Solyc09g007020	Down regulated
614	Solyc11g02096	Up regulated	664	Solyc03g119895	Down regulated	714	Solyc09g007790	Down regulated
615	Solyc03g09801	Up regulated	665	Solyc04g016177	Down regulated	715	Solyc09g011470	Down regulated
616	Solyc07g00767	Up regulated	666	Solyc04g040130	Down regulated	716	Solyc09g061700	Down regulated
617	Solyc09g09191	Up regulated	667	Solyc04g049930	Down regulated	717	Solyc09g074100	Down regulated
618	Solyc02g07974	Up regulated	668	Solyc04g054450	Down regulated	718	Solyc09g082340	Down regulated
619	Solyc02g09156	Down regulated	669	Solyc04g063245	Down regulated	719	Solyc09g089580	Down regulated
620	Solyc02g08357	Up regulated	670	Solyc04g064590	Down regulated	720	Solyc09g089730	Down regulated
621	Solyc00g13656	Down regulated	671	Solyc04g064763	Down regulated	721	Solyc09g090900	Down regulated
622	Solyc00g14006	Down regulated	672	Solyc04g064795	Down regulated	722	Solyc09g090990	Down regulated
623	Solyc00g23348	Down regulated	673	Solyc04g071340	Down regulated	723	Solyc09g091600	Down regulated
624	Solyc00g28251	Down regulated	674	Solyc04g076500	Down regulated	724	Solyc09g097760	Down regulated
625	Solyc01g00550	Down regulated	675	Solyc04g076980	Down regulated	725	Solyc09g098000	Down regulated
626	Solyc01g00583	Down regulated	676	Solyc04g077860	Down regulated	726	Solyc10g005920	Down regulated
627	Solyc01g00658	Down regulated	677	Solyc04g077990	Down regulated	727	Solyc10g006250	Down regulated
628	Solyc01g00887	Down regulated	678	Solyc04g078450	Down regulated	728	Solyc10g017960	Down regulated
629	Solyc01g05700	Down regulated	679	Solyc05g012110	Down regulated	729	Solyc10g054670	Down regulated
630	Solyc01g06645	Down regulated	680	Solyc05g016460	Down regulated	730	Solyc10g076840	Down regulated
631	Solyc01g07920	Down regulated	681	Solyc05g052880	Down regulated	731	Solyc10g081000	Down regulated
632	Solyc01g08142	Down regulated	682	Solyc05g054350	Down regulated	732	Solyc10g083380	Down regulated
633	Solyc01g09152	Down regulated	683	Solyc05g054620	Down regulated	733	Solyc10g083400	Down regulated
634	Solyc01g09405	Down regulated	684	Solyc06g005820	Down regulated	734	Solyc10g084410	Down regulated
635	Solyc01g10119	Down regulated	685	Solyc06g007430	Down regulated	735	Solyc11g008440	Down regulated
636	Solyc01g10121	Down regulated	686	Solyc06g007970	Down regulated	736	Solyc11g010790	Down regulated
637	Solyc01g10286	Down regulated	687	Solyc06g033850	Down regulated	737	Solyc11g012120	Down regulated
638	Solyc01g10421	Down regulated	688	Solyc06g051940	Down regulated	738	Solyc11g013293	Down regulated
639	Solyc01g10566	Down regulated	689	Solyc06g054610	Down regulated	739	Solyc11g020670	Down regulated
640	Solyc01g11234	Down regulated	690	Solyc06g060013	Down regulated	740	Solyc11g027840	Down regulated
641	Solyc02g01418	Down regulated	691	Solyc06g062460	Down regulated	741	Solyc11g071740	Down regulated
642	Solyc02g01419	Down regulated	692	Solyc06g068270	Down regulated	742	Solyc12g010740	Down regulated
643	Solyc02g06480	Down regulated	693	Solyc06g072840	Down regulated	743	Solyc12g010900	Down regulated
644	Solyc02g06804	Down regulated	694	Solyc06g073165	Down regulated	744	Solyc12g014620	Down regulated
645	Solyc02g07144	Down regulated	695	Solyc06g074620	Down regulated	745	Solyc12g027540	Down regulated
646	Solyc02g07156	Down regulated	696	Solyc07g009050	Down regulated	746	Solyc12g042060	Down regulated
647	Solyc02g07702	Down regulated	697	Solyc07g009100	Down regulated	747	Solyc12g042500	Down regulated
648	Solyc02g07840	Down regulated	698	Solyc07g009500	Down regulated	748	Solyc12g044983	Down regulated
649	Solyc02g08185	Down regulated	699	Solyc07g026680	Down regulated	749	Solyc12g049150	Down regulated
650	Solyc02g08291	Down regulated	700	Solyc07g044970	Down regulated	750	Solyc12g049170	Down regulated

S.N.	Gene id	Expression status	S.N.	Gene id	Expression status	S.N.	Gene id	Expression status
751	Solyc12g094380	Down regulated	801	Solyc01g091130	Up regulated	851	Solyc02g081980	Up regulated
752	Solyc12g098850	Down regulated	802	Solyc01g091200	Up regulated	852	Solyc02g082960	Up regulated
753	Solyc12g098900	Down regulated	803	Solyc01g091660	Up regulated	853	Solyc02g083200	Up regulated
754	Solyc12g100080	Down regulated	804	Solyc01g094570	Up regulated	854	Solyc02g083250	Up regulated
755	Solyc12g100090	Down regulated	805	Solyc01g094660	Up regulated	855	Solyc02g083860	Up regulated
756	Solyc12g100100	Down regulated	806	Solyc01g095500	Up regulated	856	Solyc02g083870	Up regulated
757	Solyc12g100110	Down regulated	807	Solyc01g096370	Up regulated	857	Solyc02g084790	Up regulated
758	Solyc03g094020	Down regulated	808	Solyc01g096400	Up regulated	858	Solyc02g087210	Up regulated
759	Solyc09g005610	Down regulated	809	Solyc01g096450	Up regulated	859	Solyc02g088080	Up regulated
760	Solyc12g049040	Down regulated	810	Solyc01g098720	Up regulated	860	Solyc02g088200	Up regulated
761	Solyc12g098615	Down regulated	811	Solyc01g099050	Up regulated	861	Solyc02g089850	Up regulated
762	Solyc06g060640	Down regulated	812	Solyc01g099370	Up regulated	862	Solyc02g089900	Up regulated
763	Solyc00g009060	Up regulated	813	Solyc01g100010	Up regulated	863	Solyc02g091620	Up regulated
764	Solyc00g020020	Up regulated	814	Solyc01g100030	Up regulated	864	Solyc02g093197	Up regulated
765	Solyc00g021640	Up regulated	815	Solyc01g100090	Up regulated	865	Solyc02g093600	Up regulated
766	Solyc00g022107	Up regulated	816	Solyc01g100270	Up regulated	866	Solyc02g094150	Up regulated
767	Solyc00g071180	Up regulated	817	Solyc01g100310	Up regulated	867	Solyc02g094400	Up regulated
768	Solyc00g072400	Up regulated	818	Solyc01g102390	Up regulated	868	Solyc03g005550	Up regulated
769	Solyc00g075035	Up regulated	819	Solyc01g104740	Up regulated	869	Solyc03g006050	Up regulated
770	Solyc00g136565	Up regulated	820	Solyc01g104780	Up regulated	870	Solyc03g006410	Up regulated
771	Solyc00g178340	Up regulated	821	Solyc01g105880	Up regulated	871	Solyc03g007760	Up regulated
772	Solyc00g244290	Up regulated	822	Solyc01g106630	Up regulated	872	Solyc03g008010	Up regulated
773	Solyc00g277510	Up regulated	823	Solyc01g107400	Up regulated	873	Solyc03g020040	Up regulated
774	Solyc01g006400	Up regulated	824	Solyc01g109100	Up regulated	874	Solyc03g020080	Up regulated
775	Solyc01g008320	Up regulated	825	Solyc01g110060	Up regulated	875	Solyc03g034420	Up regulated
776	Solyc01g009500	Up regulated	826	Solyc01g110600	Up regulated	876	Solyc03g044670	Up regulated
777	Solyc01g009760	Up regulated	827	Solyc01g110913	Up regulated	877	Solyc03g063480	Up regulated
778	Solyc01g010180	Up regulated	828	Solyc01g111145	Up regulated	878	Solyc03g079960	Up regulated
779	Solyc01g010250	Up regulated	829	Solyc01g112260	Up regulated	879	Solyc03g080190	Up regulated
780	Solyc01g057260	Up regulated	830	Solyc02g005115	Up regulated	880	Solyc03g093470	Up regulated
781	Solyc01g067295	Up regulated	831	Solyc02g062170	Up regulated	881	Solyc03g096870	Up regulated
782	Solyc01g067380	Up regulated	832	Solyc02g065280	Up regulated	882	Solyc03g097570	Up regulated
783	Solyc01g067850	Up regulated	833	Solyc02g065430	Up regulated	883	Solyc03g098030	Up regulated
784	Solyc01g067940	Up regulated	834	Solyc02g065480	Up regulated	884	Solyc03g098780	Up regulated
785	Solyc01g068630	Up regulated	835	Solyc02g067160	Up regulated	885	Solyc03g111820	Up regulated
786	Solyc01g073940	Up regulated	836	Solyc02g067660	Up regulated	886	Solyc03g112297	Up regulated
787	Solyc01g074000	Up regulated	837	Solyc02g068790	Up regulated	887	Solyc03g112300	Up regulated
788	Solyc01g079980	Up regulated	838	Solyc02g069250	Up regulated	888	Solyc03g113090	Up regulated
789	Solyc01g080750	Up regulated	839	Solyc02g071610	Up regulated	889	Solyc03g114310	Up regulated
790	Solyc01g080790	Up regulated	840	Solyc02g071700	Up regulated	890	Solyc03g114530	Up regulated
791	Solyc01g080800	Up regulated	841	Solyc02g071750	Up regulated	891	Solyc03g115950	Up regulated
792	Solyc01g081620	Up regulated	842	Solyc02g076980	Up regulated	892	Solyc03g116630	Up regulated
793	Solyc01g086920	Up regulated	843	Solyc02g077040	Up regulated	893	Solyc03g117860	Up regulated
794	Solyc01g087570	Up regulated	844	Solyc02g077330	Up regulated	894	Solyc03g118780	Up regulated
795	Solyc01g088250	Up regulated	845	Solyc02g078040	Up regulated	895	Solyc03g120040	Up regulated
796	Solyc01g089850	Up regulated	846	Solyc02g078100	Up regulated	896	Solyc03g120050	Up regulated
797	Solyc01g090210	Up regulated	847	Solyc02g078480	Up regulated	897	Solyc03g120950	Up regulated
798	Solyc01g090660	Up regulated	848	Solyc02g079150	Up regulated	898	Solyc03g121170	Up regulated
799	Solyc01g090890	Up regulated	849	Solyc02g080480	Up regulated	899	Solyc03g121190	Up regulated
800	Solyc01g090980	Up regulated	850	Solyc02g081360	Up regulated	900	Solyc03g121420	Up regulated

S.N.	Gene id	Expression status	S.N.	Gene id	Expression status	S.N.	Gene id	Expression status
901	Solyc03g121940	Up regulated	951	Solyc05g013530	Up regulated	1001	Solyc07g017570	Up regulated
902	Solyc03g123630	Up regulated	952	Solyc05g014370	Up regulated	1002	Solyc07g042100	Up regulated
903	Solyc04g006950	Up regulated	953	Solyc05g015300	Up regulated	1003	Solyc07g043480	Up regulated
904	Solyc04g007050	Up regulated	954	Solyc05g026310	Up regulated	1004	Solyc07g043630	Up regulated
905	Solyc04g007730	Up regulated	955	Solyc05g050730	Up regulated	1005	Solyc07g043660	Up regulated
906	Solyc04g007825	Up regulated	956	Solyc05g051610	Up regulated	1006	Solyc07g045440	Up regulated
907	Solyc04g008615	Up regulated	957	Solyc05g051870	Up regulated	1007	Solyc07g045460	Up regulated
908	Solyc04g009590	Up regulated	958	Solyc05g052270	Up regulated	1008	Solyc07g048090	Up regulated
909	Solyc04g009900	Up regulated	959	Solyc05g052400	Up regulated	1009	Solyc07g049200	Up regulated
910	Solyc04g011480	Up regulated	960	Solyc05g054090	Up regulated	1010	Solyc07g049300	Up regulated
911	Solyc04g012080	Up regulated	961	Solyc05g054470	Up regulated	1011	Solyc07g052530	Up regulated
912	Solyc04g015120	Up regulated	962	Solyc05g056380	Up regulated	1012	Solyc07g052600	Up regulated
913	Solyc04g015210	Up regulated	963	Solyc06g005470	Up regulated	1013	Solyc07g053030	Up regulated
914	Solyc04g016490	Up regulated	964	Solyc06g007130	Up regulated	1014	Solyc07g053900	Up regulated
915	Solyc04g024340	Up regulated	965	Solyc06g011490	Up regulated	1015	Solyc07g055010	Up regulated
916	Solyc04g054500	Up regulated	966	Solyc06g018100	Up regulated	1016	Solyc07g055950	Up regulated
917	Solyc04g064800	Up regulated	967	Solyc06g036340	Up regulated	1017	Solyc07g055990	Up regulated
918	Solyc04g071060	Up regulated	968	Solyc06g048570	Up regulated	1018	Solyc07g056460	Up regulated
919	Solyc04g071165	Up regulated	969	Solyc06g053520	Up regulated	1019	Solyc07g056510	Up regulated
920	Solyc04g071615	Up regulated	970	Solyc06g053620	Up regulated	1020	Solyc07g063490	Up regulated
921	Solyc04g071620	Up regulated	971	Solyc06g053625	Up regulated	1021	Solyc07g063880	Up regulated
922	Solyc04g072450	Up regulated	972	Solyc06g054640	Up regulated	1022	Solyc07g064420	Up regulated
923	Solyc04g072800	Up regulated	973	Solyc06g060600	Up regulated	1023	Solyc07g064820	Up regulated
924	Solyc04g074100	Up regulated	974	Solyc06g062380	Up regulated	1024	Solyc07g066670	Up regulated
925	Solyc04g074810	Up regulated	975	Solyc06g062540	Up regulated	1025	Solyc08g005550	Up regulated
926	Solyc04g077775	Up regulated	976	Solyc06g062550	Up regulated	1026	Solyc08g005620	Up regulated
927	Solyc04g077920	Up regulated	977	Solyc06g062770	Up regulated	1027	Solyc08g005960	Up regulated
928	Solyc04g078090	Up regulated	978	Solyc06g065580	Up regulated	1028	Solyc08g006640	Up regulated
929	Solyc04g078110	Up regulated	979	Solyc06g066180	Up regulated	1029	Solyc08g007080	Up regulated
930	Solyc04g078270	Up regulated	980	Solyc06g066750	Up regulated	1030	Solyc08g008500	Up regulated
931	Solyc04g078710	Up regulated	981	Solyc06g066830	Up regulated	1031	Solyc08g013840	Up regulated
932	Solyc04g079100	Up regulated	982	Solyc06g067910	Up regulated	1032	Solyc08g023500	Up regulated
933	Solyc04g079520	Up regulated	983	Solyc06g068770	Up regulated	1033	Solyc08g060920	Up regulated
934	Solyc04g079910	Up regulated	984	Solyc06g072830	Up regulated	1034	Solyc08g062340	Up regulated
935	Solyc04g080550	Up regulated	985	Solyc06g073380	Up regulated	1035	Solyc08g066590	Up regulated
936	Solyc04g080685	Up regulated	986	Solyc06g074000	Up regulated	1036	Solyc08g066760	Up regulated
937	Solyc05g005470	Up regulated	987	Solyc06g074790	Up regulated	1037	Solyc08g067620	Up regulated
938	Solyc05g005535	Up regulated	988	Solyc06g083160	Up regulated	1038	Solyc08g074620	Up regulated
939	Solyc05g005540	Up regulated	989	Solyc06g083490	Up regulated	1039	Solyc08g074630	Up regulated
940	Solyc05g006740	Up regulated	990	Solyc06g084460	Up regulated	1040	Solyc08g074680	Up regulated
941	Solyc05g006750	Up regulated	991	Solyc07g007220	Up regulated	1041	Solyc08g074683	Up regulated
942	Solyc05g007330	Up regulated	992	Solyc07g007270	Up regulated	1042	Solyc08g074690	Up regulated
943	Solyc05g007720	Up regulated	993	Solyc07g007320	Up regulated	1043	Solyc08g075550	Up regulated
944	Solyc05g009470	Up regulated	994	Solyc07g007660	Up regulated	1044	Solyc08g075790	Up regulated
945	Solyc05g009610	Up regulated	995	Solyc07g008210	Up regulated	1045	Solyc08g076885	Up regulated
946	Solyc05g009960	Up regulated	996	Solyc07g008280	Up regulated	1046	Solyc08g076890	Up regulated
947	Solyc05g010080	Up regulated	997	Solyc07g008290	Up regulated	1047	Solyc08g076970	Up regulated
948	Solyc05g011940	Up regulated	998	Solyc07g008380	Up regulated	1048	Solyc08g078210	Up regulated
949	Solyc05g011970	Up regulated	999	Solyc07g008710	Up regulated	1049	Solyc08g078520	Up regulated
950	Solyc05g012260	Up regulated	1000	Solyc07g009290	Up regulated	1050	Solyc08g079080	Up regulated

S.N.	Gene id	Expression status	S.N.	Gene id	Expression status	S.N.	Gene id	Expression status
1051	Solyc08g07959	Up regulated	1101	Solyc09g092720	Up regulated	1151	Solyc12g005670	Up regulated
1052	Solyc08g08015	Up regulated	1102	Solyc09g097780	Up regulated	1152	Solyc12g005940	Up regulated
1053	Solyc08g08019	Up regulated	1103	Solyc10g005020	Up regulated	1153	Solyc12g006380	Up regulated
1054	Solyc08g08144	Up regulated	1104	Solyc10g005210	Up regulated	1154	Solyc12g006680	Up regulated
1055	Solyc08g08147	Up regulated	1105	Solyc10g005340	Up regulated	1155	Solyc12g007080	Up regulated
1056	Solyc08g08182	Up regulated	1106	Solyc10g005750	Up regulated	1156	Solyc12g008650	Up regulated
1057	Solyc08g08216	Up regulated	1107	Solyc10g006920	Up regulated	1157	Solyc12g009310	Up regulated
1058	Solyc08g08245	Up regulated	1108	Solyc10g007870	Up regulated	1158	Solyc12g009480	Up regulated
1059	Solyc08g08311	Up regulated	1109	Solyc10g008410	Up regulated	1159	Solyc12g009820	Up regulated
1060	Solyc09g00540	Up regulated	1110	Solyc10g017570	Up regulated	1160	Solyc12g010960	Up regulated
1061	Solyc09g00715	Up regulated	1111	Solyc10g018907	Up regulated	1161	Solyc12g011340	Up regulated
1062	Solyc09g00765	Up regulated	1112	Solyc10g047040	Up regulated	1162	Solyc12g015920	Up regulated
1063	Solyc09g00852	Up regulated	1113	Solyc10g048060	Up regulated	1163	Solyc12g017460	Up regulated
1064	Solyc09g00852	Up regulated	1114	Solyc10g049660	Up regulated	1164	Solyc12g040640	Up regulated
1065	Solyc09g00891	Up regulated	1115	Solyc10g052600	Up regulated	1165	Solyc12g042930	Up regulated
1066	Solyc09g00919	Up regulated	1116	Solyc10g075110	Up regulated	1166	Solyc12g055920	Up regulated
1067	Solyc09g01054	Up regulated	1117	Solyc10g076210	Up regulated	1167	Solyc12g056240	Up regulated
1068	Solyc09g01151	Up regulated	1118	Solyc10g076243	Up regulated	1168	Solyc12g062340	Up regulated
1069	Solyc09g01155	Up regulated	1119	Solyc10g076710	Up regulated	1169	Solyc12g088130	Up regulated
1070	Solyc09g01163	Up regulated	1120	Solyc10g079650	Up regulated	1170	Solyc12g088370	Up regulated
1071	Solyc09g01448	Up regulated	1121	Solyc10g080050	Up regulated	1171	Solyc12g089330	Up regulated
1072	Solyc09g01502	Up regulated	1122	Solyc10g084540	Up regulated	1172	Solyc12g096770	Up regulated
1073	Solyc09g01587	Up regulated	1123	Solyc10g084680	Up regulated	1173	Solyc12g098770	Up regulated
1074	Solyc09g05776	Up regulated	1124	Solyc10g086490	Up regulated	1174	Solyc12g099430	Up regulated
1075	Solyc09g05917	Up regulated	1125	Solyc11g006490	Up regulated	1175	Solyc01g098570	Up regulated
1076	Solyc09g05947	Up regulated	1126	Solyc11g007590	Up regulated	1176	Solyc02g086400	Up regulated
1077	Solyc09g06173	Up regulated	1127	Solyc11g008810	Up regulated	1177	Solyc03g095970	Up regulated
1078	Solyc09g06493	Up regulated	1128	Solyc11g010400	Up regulated	1178	Solyc03g097560	Up regulated
1079	Solyc09g06540	Up regulated	1129	Solyc11g010630	Up regulated	1179	Solyc04g072700	Up regulated
1080	Solyc09g07526	Up regulated	1130	Solyc11g010700	Up regulated	1180	Solyc04g080920	Up regulated
1081	Solyc09g07579	Up regulated	1131	Solyc11g011240	Up regulated	1181	Solyc07g064100	Up regulated
1082	Solyc09g07597	Up regulated	1132	Solyc11g013150	Up regulated	1182	Solyc08g005940	Up regulated
1083	Solyc09g08223	Up regulated	1133	Solyc11g019910	Up regulated	1183	Solyc09g008500	Up regulated
1084	Solyc09g08224	Up regulated	1134	Solyc11g056330	Up regulated	1184	Solyc09g089505	Up regulated
1085	Solyc09g08253	Up regulated	1135	Solyc11g066400	Up regulated	1185	Solyc10g046830	Up regulated
1086	Solyc09g08272	Up regulated	1136	Solyc11g066580	Up regulated	1186	Solyc12g006130	Up regulated
1087	Solyc09g08297	Up regulated	1137	Solyc11g066940	Up regulated	1187	Solyc01g067900	Up regulated
1088	Solyc09g08309	Up regulated	1138	Solyc11g068515	Up regulated	1188	Solyc01g094870	Up regulated
1089	Solyc09g08344	Up regulated	1139	Solyc11g069070	Up regulated	1189	Solyc07g007860	Up regulated
1090	Solyc09g08445	Up regulated	1140	Solyc11g069280	Up regulated	1190	Solyc08g006850	Up regulated
1091	Solyc09g08448	Up regulated	1141	Solyc11g069940	Up regulated	1191	Solyc08g062570	Up regulated
1092	Solyc09g09007	Up regulated	1142	Solyc11g071470	Up regulated	1192	Solyc08g078930	Up regulated
1093	Solyc09g09060	Up regulated	1143	Solyc11g071720	Up regulated	1193	Solyc08g078940	Up regulated
1094	Solyc09g09103	Up regulated	1144	Solyc11g072030	Up regulated	1194	Solyc08g079190	Up regulated
1095	Solyc09g09106	Up regulated	1145	Solyc11g072410	Up regulated	1195	Solyc08g079200	Up regulated
1096	Solyc09g09113	Up regulated	1146	Solyc11g072800	Up regulated	1196	Solyc10g018200	Up regulated
1097	Solyc09g09155	Up regulated	1147	Solyc11g073090	Up regulated	1197	Solyc10g076340	Up regulated
1098	Solyc09g09180	Up regulated	1148	Solyc11g073260	Up regulated	1198	Solyc11g010390	Up regulated
1099	Solyc09g09241	Up regulated	1149	Solyc12g005430	Up regulated	1199	Solyc12g010545	Up regulated
1100	Solyc09g09248	Up regulated	1150	Solyc12g005440	Up regulated	1200	Solyc03g113930	Up regulated
						1201	Solyc11g042630	Up regulated

Bibliography:

1. Plaxton, W.C.; Carswell, M.C. Metabolic Aspects of the Phosphate Starvation Response in Plants. *Plant Responses to Environ. Stress.* **2018**, 349–372, doi:10.1201/9780203743157-16.
2. Marschner, H. Marschner's Mineral Nutrition of Higher. *Plants*, 2011.
3. Raghothama, K.G. Phosphate Aquisition. *Annu. Rev. Plant Physiol. Plant Mol. Biol.* **1999,** 37-49, https://doi.org/10.1007/s11104-004-2005-6.
4. Cordell, D.; Drangert, J.O.; White, S. The Story of Phosphorus: Global Food Security and Food for Thought. *Glob. Environ. Chang.* **2009**, *19*, 292–305, doi:10.1016/j.gloenvcha.2008.10.009.
5. Heldt, H.W.; Chon, C.J.; Maronde, D.; Herold, A.; Stankovic, Z.S.; Walker, D.A.; Kraminer, A.; Kirk, M.R.; Heber, U. Role of Orthophosphate and Other Factors in the Regulation of Starch Formation in Leaves and Isolated Chloroplasts. *Plant Physiol.* **1977**, *59*, 1146–1155, doi:10.1104/pp.59.6.1146.
6. Foyer, C.; Spencer, C. The Relationship between Phosphate Status and Photosynthesis in Leaves Effects on Intracelular Orthophosphate Distribution, Photosynthesis and Assimilate Partitioning.*Planta*, **1986,** 167, 369-375, doi: 10.1007/BF00391341.
7. Thibaud, M.C.; Arrighi, J.F.; Bayle, V.; Chiarenza, S.; Creff, A.; Bustos, R.; Paz-Ares, J.; Poirier, Y.; Nussaume, L. Dissection of Local and Systemic Transcriptional Responses to Phosphate Starvation in Arabidopsis. *Plant J.* **2010**, *64*, 775-789 , doi:10.1111/j.1365-313X.2010.04375.x.
8. Chiou, T.J.; Lin, S.I. Signaling Network in Sensing Phosphate Availability in Plants. *Annu. Rev. Plant Biol.* **2011**, *62*, 185-206, doi:10.1146/annurev-arplant-042110-103849.
9. Mollier, A.; De Willigen, P.; Heinen, M.; Morel, C.; Schneider, A.; Pellerin, S. A Two-Dimensional Simulation Model of Phosphorus Uptake Including Crop Growth and P-Response. *Ecol. Modell.* **2008**, *210*, 453–464, doi:10.1016/j.ecolmodel.2007.08.008.
10. Li, X.; Zeng, R.; Liao, H. Improving Crop Nutrient Efficiency through Root Architecture Modifications. *J. Integr. Plant Biol.* **2016**, *58*, 193–202, doi:10.1111/jipb.12434.
11. Péret, B.; Clément, M.; Nussaume, L.; Desnos, T. Root Developmental Adaptation to Phosphate Starvation: Better Safe than Sorry. *Trends Plant Sci.* **2011**, *16*, 442–450, doi:10.1016/j.tplants.2011.05.006.
12. Péret, B.; Desnos, T.; Jost, R.; Kanno, S.; Berkowitz, O.; Nussaume, L. Root Architecture Responses: In Search of Phosphate. *Plant Physiol.* **2014**, *166*, 1713-1723, doi:10.1104/pp.114.244541.
13. Williamson, L.C.; Ribrioux, S.P.C.P.; Fitter, A.H.; Leyser, H.M.O. Phosphate Availability Regulates Root System Architecture in Arabidopsis. *Plant Physiol.* **2001**, *126*, 875–882, doi:10.1104/pp.126.2.875.
14. Lynch, J.P.; Brown, K.M. Topsoil Foraging – an Architectural Adaptation of Plants to Low Phosphorus Availability. *Plant Soil* **2001**, *237*, 225–237, doi:10.1023/A:1013324727040.
15. Vance, C.P.; Uhde-Stone, C.; Allan, D.L. Phosphorus Acquisition and Use: Critical Adaptations by Plants for Securing a Nonrenewable Resource. *New Phytol.* 2003, 423-447, doi:10.1046/j.1469-8137.2003.00695.x
16. Lynch, J.P. Roots of the Second Green Revolution. *Aust. J. Bot.* **2007**, *55*, 493-512., doi:10.1071/BT06118.
17. Richardson, A.E.; Lynch, J.P.; Ryan, P.R.; Delhaize, E.; Smith, F.A.; Smith, S.E.; Harvey, P.R.; Ryan, M.H.; Veneklaas, E.J.; Lambers, H.; et al. Plant and Microbial Strategies to Improve the Phosphorus Efficiency of Agriculture. *Plant Soil* **2011**, *349*, 121–156, doi:10.1007/s11104-011-0950-4.
18. van de Wiel, C.C.M.; van der Linden, C.G.; Scholten, O.E. Improving Phosphorus Use Efficiency in Agriculture: Opportunities for Breeding. *Euphytica* **2016**, *207*, 1–22, doi:10.1007/s10681-015-1572-3.
19. Campos, P.; Borie, F.; Cornejo, P.; López-Ráez, J.A.; López-García, Á.; Seguel, A. Phosphorus Acquisition Efficiency Related to Root Traits: Is Mycorrhizal Symbiosis a Key Factor to Wheat and Barley Cropping? *Front. Plant Sci.* **2018**, *9*, 752, doi:10.3389/fpls.2018.00752.
20. Mollier, A.; Pellerin, S. Maize Root System Growth and Development as Influenced by Phosphorus Deficiency. *J. Exp. Bot.* **1999**, *50*, 487–497., doi:10.1093/jxb/50.333.487.
21. Giri, J.; Bhosale, R.; Huang, G.; Pandey, B.K.; Parker, H.; Zappala, S.; Yang, J.; Dievart, A.; Bureau, C.;

Ljung, K.; et al. Rice Auxin Influx Carrier *OsAUX1* Facilitates Root Hair Elongation in Response to Low External Phosphate. *Nat. Commun.* **2018**, *9*, 1-7, doi:10.1038/s41467-018-03850-4.

22. Chevalier, F.; Pata, M.; Nacry, P.; Doumas, P.; Rossignol, M. Effects of Phosphate Availability on the Root System Architecture: Large-Scale Analysis of the Natural Variation between Arabidopsis Accessions. *Plant. Cell Environ.* **2003**, *26*, 1839–1850, doi:10.1046/j.1365-3040.2003.01100.x.
23. Srivastava, R.; Sirohi, P.; Chauhan, H.; Kumar, R. The Enhanced Phosphorus Use Efficiency in Phosphate-Deficient and Mycorrhiza-Inoculated Barley Seedlings Involves Activation of Different Sets of PHT1 Transporters in Roots. *Planta* **2021**, *254*, 38, doi:10.1007/s00425-021-03687-0.
24. Shimizu, A.; Yanagihara, S.; Kawasaki, S.; Ikehashi, H. Phosphorus Deficiency-Induced Root Elongation and Its QTL in Rice (*Oryza sativa L.*). *Theor. Appl. Genet.* **2004**, *109*, 1361–1368, doi:10.1007/S00122-004-1751-4/FIGURES/6.
25. Niu, Y.F.; Chai, R.S.; Jin, G.L.; Wang, H.; Tang, C.X.; Zhang, Y.S. Responses of Root Architecture Development to Low Phosphorus Availability: A Review. *Ann. Bot.* **2013**, *112*, 391–408, doi:10.1093/aob/mcs285.
26. Zhao, J.; Fu, J.; Liao, H.; He, Y.; Nian, H.; Hu, Y.; Qiu, L.; Dong, Y.; Yan, X. Characterization of Root Architecture in an Applied Core Collection for Phosphorus Efficiency of Soybean Germplasm. *Chinese Sci. Bull.*, **2004**, *49*, 1611–1620, doi:10.1007/BF03184131.
27. Calderón-Vázquez, C.; Alatorre-Cobos, F.; Simpson-Williamson, J.; Herrera-Estrella, L. Maize Under Phosphate Limitation. *Handb. Maize Its Biol.* **2009**, 381–404, doi:10.1007/978-0-387-79418-1_19.
28. Lynch, J.P. Root Phenes for Enhanced Soil Exploration and Phosphorus Acquisition: Tools for Future Crops. *Plant Physiol.* **2011**, *156*, 1041–1049, doi:10.1104/pp.111.175414.
29. Huang, G.; Liang, W.; Sturrock, C.J.; Pandey, B.K.; Giri, J.; Mairhofer, S.; Wang, D.; Muller, L.; Tan, H.; York, L.M.; et al. Rice Actin Binding Protein RMD Controls Crown Root Angle in Response to External Phosphate. *Nat. Commun.* **2018**, *9*, 2346, doi:10.1038/s41467-018-04710-x.
30. Neumann, G.; Martinoia, E. Cluster Roots an Underground Adaptation for Survival in Extreme Environments. *Trends Plant Sci.* **2002**, *7*, 162–167, doi:10.1016/S1360-1385(02)02241-0.
31. Lambers, H.; Shane, M.W.; Cramer, M.D.; Pearse, S.J.; Veneklaas, E.J. Root Structure and Functioning for Efficient Acquisition of Phosphorus: Matching Morphological and Physiological Traits. *Ann. Bot.* **2006**, *98*, 693–713, doi:10.1093/aob/mcl114.
32. Gilroy, S.; Jones, D.L. Through Form to Function: Root Hair Development and Nutrient Uptake. *Trends Plant Sci.* **2000**, *5*, 56–60, doi:10.1016/S1360-1385(99)01551-4.
33. Singh, S.K.; Fischer, U.; Singh, M.; Grebe, M.; Marchant, A. Insight into the Early Steps of Root Hair Formation Revealed by the Procuste1 Cellulose Synthase Mutant of *Arabidopsis thaliana*. *BMC Plant Biol.* **2008**, *8*, 57, doi:10.1186/1471-2229-8-57.
34. Jungk, A. Root Hairs and the Acquisition of Plant Nutrients from Soil. *J. Plant Nutr. Soil Sci.* **2001**, 164, 121-129, doi:10.1002/1522-2624(200104)164:2<121::AID-JPLN121>3.0.CO;2-6.
35. Wang, Y.; Thorup-Kristensen, K.; Jensen, L.S.; Magid, J. Vigorous Root Growth Is a Better Indicator of Early Nutrient Uptake than Root Hair Traits in Spring Wheat Grown under Low Fertility. *Front. Plant Sci.* **2016**, *7*, 865, doi:10.3389/fpls.2016.00865.
36. Ma, Z.; Bielenberg, D.G.; Brown, K.M.; Lynch, J.P. Regulation of Root Hair Density by Phosphorus Availability in *Arabidopsis thaliana*. *Plant. Cell Environ.* **2001**, *24*, 459–467, doi:10.1046/j.1365-3040.2001.00695.x.
37. Bates, T.R.; Lynch, J.P. Root Hairs Confer a Competitive Advantage under Low Phosphorus Availability. *Plant Soil* **2001**, 2- 243-250, doi:10.1023/A:1012791706800.
38. Wang, L.; Liao, H.; Yan, X.; Zhuang, B.; Dong, Y. Genetic Variability for Root Hair Traits as Related to Phosphorus Status in Soybean. *Plant Soil* **2004**, *261*, 77–84, doi:10.1023/B:PLSO.0000035552.94249.6a.
39. Hammond, J.P.; White, P.J. Sucrose Transport in the Phloem: Integrating Root Responses to Phosphorus Starvation. In Proceedings of the *J. Exp. Bot.*; **2008**, 59, 93-109, doi:10.1093/jxb/erm221.
40. Keyes, S.D.; Daly, K.R.; Gostling, N.J.; Jones, D.L.; Talboys, P.; Pinzer, B.R.; Boardman, R.; Sinclair, I.;

Marchant, A.; Roose, T. High Resolution Synchrotron Imaging of Wheat Root Hairs Growing in Soil and Image Based Modelling of Phosphate Uptake. *New Phytol.* **2013**, *198*, 1023–1029, doi:10.1111/nph.12294.
41. Kohli, P.S.; Pazhamala, L.T.; Mani, B.; Thakur, J.K.; Giri, J. Root Hair-Specific Transcriptome Reveals Response to Low Phosphorus in Cicer Arietinum. *Front. Plant Sci.* **2022**, *13*, doi:10.3389/fpls.2022.983969.
42. He, Z.; Ma, Z.; Brown, K.M.; Lynch, J.P. Assessment of Inequality of Root Hair Density in *Arabidopsis thaliana* Using the Gini Coefficient: A Close Look at the Effect of Phosphorus and its Interaction with Ethylene. *Ann. Bot.* **2005**, *95*, 287–293, doi:10.1093/aob/mci024.
43. Raya-González, J.; Ojeda-Rivera, J.O.; Mora-Macias, J.; Oropeza-Aburto, A.; Ruiz-Herrera, L.F.; López-Bucio, J.; Herrera-Estrella, L. *MEDIATOR16* Orchestrates Local and Systemic Responses to Phosphate Scarcity in Arabidopsis Roots. *New Phytol.* **2021**, *229*, 1278-1288, doi:10.1111/nph.16989.
44. Marin, M.; Feeney, D.S.; Brown, L.K.; Naveed, M.; Ruiz, S.; Koebernick, N.; Bengough, A.G.; Hallett, P.D.; Roose, T.; Puértolas, J.; et al. Significance of Root Hairs for Plant Performance under Contrasting Field Conditions and Water Deficit. *Ann. Bot.* **2021**, *128*, 1–16, doi:10.1093/aob/mcaa181.
45. Haran, S.; Logendra, S.; Seskar, M.; Bratanova, M.; Raskin, I. Characterization of Arabidopsis Acid Phosphatase Promoter and Regulation of Acid Phosphatase Expression. *Plant Physiol.* **2000**, *124*, 615-626, doi:10.1104/pp.124.2.615.
46. George, T.S.; Richardson, A.E. Potential and Limitations to Improving Crops for Enhanced Phosphorus Utilization. **2008**, 247–270, doi:10.1007/978-1-4020-8435-5_11.
47. Adesemoye, A.O.; Kloepper, J.W. Plant-Microbes Interactions in Enhanced Fertilizer-Use Efficiency. *Appl. Microbiol. Biotechnol.* **2009**, *85*, 1–12, doi:10.1007/S00253-009-2196-0.
48. Smith, S.; Read, D. *Mycorrhizal Symbiosis*; 2010.
49. Wu, Q.S.; Li, G.H.; Zou, Y.N. Improvement of Root System Architecture in Peach (*Prunus Persica*) Seedlings by Arbuscular Mycorrhizal Fungi, Related to Allocation of Glucose/Sucrose to Root. *Not. Bot. Horti Agrobot. Cluj-Napoca* **2011**, *39*, 232-236, doi:10.15835/nbha3926232.
50. Liu, C.Y.; Huang, Y.M.; Zou, Y.N.; Wu, Q.S. Regulation of Root Length and Lateral Root Number in Trifoliate Orange Applied by Peroxide Hydrogen and Arbuscular Mycorrhizal Fungi. *Not. Bot. Horti Agrobot. Cluj-Napoca* **2014**, *42*, 94-98, doi:10.15835/nbha4219442.
51. Xiao, K.; Katagi, H.; Harrison, M.; Wang, Z.-Y. Improved Phosphorus Acquisition and Biomass Production in Arabidopsis by Transgenic Expression of a Purple Acid Phosphatase Gene from M. Truncatula. *Plant Sci.* **2006**, *170*, 191–202, doi:10.1016/j.plantsci.2005.08.001.
52. Yu, X.; Chen, Q.; Shi, W.; Gao, Z.; Sun, X.; Dong, J.; Li, J.; Wang, H.; Gao, J.; Liu, Z. Interactions between Phosphorus Availability and Microbes in a Wheat–Maize Double Cropping System: A Reduced Fertilization Scheme. *J. Integr. Agric.* **2022**, *21*, 840–854, doi:10.1016/S2095-3119(20)63599-7.
53. Qi, S.; Wang, J.; Wan, L.; Dai, Z.; da Silva Matos, D.M.; Du, D.; Egan, S.; Bonser, S.P.; Thomas, T.; Moles, A.T. Arbuscular Mycorrhizal Fungi Contribute to Phosphorous Uptake and Allocation Strategies of Solidago Canadensis in a Phosphorous-Deficient Environment. *Front. Plant Sci.* **2022**, *13*, doi:10.3389/fpls.2022.831654.
54. Plassard, C.; Becquer, A.; Garcia, K. Phosphorus Transport in Mycorrhiza: How Far Are We? *Trends Plant Sci.* **2019**, *24*, 794–801, doi:10.1016/j.tplants.2019.06.004.
55. Harvey, P.R.; Warren, R.A.; Wakelin, S. Potential to Improve Root Access to Phosphorus: The Role of Non-Symbiotic Microbial Inoculants in the Rhizosphere. *Crop Pasture Sci.* **2009**, *60*, 144-151, doi:10.1071/CP08084.
56. Khan, M.S.; Zaidi, A.; Ahemad, M.; Oves, M.; Wani, P.A. Plant Growth Promotion by Phosphate Solubilizing Fungi – Current Perspective. *Arch. Agron. Soil Sci.* **2010**, *56*, 73–98, doi:10.1080/03650340902806469.
57. Richardson, A.E.; Simpson, R.J. Soil Microorganisms Mediating Phosphorus Availability Update on Microbial Phosphorus. *Plant Physiol.* **2011**, *156*, 989–996, doi:10.1104/pp.111.175448.
58. Pereira, N.C.M.; Galindo, F.S.; Gazola, R.P.D.; Dupas, E.; Rosa, P.A.L.; Mortinho, E.S.; Filho, M.C.M.T. Corn Yield and Phosphorus Use Efficiency Response to Phosphorus Rates Associated With Plant Growth Promoting Bacteria. *Front. Environ. Sci.* **2020**, *8*, doi:10.3389/fenvs.2020.00040.

59. Dörmann, P.; Benning, C. Galactolipids Rule in Seed Plants. *Trends Plant Sci.* **2002**, *7*, 112–118, doi:10.1016/S1360-1385(01)02216-6.
60. Veneklaas, E.J.; Lambers, H.; Bragg, J.; Finnegan, P.M.; Lovelock, C.E.; Plaxton, W.C.; Price, C.A.; Scheible, W.R.; Shane, M.W.; White, P.J.; et al. Opportunities for Improving Phosphorus-Use Efficiency in Crop Plants. *New Phytol.* 2012, 306-320, doi: 10.1111/j.1469-8137.2012.04190.x
61. Andersson, M.X.; Larsson, K.E.; Tjellström, H.; Liljenberg, C.; Sandelius, A.S. Phosphate-Limited Oat. *J. Biol. Chem.* **2005**, *280*, 27578–27586, doi:10.1074/jbc.M503273200.
62. Andersson, M.X.; Stridh, M.H.; Larsson, K.E.; Liljenberg, C.; Sandelius, A.S. Phosphate-Deficient Oat Replaces a Major Portion of the Plasma Membrane Phospholipids with the Galactolipid Digalactosyldiacylglycerol. *FEBS Lett.* **2003**, *537*, 128–132, doi:10.1016/S0014-5793(03)00109-1.
63. Russo, M.A.; Quartacci, M.F.; Izzo, R.; Belligno, A.; Navari-Izzo, F. Long- and Short-Term Phosphate Deprivation in Bean Roots: Plasma Membrane Lipid Alterations and Transient Stimulation of Phospholipases. *Phytochemistry* **2007**, *68*, 1564–1571, doi:10.1016/j.phytochem.2007.03.017.
64. Tjellström, H.; Andersson, M.X.; Larsson, K.E.; Sandelius, A.S. Membrane Phospholipids as a Phosphate Reserve: The Dynamic Nature of Phospholipid-to-Digalactosyl Diacylglycerol Exchange in Higher Plants. *Plant. Cell Environ.* **2008**, *31*, 1388–1398, doi:10.1111/j.1365-3040.2008.01851.x.
65. Corda, D.; Mosca, M.G.; Ohshima, N.; Grauso, L.; Yanaka, N.; Mariggiò, S. The Emerging Physiological Roles of the Glycerophosphodiesterase Family. *FEBS J.* **2014**, *281*, 998–1016, doi:10.1111/febs.12699.
66. Larson, T.J.; Ehrmann, M.; Boos, W. Periplasmic Glycerophosphodiester Phosphodiesterase of Escherichia Coli, a New Enzyme of the Glp Regulon. *J. Biol. Chem.* **1983**, *258*, 5428–5432, doi:10.1016/S0021-9258(20)81908-5.
67. Lemieux, M.J.; Huang, Y.; Wang, D.-N. Glycerol-3-Phosphate Transporter of Escherichia Coli: Structure, Function and Regulation. *Res. Microbiol.* **2004**, *155*, 623–629, doi:10.1016/j.resmic.2004.05.016.
68. Schwan, T.G.; Battisti, J.M.; Porcella, S.F.; Raffel, S.J.; Schrumpf, M.E.; Fischer, E.R.; Carroll, J.A.; Stewart, P.E.; Rosa, P.; Somerville, G.A. Glycerol-3-Phosphate Acquisition in Spirochetes: Distribution and Biological Activity of Glycerophosphodiester Phosphodiesterase (GlpQ) among *Borrelia* Species. *J. Bacteriol.* **2003**, *185*, 1346–1356, doi:10.1128/JB.185.4.1346-1356.2003.
69. Ohshima, N.; Yamashita, S.; Takahashi, N.; Kuroishi, C.; Shiro, Y.; Takio, K. *Escherichia Coli* Cytosolic Glycerophosphodiester Phosphodiesterase (UgpQ) Requires Mg^{2+}, Co^{2+}, or Mn^{2+} for Its Enzyme Activity. *J. Bacteriol.* **2008**, *190*, 1219–1223, doi:10.1128/JB.01223-07.
70. Nakamura, Y. Phosphate Starvation and Membrane Lipid Remodeling in Seed Plants. *Prog. Lipid Res.* **2013**, *52*, 43–50, doi:10.1016/j.plipres.2012.07.002.
71. Cheng, L.; Bucciarelli, B.; Liu, J.; Zinn, K.; Miller, S.; Patton-Vogt, J.; Allan, D.; Shen, J.; Vance, C.P. White Lupin Cluster Root Acclimation to Phosphorus Deficiency and Root Hair Development Involve Unique Glycerophosphodiester Phosphodiesterases. *Plant Physiol.* **2011**, *156*, 1131–1148, doi:10.1104/pp.111.173724.
72. Mehra, P.; Giri, J. Rice and Chickpea GDPDs Are Preferentially Influenced by Low Phosphate and *CaGDPD1* Encodes an Active Glycerophosphodiester Phosphodiesterase Enzyme. *Plant Cell Rep.* **2016**, *35*, 1699–1717, doi:10.1007/S00299-016-1984-0.
73. Mehra, P.; Pandey, B.K.; Verma, L.; Giri, J. A Novel Glycerophosphodiester Phosphodiesterase Improves Phosphate Deficiency Tolerance in Rice. *Plant. Cell Environ.* **2019**, *42*, 1167–1179, doi:10.1111/pce.13459.
74. Ngo, A.H.; Nakamura, Y. Phosphate Starvation Inducible *GLYCEROPHOSPHODIESTER PHOSPHODIESTERASE 6* is Involved in Arabidopsis Root Growth. *J. Exp. Bot.* **2022**, *73*, 2995–3003, doi:10.1093/jxb/erac064.
75. Harrison, M.J. The Arbuscular Mycorrhizal Symbiosis: An Underground Association. *Trends Plant Sci.* **1997**, *2*, 54–60, doi:10.1016/S1360-1385(97)82563-0.
76. Ali, W.; Nadeem, M.; Ashiq, W.; Zaeem, M.; Gilani, S.S.M.; Rajabi-Khamseh, S.; Pham, T.H.; Kavanagh, V.; Thomas, R.; Cheema, M. The Effects of Organic and Inorganic Phosphorus Amendments on the Biochemical Attributes and Active Microbial Population of Agriculture Podzols Following Silage Corn

Cultivation in Boreal Climate. *Sci. Rep.* **2019**, *9*, 1-7, doi:10.1038/s41598-019-53906-8.
77. Ryan, P.; Delhaize, E.; Jones, D. F. Function and Mechanism of Organic Anion Exudation from Plant Roots. *Annu. Rev. Plant Physiol. Plant Mol. Biol.* **2001**, *52*, 527–560, doi:10.1146/annurev.arplant.52.1.527.
78. Nadeem, M.; Wu, J.; Ghaffari, H.; Kedir, A.J.; Saleem, S.; Mollier, A.; Singh, J.; Cheema, M. Understanding the Adaptive Mechanisms of Plants to Enhance Phosphorus Use Efficiency on Podzolic Soils in Boreal Agroecosystems. *Front. Plant Sci.* **2022**, *13*, 15:337, doi:10.3389/fpls.2022.804058.
79. Dinkelaker, B.; Romheld, V.; Marschner, H. Citric Acid Excretion and Precipitation of Calcium Citrate in the Rhizosphere of White Lupin (*Lupinus albus L.*). *Plant, Cell Environ.* **1989**, *12*, 285–292, doi:10.1111/j.1365-3040.1989.tb01942.x.
80. Delhaize, E.; Ryan, P.R.; Randall, P.J. Aluminum Tolerance in Wheat (*Triticum aestivum L.*) (II. Aluminum-Stimulated Excretion of Malic Acid from Root Apices). *Plant Physiol.* **1993**, *103*, 695–702, doi:10.1104/pp.103.3.695.
81. Delhaize, E.; Ryan, P.R. Aluminum Toxicity and Tolerance in Plants. *Plant Physiol.* **1995**, *107*, 315–321, doi:10.1104/pp.107.2.315.
82. Larsen, P.B.; Degenhardt, J.; Tai, C.-Y.; Stenzler, L.M.; Howell, S.H.; Kochian, L. V. Aluminum-Resistant Arabidopsis Mutants That Exhibit Altered Patterns of Aluminum Accumulation and Organic Acid Release from Roots1. *Plant Physiol.* **1998**, *117*, 9–17, doi:10.1104/pp.117.1.9.
83. Neumann, G. Physiological Aspects of Cluster Root Function and Development in Phosphorus-Deficient White Lupin (*Lupinus albus L.*). *Ann. Bot.* **2000**, *85*, 909–919, doi:10.1006/anbo.2000.1135.
84. Mehra, P.; Pandey, B.K.; Giri, J. Improvement in Phosphate Acquisition and Utilization by a Secretory Purple Acid Phosphatase (*OsPAP21b*) in Rice. *Plant Biotechnol. J.* **2017**, doi:10.1111/pbi.12699.
85. Pandey, B.K.; Mehra, P.; Verma, L.; Bhadouria, J.; Giri, J. OsHAD1, a Haloacid Dehalogenase-like Apase, Enhances Phosphate Accumulation. *Plant Physiol.* **2017**, doi:10.1104/pp.17.00571.
86. Wang, F.; Deng, M.; Chen, J.; He, Q.; Jia, X.; Guo, H.; Xu, J.; Liu, Y.; Zhang, S.; Shou, H.; et al. CASEIN KINASE2-Dependent Phosphorylation of PHOSPHATE2 Fine-Tunes Phosphate Homeostasis in Rice. *Plant Physiol.* **2020**, *183*, 250–262, doi:10.1104/pp.20.00078.
87. Hinsinger, P. Bioavailability of Soil Inorganic P in the Rhizosphere as Affected by Root-Induced Chemical Changes: A Review. *Plant Soil* **2001**, *237*, 173–195, doi:10.1023/A:1013351617532.
88. Menezes-Blackburn, D.; Paredes, C.; Zhang, H.; Giles, C.D.; Darch, T.; Stutter, M.; George, T.S.; Shand, C.; Lumsdon, D.; Cooper, P.; et al. Organic Acids Regulation of Chemical–Microbial Phosphorus Transformations in Soils. *Environ. Sci. Technol.* **2016**, *50*, 11521–11531, doi:10.1021/acs.est.6b03017.
89. Ström, L.; Owen, A.G.; Godbold, D.L.; Jones, D.L. Organic Acid Mediated P Mobilization in the Rhizosphere and Uptake by Maize Roots. *Soil Biol. Biochem.* **2002**, *34*, 703–710, doi:10.1016/S0038-0717(01)00235-8.
90. López-Bucio, J.; De la Vega, O.M.; Guevara-García, A.; Herrera-Estrella, L. Enhanced Phosphorus Uptake in Transgenic Tobacco Plants That Overproduce Citrate. *Nat. Biotechnol.* **2000**, 15:337, doi:10.1038/74531.
91. Ma, X.-F.; Wright, E.; Ge, Y.; Bell, J.; Xi, Y.; Bouton, J.H.; Wang, Z.-Y. Improving Phosphorus Acquisition of White Clover (Trifolium Repens L.) by Transgenic Expression of Plant-Derived Phytase and Acid Phosphatase Genes. *Plant Sci.* **2009**, *176*, 479–488, doi:10.1016/j.plantsci.2009.01.001.
92. Wang, X.; Wang, Y.; Tian, J.; Lim, B.L.; Yan, X.; Liao, H. Overexpressing *AtPAP15* Enhances Phosphorus Efficiency in Soybean. *Plant Physiol.* **2009**, *151*, 233–240, doi:10.1104/pp.109.138891.
93. Tomscha, J.L.; Trull, M.C.; Deikman, J.; Lynch, J.P.; Guiltinan, M.J. Phosphatase Under-Producer Mutants Have Altered Phosphorus Relations. *Plant Physiol.* **2004**, *135*, 334–345, doi:10.1104/pp.103.036459.
94. Ozawa, K.; Osaki, M.; Matsui, H.; Honma, M.; Tadano, T. Purification and Properties of Acid Phosphatase Secreted from Lupin Roots under Phosphorus-Deficiency Conditions. *Soil Sci. Plant Nutr.* **1995**, *41*, 461–469, doi:10.1080/00380768.1995.10419608.
95. Li, M.; Tadano, T. Comparison of Characteristics of Acid Phosphatases Secreted from Roots of Lupin and Tomato. *Soil Sci. Plant Nutr.* **1996**, *42*, 753–763, doi:10.1080/00380768.1996.10416623.
96. Miller, S.S.; Liu, J.; Allan, D.L.; Menzhuber, C.J.; Fedorova, M.; Vance, C.P. Molecular Control of Acid Phosphatase Secretion into the Rhizosphere of Proteoid Roots from Phosphorus-Stressed White Lupin. *Plant*

Physiol. **2001**, *127*, 594–606, doi:10.1104/pp.010097.

97. Bozzo, G.G.; Raghothama, K.G.; Plaxton, W.C. Structural and Kinetic Properties of a Novel Purple Acid Phosphatase from Phosphate-Starved Tomato (*Lycopersicon esculentum*) Cell Cultures. *Biochem. J.* **2004**, *377*, 419–428, doi:10.1042/bj20030947.
98. Bozzo, G.G.; Dunn, E.L.; Plaxton, W.C. Differential Synthesis of Phosphate-Starvation Inducible Purple Acid Phosphatase Isozymes in Tomato (Lycopersicon Esculentum) Suspension Cells and Seedlings. *Plant, Cell Environ.* **2006**, *29*, 303–313, doi:10.1111/j.1365-3040.2005.01422.x.
99. Liang, C.; Tian, J.; Lam, H.-M.; Lim, B.L.; Yan, X.; Liao, H. Biochemical and Molecular Characterization of *PvPAP3*, a Novel Purple Acid Phosphatase Isolated from Common Bean Enhancing Extracellular ATP Utilization. *Plant Physiol.* **2010**, *152*, 854–865, doi:10.1104/pp.109.147918.
100. Lung, S.-C.; Leung, A.; Kuang, R.; Wang, Y.; Leung, P.; Lim, B.-L. Phytase Activity in Tobacco (Nicotiana *tabacum*) Root Exudates is Exhibited by a Purple Acid Phosphatase. *Phytochemistry* **2008**, *69*, 365–373, doi:10.1016/j.phytochem.2007.06.036.
101. Tran, H.T.; Qian, W.; Hurley, B.A.; She, Y.-M.; Wang, D.; Plaxton, W.C. Biochemical and Molecular Characterization of *AtPAP12* and *AtPAP26*: The Predominant Purple Acid Phosphatase Isozymes Secreted by Phosphate-Starved *Arabidopsis thaliana*. *Plant. Cell Environ.* **2010**, *33*, 1789–1803, doi:10.1111/j.1365-3040.2010.02184.x.
102. del Pozo, J.C.; Allona, I.; Rubio, V.; Leyva, A.; de la Pena, A.; Aragoncillo, C.; Paz-Ares, J. A Type 5 Acid Phosphatase Gene from *Arabidopsis thaliana* is Induced by Phosphate Starvation and by Some Other Types of Phosphate Mobilising/Oxidative Stress Conditions. *Plant J.* **1999**, *19*, 579–589, doi:10.1046/j.1365-313X.1999.00562.x.
103. O'Gallagher, B.; Ghahremani, M.; Stigter, K.; Walker, E.J.L.; Pyc, M.; Liu, A.-Y.; MacIntosh, G.C.; Mullen, R.T.; Plaxton, W.C. Arabidopsis *PAP17* Is a Dual-Localized Purple Acid Phosphatase up-Regulated during Phosphate Deprivation, Senescence, and Oxidative Stress. *J. Exp. Bot.* **2022**, *73*, 382–399, doi:10.1093/jxb/erab409.
104. Wang, L.; Li, Z.; Qian, W.; Guo, W.; Gao, X.; Huang, L.; Wang, H.; Zhu, H.; Wu, J.-W.; Wang, D.; et al. The Arabidopsis Purple Acid Phosphatase AtPAP10 Is Predominantly Associated with the Root Surface and Plays an Important Role in Plant Tolerance to Phosphate Limitation. *Plant Physiol.* **2011**, *157*, 1283–1299, doi:10.1104/pp.111.183723.
105. May, A.; Berger, S.; Hertel, T.; Köck, M. The *Arabidopsis haliana* Phosphate Starvation Responsive Gene AtPPsPase1 Encodes a Novel Type of Inorganic Pyrophosphatase. *Biochim. Biophys. Acta - Gen. Subj.* **2011**, *1810*, 178–185, doi:10.1016/j.bbagen.2010.11.006.
106. Burroughs, A.M.; Allen, K.N.; Dunaway-Mariano, D.; Aravind, L. Evolutionary Genomics of the HAD Superfamily: Understanding the Structural Adaptations and Catalytic Diversity in a Superfamily of Phosphoesterases and Allied Enzymes. *J. Mol. Biol.* **2006**, *361*, 1003–1034, doi:10.1016/j.jmb.2006.06.049.
107. Kuznetsova, E.; Proudfoot, M.; Gonzalez, C.F.; Brown, G.; Omelchenko, M. V.; Borozan, I.; Carmel, L.; Wolf, Y.I.; Mori, H.; Savchenko, A. V.; et al. Genome-Wide Analysis of Substrate Specificities of the *Escherichia coli* Haloacid Dehalogenase-like Phosphatase Family. *J. Biol. Chem.* **2006**, *281*, 36149–36161, doi:10.1074/jbc.M605449200.
108. Baldwin, J.C.; Karthikeyan, A.S.; Raghothama, K.G. *LEPS2*, a Phosphorus Starvation-Induced Novel Acid Phosphatase from Tomato. *Plant Physiol.* **2001**, 728-737 doi:10.1104/pp.125.2.728.
109. Baldwin, J.C.; Karthikeyan, A.S.; Cao, A.; Raghothama, K.G. Biochemical and Molecular Analysis of *LePS2;1*: A Phosphate Starvation Induced Protein Phosphatase Gene from Tomato. *Planta* **2008**, *228*, 273–280, doi:10.1007/s00425-008-0736-y.
110. Liu, J.-Q.; Allan, D.L.; Vance, C.P. Systemic Signaling and Local Sensing of Phosphate in Common Bean: Cross-Talk between Photosynthate and MicroRNA399. *Mol. Plant* **2010**, *3*, 428–437, doi:10.1093/mp/ssq008.
111. Liang, C.-Y.; Chen, Z.-J.; Yao, Z.-F.; Tian, J.; Liao, H. Characterization of Two Putative Protein Phosphatase Genes and Their Involvement in Phosphorus Efficiency in *Phaseolus vulgaris*. F. *J. Integr. Plant Biol.* **2012**, *54*, 400–411, doi:10.1111/j.1744-7909.2012.01126.x.

112. Pandey, B.K.; Mehra, P.; Verma, L.; Bhadouria, J.; Giri, J. *OsHAD1*, a Haloacid Dehalogenase-Like APase, Enhances Phosphate Accumulation. *Plant Physiol.* **2017**, *174*, 2316–2332, doi:10.1104/pp.17.00571.
113. Duff, S.M.G.; Moorhead, G.B.G.; Lefebvre, D.D.; Plaxton, W.C. Phosphate Starvation Inducible `Bypasses' of Adenylate and Phosphate Dependent Glycolytic Enzymes in *Brassica nigra* Suspension Cells. *Plant Physiol.* **1989**, 1275-1278, doi:10.1104/pp.90.4.1275.
114. Plaxton, W.C.; Podestá, F.E. The Functional Organization and Control of Plant Respiration. *CRC. Crit. Rev. Plant Sci.* 2006, doi: 159-198, 10.1080/07352680600563876.
115. Plaxton, W.C.; Tran, H.T. Metabolic Adaptations of Phosphate-Starved Plants. *Plant Physiol.* **2011**, 1006-1015, doi:10.1104/pp.111.175281.
116. Sieger, S.M.; Kristensen, B.K.; Robson, C.A.; Amirsadeghi, S.; Eng, E.W.Y.; Abdel-Mesih, A.; Møller, I.M.; Vanlerberghe, G.C. The Role of Alternative Oxidase in Modulating Carbon Use Efficiency and Growth during Macronutrient Stress in Tobacco Cells. *J. Exp. Bot.* **2005**, 1499-1515, doi:10.1093/jxb/eri146.
117. Karthikeyan, A.S.; Varadarajan, D.K.; Jain, A.; Held, M.A.; Carpita, N.C.; Raghothama, K.G. Phosphate Starvation Responses Are Mediated by Sugar Signaling in Arabidopsis. *Planta* **2007,** 907-918,doi:10.1007/s00425-006-0408-8.
118. Abdelrahman, M.; El-Sayed, M.A.; Hashem, A.; Abd-Allah, E.F.; Alqarawi, A.A.; Burritt, D.J.; Tran, L.S.P. Metabolomics and Transcriptomics in Legumes under Phosphate Deficiency in Relation to Nitrogen Fixation by Root Nodules. *Front. Plant Sci.* 2018, 922, doi: 10.3389/fpls.2018.00922.
119. Song, Z.; Luo, Y.; Wang, W.; Fan, N.; Wang, D.; Yang, C.; Jia, H. *NtMYB12* Positively Regulates Flavonol Biosynthesis and Enhances Tolerance to Low Pi Stress in *Nicotiana tabacum*. *Front. Plant Sci.* **2020**, *10*, 1683, doi:10.3389/fpls.2019.01683.
120. Song, Z.; Luo, Y.; Wang, W.; Fan, N.; Wang, D.; Yang, C.; Jia, H. *NtMYB12* Positively Regulates Flavonol Biosynthesis and Enhances Tolerance to Low Pi Stress in *Nicotiana iabacum*. *Front. Plant Sci.* **2020**, *10*, 1683, doi:10.3389/fpls.2019.01683.
121. Pant, Bikram Datt, Asdrubal Burgos, Pooja Pant, Alvaro Cuadros-Inostroza, Lothar Willmitzer, and Wolf-Rüdiger Scheible. "The transcription factor PHR1 regulates lipid remodeling and triacylglycerol accumulation in *Arabidopsis thaliana* during phosphorus starvation. *J. Exp. Bot*. 2015, 1907-1918, doi: 10.1093/jxb/eru535.
122. Pérez-Torres, C.A.; López-Bucio, J.; Cruz-Ramírez, A.; Ibarra-Laclette, E.; Dharmasiri, S.; Estelle, M.; Herrera-Estrella, L. Phosphate Availability Alters Lateral Root Development in Arabidopsis by Modulating Auxin Sensitivity via a Mechanism Involving the TIR1 Auxin Receptor. *Plant Cell* **2008**, 3258-3272, doi:10.1105/tpc.108.058719.
123. Akiyama, K.; Matsuoka, H.; Hayashi, H. Isolation and Identification of a Phosphate Deficiency-Induced C-Glycosylflavonoid That Stimulates Arbuscular Mycorrhiza Formation in Melon Roots. *Mol. Plant-Microbe Interact.* **2002**, 334-340, doi:10.1094/MPMI.2002.15.4.334.
124. Tesfaye, M.; Temple, S.J.; Allan, D.L.; Vance, C.P.; Samac, D.A. Overexpression of Malate Dehydrogenase in Transgenic Alfalfa Enhances Organic Acid Synthesis and Confers Tolerance to Aluminum. *Plant Physiol.* **2001**, 1836-1844, doi:10.1104/pp.010376.
125. López-Arredondo, D.L.; Leyva-González, M.A.; González-Morales, S.I.; López-Bucio, J.; Herrera-Estrella, L. Phosphate Nutrition: Improving Low-Phosphate Tolerance in Crops. *Annu. Rev. Plant Biol.* 2014, 95-123, doi: 10.1146/annurev-arplant-050213-035949.
126. Veneklaas, E.J.; Lambers, H.; Bragg, J.; Finnegan, P.M.; Lovelock, C.E.; Plaxton, W.C.; Price, C.A.; Scheible, W.; Shane, M.W.; White, P.J.; et al. Opportunities for Improving Phosphorus-use Efficiency in Crop Plants. *New Phytol.* **2012**, *195*, 306–320, doi:10.1111/j.1469-8137.2012.04190.x.
127. Pearse, S.J.; Veneklaas, E.J.; Cawthray, G.; Bolland, M.D.A.; Lambers, H. Carboxylate Composition of Root Exudates Does Not Relate Consistently to a Crop Species' Ability to Use Phosphorus from Aluminium, Iron or Calcium Phosphate Sources. *New Phytol.* **2007**, 181-190, doi:10.1111/j.1469-8137.2006.01897.x.
128. Wu, P.; Shou, H.; Xu, G.; Lian, X. Improvement of Phosphorus Efficiency in Rice on the Basis of Understanding Phosphate Signaling and Homeostasis. *Curr. Opin. Plant Biol.* 2013, 205-212, doi: 10.1016/j.pbi.2013.03.002.

129. Ozturk, L.; Eker, S.; Torun, B.; Cakmak, I. Variation in Phosphorus Efficiency among 73 Bread and Durum Wheat Genotypes Grown in a Phosphorus-Deficient Calcareous Soil. In Proceedings of the Plant and Soil 2005, 69-80, doi: 10.1007/s11104-004-0469-z.
130. Hammond, J.P.; Broadley, M.R.; White, P.J.; King, G.J.; Bowen, H.C.; Hayden, R.; Meacham, M.C.; Mead, A.; Overs, T.; Spracklen, W.P.; et al. Shoot Yield Drives Phosphorus Use Efficiency in Brassica Oleracea and Correlates with Root Architecture Traits. *J. Exp. Bot.* **2009**, 1953-1968, doi:10.1093/jxb/erp083.
131. Misson, J.; Raghothama, K.G.; Jain, A.; Jouhet, J.; Block, M.A.; Bligny, R.; Ortet, P.; Creff, A.; Somerville, S.; Rolland, N.; et al. A Genome-Wide Transcriptional Analysis Using *Arabidopsis thaliana* Affymetrix Gene Chips Determined Plant Responses to Phosphate Deprivation. *Proc. Natl. Acad. Sci.* **2005**, *102*, 11934–11939, doi:10.1073/pnas.0505266102.
132. Bustos, R.; Castrillo, G.; Linhares, F.; Puga, M.I.; Rubio, V.; Pérez-Pérez, J.; Solano, R.; Leyva, A.; Paz-Ares, J. A Central Regulatory System Largely Controls Transcriptional Activation and Repression Responses to Phosphate Starvation in Arabidopsis. *PLoS Genet.* **2010**, *6*, e1001102, doi:10.1371/journal.pgen.1001102.
133. Tian, P.; Lin, Z.; Lin, D.; Dong, S.; Huang, J.; Huang, T. The Pattern of DNA Methylation Alteration, and Its Association with the Changes of Gene Expression and Alternative Splicing during Phosphate Starvation in Tomato. *Plant J.* **2021**, *108*, 841–858, doi:10.1111/TPJ.15486.
134. Pfaff, J.; Denton, A.K.; Usadel, B.; Pfaff, C. Phosphate Starvation Causes Different Stress Responses in the Lipid Metabolism of Tomato Leaves and Roots. *Biochim. Biophys. Acta - Mol. Cell Biol. Lipids* **2020**, 158763, doi:10.1016/j.bbalip.2020.158763.
135. Satheesh, V.; Zhang, J.; Li, J.; You, Q.; Zhao, P.; Wang, P.; Lei, M. High Transcriptome Plasticity Drives Phosphate Starvation Responses in Tomato. *Stress Biol.* **2022**, 1-23, doi:10.1007/s44154-022-00035-4.
136. Wang, Q.-J.; Yuan, Y.; Liao, Z.; Jiang, Y.; Wang, Q.; Zhang, L.; Gao, S.; Wu, F.; Li, M.; Xie, W.; et al. Genome-Wide Association Study of 13 Traits in Maize Seedlings under Low Phosphorus Stress. *Plant Genome* **2019**, 190039, doi:10.3835/plantgenome2019.06.0039.
137. Wasaki, J.; Shinano, T.; Onishi, K.; Yonetani, R.; Yazaki, J.; Fujii, F.; Shimbo, K.; Ishikawa, M.; Shimatani, Z.; Nagata, Y.; et al. Transcriptomic Analysis Indicates Putative Metabolic Changes Caused by Manipulation of Phosphorus Availability in Rice Leaves. In Proceedings of the Journal of Experimental Botany; 2006, 2049-2059, doi: 10.1093/jxb/erj158.
138. Li, L.H.; Qiu, X.H.; Li, X.H.; Wang, S.P.; Zhang, Q.F.; Lian, X.M. Transcriptomic Analysis of Rice Responses to Low Phosphorus Stress. *Chinese Sci. Bull.* **2010**, 2049-2059, doi:10.1007/s11434-010-0012-y.
139. Secco, D.; Jabnoune, M.; Walker, H.; Shou, H.; Wu, P.; Poirier, Y.; Whelan, J. Spatio-Temporal Transcript Profiling of Rice Roots and Shoots in Response to Phosphate Starvation and Recovery. *Plant Cell* **2013**, 4285-4304, doi:10.1105/tpc.113.117325.
140. Oono, Y.; Kobayashi, F.; Kawahara, Y.; Yazawa, T.; Handa, H.; Itoh, T.; Matsumoto, T. Characterisation of the Wheat (*Triticum aestivum L.*) Transcriptome by de Novo Assembly for the Discovery of Phosphate Starvation-Responsive Genes: Gene Expression in Pi-Stressed Wheat. *BMC Genomics* **2013**, 1-14, doi:10.1186/1471-2164-14-77.
141. Du, Q.; Wang, K.; Xu, C.; Zou, C.; Xie, C.; Xu, Y.; Li, W.X. Strand-Specific RNA-Seq Transcriptome Analysis of Genotypes with and without Low-Phosphorus Tolerance Provides Novel Insights into Phosphorus-Use Efficiency in Maize. *BMC Plant Biol.* **2016**, 1-12, doi:10.1186/s12870-016-0903-4.
142. Deng, Y.; Teng, W.; Tong, Y.P.; Chen, X.P.; Zou, C.Q. Phosphorus Efficiency Mechanisms of Two Wheat Cultivars as Affected by a Range of Phosphorus Levels in the Field. *Front. Plant Sci.* **2018**, 1614, doi:10.3389/fpls.2018.01614.
143. Zhang, J.; Jiang, F.; Shen, Y.; Zhan, Q.; Bai, B.; Chen, W.; Chi, Y. Transcriptome Analysis Reveals Candidate Genes Related to Phosphorus Starvation Tolerance in Sorghum. *BMC Plant Biol.* **2019**, 1-18, doi:10.1186/s12870-019-1914-8.
144. Aparicio-Fabre, R.; Guillén, G.; Loredo, M.; Arellano, J.; Valdés-López, O.; Ramírez, M.; Íñiguez, L.P.; Panzeri, D.; Castiglioni, B.; Cremonesi, P.; et al. Common Bean (*Phaseolus vulgaris L.*) *PvTIFY* Orchestrates Global Changes in Transcript Profile Response to Jasmonate and Phosphorus Deficiency. *BMC Plant Biol.*

2013, 1-22, doi:10.1186/1471-2229-13-26.

145. O'Rourke, J.A.; Yang, S.S.; Miller, S.S.; Bucciarelli, B.; Liu, J.; Rydeen, A.; Bozsoki, Z.; Uhde-Stone, C.; Tu, Z.J.; Allan, D.; et al. An RNA-Seq Transcriptome Analysis of Orthophosphate-Deficient White lupin Reveals Novel Insights into Phosphorus Acclimation in Plants. *Plant Physiol.* **2013**, *161*, 705–724, doi:10.1104/pp.112.209254.
146. Wang, Z.; Straub, D.; Yang, H.; Kania, A.; Shen, J.; Ludewig, U.; Neumann, G. The Regulatory Network of Cluster-Root Function and Development in Phosphate-Deficient White Lupin (*Lupinus albus*) Identified by Transcriptome Sequencing. *Physiol. Plant.* **2014**, *151*, 323–338, doi:10.1111/ppl.12187.
147. Zeng, H.; Wang, G.; Zhang, Y.; Hu, X.; Pi, E.; Zhu, Y.; Wang, H.; Du, L. Genome-Wide Identification of Phosphate-Deficiency-Responsive Genes in Soybean Roots by High-Throughput Sequencing. *Plant Soil* **2016**, *398*, 207–227, doi:10.1007/s11104-015-2657-4.
148. Svistoonoff, S.; Creff, A.; Reymond, M.; Sigoillot-Claude, C.; Ricaud, L.; Blanchet, A.; Nussaume, L.; Desnos, T. Root Tip Contact with Low-Phosphate Media Reprograms Plant Root Architecture. *Nat. Genet. 2007 396* **2007**, *39*, 792–796, doi:10.1038/ng2041.
149. Lai, F.; Thacker, J.; Li, Y.; Journal, P.D.-T.P.; 2007, undefined Cell Division Activity Determines the Magnitude of Phosphate Starvation Responses in Arabidopsis. *Wiley Online Libr.* **2007**, *50*, 545–556, doi:10.1111/j.1365-313X.2007.03070.x.
150. Giots, F.; Donaton, M.C. V.; Thevelein, J.M. Inorganic Phosphate Is Sensed by Specific Phosphate Carriers and Acts in Concert with Glucose as a Nutrient Signal for Activation of the Protein Kinase A Pathway in the Yeast *Saccharomyces cerevisiae*. *Mol. Microbiol.* **2003**, *47*, 1163–1181, doi:10.1046/j.1365-2958.2003.03365.x.
151. Popova, Y.; Thayumanavan, P.; Lonati, E.; Agrochão, M.; Thevelein, J.M. Transport and Signaling through the Phosphate-Binding Site of the Yeast Pho84 Phosphate Transceptor. *Proc. Natl. Acad. Sci. U. S. A.* **2010**, *107*, 2890–2895, doi:10.1073/PNAS.0906546107.
152. Harrison, M.J.; Dewbre, G.R.; Liu, J. A Phosphate Transporter from *Medicago Truncatula* Involved in the Acquisition of Phosphate Released by Arbuscular Mycorrhizal Fungi. *Plant Cell* **2002**, *14*, 2413–2429, doi:10.1105/tpc.004861.
153. Raghothama, K.G.; Karthikeyan, A.S. Phosphate Acquisition. *Plant Soil* **2005**, *274*, 37–49, doi:10.1007/s11104-004-2005-6.
154. Versaw, W.K.; Harrison, M.J. A Chloroplast Phosphate Transporter, PHT2;1, Influences Allocation of Phosphate within the Plant and Phosphate-Starvation Responses. *Plant Cell* **2002**, *14*, 1751–1766, doi:10.1105/tpc.002220.
155. Dissanayaka, D.M.S.B.; Ghahremani, M.; Siebers, M.; Wasaki, J.; Plaxton, W.C. Recent Insights into the Metabolic Adaptations of Phosphorus-Deprived Plants. *J. Exp. Bot.* **2021**, *72*, 199–223, doi:10.1093/jxb/eraa482.
156. Mudge, S.R.; Rae, A.L.; Diatloff, E.; Smith, F.W. Expression Analysis Suggests Novel Roles for Members of the Pht1 Family of Phosphate Transporters in Arabidopsis. *Plant J.* **2002**, *31*, 341–353, doi:10.1046/j.1365-313X.2002.01356.x.
157. Misson, J.; Thibaud, M.-C.; Bechtold, N.; Raghothama, K.; Nussaume, L. Transcriptional Regulation and Functional Properties of Arabidopsis Pht1;4, a High Affinity Transporter Contributing Greatly to Phosphate Uptake in Phosphate Deprived Plants. *Plant Mol. Biol.* **2004**, *55*, 727–741, doi:10.1007/s11103-004-1965-5.
158. Shin, H.; Shin, H.-S.; Dewbre, G.R.; Harrison, M.J. Phosphate Transport in *Arabidopsis* : Pht1;1 and Pht1;4 Play a Major Role in Phosphate Acquisition from Both Low- and High-Phosphate Environments. *Plant J.* **2004**, *39*, 629–642, doi:10.1111/j.1365-313X.2004.02161.x.
159. Paszkowski, U.; Kroken, S.; Roux, C.; Briggs, S.P. Rice Phosphate Transporters Include an Evolutionarily Divergent Gene Specifically Activated in Arbuscular Mycorrhizal Symbiosis. *Proc. Natl. Acad. Sci.* **2002**, *99*, 13324–13329, doi:10.1073/pnas.202474599.
160. PREUSS, C.P.; HUANG, C.Y.; TYERMAN, S.D. Proton-Coupled High-Affinity Phosphate Transport Revealed from Heterologous Characterization in Xenopus of Barley-Root Plasma Membrane Transporter,

HvPHT1;1. *Plant. Cell Environ.* **2011**, *34*, 681–689, doi:10.1111/j.1365-3040.2010.02272.x.
161. Sisaphaithong, T.; Kondo, D.; Matsunaga, H.; Kobae, Y.; Hata, S. Expression of Plant Genes for Arbuscular Mycorrhiza-Inducible Phosphate Transporters and Fungal Vesicle Formation in Sorghum, Barley, and Wheat Roots. *Biosci. Biotechnol. Biochem.* **2012**, *76*, 2364–2367, doi:10.1271/bbb.120782.
162. Hufnagel, B.; de Sousa, S.M.; Assis, L.; Guimaraes, C.T.; Leiser, W.; Azevedo, G.C.; Negri, B.; Larson, B.G.; Shaff, J.E.; Pastina, M.M.; et al. Duplicate and Conquer: Multiple Homologs of *PHOSPHORUS-STARVATION TOLERANCE1* Enhance Phosphorus Acquisition and Sorghum Performance on Low-Phosphorus Soils. *Plant Physiol.* **2014**, *166*, 659–677, doi:10.1104/pp.114.243949.
163. Rausch, C.; Daram, P.; Brunner, S.; Jansa, J.; Laloi, M.; Leggewie, G.; Amrhein, N.; Bucher, M. A Phosphate Transporter Expressed in Arbuscule-Containing Cells in Potato. *Nature* **2001**, *414*, 462–465, doi:10.1038/35106601.
164. Smith, F.W. Sulphur and Phosphorus Transport Systems in Plants. *Plant Soil* **2001**, *232*, 109–118, doi:10.1023/A:1010390120820.
165. Smith, F.W., Mudge, S.R., Rae, A.L. et al. Phosphate transport in plants. Plant and Soil, 2003, 248, 71–83, doi:10.1023/A:1022376332180.
166. Morcuende, R.; Bari, R.; Gibon, Y.; Zheng, W.; Pant, B.D.; Bläsing, O.; Usadel, B.; Czechowski, T.; Udvardi, M.K.; Stitt, M.; et al. Genome-Wide Reprogramming of Metabolism and Regulatory Networks of Arabidopsis in Response to Phosphorus. *Plant, Cell Environ.* **2007**, *30*, 85–112, doi:10.1111/j.1365-3040.2006.01608.x.
167. Chiou, T.-J.; Aung, K.; Lin, S.-I.; Wu, C.-C.; Chiang, S.-F.; Su, C. Regulation of Phosphate Homeostasis by MicroRNA in *Arabidopsis*. *Plant Cell* **2006**, *18*, 412–421, doi:10.1105/tpc.105.038943.
168. Huang, T.K.; Han, C.L.; Lin, S.I.; Chen, Y.J.; Tsai, Y.C.; Chen, Y.R.; Chen, J.W.; Lin, W.Y.; Chen, P.M.; Liu, T.Y. Identification of Downstream Components of Ubiquitin-Conjugating Enzyme PHOSPHATE2 by Quantitative Membrane Proteomics in Arabidopsis Roots. *Plant Cell* **2013**, 4044-4060, doi:10.1105/tpc.113.115998.
169. Yang, Z.; Yang, J.; Wang, Y.; Wang, F.; Mao, W.; He, Q.; Xu, J.; Wu, Z.; Mao, C. PROTEIN PHOSPHATASE95 Regulates Phosphate Homeostasis by Affecting Phosphate Transporter Trafficking in Rice. *Plant Cell* **2020**, *32*, 740–757, doi:10.1105/tpc.19.00685.
170. Wang, Y.; Chen, Y.; Wu, W. Potassium and Phosphorus Transport and Signaling in Plants. *J. Integr. Plant Biol.* **2021**, *63*, 34–52, doi:10.1111/jipb.13053.
171. Che, J.; Yamaji, N.; Miyaji, T.; Mitani-Ueno, N.; Kato, Y.; Shen, R.F.; Ma, J.F. Node-Localized Transporters of Phosphorus Essential for Seed Development in Rice. *Plant Cell Physiol.* **2020**, *61*, 1387–1398, doi:10.1093/pcp/pcaa074.
172. Ma, B.; Zhang, L.; Gao, Q.; Wang, J.; Li, X.; Wang, H.; Liu, Y.; Lin, H.; Liu, J.; Wang, X.; et al. A Plasma Membrane Transporter Coordinates Phosphate Reallocation and Grain Filling in Cereals. *Nat. Genet.* **2021**, *53*, 906–915, doi:10.1038/s41588-021-00855-6.
173. Liu, J.; Yang, L.; Luan, M.; Wang, Y.; Zhang, C.; Zhang, B.; Shi, J.; Zhao, F.-G.; Lan, W.; Luan, S. A Vacuolar Phosphate Transporter Essential for Phosphate Homeostasis in *Arabidopsis*. *Proc. Natl. Acad. Sci.* **2015**, E6571-E6578, doi:10.1073/pnas.1514598112.
174. Liu, T.-Y.; Huang, T.-K.; Yang, S.-Y.; Hong, Y.-T.; Huang, S.-M.; Wang, F.-N.; Chiang, S.-F.; Tsai, S.-Y.; Lu, W.-C.; Chiou, T.-J. Identification of Plant Vacuolar Transporters Mediating Phosphate Storage. *Nat. Commun.* **2016**, 1-11,, 11095, doi:10.1038/ncomms11095.
175. Xu, L.; Zhao, H.; Wan, R.; Liu, Y.; Xu, Z.; Tian, W.; Ruan, W.; Wang, F.; Deng, M.; Wang, J.; et al. Identification of Vacuolar Phosphate Efflux Transporters in Land Plants. *Nat. Plants* **2019**, *5*, 84–94, doi:10.1038/s41477-018-0334-3.
176. Raboy, V.; Young, K.A.; Dorsch, J.A.; Cook, A. Genetics and Breeding of Seed Phosphorus and Phytic Acid. *J. Plant Physiol.* **2001**, *158*, 489–497, doi:10.1078/0176-1617-00361.
177. Sahu, A.; Banerjee, S.; Raju, A.S.; Chiou, T.-J.; Garcia, L.R.; Versaw, W.K. Spatial Profiles of Phosphate in Roots Indicate Developmental Control of Uptake, Recycling, and Sequestration. *Plant Physiol.* **2020**, *184*, 2064–2077, doi:10.1104/pp.20.01008.

178. Nilsson, L.; Müller, R.; Nielsen, T.H. Dissecting the Plant Transcriptome and the Regulatory Responses to Phosphate Deprivation. *Physiol. Plant.* **2010**, *139*, 129–143, doi:10.1111/j.1399-3054.2010.01356.x.
179. Rubio, V.; Linhares, F.; Solano, R.; Martín, A.C.; Iglesias, J.; Leyva, A.; Paz-Ares, J. A Conserved MYB Transcription Factor Involved in Phosphate Starvation Signaling Both in Vascular Plants and in Unicellular Algae. *Genes Dev.* **2001**, doi:10.1101/gad.204401.
180. Miura, K.; Rus, A.; Sharkhuu, A.; Yokoi, S.; Karthikeyan, A.S.; Raghothama, K.G.; Baek, D.; Koo, Y.D.; Jin, J.B.; Bressan, R.A.; et al. The *Arabidopsis* SUMO E3 Ligase SIZ1 Controls Phosphate Deficiency Responses. *Proc. Natl. Acad. Sci.* **2005**, *102*, 7760–7765, doi:10.1073/pnas.0500778102.
181. Müller, R.; Morant, M.; Jarmer, H.; Nilsson, L.; Nielsen, T.H. Genome-Wide Analysis of the Arabidopsis Leaf Transcriptome Reveals Interaction of Phosphate and Sugar Metabolism. *Plant Physiol.* **2007**, *143*, 156–171, doi:10.1104/pp.106.090167.
182. Zhou, J.; Jiao, F.; Wu, Z.; Li, Y.; Wang, X.; He, X.; Zhong, W.; Wu, P. *OsPHR2* Is Involved in Phosphate-Starvation Signaling and Excessive Phosphate Accumulation in Shoots of Plants. *Plant Physiol.* **2008**, *146*, 1673–1686, doi:10.1104/pp.107.111443.
183. Bustos, R.; Castrillo, G.; Linhares, F.; Puga, M.I.; Rubio, V.; Pérez-Pérez, J.; Solano, R.; Leyva, A.; Paz-Ares, J. A Central Regulatory System Largely Controls Transcriptional Activation and Repression Responses to Phosphate Starvation in Arabidopsis. *PLoS Genet.* **2010**, e1001102, doi:10.1371/journal.pgen.1001102.
184. Guo, M.; Ruan, W.; Li, C.; Huang, F.; Zeng, M.; Liu, Y.; Yu, Y.; Ding, X.; Wu, Y.; Wu, Z.; et al. Integrative Comparison of the Role of the PHOSPHATE RESPONSE1 Subfamily in Phosphate Signaling and Homeostasis in Rice. *Plant Physiol.* **2015**, *168*, 1762–1776, doi:10.1104/pp.15.00736.
185. Zhang, Yongqiang, Yi Wang, Enhui Wang, Xueqian Wu, Qinghua Zheng, Yizhen Han, Weiwei Lin, Zhongjuan Liu, and Wenxiong Lin. "SlPHL1, a MYB-CC transcription factor identified from tomato, positively regulates the phosphate starvation response. Physiol. Plant. 2021, 1063-1077, doi:10.1111/ppl.13503.
186. Ruan, W.; Guo, M.; Cai, L.; Hu, H.; Li, C.; Liu, Y.; Wu, Z.; Mao, C.; Yi, K.; Wu, P.; et al. Genetic Manipulation of a High-Affinity PHR1 Target Cis-Element to Improve Phosphorous Uptake in *Oryza sativa L. Plant Mol. Biol.* **2015**, *87*, 429–440, doi:10.1007/S11103-015-0289-Y/FIGURES/6.
187. Wang, F.; Deng, M.; Xu, J.; Zhu, X.; Mao, C. Molecular Mechanisms of Phosphate Transport and Signaling in Higher Plants. *Semin. Cell Dev. Biol.* **2018**, *74*, 114–122, doi:10.1016/j.semcdb.2017.06.013.
188. Mukatira, U.T.; Liu, C.; Varadarajan, D.K.; Raghothama, K.G. Negative Regulation of Phosphate Starvation-Induced Genes. *Plant Physiol.* **2001**, *127*, 1854–1862, doi:10.1104/pp.010876.
189. Hammond, J.P.; Bennett, M.J.; Bowen, H.C.; Broadley, M.R.; Eastwood, D.C.; May, S.T.; Rahn, C.; Swarup, R.; Woolaway, K.E.; White, P.J. Changes in Gene Expression in Arabidopsis Shoots during Phosphate Starvation and the Potential for Developing Smart Plants. *Plant Physiol.* **2003**, doi:10.1104/pp.103.020941.
190. Misson, J.; Raghothama, K.G.; Jain, A.; Jouhet, J.; Block, M.A.; Bligny, R.; Ortet, P.; Creff, A.; Somerville, S.; Rolland, N.; et al. A Genome-Wide Transcriptional Analysis Using *Arabidopsis thaliana* Affymetrix Gene Chips Determined Plant Responses to Phosphate Deprivation. *Proc. Natl. Acad. Sci. U. S. A.* **2005**, doi:10.1073/pnas.0505266102.
191. Bari, R.; Datt Pant, B.; Stitt, M.; Scheible, W.-R. PHO2, MicroRNA399, and PHR1 Define a Phosphate-Signaling Pathway in Plants. *Plant Physiol.* **2006**, *141*, 988–999, doi:10.1104/pp.106.079707.
192. Stefanovic, A.; Ribot, C.; Rouached, H.; Wang, Y.; Chong, J.; Belbahri, L.; Delessert, S.; Poirier, Y. Members of the PHO1 Gene Family Show Limited Functional Redundancy in Phosphate Transfer to the Shoot, and Are Regulated by Phosphate Deficiency via Distinct Pathways. *Plant J.* **2007**, *50*, 982–994, doi:10.1111/j.1365-313X.2007.03108.x.
193. Duan, K.; Yi, K.; Dang, L.; Huang, H.; Wu, W.; Wu, P. Characterization of a Sub-Family of Arabidopsis Genes with the SPX Domain Reveals Their Diverse Functions in Plant Tolerance to Phosphorus Starvation. *Plant J.* **2008**, *54*, 965–975, doi:10.1111/j.1365-313X.2008.03460.x.
194. Bayle, V.; Arrighi, J.-F.; Creff, A.; Nespoulous, C.; Vialaret, J.; Rossignol, M.; Gonzalez, E.; Paz-Ares, J.; Nussaume, *L. Arabidopsis thaliana* High-Affinity Phosphate Transporters Exhibit Multiple Levels of

Posttranslational Regulation. *Plant Cell* **2011**, *23*, 1523–1535, doi:10.1105/tpc.110.081067.

195. Chen, N.; Tong, S.; Yang, J.; Qin, J.; Wang, W.; Chen, K.; Shi, W.; Li, J.; Liu, J.; Jiang, Y. PtoWRKY40 Interacts with PtoPHR1-LIKE3 While Regulating the Phosphate Starvation Response in Poplar. *Plant Physiol.* **2022**, 2688-2705, doi:10.1093/plphys/kiac404.
196. Huang, K.L.; Ma, G.J.; Zhang, M.L.; Xiong, H.; Wu, H.; Zhao, C.Z.; Liu, C. Sen; Jia, H.X.; Chen, L.; Kjorven, J.O. The ARF7 and ARF19 Transcription Factors Positively Regulate PHOSPHATE STARVATION RESPONSE1 in Arabidopsis Roots. *Plant Physiol.* **2018**, *178*, 413, doi:10.1104/PP.17.01713.
197. Dai, X.; Zhou, L.; Zhang, W.; Cai, L.; Guo, H.; Tian, H.; Schiefelbein, J.; Wang, S. A Single Amino Acid Substitution in the R3 Domain of GLABRA1 Leads to Inhibition of Trichome Formation in Arabidopsis without Affecting Its Interaction with GLABRA3. *Plant Cell Environ.* **2016**, 897-907, doi:10.1111/pce.12695.
198. Chen, Y.; Wu, P.; Zhao, Q.; Tang, Y.; Chen, Y.; Li, M.; Jiang, H.; Wu, G. Overexpression of a Phosphate Starvation Response *AP2*/*ERF* Gene From Physic Nut in Arabidopsis Alters Root Morphological Traits and Phosphate Starvation-Induced Anthocyanins Accumulation. *Front. Plant Sci.* **2018**, *9*, 1186, doi:10.3389/FPLS.2018.01186.
199. Li, Z.; Hua, X.; Zhong, W.; Yuan, Y.; Wang, Y.; Wang, Z.; Ming, R.; Zhang, J. Genome-Wide Identification and Expression Profile Analysis of WRKY Family Genes in the Autopolyploid Saccharum Spontaneum. *Plant Cell Physiol.* **2020**, 616-630. doi:10.1093/pcp/pcz227.
200. He, Q.; Lu, H.; Guo, H.; Wang, Y.; Zhao, P.; Li, Y.; Wang, F.; Xu, J.; Mo, X.; Mao, C. OsbHLH6 Interacts with OsSPX4 and Regulates the Phosphate Starvation Response in Rice. *Plant J.* **2021**, *105*, 649–667, doi:10.1111/tpj.15061.
201. Chen, Z.-H.; Nimmo, G.A.; Jenkins, G.I.; Nimmo, H.G. BHLH32 Modulates Several Biochemical and Morphological Processes That Respond to Pi Starvation in Arabidopsis. *Biochem. J.* **2007**, *405*, 191–198, doi:10.1042/BJ20070102.
202. Secco, D.; Wang, C.; Arpat, B.A.; Wang, Z.; Poirier, Y.; Tyerman, S.D.; Wu, P.; Shou, H.; Whelan, J. The Emerging Importance of the SPX Domain-Containing Proteins in Phosphate Homeostasis. *New Phytol.* 2012, 842-851, doi: 10.1111/j.1469-8137.2011.04002.x
203. Wang, Z.; Kuo, H.-F.; Chiou, T.-J. Intracellular Phosphate Sensing and Regulation of Phosphate Transport Systems in Plants. *Plant Physiol.* **2021**, *187*, 2043–2055, doi:10.1093/plphys/kiab343.
204. Wild, R.; Gerasimaite, R.; Jung, J.-Y.; Truffault, V.; Pavlovic, I.; Schmidt, A.; Saiardi, A.; Jessen, H.J.; Poirier, Y.; Hothorn, M.; et al. Control of Eukaryotic Phosphate Homeostasis by Inositol Polyphosphate Sensor Domains. *Science.*. **2016**, *352*, 986–990, doi:10.1126/science.aad9858.
205. Puga, M.I.; Mateos, I.; Charukesi, R.; Wang, Z.; Franco-Zorrilla, J.M.; De Lorenzo, L.; Irigoyen, M.L.; Masiero, S.; Bustos, R.; Rodríguez, J. *SPX1* is a Phosphate-Dependent Inhibitor of Phosphate Starvation Response 1 in Arabidopsis. *Proc. Natl. Acad. Sci. U. S. A.* **2014**, 14947-14952, doi:10.1073/pnas.1404654111.
206. Wang, Z.; Ruan, W.; Shi, J.; Zhang, L.; Xiang, D.; Yang, C.; Li, C.; Wu, Z.; Liu, Y.; Yu, Y.; et al. Rice *SPX1* and *SPX2* Inhibit Phosphate Starvation Responses through Interacting with PHR2 in a Phosphate-Dependent Manner. *Proc. Natl. Acad. Sci. U. S. A.* **2014**, 14953-14958, doi:10.1073/pnas.1404680111.
207. Lv, Q.; Zhong, Y.; Wang, Y.; Wang, Z.; Zhang, L.; Shi, J.; Wu, Z.; Liu, Y.; Mao, C.; Yi, K.; et al. *SPX4* Negatively Regulates Phosphate Signaling and Homeostasis through Its Interaction with *PHR2* in Rice. *Plant Cell* **2014**, *26*, 1586–1597, doi:10.1105/tpc.114.123208.
208. Liu, J.; Fu, S.; Yang, L.; Luan, M.; Zhao, F.; Luan, S.; Lan, W. Vacuolar SPX-MFS Transporters Are Essential for Phosphate Adaptation in Plants. *Plant Signal. Behav.* **2016**, *11*, e1213474, doi:10.1080/15592324.2016.1213474.
209. Nacry, P.; Canivenc, G.; Muller, B.; Azmi, A.; Van Onckelen, H.; Rossignol, M.; Doumas, P. A Role for Auxin Redistribution in the Responses of the Root System Architecture to Phosphate Starvation in Arabidopsis. *Plant Physiol.* **2005**, *138*, 2061–2074, doi:10.1104/pp.105.060061.
210. Dong, J.; Piñeros, M.A.; Li, X.; Yang, H.; Liu, Y.; Murphy, A.S.; Kochian, L. V; Liu, D. An Arabidopsis ABC Transporter Mediates Phosphate Deficiency-Induced Remodeling of Root Architecture by Modulating Iron Homeostasis in Roots. *Mol. Plant* **2017** 244-259, doi:10.1016/j.molp.2016.11.001.

211. Uhde-Stone, C. White lupin: Legume Nitrogen Fixation in Soils with Low Phosphorus AvailabilitySpringer International Publishing: Cham, 2017, 243–280, doi: 10.1007/978-3-319-55729-8
212. Bhosale, R.; Giri, J.; Pandey, B.K.; Giehl, R.F.H.; Hartmann, A.; Traini, R.; Truskina, J.; Leftley, N.; Hanlon, M.; Swarup, K. A Mechanistic Framework for Auxin Dependent Arabidopsis Root Hair Elongation to Low External Phosphate. *Nat. Commun.* **2018**, *9*, 1409, doi:10.1038/s41467-018-03851-3.
213. Vejchasarn, P.; Lynch, J.P.; Brown, K.M. Genetic Variability in Phosphorus Responses of Rice Root Phenotypes. *Rice* **2016**, *9*, 1-16, doi:10.1186/s12284-016-0102-9.
214. Borch, K.; Bouma, T.J.; Lynch, J.P.; Brown, K.M. Ethylene: A Regulator of Root Architectural Responses to Soil Phosphorus Availability. *Plant, Cell Environ.* **1999**, *22*, 425–431, doi:10.1046/j.1365-3040.1999.00405.x.
215. Castrillo, G.; Teixeira, P.J.P.L.; Paredes, S.H.; Law, T.F.; de Lorenzo, L.; Feltcher, M.E.; Finkel, O.M.; Breakfield, N.W.; Mieczkowski, P.; Jones, C.D.; et al. Root Microbiota Drive Direct Integration of Phosphate Stress and Immunity. *Nature* **2017**, *543*, 513–518, doi:10.1038/nature21417.
216. Crombez, H.; Motte, H.; Beeckman, T. Tackling Plant Phosphate Starvation by the Roots. *Dev. Cell* **2019**, *48*, 599–615, doi:10.1016/j.devcel.2019.01.002.
217. Wang, Z.; Ruan, W.; Shi, J.; Zhang, L.; Xiang, D.; Yang, C.; Li, C.; Wu, Z.; Liu, Y.; Yu, Y.; et al. Rice *SPX1* and *SPX2* Inhibit Phosphate Starvation Responses through Interacting with PHR2 in a Phosphate-Dependent Manner., doi:10.1073/pnas.1404680111.
218. Shen, C.; Wang, S.; Zhang, S.; Xu, Y.; Qian, Q.; Qi, Y.; Jiang, D.A. *OsARF16*, a Transcription Factor, Is Required for Auxin and Phosphate Starvation Response in Rice (*Oryza sativa* L.). *Plant. Cell Environ.* **2013**, *36*, 607–620, doi:10.1111/pce.12001.
219. Narise, T.; Kobayashi, K.; Baba, S.; Shimojima, M.; Masuda, S.; Fukaki, H.; Ohta, H. Involvement of Auxin Signaling Mediated by *IAA14* and *ARF7*/*19* in Membrane Lipid Remodeling during Phosphate Starvation. *Plant Mol. Biol.* **2010**, *72*, 533–544, doi:10.1007/s11103-009-9589-4.
220. Gahoonia, T.S.; Nielsen, N.E. Variation in Root Hairs of Barley Cultivars Doubled Soil Phosphorus Uptake. *Euphytica* **1997**, *98*, 177–182, doi:10.1023/A:1003113131989.
221. Bates, T.R.; Lynch, J.P. Stimulation of Root Hair Elongation in *Arabidopsis thaliana* by Low Phosphorus Availability. *Plant, Cell Environ.* **1996**, *19*, 529–538, doi:10.1111/J.1365-3040.1996.TB00386.X.
222. Föshe, D., N. Classen, and A. Jungk. Phosphorus efficiency of plants: II. Significance of root radius, root hairs and catio-anion balance for phosphorus influx in seven plant species. *Plant and Soil*. 1991, 261-272.
223. Brown, L.K.; George, T.S.; Dupuy, L.X.; White, P.J. A Conceptual Model of Root Hair Ideotypes for Future Agricultural Environments: What Combination of Traits Should Be Targeted to Cope with Limited P Availability? *Ann. Bot.* **2013**, *112*, 317–330, doi:10.1093/aob/mcs231.
224. Yan, X.; Liao, H.; Beebe, S.E.; Blair, M.W.; Lynch, J.P. QTL Mapping of Root Hair and Acid Exudation Traits and Their Relationship to Phosphorus Uptake in Common Bean. *Plant Soil* **2004**, *265*, 17–29, doi:10.1007/s11104-005-0693-1.
225. Mangano, S.; Denita-Juarez, S.P.; Marzol, E.; Borassi, C.; Estevez, J.M. High Auxin and High Phosphate Impact on *RSL2* Expression and ROS-Homeostasis Linked to Root Hair Growth in *Arabidopsis haliana*. *Front. Plant Sci.* **2018**, *9*, doi:10.3389/fpls.2018.01164.
226. Velasquez, S.M.; Barbez, E.; Kleine-Vehn, J.; Estevez, J.M. Auxin and Cellular Elongation. *Plant Physiol.* **2016**, *170*, 1206–1215, doi:10.1104/pp.15.01863.
227. He, C.; Morgan, P.; Physiology, M.D.-P.; 1992, undefined Enhanced Sensitivity to Ethylene in Nitrogen- or Phosphate-Starved Roots of *Zea mays L*. during Aerenchyma Formation. *academic.oup.com* **1992**, *98*, 137–142.
228. Borch, K.; Bouma, T.J.; Lynch, J.P.; Brown, K.M. Ethylene: A Regulator of Root Architectural Responses to Soil Phosphorus Availability. *Plant, Cell Environ.* **1999**, *22*, 425–431, doi:10.1046/j.1365-3040.1999.00405.x.
229. Gilbert, G. Proteoid Root Development of Phosphorus Deficient Lupin Is Mimicked by Auxin and Phosphonate. *Ann. Bot.* **2000**, *85*, 921–928, doi:10.1006/anbo.2000.1133.

230. Lei, M.; Zhu, C.; Liu, Y.; Karthikeyan, A.S.; Bressan, R.A.; Raghothama, K.G.; Liu, D. Ethylene Signalling Is Involved in Regulation of Phosphate Starvation-induced Gene Expression and Production of Acid Phosphatases and Anthocyanins in Arabidopsis. *New Phytol.* **2011**, *189*, 1084–1095, doi:10.1111/j.1469-8137.2010.03555.x.
231. He, C.-J.; Morgan, P.W.; Drew, M.C. Enhanced Sensitivity to Ethylene in Nitrogen- or Phosphate-Starved Roots of *Zea Mays* L. during Aerenchyma Formation. *Plant Physiol.* **1992**, *98*, 137–142, doi:10.1104/pp.98.1.137.
232. Kim, H.-J.; Lynch, J.P.; Brown, K.M. Ethylene Insensitivity Impedes a Subset of Responses to Phosphorus Deficiency in Tomato and Petunia. *Plant. Cell Environ.* **2008**, *31*, 1744–1755, doi:10.1111/j.1365-3040.2008.01886.x.
233. Wang, Z.; Rahman, A.B.M.M.; Wang, G.; Ludewig, U.; Shen, J.; Neumann, G. Hormonal Interactions during Cluster-Root Development in Phosphate-Deficient White Lupin (*Lupinus albus L.*). *J. Plant Physiol.* **2015**, *177*, 74–82, doi:10.1016/j.jplph.2014.10.022.
234. Basu, P.; Zhang, Y.-J.; Lynch, J.P.; Brown, K.M. Ethylene Modulates Genetic, Positional, and Nutritional Regulation of Root Plagiogravitropism. *Funct. Plant Biol.* **2007**, *34*, 41-51, doi:10.1071/FP06209.
235. Zhang, Y.-J. Ethylene and Phosphorus Availability Have Interacting yet Distinct Effects on Root Hair Development. *J. Exp. Bot.* **2003**, *54*, 2351–2361, doi:10.1093/jxb/erg250.
236. Song, L.; Yu, H.; Dong, J.; Che, X.; Jiao, Y.; Liu, D. The Molecular Mechanism of Ethylene-Mediated Root Hair Development Induced by Phosphate Starvation. *PLOS Genet.* **2016**, *12*, e1006194, doi:10.1371/journal.pgen.1006194.
237. Ma, Z.; Baskin, T.I.; Brown, K.M.; Lynch, J.P. Regulation of Root Elongation under Phosphorus Stress Involves Changes in Ethylene Responsiveness. *Plant Physiol.* **2003**, *131*, 1381–1390, doi:10.1104/pp.012161.
238. Umehara, M.; Hanada, A.; Yoshida, S.; Akiyama, K.; Arite, T.; Takeda-Kamiya, N.; Magome, H.; Kamiya, Y.; Shirasu, K.; Yoneyama, K. Inhibition of Shoot Branching by New Terpenoid Plant Hormones. *Nat. 2008 4557210* **2008**, *455*, 195–200, doi:10.1038/nature07272.
239. López-Ráez, J.A.; Charnikhova, T.; Gómez-Roldán, V.; Matusova, R.; Kohlen, W.; De Vos, R.; Verstappen, F.; Puech-Pages, V.; Bécard, G.; Mulder, P.. Tomato Strigolactones Are Derived from Carotenoids and Their Biosynthesis Is Promoted by Phosphate Starvation. *New Phytol.* **2008**, *178*, 863–874, doi:10.1111/j.1469-8137.2008.02406.x.
240. Czarnecki, O.; Yang, J.; Weston, D.; Tuskan, G.; Chen, J.-G. A Dual Role of Strigolactones in Phosphate Acquisition and Utilization in Plants. *Int. J. Mol. Sci.* **2013**, *14*, 7681–7701, doi:10.3390/ijms14047681.
241. Kapulnik, Y.; Delaux, P.M.; Resnick, N.; Mayzlish-Gati, E.; Wininger, S.; Bhattacharya, C.; Séjalon-Delmas, N.; Combier, J.P.; Bécard, G.; Belausov, E.. Strigolactones Affect Lateral Root Formation and Root-Hair Elongation in Arabidopsis. *Planta* **2011**, *233*, 209–216, doi:10.1007/S00425-010-1310-Y.
242. Ruyter-Spira, C.; Kohlen, W.; Charnikhova, T.; van Zeijl, A.; van Bezouwen, L.; de Ruijter, N.; Cardoso, C.; Lopez-Raez, J.A.; Matusova, R.; Bours, R. Physiological Effects of the Synthetic Strigolactone Analog GR24 on Root System Architecture in Arabidopsis: Another Belowground Role for Strigolactones?. *Plant Physiol.* **2011**, *155*, 721–734, doi:10.1104/pp.110.166645.
243. Rasmussen, A.; Mason, M.G.; De Cuyper, C.; Brewer, P.B.; Herold, S.; Agusti, J.; Geelen, D.; Greb, T.; Goormachtig, S.; Beeckman.. Strigolactones Suppress Adventitious Rooting in Arabidopsis and Pea. *Plant Physiol.* **2012**, *158*, 1976–1987, doi:10.1104/pp.111.187104.
244. Kohlen, W., Charnikhova, T., Liu, Q., Bours, R., Domagalska, M.A., Beguerie, S., Verstappen, F., Leyser, O., Bouwmeester, H. and Ruyter-Spira, C.Strigolactones Are Transported through the Xylem and Play a Key Role in Shoot Architectural Response to Phosphate Deficiency in Nonarbuscular Mycorrhizal Host. *Plant physiol*. 2011, 974-987. doi: 10.1104/pp.110.164640
245. Yoneyama, K.; Xie, X.; Sekimoto, H.; Takeuchi, Y.; Ogasawara, S.; Akiyama, K.; Hayashi, H.; Yoneyama, K. Strigolactones, Host Recognition Signals for Root Parasitic Plants and Arbuscular Mycorrhizal Fungi, from Fabaceae Plants. *New Phytol.* **2008**, *179*, 484–494, doi:10.1111/j.1469-8137.2008.02462.x.
246. Marro, N., Lidoy, J., Chico, M.Á., Rial, C., García, J., Varela, R.M., Macías, F.A., Pozo, M.J., Janoušková,

M. and López-Ráez, J.A.,Strigolactones: New Players in the Nitrogen-Phosphorus Signalling Interplay. *Plant Cell Environ.* **2021**, 512-527, doi:10.1111/pce.14212.

247. Haq, B.U.I.; Ahmad, M.Z.; Ur Rehman, N.; Wang, J.; Li, P.; Li, D.; Zhao, J. Functional Characterization of Soybean Strigolactone Biosynthesis and Signaling Genes in Arabidopsis MAX Mutants and GmMAX3 in Soybean Nodulation. *BMC Plant Biol.* **2017**, *17*, 1-20, doi:10.1186/S12870-017-1182-4.
248. Sun, H.; Xu, F.; Guo, X.; Wu, D.; Zhang, X.; Lou, M.; Luo, F.; Zhao, Q.; Xu, G.; Zhang, Y. A Strigolactone Signal Inhibits Secondary Lateral Root Development in Rice. *Front. Plant Sci.* **2019**, *10*, doi:10.3389/fpls.2019.01527.
249. Sun, H.; Tao, J.; Hou, M.; Huang, S.; Chen, S.; Liang, Z.; Xie, T.; Wei, Y.; Xie, X.; Yoneyama, K. A Strigolactone Signal is Required for Adventitious Root Formation in Rice. *Ann. Bot.* **2015**, *115*, 1155–1162, doi:10.1093/aob/mcv052.
250. Koltai, H.; Dor, E.; Hershenhorn, J.; Joel, D.M.; Weininger, S.; Lekalla, S.; Shealtiel, H.; Bhattacharya, C.; Eliahu, E.; Resnick, N.; et al. Strigolactones' Effect on Root Growth and Root-Hair Elongation May Be Mediated by Auxin-Efflux Carriers. *J. Plant Growth Regul.* **2010**, *29*, 129–136, doi:10.1007/S00344-009-9122-7/FIGURES/4.
251. Santoro, V.; Schiavon, M.; Gresta, F.; Ertani, A.; Cardinale, F.; Sturrock, C.J.; Celi, L.; Schubert, A. Strigolactones Control Root System Architecture and Tip Anatomy in *Solanum lycopersicum L*. Plants under P Starvation. *Plants* **2020**, *9*, 612, doi:10.3390/plants9050612.
252. Marro, N.; Lidoy, J.; Chico, M.Á.; Rial, C.; García, J.; Varela, R.M.; Macías, F.A.; Pozo, M.J.; Janoušková, M.; López-Ráez, J.A. Strigolactones: New Players in the Nitrogen–Phosphorus Signalling Interplay. *Plant. Cell Environ.* **2022**, *45*, 512–527, doi:10.1111/pce.14212.
253. Khan, G.A.; Vogiatzaki, E.; Glauser, G.; Poirier, Y. Phosphate Deficiency Induces the Jasmonate Pathway and Enhances Resistance to Insect Herbivory. *Plant Physiol.* **2016**, *171*, 632–644, doi:10.1104/pp.16.00278.
254. Chevalier, F.; Cuyas, L.; Jouhet, J.; Gros, V.; Chiarenza, S.; Secco, D.; Whelan, J.; Seddiki, K.; Block, M.A.; Nussaume, L.; et al. Interplay between Jasmonic Acid, Phosphate Signaling and the Regulation of Glycerolipid Homeostasis in Arabidopsis. *Plant Cell Physiol.* **2019**, *60*, 1260–1273, doi:10.1093/pcp/pcz027.
255. Hammond, J.P.; Bennett, M.J.; Bowen, H.C.; Broadley, M.R.; Eastwood, D.C.; May, S.T.; Rahn, C.; Swarup, R.; Woolaway, K.E.; White, P.J. Changes in Gene Expression in Arabidopsis Shoots during Phosphate Starvation and the Potential for Developing Smart Plants. *Plant Physiol.* **2003**, *132*, 578–596, doi:10.1104/pp.103.020941.
256. Müller, R.; Morant, M.; Jarmer, H.; Nilsson, L.; Nielsen, T.H. Genome-Wide Analysis of the Arabidopsis Leaf Transcriptome Reveals Interaction of Phosphate and Sugar Metabolism. *Plant Physiol.* **2007**, *143*, 156-171, doi:10.1104/PP.106.090167.
257. Woo, J.; MacPherson, C.R.; Liu, J.; Wang, H.; Kiba, T.; Hannah, M.A.; Wang, X.-J.; Bajic, V.B.; Chua, N.-H. The Response and Recovery of the *Arabidopsis thaliana* transcriptome to Phosphate Starvation. *BMC Plant Biol.* **2012**, 62, 1-22, doi:10.1186/1471-2229-12-62.
258. Chacón-López, A.; Ibarra-Laclette, E.; Sánchez-Calderón, L.; Gutiérrez-Alanis, D.; Herrera-Estrella, L. Global Expression Pattern Comparison between *Low Phosphorus Insensitive 4* and WT Arabidopsis Reveals an Important Role of Reactive Oxygen Species and Jasmonic Acid in the Root Tip Response to Phosphate Starvation. *Plant Signal. Behav.* **2011**, *6*, 382–392, doi:10.4161/psb.6.3.14160.
259. Han, X.; Zhang, M.; Yang, M.; Hu, Y. Arabidopsis JAZ Proteins Interact with and Suppress RHD6 Transcription Factor to Regulate Jasmonate-Stimulated Root Hair Development. *Plant Cell* **2020**, *32*, 1049–1062, doi:10.1105/tpc.19.00617.
260. EI-D, A. M. S. A., A. Salama, and P. F. Wareing. "Effects of mineral nutrition on endogenous cytokinins in plants of sunflower (*Helianthus annuus L.*). *J. Exp Bot.* 1979, 971-981, doi: 10.1093/jxb/30.5.971.
261. Horgan, J.M.; Wareing, P.F. Cytokinins and the Growth Responses of Seedlings of *Betula Pendula* Roth. and *Acer Pseudoplatanus* L. to Nitrogen and Phosphorus Deficiency. *J. Exp. Bot.* **1980**, *31*, 525–532, doi:10.1093/jxb/31.2.525.
262. Martin, A.C.; del Pozo, J.C.; Iglesias, J.; Rubio, V.; Solano, R.; de la Pena, A.; Leyva, A.; Paz-Ares, J.

Influence of Cytokinins on the Expression of Phosphate Starvation Responsive Genes in Arabidopsis. *Plant J.* **2000**, *24*, 559–567, doi:10.1046/j.1365-313x.2000.00893.x.

263. López-Bucio, J.; Hernández-Abreu, E.; Sánchez-Calderón, L.; Nieto-Jacobo, M.F.; Simpson, J.; Herrera-Estrella, L. Phosphate Availability Alters Architecture and Causes Changes in Hormone Sensitivity in the Arabidopsis Root System. *Plant Physiol.* **2002**, *129*, 244–256, doi:10.1104/pp.010934.
264. Devaiah, B.N.; Madhuvanthi, R.; Karthikeyan, A.S.; Raghothama, K.G. Phosphate Starvation Responses and Gibberellic Acid Biosynthesis Are Regulated by the MYB62 Transcription Factor in Arabidopsis. *Mol. Plant* **2009**, *2*, 43–58, doi:10.1093/mp/ssn081.
265. Trull, M.C.; Guiltinan, M.J.; Lynch, J.P.; Deikman, J. The Responses of Wild-Type and ABA Mutant A*rabidopsis thaliana* Plants to Phosphorus Starvation. *Plant, Cell Environ.* **1997**, *20*, 85–92, doi:10.1046/j.1365-3040.1997.d01-4.x.
266. Shin, H.; Shin, H.-S.; Chen, R.; Harrison, M.J. Loss of *At4* Function Impacts Phosphate Distribution between the Roots and the Shoots during Phosphate Starvation. *Plant J.* **2006**, *45*, 712–726, doi:10.1111/j.1365-313X.2005.02629.x.
267. Ribot, C.; Wang, Y.; Poirier, Y. Expression Analyses of Three Members of the *AtPHO1* Family Reveal Differential Interactions between Signaling Pathways Involved in Phosphate Deficiency and the Responses to Auxin, Cytokinin, and Abscisic Acid. *Planta* **2008**, *227*, 1025–1036, doi:10.1007/S00425-007-0677-X/FIGURES/6.
268. Jiang, K.; Feldman, L.J. Root Meristem Establishment and Maintenance: The Role of Auxin. *J. Plant Growth Regul.* **2002**, *21*, 432–440, doi:10.1007/S00344-002-0037-9/FIGURES/7.
269. Liszkay, A.; Van Der Zalm, E.; Schopfer, P. Production of Reactive Oxygen Intermediates (O2.-, H2O2, and .OH) by Maize Roots and Their Role in Wall Loosening and Elongation Growth. *Plant Physiol.* **2004**, 136, 3114-3123. doi:10.1104/pp.104.044784.
270. Sagi, M.; Fluhr, R. Production of Reactive Oxygen Species by Plant NADPH Oxidases. *Plant Physiol.* **2006**, *141*, 336–340, doi:10.1104/pp.106.078089.
271. Marino, D.; Andrio, E.; Danchin, E.G.J.; Oger, E.; Gucciardo, S.; Lambert, A.; Puppo, A.; Pauly, N. A *Medicago Truncatula* NADPH Oxidase Is Involved in Symbiotic Nodule Functioning. *New Phytol.* **2011**, *189*, 580–592, doi:10.1111/j.1469-8137.2010.03509.x.
272. Miller, G.; Suzuki, N.; Ciftci-Yilmaz, S.; Mittler, R. Reactive Oxygen Species Homeostasis and Signalling during Drought and Salinity Stresses. *Plant. Cell Environ.* **2010**, *33*, 453–467, doi:10.1111/j.1365-3040.2009.02041.x.
273. Mittler, R.; Vanderauwera, S.; Suzuki, N.; Miller, G.; Tognetti, V.B.; Vandepoele, K.; Gollery, M.; Shulaev, V.; Van Breusegem, F. ROS Signaling: The New Wave? *Trends Plant Sci.* **2011**, *16*, 300–309, doi:10.1016/j.tplants.2011.03.007.
274. Kadota, Y.; Shirasu, K.; Zipfel, C. Regulation of the NADPH Oxidase *RBOHD* during Plant Immunity. *Plant Cell Physiol.* **2015**, doi:10.1093/pcp/pcv063.
275. Barceló, A.R.; Laura, V.G.R. Reactive Oxygen Species in Plant Cell Walls. **2009**, 73–93, doi:10.1007/978-3-642-00390-5_5.
276. Jaspers, P.; Kangasjärvi, J. Reactive Oxygen Species in Abiotic Stress Signaling. *Physiol. Plant.* **2010**, *138*, 405–413, doi:10.1111/j.1399-3054.2009.01321.x.
277. Devireddy, A.R.; Arbogast, J.; Mittler, R. Coordinated and Rapid Whole-Plant Systemic Stomatal Responses. *New Phytol.* 2020, *225*, 21–25, doi.org/10.1111/nph.16143.
278. Boyd, E.S.; Thomas, K.M.; Dai, Y.; Boyd, J.M.; Outten, F.W. Interplay between Oxygen and Fe–S Cluster Biogenesis: Insights from the Suf Pathway. *Biochemistry* **2014**, *53*, 5834–5847, doi:10.1021/bi500488r.
279. Miller, G.; Schlauch, K.; Tam, R.; Cortes, D.; Torres, M.A.; Shulaev, V.; Dangl, J.L.; Mittler, R. The Plant NADPH Oxidase *RBOHD* Mediates Rapid Systemic Signaling in Response to Diverse Stimuli. *Sci. Signal.* **2009**, *84, ra45-ra45*, doi:10.1126/scisignal.2000448.
280. Takahashi, F.; Mizoguchi, T.; Yoshida, R.; Ichimura, K.; Shinozaki, K. Calmodulin-Dependent Activation of MAP Kinase for ROS Homeostasis in Arabidopsis. *Mol. Cell* **2011**, *41*, 649–660,

doi:10.1016/j.molcel.2011.02.029.

281. Si, T.; Wang, X.; Wu, L.; Zhao, C.; Zhang, L.; Huang, M.; Cai, J.; Zhou, Q.; Dai, T.; Zhu, J.-K.; et al. Nitric Oxide and Hydrogen Peroxide Mediate Wounding-Induced Freezing Tolerance through Modifications in Photosystem and Antioxidant System in Wheat. *Front. Plant Sci.* **2017**, 1284, doi:10.3389/fpls.2017.01284.
282. Kwak, J.M. NADPH Oxidase *AtrbohD* and *AtrbohF* Genes Function in ROS-Dependent ABA Signaling in Arabidopsis. *EMBO J.* **2003**, *22*, 2623–2633, doi:10.1093/emboj/cdg277.
283. Zhang, Y.; Zhang, Y.; Luo, L.; Lu, C.; Kong, W.; Cheng, L.; Xu, X.; Liu, J. Genome Wide Identification of Respiratory Burst Oxidase Homolog (Rboh) Genes in Citrus Sinensis and Functional Analysis of *CsRbohD* in Cold Tolerance. *Int. J. Mol. Sci.* **2022**, *23*, 648, doi:10.3390/ijms23020648.
284. Zhang, Y.; Zhu, H.; Zhang, Q.; Li, M.; Yan, M.; Wang, R.; Wang, L.; Welti, R.; Zhang, W.; Wang, X. Phospholipase Dα1 and Phosphatidic Acid Regulate NADPH Oxidase Activity and Production of Reactive Oxygen Species in ABA-Mediated Stomatal Closure in Arabidopsis. *Plant Cell* **2009**, *21*, 2357–2377, doi:10.1105/tpc.108.062992.
285. Maruta, T.; Inoue, T.; Tamoi, M.; Yabuta, Y.; Yoshimura, K.; Ishikawa, T.; Shigeoka, S. Arabidopsis NADPH Oxidases, *AtrbohD* and *AtrbohF*, Are Essential for Jasmonic Acid-Induced Expression of Genes Regulated by MYC2 Transcription Factor. *Plant Sci.* **2011**, *180*, 655–660, doi:10.1016/j.plantsci.2011.01.014.
286. Maruta, T., Ojiri, M., Noshi, M., Tamoi, M., Ishikawa, T. and Shigeoka, S., 2013. Activation of γ-aminobutyrate production by chloroplastic H_2O_2 is associated with the oxidative stress response. BBiosci. Biotechnol. Biochem. 2013, 77, 422-425, doi:10.1271/bbb.120825.
287. Wang, Q.; Ni, L.; Cui, Z.; Jiang, J.; Chen, C.; Jiang, M. The NADPH Oxidase *OsRbohA* Increases Salt Tolerance by Modulating K^+ Homeostasis in Rice. *Crop J.* **2022**, doi:10.1016/j.cj.2022.03.004.
288. Yao, Y.; He, R.J.; Xie, Q.L.; Zhao, X. hai; Deng, X. mei; He, J. bo; Song, L.; He, J.; Marchant, A.; Chen, X.; et al. *ETHYLENE RESPONSE FACTOR 74* (*ERF74*) Plays an Essential Role in Controlling a *Respiratory Burst Oxidase Homolog D* (*RbohD*)-dependent Mechanism in Response to Different Stresses in Arabidopsis. *New Phytol.* **2017**, *213*, 1667–1681, doi:10.1111/nph.14278.
289. He, H.; Yan, J.; Yu, X.; Liang, Y.; Fang, L.; Scheller, H.V.; Zhang, A. The NADPH-Oxidase *AtRbohI* Plays a Positive Role in Drought-Stress Response in *Arabidopsis thaliana*. *Biochem. Biophys. Res. Commun.* **2017**, *491*, 834–839, doi:10.1016/j.bbrc.2017.05.131.
290. Huang, W.; Zhang, Y.; Zhou, J.; Wei, F.; Feng, Z.; Zhao, L.; Shi, Y.; Feng, H.; Zhu, H. The *Respiratory Burst Oxidase Homolog Protein D* (*GhRbohD*) Positively Regulates the Cotton Resistance to Verticillium Dahliae. *Int. J. Mol. Sci.* **2021**, *22*, 13041, doi:10.3390/ijms222313041.
291. Peleg-Grossman, S.; Volpin, H.; Levine, A. Root Hair Curling and Rhizobium Infection in Medicago Truncatula Are Mediated by Phosphatidylinositide-Regulated Endocytosis and Reactive Oxygen Species. *J. Exp. Bot.* **2007**, *58*, 1637–1649, doi:10.1093/jxb/erm013.
292. D'Haeze, W.; De Rycke, R.; Mathis, R.; Goormachtig, S.; Pagnotta, S.; Verplancke, C.; Capoen, W.; Holsters, M. Reactive Oxygen Species and Ethylene Play a Positive Role in Lateral Root Base Nodulation of a Semiaquatic Legume. *Proc. Natl. Acad. Sci.* **2003**, *100*, 11789–11794, doi:10.1073/pnas.1333899100.
293. Marino, D.; Damiani, I.; Gucciardo, S.; Mijangos, I.; Pauly, N.; Puppo, A. Inhibition of Nitrogen Fixation in Symbiotic Medicago Truncatula upon Cd Exposure Is a Local Process Involving Leghaemoglobin. *J. Exp. Bot.* **2013**, *64*, 5651–5660, doi:10.1093/jxb/ert334.
294. Kiirika, L.M.; Bergmann, H.F.; Schikowsky, C.; Wimmer, D.; Korte, J.; Schmitz, U.; Niehaus, K.; Colditz, F. Silencing of the Rac1 GTPase *MtROP9* in *Medicago Truncatula* Stimulates Early Mycorrhizal and Oomycete Root Colonizations But Negatively Affects Rhizobial Infection. *Plant Physiol.* **2012**, *159*, 501–516, doi:10.1104/pp.112.193706.
295. Belmondo, S.; Calcagno, C.; Genre, A.; Puppo, A.; Pauly, N.; Lanfranco, L. The Medicago Truncatula *MtRbohE* Gene Is Activated in Arbusculated Cells and Is Involved in Root Cortex Colonization. *Planta* **2016**, *243*, 251–262, doi:10.1007/S00425-015-2407-0.
296. Montiel, J.; Nava, N.; Cárdenas, L.; Sánchez-López, R.; Arthikala, M.-K.; Santana, O.; Sánchez, F.; Quinto, C. A Phaseolus Vulgaris NADPH Oxidase Gene Is Required for Root Infection by Rhizobia. *Plant Cell*

Physiol. **2012**, *53*, 1751–1767, doi:10.1093/pcp/pcs120.

297. Arthikala, M.-K.; Montiel, J.; Nava, N.; Santana, O.; Sánchez-López, R.; Cárdenas, L.; Quinto, C. *PvRbohB* Negatively Regulates Rhizophagus Irregularis Colonization in *Phaseolus vulgaris*. *Plant Cell Physiol.* **2013**, *54*, 1391–1402, doi:10.1093/pcp/pct089.
298. Fonseca-García, C.; Zayas, A.E.; Montiel, J.; Nava, N.; Sánchez, F.; Quinto, C. Transcriptome Analysis of the Differential Effect of the NADPH Oxidase Gene *RbohB* in *Phaseolus vulgaris* Roots Following *Rhizobium tropici* and *Rhizophagus irregularis* Inoculation. *BMC Genomics* **2019**, *20*, 1-18, doi:10.1186/s12864-019-6162-7.
299. Kaur, G.; Sharma, A.; Guruprasad, K.; Pati, P.K. Versatile Roles of Plant NADPH Oxidases and Emerging Concepts. *Biotechnol. Adv.* **2014**, *32*, 551–563, doi:10.1016/j.biotechadv.2014.02.002.
300. Chang, Y.; Li, B.; Shi, Q.; Geng, R.; Geng, S.; Liu, J.; Zhang, Y.; Cai, Y. Comprehensive Analysis of Respiratory Burst Oxidase Homologs (Rboh) Gene Family and Function of GbRboh5/18 on *Verticillium wilt* Resistance in *Gossypium barbadense*. *Front. Genet.* **2020**, *11*, 788, doi:10.3389/fgene.2020.00788.
301. Gui, T.-Y.; Gao, D.-H.; Ding, H.-C.; Yan, X.-H. Identification of Respiratory Burst Oxidase Homolog (Rboh) Family Genes From *Pyropia yezoensis* and Their Correlation With Archeospore Release. *Front. Plant Sci.* **2022**, *13*, 929299, doi:10.3389/fpls.2022.929299.
302. Mathur, J. Cell Shape Development in Plants. *Trends Plant Sci.* **2004**, *9*, 583–590, doi:10.1016/j.tplants.2004.10.006.
303. Coelho, S.M.B.; Brownlee, C.; Bothwell, J.H.F. A Tip-High, Ca2+-Interdependent, Reactive Oxygen Species Gradient Is Associated with Polarized Growth in Fucus Serratus Zygotes. *Planta* **2008**, *227*, 1037–1046, doi:10.1007/S00425-007-0678-9/FIGURES/5.
304. Foreman, J., Demidchik, V., Bothwell, J.H., Mylona, P., Miedema, H., Torres, M.A., Linstead, P., Costa, S., Brownlee, C., Jones, J.D. and Davies, J.M. Reactive oxygen species produced by NADPH oxidase regulate plant cell growth. *Nature*, 2003, 422, 442-446, 10.1038/nature01485.
305. Nanda, A.K.; Andrio, E.; Marino, D.; Pauly, N.; Dunand, C. Reactive Oxygen Species during Plant-Microorganism Early Interactions. *J. Integr. Plant Biol.* **2010**, *52*, 195–204, doi:10.1111/j.1744-7909.2010.00933.x.
306. Dunand, C.; Crèvecoeur, M.; Penel, C. Distribution of Superoxide and Hydrogen Peroxide in Arabidopsis Root and Their Influence on Root Development: Possible Interaction with Peroxidases. *New Phytol.* **2007**, *174*, 332–341, doi:10.1111/j.1469-8137.2007.01995.x.
307. Müller, K.; Carstens, A.C.; Linkies, A.; Torres, M.A.; Leubner-Metzger, G. The NADPH-oxidase *AtrbohB* Plays a Role in Arabidopsis Seed After-ripening. *New Phytol.* **2009**, *184*, 885–897, doi:10.1111/j.1469-8137.2009.03005.x.
308. Tonón, C.; Terrile, M.C.; Iglesias, M.J.; Lamattina, L. and Casalongué, C. Extracellular ATP, nitric oxide and superoxide act coordinately to regulate hypocotyl growth in etiolated Arabidopsis seedlings. *J. plant physiol.* 2010, *167*, 540-546, doi: 10.1016/j.jplph.2009.11.002.
309. Sagi, M.; Davydov, O.; Orazova, S.; Yesbergenova, Z.; Ophir, R.; Stratmann, J.W.; Fluhr, R. Plant Respiratory Burst Oxidase Homologs Impinge on Wound Responsiveness and Development in *Lycopersicon esculentum*. *Plant Cell* **2004**, *16*, 616–628, doi:10.1105/tpc.019398.
310. Zhang, A.; Zhang, J.; Ye, N.; Cao, J.; Tan, M.; Zhang, J.; Jiang, M. ZmMPK5 Is Required for the NADPH Oxidase-Mediated Self-Propagation of Apoplastic H_2O_2 in Brassinosteroid-Induced Antioxidant Defence in Leaves of Maize. *J. Exp. Bot.* **2010**, *61*, 4399–4411, doi:10.1093/jxb/erq243.
311. Livanos, P.; Galatis, B.; Quader, H.; Apostolakos, P. Disturbance of Reactive Oxygen Species Homeostasis Induces Atypical Tubulin Polymer Formation and Affects Mitosis in Root-Tip Cells of *Triticum turgidum* and A*rabidopsis thaliana*. *Cytoskeleton* **2012**, *69*, 1–21, doi:10.1002/cm.20538.
312. Linkohr, B.I.; Williamson, L.C.; Fitter, A.H.; Leyser, H.M.O. Nitrate and Phosphate Availability and Distribution Have Different Effects on Root System Architecture of Arabidopsis. *Plant J.* **2002**, *29*, 751–760, doi:10.1046/j.1365-313X.2002.01251.x.
313. Jain, A.; Poling, M.D.; Karthikeyan, A.S.; Blakeslee, J.J.; Peer, W.A.; Titapiwatanakun, B.; Murphy, A.S.;

Raghothama, K.G. Differential Effects of Sucrose and Auxin on Localized Phosphate Deficiency-Induced Modulation of Different Traits of Root System Architecture in Arabidopsis. *Plant Physiol.* **2007**, *144*, 232–247, doi:10.1104/pp.106.092130.

314. Tyburski, J.; Dunajska, K.; Tretyn, A. A Role for Redox Factors in Shaping Root Architecture under Phosphorus Deficiency. *Plant Signal. Behav.* **2010**, 5, 64-66,doi:10.4161/psb.5.1.10199.
315. Potters, G.; De Gara, L.; Asard, H.; Horemans, N. Ascorbate and Glutathione: Guardians of the Cell Cycle, Partners in Crime? *Plant Physiol. Biochem.* **2002**, *40*, 537–548, doi:10.1016/S0981-9428(02)01414-6.
316. Shin, R.; Berg, R.H.; Schachtman, D.P. Reactive Oxygen Species and Root Hairs in Arabidopsis Root Response to Nitrogen, Phosphorus and Potassium Deficiency. *Plant Cell Physiol.* **2005**, *46*, 1350–1357, doi:10.1093/pcp/pci145.
317. Tyburski, J.; Dunajska, K.; Tretyn, A. Reactive Oxygen Species Localization in Roots of *Arabidopsis thaliana* Seedlings Grown under Phosphate Deficiency. *Plant Growth Regul.* **2009**, *59*, 27–36, doi:10.1007/s10725-009-9385-9.
318. Smalle, J.; Vierstra, R.D. The Ubiquitin 26S Proteasome Proteolytic Pathway. *Annu. Rev. Plant Biol.* **2004**, *55*, 555–590, doi:10.1146/annurev.arplant.55.031903.141801.
319. Lechner, E.; Achard, P.; Vansiri, A.; Potuschak, T.; Genschik, P. F-Box Proteins. Everywhere. *Curr. Opin. Plant Biol.* 2006, 631-638, doi: 10.1016/j.pbi.2006.09.003.
320. Jain, M.; Nijhawan, A.; Arora, R.; Agarwal, P.; Ray, S.; Sharma, P.; Kapoor, S.; Tyagi, A.K.; Khurana, J.P. F-Box Proteins in Rice. Genome-Wide Analysis, Classification, Temporal and Spatial Gene Expression during Panicle and Seed Development, and Regulation by Light and Abiotic Stress. *Plant Physiol.* **2007**, 143, 1467-1483. doi:10.1104/pp.106.091900.
321. Bai, C.; Richman, R.; Elledge, S.J. Human Cyclin F. *EMBO J.* **1994**, 13, 6087-6098, doi:10.1002/j.1460-2075.1994.tb06955.x.
322. Hermand, D. F-Box Proteins: More than Baits for the SCF? *Cell Div.* 2006, 1, 1-6, doi: 10.1186/1747-1028-1-30.
323. Xu, G.; Ma, H.; Nei, M.; Kong, H. Evolution of F-Box Genes in Plants: Different Modes of Sequence Divergence and Their Relationships with Functional Diversification. *Proc. Natl. Acad. Sci. U. S. A.* **2009**, 835-840, doi:10.1073/pnas.0812043106.
324. Yang, X.; Kalluri, U.C.; Jawdy, S.; Gunter, L.E.; Yin, T.; Tschaplinski, T.J.; Weston, D.J.; Ranjan, P.; Tuskan, G.A. The F-Box Gene Family Is Expanded in Herbaceous Annual Plants Relative to Woody Perennial Plants. *Plant Physiol.* **2008**, 148, 1189-1200, doi:10.1104/pp.108.121921.
325. Zhang, X.; Gonzalez-Carranza, Z.H.; Zhang, S.; Miao, Y.; Liu, C.-J.; Roberts, J.A. F-Box Proteins in Plants. *Annu. Plant Rev.* 2019, 2, 307–328, doi: 10.1002/9781119312994.apr0701
326. Hepworth, S.R.; Klenz, J.E.; Haughn, G.W. UFO in the Arabidopsis Inflorescence Apex Is Required for Floral-Meristem Identity and Bract Suppression. *Planta* **2006**, 223, 769-778, doi:10.1007/s00425-005-0138-3.
327. Laufs, P.; Coen, E.; Kronenberger, J.; Traas, J.; Doonan, J. Separable Roles of UFO during Floral Development Revealed by Conditional Restoration of Gene Function. *Dev.* 2003, 785-796, doi: 10.1242/dev.00295.
328. Levin, J.Z.; Meyerowitz, E.M. UFO: An Arabidopsis Gene Involved in Both Floral Meristem and Floral Organ Development. *Plant Cell* **1995**, 7, 529-548. doi:10.1105/tpc.7.5.529.
329. Imaizumi, T.; Tran, H.G.; Swartz, T.E.; Briggs, W.R.; Kay, S.A. FKF1 Is Essential for Photoperiodic-Specific Light Signalling in Arabidopsis. *Nature*, **2003**, 426, 302-306, doi:10.1038/nature02090.
330. Nelson, D.C.; Lasswell, J.; Rogg, L.E.; Cohen, M.A.; Bartel, B. FKF1, a Clock-Controlled Gene That Regulates the Transition to Flowering in Arabidopsis. *Cell*, **2000**, *101*, 331-340, doi:10.1016/S0092-8674(00)80842-9.
331. Schultz, T.F.; Kiyosue, T.; Yanovsky, M.; Wada, M.; Kay, S.A. A Role for LKP2 in the Circadian Clock of Arabidopsis. *Plant Cell.* **2001**, *13*, 2659-2670, doi:10.1105/tpc.010332.
332. Somers, D.E.; Kim, W.Y.; Geng, R. The F-Box Protein ZEITLUPE Confers Dosage-Dependent Control on

the Circadian Clock, Photomorphogenesis, and Flowering Time. *Plant Cell* **2004**, 16, 769-782, doi:10.1105/tpc.016808.

333. Liu, Q.; Guo, X.; Chen, G.; Zhu, Z.; Yin, W.; Hu, Z. Silencing *SlGID2*, a Putative F-Box Protein Gene, Generates a Dwarf Plant and Dark-Green Leaves in Tomato. *Plant Physiol. Biochem.* **2016**, *109*, 491–501, doi:10.1016/j.plaphy.2016.10.030.
334. Borah, P.; Khurana, J.P. The OsFBK1 E3 Ligase Subunit Affects Anther and Root Secondary Cell Wall Thickenings by Mediating Turnover of a Cinnamoyl-CoA Reductase. *Plant Physiol.* **2018**, 176, 2148-2165, doi:10.1104/pp.17.01733.
335. Zhang, X.; Gou, M.; Liu, C.J. Arabidopsis Kelch Repeat F-Box Proteins Regulate Phenylpropanoid Biosynthesis via Controlling the Turnover of Phenylalanine Ammonia-Lyase. *Plant Cell.* **2013**, *25*, 4994-5010, doi:10.1105/tpc.113.119644.
336. Baute, J.; Polyn, S.; De Block, J.; Blomme, J.; Van Lijsebettens, M.; Inzé, D. F-Box Protein FBX92 Affects Leaf Size in *Arabidopsis thaliana*. *Plant Cell Physiol.* **2017**, *58*, 962-975, doi:10.1093/pcp/pcx035.
337. Zhang, Y.; Zhang, J.; Guo, J.; Zhou, F.; Singh, S.; Xu, X.; Xie, Q.; Yang, Z.; Huang, C.F. F-Box Protein RAE1 Regulates the Stability of the Aluminum-Resistance Transcription Factor STOP1 in Arabidopsis. *Proc. Natl. Acad. Sci. U. S. A.* **2019**, *116*, 319-327, doi:10.1073/pnas.1814426116.
338. Chen, Y.; Xu, Y.; Luo, W.; Li, W.; Chen, N.; Zhang, D.; Chong, K. The F-Box Protein OsFBK12 Targets OsSAMS1 for Degradation and Affects Pleiotropic Phenotypes, Including Leaf Senescence, in Rice. *PLANT Physiol.* **2013**, *163*, 1673–1685, doi:10.1104/pp.113.224527.
339. Borah, P.; Sharma, A.; Sharma, A.K.; Khurana, P.; Khurana, J.P. SCFOsFBK1 E3 Ligase Mediates Jasmonic Acid-Induced Turnover of *OsATL53* and *OsCCR14* to Regulate Lignification of Rice Anthers and Roots. *J. Exp. Bot.* **2022**, doi:10.1093/jxb/erac434.
340. Jia, F.; Wang, C.; Huang, J.; Yang, G.; Wu, C.; Zheng, C. SCF E3 Ligase PP2-B11 Plays a Positive Role in Response to Salt Stress in Arabidopsis. *J. Exp. Bot.* **2015**, *66*, 4683–4697, doi:10.1093/JXB/ERV245.
341. Cheng, C.; Wang, Z.; Ren, Z.; Zhi, L.; Yao, B.; Su, C.; Liu, L.; Li, X. *SCFAtPP2-B11* modulates ABA Signaling by Facilitating *SnRK2*.3 Degradation in *Arabidopsis thaliana*. *PLoS Genet.* **2017**, 13, e1006947, doi:10.1371/journal.pgen.1006947.
342. Dharmasiri, N.; Dharmasiri, S.; Estelle, M. The F-Box Protein TIR1 Is an Auxin Receptor. *Nature*, **2005**, *7041*, 441-445, doi:10.1038/nature03543.
343. Gray, W.M.; Kepinski, S.; Rouse, D.; Leyser, O.; Estelle, M. Auxin Regulates SCF(TIR1)-Dependent Degradation of AUX/IAA Proteins. *Nature*, **2001**, *414*, 271–276, doi:10.1038/35104500.
344. Kepinski, S.; Leyser, O. The Arabidopsis F-Box Protein TIR1 Is an Auxin Receptor. *Nature*, **2005**, *4071*, 446-451, doi:10.1038/nature03542.
345. Potuschak, T.; Lechner, E.; Parmentier, Y.; Yanagisawa, S.; Grava, S.; Koncz, C.; Genschik, P. EIN3-Dependent Regulation of Plant Ethylene Hormone Signaling by Two Arabidopsis F Box Proteins: EBF1 and EBF2. *Cell* **2003**, *115*, 679-689, doi:10.1016/S0092-8674(03)00968-1.
346. Thines, B.; Katsir, L.; Melotto, M.; Niu, Y.; Mandaokar, A.; Liu, G.; Nomura, K.; He, S.Y.; Howe, G.A.; Browse, J. JAZ Repressor Proteins Are Targets of the SCFCOI1 Complex during Jasmonate Signalling. *Nature*, **2007**, *5154*, 661-665, doi:10.1038/nature05960.
347. Yan, J.; Zhang, C.; Gu, M.; Bai, Z.; Zhang, W.; Qi, T.; Cheng, Z.; Peng, W.; Luo, H.; Nan, F.. The Arabidopsis CORONATINE INSENSITIVE1 Protein is a Jasmonate Receptor. *Plant Cell*, **2009**, *21*, 2220-2236, doi:10.1105/tpc.109.065730.
348. Piisilä, M.; Keceli, M.A.; Brader, G.; Jakobson, L.; Jöesaar, I.; Sipari, N.; Kollist, H.; Palva, E.T.; Kariola, T. The F-Box Protein MAX2 Contributes to Resistance to Bacterial Phytopathogens in *Arabidopsis thaliana. BMC Plant Biol.* **2015**, *15*, 1-7, doi:10.1186/s12870-015-0434-4.
349. Wang, L.; Wang, B.; Yu, H.; Guo, H.; Lin, T.; Kou, L.; Wang, A.; Shao, N.; Ma, H.; Xiong, G.. Transcriptional Regulation of Strigolactone Signalling in Arabidopsis. *Nature* **2020**, *583*, 277-281, doi:10.1038/s41586-020-2382-x.
350. Dill, A.; Thomas, S.G.; Hu, J.; Steber, C.M.; Sun, T.P. The Arabidopsis F-Box Protein SLEEPY1 Targets

Gibberellin Signaling Repressors for Gibberellin-Induced Degradation. *Plant Cell*, **2004**, *16*, 1392-1405, doi:10.1105/tpc.020958.

351. Fu, X.; Richards, D.E.; Fleck, B.; Xie, D.; Burton, N.; Harberd, N.P. The Arabidopsis Mutant Sleepy1gar2-1 Protein Promotes Plant Growth by Increasing the Affinity of the SCFSLY1 E3 Ubiquitin Ligase for DELLA Protein Substrates. *Plant Cell*, **2004**, *16*, 1406-1418, doi:10.1105/tpc.021386.
352. Chen, Z.H.; Jenkins, G.I.; Nimmo, H.G. Identification of an F-Box Protein That Negatively Regulates Pi Starvation Responses. *Plant Cell Physiol.* **2008**, *49*, 1902–1906, doi:10.1093/pcp/pcn157.
353. Cui, H.R.; Zhang, Z.R.; lv, W.; Xu, J.N.; Wang, X.Y. Genome-Wide Characterization and Analysis of F-Box Protein-Encoding Genes in the Malus Domestica Genome. *Mol. Genet. Genomics* **2015**, *290*, 1435-1446, doi:10.1007/s00438-015-1004-z.
354. Gupta, S.; Garg, V.; Kant, C.; Bhatia, S. Genome-Wide Survey and Expression Analysis of F-Box Genes in Chickpea. *BMC Genomics*, **2015**, *16*, 1-15, doi:10.1186/s12864-015-1293-y.
355. Jain, M.; Khurana, P.; Tyagi, A.K.; Khurana, J.P. Genome-Wide Analysis of Intronless Genes in Rice and Arabidopsis. *Funct. Integr. Genomics*, **2008**, *8*, 69-78, doi:10.1007/s10142-007-0052-9.
356. Jia, F.; Wu, B.; Li, H.; Huang, J.; Zheng, C. Genome-Wide Identification and Characterisation of F-Box Family in Maize. *Mol. Genet. Genomics* **2013**, *288*, 559-577, doi:10.1007/s00438-013-0769-1.
357. Jia, Q.; Xiao, Z.X.; Wong, F.L.; Sun, S.; Liang, K.J.; Lam, H.M. Genome-Wide Analyses of the Soybean F-Box Gene Family in Response to Salt Stress. *Int. J. Mol. Sci.* **2017**, *18*, 818, doi:10.3390/ijms18040818.
358. Song, J.B.; Wang, Y.X.; Li, H.B.; Li, B.W.; Zhou, Z.S.; Gao, S.; Yang, Z.M. The F-Box Family Genes as Key Elements in Response to Salt, Heavy Mental, and Drought Stresses in *Medicago runcatula*. *Funct. Integr. Genomics* **2015**, *15*, 495-507, doi:10.1007/s10142-015-0438-z.
359. Wang, G.M.; Yin, H.; Qiao, X.; Tan, X.; Gu, C.; Wang, B.H.; Cheng, R.; Wang, Y.Z.; Zhang, S.L. F-Box Genes: Genome-Wide Expansion, Evolution and Their Contribution to Pollen Growth in Pear (*Pyrus retschneideri*). *Plant Sci.* **2016**, *253*, 164-175, doi:10.1016/j.plantsci.2016.09.009.
360. Zhang, S.; Tian, Z.; Li, H.; Guo, Y.; Zhang, Y.; Roberts, J.A.; Zhang, X.; Miao, Y. Genome-Wide Analysis and Characterization of F-Box Gene Family in *Gossypium hirsutum L*. *BMC Genomics* **2019**, *20*, 116, doi:10.1186/s12864-019-6280-2.
361. Amoanimaa-Dede, H.; Shao, Z.; Su, C.; Yeboah, A.; Zhu, H. Genome-Wide Identification and Characterization of F-Box Family Proteins in Sweet Potato and Its Expression Analysis under Abiotic Stress. *Gene* **2022**, *817*, 146191, doi:10.1016/j.gene.2022.146191.
362. Fan, G.; Xia, X.; Yao, W.; Cheng, Z.; Zhang, X.; Jiang, J.; Zhou, B.; Jiang, T. Genome-Wide Identification and Expression Patterns of the F-Box Family in Poplar under Salt Stress. *Int. J. Mol. Sci.* **2022**, *23*, 10934, doi:10.3390/ijms231810934.
363. Kumar, R.; Agarwal, P.; Pareek, A.; Tyagi, A.K.; Sharma, A.K. Genomic Survey, Gene Expression, and Interaction Analysis Suggest Diverse Roles of ARF and Aux/IAA Proteins in Solanaceae. *Plant Mol. Biol. Report.* **2015**, *33*, 1552–1572, doi:10.1007/s11105-015-0856-z.
364. Kumar, R.; Chauhan, P.K.; Khurana, A. Identification and Expression Profiling of DNA Methyltransferases during Development and Stress Conditions in Solanaceae. *Funct. Integr. Genomics* **2016**, *16*, 513-528, doi:10.1007/s10142-016-0502-3.
365. Foehse, D.; Jungk, A. Influence of Phosphate and Nitrate Supply on Root Hair Formation of Rape, Spinach and Tomato Plants. *Plant Soil* **1983**, *I74*, 359-368, doi:10.1007/BF02181353.
366. Ames, B.N. Assay of Inorganic Phosphate, Total Phosphate and Phosphatases. *Methods Enzymol.* **1966**, *8*, 115-118, doi:10.1016/0076-6879(66)08014-5.
367. Achard, P.; Renou, J.-P.; Berthomé, R.; Harberd, N.P.; Genschik, P. Plant DELLAs Restrain Growth and Promote Survival of Adversity by Reducing the Levels of Reactive Oxygen Species. *Curr. Biol.* **2008**, *18*, 656–660, doi:10.1016/j.cub.2008.04.034.
368. Sims, D.A.; Gamon, J.A. Relationships between Leaf Pigment Content and Spectral Reflectance across a Wide Range of Species, Leaf Structures and Developmental Stages. *Remote Sens. Environ.* **2002**, *81*, 337-354, doi:10.1016/S0034-4257(02)00010-X.

369. Zhang, Y.; Wang, X.; Lu, S.; Liu, D. A Major Root-Associated Acid Phosphatase in Arabidopsis, *AtPAP10*, Is Regulated by Both Local and Systemic Signals under Phosphate Starvation. *J. Exp. Bot.* **2014**, *65*, 6577–6588, doi:10.1093/jxb/eru377.
370. Bodanapu, R.; Gupta, S.K.; Basha, P.O.; Sakthivel, K.; Sadhana; Sreelakshmi, Y.; Sharma, R. Nitric Oxide Overproduction in Tomato Shr Mutant Shifts Metabolic Profiles and Suppresses Fruit Growth and Ripening. *Front. Plant Sci.* **2016**, *7*, 1714, doi:10.3389/fpls.2016.01714.
371. Xia, J.; Mandal, R.; Sinelnikov, I. V.; Broadhurst, D.; Wishart, D.S. MetaboAnalyst 2.0-a Comprehensive Server for Metabolomic Data Analysis. *Nucleic Acids Res.* **2012**, 40, W127-W133, doi:10.1093/nar/gks374.
372. Sagi, M.; Fluhr, R. Superoxide Production by Plant Homologues of the Gp91phox NADPH Oxidase. Modulation of Activity by Calcium and by *Tobacco Mosaic Virus* Infection. *Plant Physiol.* **2001**, *126*, 1281–1290, doi:10.1104/pp.126.3.1281.
373. Livak, K.J.; Schmittgen, T.D. Analysis of Relative Gene Expression Data Using Real-Time Quantitative PCR and the 2-ΔΔCT Method. *Methods* **2001**, *25*, 402-408, doi:10.1006/meth.2001.1262.
374. Voorrips R.E. MapChart: Software for the Graphical Presentation of Linkage Maps and QTLs. *J. Hered.* **2002**, 93, 77-78, doi:10.1093/jhered/93.1.77
375. Shiu, S.-H.; Bleecker, A.B. Expansion of the Receptor-Like Kinase/Pelle Gene Family and Receptor-Like Proteins in Arabidopsis. *Plant Physiol.* **2003**, *132*, 530–543, doi:10.1104/pp.103.021964.
376. Krzywinski, M.; Schein, J.; Birol, I.; Connors, J.; Gascoyne, R.; Horsman, D.; Jones, S.J.; Marra, M.A. Circos: An Information Aesthetic for Comparative Genomics. *Genome Res.* **2009**, *19*, 1639-1645, doi:10.1101/gr.092759.109.
377. Tamura, K.; Stecher, G.; Peterson, D.; Filipski, A.; Kumar, S. MEGA6: Molecular Evolutionary Genetics Analysis Version 6.0. *Mol. Biol. Evol.* **2013**, *30*, 2725-2729, doi:10.1093/molbev/mst197.
378. Sato, S.; Tabata, S.; Hirakawa, H.; Asamizu, E.; Shirasawa, K.; Isobe, S.; Kaneko, T.; Nakamura, Y.; Shibata, D.; Aoki, K.; et al. The Tomato Genome Sequence Provides Insights into Fleshy Fruit Evolution. *Nature* **2012**, *485*, 635–641, doi:10.1038/nature11119.
379. Sravankumar, T.; Akash; Naik, N.K.; Kumar, R. A Ripening-Induced *SlGH3*-2 Gene Regulates Fruit Ripening via Adjusting Auxin-Ethylene Levels in Tomato (S*olanum lycopersicum L.*). *Plant Mol. Biol.* **2018**, doi:10.1007/s11103-018-0790-1.
380. Bozzola, J.J. The Champagne Artifact in Negative Staining TEM. *Micros. Today* **1998**, *6*, 24–25, doi:10.1017/S1551929500069704.
381. Kaur, G.; Shukla, V.; Kumar, A.; Kaur, M.; Goel, P.; Singh, P.; Shukla, A.; Meena, V.; Kaur, J.; Singh, J.; et al. Integrative Analysis of Hexaploid Wheat Roots Identifies Signature Components during Iron Starvation. *J. Exp. Bot.* **2019**, *70*, 6141–6161, doi:10.1093/jxb/erz358.
382. Barber, S.A.; Walker, J.M.; Vasey, E.H. Mechanisms for the Movement of Plant Nutrients from the Soil and Fertilizer to the Plant Root. *J. Agric. Food Chem.* **1963**, *485*, 635-641, doi:10.1021/jf60127a017.
383. Misson, J.; Raghothama, K.G.; Jain, A.; Jouhet, J.; Block, M.A.; Bligny, R.; Ortet, P.; Creff, A.; Somerville, S.; Rolland, N.; et al. A Genome-Wide Transcriptional Analysis Using *Arabidopsis thaliana* Affymetrix Gene Chips Determined Plant Responses to Phosphate Deprivation. *Proc. Natl. Acad. Sci.* **2005**, *102*, 11934–11939, doi:10.1073/pnas.0505266102.
384. Thibaud, M.C.; Arrighi, J.F.; Bayle, V.; Chiarenza, S.; Creff, A.; Bustos, R.; Paz-Ares, J.; Poirier, Y.; Nussaume, L. Dissection of Local and Systemic Transcriptional Responses to Phosphate Starvation in Arabidopsis. *Plant J.* **2010**, 64, 775-789, doi:10.1111/j.1365-313X.2010.04375.x.
385. Bozzo, G.G.; Dunn, E.L.; Plaxton, W.C. Differential Synthesis of Phosphate-Starvation Inducible Purple Acid Phosphatase Isozymes in Tomato (*Lycopersicon esculentum*) Suspension Cells and Seedlings. *Plant, Cell Environ.* **2006**, *29*, 303-313, doi:10.1111/j.1365-3040.2005.01422.x.
386. Singh, S.; Singh, H.; Seema; Singh, J.; Sharma, V.K. Effect of Integrated Use of Rock Phosphate, Molybdenum and Phosphate Solubilizing Bacteria on Lentil (*Lens culinaris*) in an Alluvial Soil. *Indian J. Agron.* **2014**, 59, 433-438.
387. Fang, Z.; Shao, C.; Meng, Y.; Wu, P.; Chen, M. Phosphate Signaling in Arabidopsis and *Oryza sativa*. *Plant*

Sci. 2009.

388. Liu, C.; Muchhal, U.S.; Uthappa, M.; Kononowicz, A.K.; Raghothama, K.G. Tomato Phosphate Transporter Genes Are Differentially Regulated in Plant Tissues by Phosphorus. *Plant Physiol.* **1998**, *116*, 91-99, doi:10.1104/pp.116.1.91.
389. Baldwin, J.C.; Karthikeyan, A.S.; Raghothama, K.G. *LEPS2* , a Phosphorus Starvation-Induced Novel Acid Phosphatase from Tomato. *Plant Physiol.* **2001**, *125*, 728–737, doi:10.1104/pp.125.2.728.
390. Khurana, A.; Akash; Roychowdhury, A. Identification of Phosphorus Starvation Inducible SnRK Genes in Tomato (*Solanum lycopersicum L.*). *J. Plant Biochem. Biotechnol.***2021**, *30*, 1–12, doi:10.1007/S13562-021-00701-0.
391. Kumar, R.; Khurana, A. Functional Genomics of Tomato: Opportunities and Challenges in Post-Genome NGS Era. *J. Biosci.* 2014, 39, 917-929, doi: 10.1007/s12038-014-9480-6
392. Wang, Y.; Yan, H.; Qiu, Z.; Hu, B.; Zeng, B.; Zhong, C.; Fan, C. Comprehensive Analysis of SNRK Gene Family and Their Responses to Salt Stress in *Eucalyptus grandis*. *Int. J. Mol. Sci.* **2019**, *20*, 2786, doi:10.3390/ijms20112786.
393. Zeng, H.; Wang, G.; Zhang, Y.; Hu, X.; Pi, E.; Zhu, Y.; Wang, H.; Du, L. Genome-Wide Identification of Phosphate-Deficiency-Responsive Genes in Soybean Roots by High-Throughput Sequencing. *Plant Soil* **2016**, *398*, 207-227, doi:10.1007/s11104-015-2657-4.
394. Wang, Y.; Gao, H.; He, L.; Zhu, W.; Yan, L.; Chen, Q.; He, C. The *PHOSPHATE1* Genes Participate in Salt and Pi Signaling Pathways and Play Adaptive Roles during Soybean Evolution. *BMC Plant Biol.* **2019**, *19*, 1-19, doi:10.1186/s12870-019-1959-8.
395. Kumar Sharma, A.; Mühlroth, A.; Jouhet, J.; Maréchal, E.; Alipanah, L.; Kissen, R.; Brembu, T.; Bones, A.M.; Winge, P. The Myb-like Transcription Factor Phosphorus Starvation Response (PtPSR) Controls Conditional P Acquisition and Remodelling in *Marine microalgae*. *New Phytol.* **2020**, *225*, 2380-2395, doi:10.1111/nph.16248.
396. Zhou, J.; Jiao, F.C.; Wu, Z.; Li, Y.; Wang, X.; He, X.; Zhong, W.; Wu, P. *OsPHR2* is Involved in Phosphate-Starvation Signaling and Excessive Phosphate Accumulation in Shoots of Plants. *Plant Physiol.* **2008**, *225*, 2380-2395, doi:10.1104/pp.107.111443.
397. Wykoff, D.D.; Grossman, A.R.; Weeks, D.P.; Usuda, H.; Shimogawara, K. Psr1, a Nuclear Localized Protein That Regulates Phosphorus Metabolism in Chlamydomonas. *Proc. Natl. Acad. Sci. U. S. A.* **1999**, *26*, 15336-15341, doi:10.1073/pnas.96.26.15336.
398. Rubio, V.; Linhares, F.; Solano, R.; Martín, A.C.; Iglesias, J.; Leyva, A.; Paz-Ares, J. A Conserved MYB Transcription Factor Involved in Phosphate Starvation Signaling Both in Vascular Plants and in Unicellular Algae. *Genes Dev.* **2001**, *15*, 2122–2133, doi:10.1101/gad.204401.
399. Dubos, C.; Stracke, R.; Grotewold, E.; Weisshaar, B.; Martin, C.; Lepiniec, L. MYB Transcription Factors in Arabidopsis. *Trends Plant Sci.* 2010, *15*, 573-581, doi: 10.1016/j.tplants.2010.06.005.
400. Li, Z.; Peng, R.; Tian, Y.; Han, H.; Xu, J.; Yao, Q. Genome-Wide Identification and Analysis of the MYB Transcription Factor Superfamily in Solanum Lycopersicum. *Plant Cell Physiol.* **2016**, doi:10.1093/pcp/pcw091.
401. Rubio, V.; Bustos, R.; Irigoyen, M.L.; Cardona-López, X.; Rojas-Triana, M.; Paz-Ares, J. Plant Hormones and Nutrient Signaling. *Plant Mol. Biol.* 2009, *69*, 361-373, doi: 10.1007/s11103-008-9380-y.
402. Gamir, J.; Torres-Vera, R.; Rial, C.; Berrio, E.; de Souza Campos, P.M.; Varela, R.M.; Macías, F.A.; Pozo, M.J.; Flors, V.; López-Ráez, J.A. Exogenous Strigolactones Impact Metabolic Profiles and Phosphate Starvation Signalling in Roots. *Plant Cell Environ.* **2020**, *43*, 1655-1668, doi:10.1111/pce.13760.
403. Chen, A.; Chen, X.; Wang, H.; Liao, D.; Gu, M.; Qu, H.; Sun, S.; Xu, G. Genome-Wide Investigation and Expression Analysis Suggest Diverse Roles and Genetic Redundancy of Pht1 Family Genes in Response to Pi Deficiency in Tomato. *BMC Plant Biol.* **2014**, *14*, 1-15, doi:10.1186/1471-2229-14-61.
404. Ramaiah, M.; Jain, A.; Baldwin, J.C.; Karthikeyan, A.S.; Raghothama, K.G. Characterization of the Phosphate Starvation-Induced Glycerol-3-Phosphate Permease Gene Family in Arabidopsis. *Plant Physiol.* **2011**, *157*, 279-291, doi:10.1104/pp.111.178541.

405. Bosse, D.; Köck, M. Influence of Phosphate Starvation on Phosphohydrolases during Development of Tomato Seedlings. *Plant, Cell Environ.* **1998**, *21*, 325-332, doi:10.1046/j.1365-3040.1998.00289.x.
406. Bozzo, G.G.; Dunn, E.L.; Plaxton, W.C. Differential Synthesis of Phosphate-Starvation Inducible Purple Acid Phosphatase Isozymes in Tomato (Lycopersicon Esculentum) Suspension Cells and Seedlings. *Plant, Cell Environ.* **2006**, *29*, 303-313, doi:10.1111/j.1365-3040.2005.01422.x.
407. Suen, P.K.; Zhang, S.; Sun, S.S.M. Molecular Characterization of a Tomato Purple Acid Phosphatase during Seed Germination and Seedling Growth under Phosphate Stress. *Plant Cell Rep.* **2015**, *34*, 981-992, doi:10.1007/s00299-015-1759-z.
408. Kuang, R.; Chan, K.-H.; Yeung, E.; Lim, B.L. Molecular and Biochemical Characterization of AtPAP15, a Purple Acid Phosphatase with Phytase Activity, in Arabidopsis 1[W][OA]. *Am Soc Plant Biol* **2009**, *151*, 199-209, doi:10.1104/pp.109.143180.
409. Zhang, Q.; Wang, C.; Tian, J.; Li, K.; Shou, H. Identification of Rice Purple Acid Phosphatases Related to Posphate Starvation Signalling. *Plant Biol.* **2011**, *13*, 7-5, doi:10.1111/j.1438-8677.2010.00346.x.
410. Robinson, W.D.; Park, J.; Tran, H.T.; Del Vecchio, H.A.; Ying, S.; Zins, J.L.; Patel, K.; McKnight, T.D.; Plaxton, W.C. The Secreted Purple Acid Phosphatase Isozymes *AtPAP12* and *AtPAP26* Play a Pivotal Role in Extracellular Phosphate-Scavenging by *Arabidopsis haliana. J. Exp. Bot.* **2012**, doi:10.1093/jxb/ers309.
411. Yan, F.; Zhu, Y.; Müller, C.; Schubert, S. Adaptation of Plasma Membrane H+-ATPase of Proteoid Roots of White lupin (*Lupinus albus L.*) to Phosphorus Deficiency. In *Plant Nutrition*; 2001.
412. Gregory, A.L.; Hurley, B.A.; Tran, H.T.; Valentine, A.J.; She, Y.M.; Knowles, V.L.; Plaxton, W.C. In Vivo Regulatory Phosphorylation of the Phosphoenolpyruvate Carboxylase AtPPC1 in Phosphate-Starved *Arabidopsis thaliana*. *Biochem. J.* **2009**, 186-187, doi:10.1042/BJ20082397.
413. Baxter, A.; Mittler, R.; Suzuki, N. ROS as Key Players in Plant Stress Signalling. *J. Exp. Bot.* **2014**, *65*, 1229–1240, doi:10.1093/jxb/ert375.
414. Kaya, C.; Higgs, D.; Burton, A. Phosphorus and Acid Phosphatase Enzyme Activity in Leaves of Tomato Cultivars in Relation to Zinc Supply. *Commun. Soil Sci. Plant Anal.* **2000**, *31*, 3239–3248, doi:10.1080/00103620009370664.
415. Huang, C.; Barker, S.J.; Langridge, P.; Smith, F.W.; Graham, R.D. Zinc Deficiency Up-Regulates Expression of High-Affinity Phosphate Transporter Genes in Both Phosphate-Sufficient and -Deficient Barley Roots. *Plant Physiol.* **2000**, *124*, 415–422, doi:10.1104/pp.124.1.415.
416. Awasthi, P.; Laxmi, A. Root Architectural Plasticity in Changing Nutrient Availability. In; 2021, 25–37, doi: 10.1007/978-3-030-84985-6_2.
417. Eljebbawi, A.; Guerrero, Y. del C.R.; Dunand, C.; Estevez, J.M. Highlighting Reactive Oxygen Species as Multitaskers in Root Development. *iScience* **2021**, *24*, 101978, doi:10.1016/j.isci.2020.101978.
418. Chapman, J.M.; Muhlemann, J.K.; Gayomba, S.R.; Muday, G.K. RBOH-Dependent ROS Synthesis and ROS Scavenging by Plant Specialized Metabolites to Modulate Plant Development and Stress Responses. *Chem. Res. Toxicol.* **2019**, *32*, 370–396, doi:10.1021/acs.chemrestox.9b00028.
419. Pandey, M.; Paladi, R.K.; Srivastava, A.K.; Suprasanna, P. Thiourea and Hydrogen Peroxide Priming Improved K+ Retention and Source-Sink Relationship for Mitigating Salt Stress in Rice. *Sci. Rep.* **2021**, *11*, 1-15, doi:10.1038/s41598-020-80419-6.
420. Deng, X.P.; Cheng, Y.J.; Wu, X.B.; Kwak, S.S.; Chen, W.; Eneji, A.E. Exogenous Hydrogen Peroxide Positively Influences Root Growth and Exogenous Hydrogen Peroxide Positively Influences Root Growth and Metabolism in Leaves of Sweet Potato Seedlings. *Aust. J. Crop Sci.* **2012**, *6*, 1572–1578.
421. Hua, Z.; Zou, C.; Shiu, S.H.; Vierstra, R.D. Phylogenetic Comparison of F-Box (FBX) Gene Superfamily within the Plant Kingdom Reveals Divergent Evolutionary Histories Indicative of Genomic Drift. *PLoS One* **2011**, *6*, e16219, doi:10.1371/journal.pone.0016219.
422. Gagne, J.M.; Downes, B.P.; Shiu, S.H.; Durski, A.M.; Vierstra, R.D. The F-Box Subunit of the SCF E3 Complex Is Encoded by a Diverse Superfamily of Genes in Arabidopsis. *Proc. Natl. Acad. Sci. U. S. A.* **2002**, *99*, 11519-11524, doi:10.1073/pnas.162339999.
423. Cannon, S.B.; Mitra, A.; Baumgarten, A.; Young, N.D.; May, G. The Roles of Segmental and Tandem Gene

Duplication in the Evolution of Large Gene Families in *Arabidopsis thaliana*. *BMC Plant Biol.* **2004**, doi:10.1186/1471-2229-4-10.

424. Navarro-Quezada, A.; Schumann, N.; Quint, M. Plant F-Box Protein Evolution Is Determined by Lineage-Specific Timing of Major Gene Family Expansion Waves. *PLoS One* **2013**, *8*, e68672, doi:10.1371/journal.pone.0068672.
425. Koonin, E. V. Orthologs, Paralogs, and Evolutionary Genomics. *Annu. Rev. Genet.* 2005, *39*, 309-338, doi: 10.1146/annurev.genet.39.073003.114725
426. Kiyosue, T.; Wada, M. LKP1 (LOV Kelch Protein 1): A Factor Involved in the Regulation of Flowering Time in Arabidopsis. *Plant J.* **2000**, *23*, 807-815, doi:10.1046/j.1365-313X.2000.00850.x.
427. Más, P.; Kim, W.Y.; Somers, D.E.; Kay, S.A. Targeted Degradation of TOC1 by ZTL Modulates Circadian Function in *Arabidopsis thaliana*. *Nature* **2003**, *426*, 668-671, doi:10.1038/nature02163.
428. Baudry, A.; Ito, S.; Song, Y.H.; Strait, A.A.; Kiba, T.; Lu, S.; Henriques, R.; Pruneda-Paz, J.L.; Chua, N.H.; Tobin, E.M.. F-Box Proteins FKF1 and LKP2 Act in Concert with ZEITLUPE to Control Arabidopsis Clock Progression. *Plant Cell* **2010**, *22*, 606-622, doi:10.1105/tpc.109.072843.
429. Takase, T.; Nishiyama, Y.; Tanihigashi, H.; Ogura, Y.; Miyazaki, Y.; Yamada, Y.; Kiyosue, T. LOV KELCH PROTEIN2 and ZEITLUPE Repress Arabidopsis Photoperiodic Flowering under Non-Inductive Conditions, Dependent on FLAVIN-BINDING KELCH REPEAT F - BOX1. *Plant J.* **2011**, *67*, 608-621, doi:10.1111/j.1365-313X.2011.04618.x.
430. Majee, M.; Kumar, S.; Kathare, P.K.; Wu, S.; Gingerich, D.; Nayak, N.R.; Salaita, L.; Dinkins, R.; Martin, K.; Goodin, M. Kelch F-Box Protein Positively Influences Arabidopsis Seed Germination by Targeting Phytochrome-Interacting Factor1. *Proc. Natl. Acad. Sci. U. S. A.* **2018**, *115*, E4120-E4129, doi:10.1073/pnas.1711919115.
431. Deng, H.; Pirrello, J.; Chen, Y.; Li, N.; Zhu, S.; Chirinos, X.; Bouzayen, M.; Liu, Y.; Liu, M. A Novel Tomato F-Box Protein, SlEBF3, Is Involved in Tuning Ethylene Signaling during Plant Development and Climacteric Fruit Ripening. *Plant J.* **2018**, *95*, 648-658, doi:10.1111/tpj.13976.
432. Yang, Y.; Wu, Y.; Pirrello, J.; Regad, F.; Bouzayen, M.; Deng, W.; Li, Z. Silencing Sl-*EBF1* and Sl-*EBF2* Expression Causes Constitutive Ethylene Response Phenotype, Accelerated Plant Senescence, and Fruit Ripening in Tomato. *J. Exp. Bot.* **2010**, *61*, 697-708, doi:10.1093/jxb/erp332.
433. Kumar, R.; Sharma, M.K.; Kapoor, S.; Tyagi, A.K.; Sharma, A.K. Transcriptome Analysis of Rin Mutant Fruit and in Silico Analysis of Promoters of Differentially Regulated Genes Provides Insight into LeMADS-RIN-Regulated Ethylene-Dependent as Well as Ethylene-Independent Aspects of Ripening in Tomato. *Mol. Genet. Genomics* **2012**, *287*, 189-203, doi:10.1007/s00438-011-0671-7.
434. Gambhir, P.; Singh, V.; Parida, A.; Raghuvanshi, U.; Kumar, R.; Sharma, A.K. Ethylene Response Factor ERF.D7 Activates *Auxin Response Factor 2* Paralogs to Regulate Tomato Fruit Ripening. *Plant Physiol.* **2022**, *190*, 2775–2796, doi:10.1093/plphys/kiac441.
435. Ronen, G.; Carmel-Goren, L.; Zamir, D.; Hirschberg, J. An Alternative Pathway to β-Carotene Formation in Plant Chromoplasts Discovered by Map-Based Cloning of Beta and Old-Gold Color Mutations in Tomato. *Proc. Natl. Acad. Sci.* **2000**, *97*, 11102–11107, doi:10.1073/pnas.190177497.
436. Rosati, C.; Aquilani, R.; Dharmapuri, S.; Pallara, P.; Marusic, C.; Tavazza, R.; Bouvier, F.; Camara, B.; Giuliano, G. Metabolic Engineering of Beta-Carotene and Lycopene Content in Tomato Fruit. *Plant J.* **2000**, *24*, 413–420, doi:10.1046/j.1365-313x.2000.00880.x.
437. Li, X.; Wang, Y.; Chen, S.; Tian, H.; Fu, D.; Zhu, B.; Luo, Y.; Zhu, H. Lycopene is Enriched in Tomato Fruit by CRISPR/Cas9-Mediated Multiplex Genome Editing. *Front. Plant Sci.* **2018**, *9*, 559, doi:10.3389/fpls.2018.00559.
438. Umehara, M., Hanada, A., Magome, H., Takeda-Kamiya, N., & Yamaguchi, S. Contribution of strigolactones to the inhibition of tiller bud outgrowth under phosphate deficiency in rice. *Plant Cell Physio.*, 2010, *51*, 1118-1126, doi: 10.1093/pcp/pcq084.
439. Raya-González, J., Ojeda-Rivera, J. O., Mora-Macias, J., Oropeza-Aburto, A., Ruiz-Herrera, L. F., López-

Bucio, J., & Herrera-Estrella, L. MEDIATOR16 orchestrates local and systemic responses to phosphate scarcity in Arabidopsis roots. *New. Phytol.* 2021, *229*, 1278-1288 doi: 10.1111/nph.16989.

440. Srivastava, R., Sirohi, P., Chauhan, H., & Kumar, R. The enhanced phosphorus use efficiency in phosphate-deficient and mycorrhiza-inoculated barley seedlings involves activation of different sets of PHT1 transporters in roots. *Planta*, 2021, *254*,, 1-17, doi: 10.1007/s00425-021-03687-0.
441. Abel, S., Ticconi, C. A., & Delatorre, C. A. Phosphate sensing in higher plants. *Physiol.* 2002, *Physiol. Plant.*, *115*,, 1-8, doi: 10.1034/j.1399-3054.2002.1150101.x.
442. Matusova, R., Rani, K., Verstappen, F. W., Franssen, M. C., Beale, M. H., & Bouwmeester, H. J. The strigolactone germination stimulants of the plant-parasitic Striga and Orobanche spp. are derived from the carotenoid pathway. *Plant physiol.* 2005, *139*, 920-934, doi: 10.1104/pp.105.061382.
443. Schmidt, W., & Schikora, A. Different pathways are involved in phosphate and iron stress-induced alterations of root epidermal cell development. *Plant Physiol.* 2001, *125*, 2078-2084, doi: 10.1104/pp.125.4.2078.
444. Spurr, A. R. A low-viscosity epoxy resin embedding medium for electron microscopy. *J. Ultrastruct. Res.*, 1969, *26*, 31-43, doi: 10.1016/S0022-5320(69)90033-1.
446. Senthil-Kumar, M., Lee, H.-K., & Mysore, K. S. (2013). VIGS-mediated forward genetics screening for identification of genes involved in nonhost resistance. *J. Vis. Exp.* 78, e51033 doi: 10.3791/51033.
447. Dellaporta, S.L., Wood, J. and Hicks, J.B., 1983. A plant DNA minipreparation: version II. Plant molecular biology reporter, *1*, 19-21.
448. Hoagland, D.R. and Arnon, D.I. The water-culture method for growing plants without soil. Circular. California agricultural experiment station, 1950, 347(2nd edit).
449. Akash., Parida, A. P., Srivastava, A., Mathur, S., Sharma, A. K., & Kumar, R. Identification, evolutionary profiling, and expression analysis of F-box superfamily genes under phosphate deficiency in tomato. *Plant Physiol. Biochem.* **2021**, *162*, 349-362. doi: 10.1016/j.plaphy.2021.03.002.
450. Senthil-Kumar, M. and Mysore, K.S. Virus-induced gene silencing can persist for more than 2 years and also be transmitted to progeny seedlings in *Nicotiana benthamiana* and tomato. *Plant Biotechnol. J.* **2011**, 97, 797-806, doi: 10.1111/j.1467-7652.2011.00589.x.

List of publications

1. **Akas**h**.,** Rajat Srivastava and Kumar, R. **(2021).** VIGS-based gene silencing for assessing mineral nutrient acquisition. Plant gene silencing. Methods in Molecular Biology, 2nd edition vol. 2408. DOI: 10.1007/978-1-0716-1875-2_11.
2. **Akash.**, Parida, A. P., Srivastava, A., Mathur, S., Sharma, A. K., & Kumar, R. **(2021)**. Identification, evolutionary profiling, and expression analysis of F-box superfamily genes under phosphate deficiency in tomato. Plant Physiology and Biochemistry, DOI: 10.1016/j.plaphy.2021.03.002.
3. Ashima Khurana., **Akash.,** Abhishek Roychowdhury., **(2021)**. Identification of phosphorus starvation inducible SnRK genes in tomato (*Solanum lycopersicum L.). Journal of Plant Biochemistry and Biotechnology*, DOI: 10.1007/s13562-021-00701-0.
4. Srivastava, R., **Akash.**, Parida, A.P., Chauhan, P.K., Kumar, R., **(2020)**. Identification, structure analysis, and transcript profiling of purple acid phosphatases under Pi deficiency in tomato (*Solanum lycopersicum L*.) and its wild relatives. Int. J. Biol. Macromol. DOI: 10.1016/j.ijbiomac.2020.10.080.
5. Sravan Kumar, T., **Akash.**, Naik, N., & Kumar, R. **(2018)**. A ripening-induced SlGH3-2 gene regulates fruit ripening via adjusting auxin-ethylene levels in tomato (*Solanum lycopersicum L*.). *Plant Molecular Biology*, DOI: 10.1007/s11103-018-0790-1.

Conferences and training attended

1. Presented poster on **"Functional elucidation of tomato *FBX2L1* gene in phosphate starvation and fruit ripening using Virus-induced gene silencing and CRISPR/Cas9 mediated gene-editing"** 15th-17th December 2022, at International Conference on Virus Evolution, Infection and Disease Control (ICVEIDC-2022) by Department of Biotechnology & Bioinformatics, School of Life Sciences, University of Hyderabad, India-500046.
2. Presented poster on "**Functional elucidation of a Phosphorus starvation inducible Respiratory burst oxidase *SlRbohH* gene in the reprogramming of root system architecture"** at International conference on Frontier Areas of Science and Technology (ICFAST-2022) organized by Indian JSPS Alumni Association (IJAA), University of Hyderabad, Hyderabad, India-500046.

3. Delivered a presentation entitled **"Strategies to confirm transgenics and gene-edited lines and Virus-induced gene silencing based characterization of the gene of interest"** in online workshop on "Plant functional genomics techniques" 9th-10th may 2022, by SERB-SSR (CRG/2018/001033) at Department of Plant Sciences, University of Hyderabad.
4. Delivered a oral presentation on "**A novel phosphate starvation inducible respiratory burst oxidase homolog gene *SlRbohH* regulates phosphorus starvation responses by controlling reactive oxygen species-mediated root system architecture in tomato"** 29 October 2021, in 13th Plant Sciences Colloquium by the Department of Plant Science, University of Hyderabad.
5. Participant in online workshop on **"Hands-On Training on CRISPR/Cas9 Mediated Gene-editing in Plants"** 3rd-10th October, 2021 by SERB-SSR (CRG/2018/001033) at Department of Plant Sciences, University of Hyderabad.
6. Presented poster on **"Identification and functional characterization of low Phosphate inducible *SlFBX2L1* gene in tomato"** at National conference on Frontiers in Plant Biology, 31st January - 1st February 2020, organized by d Department of Plant Sciences, School of Life Sciences, University of Hyderabad.
7. Presented poster on **"Genome-wide identification of F-box members and functional characterization of F-box gene for its role under phosphate starvation in tomato"** at National conference on Integrative Plant Biochemistry and Biotechnology, 8th-9th November 2019, organized by Society for Plant Biochemistry and Biotechnology, New Delhi and IICAR-IRR, Hyderabad.
8. Participated in **the 59th Annual Conference of Association of Microbiologist of India (AMI-2018) and International Symposium on Host Pathogen Interactions** held on 9th-12th December 2018, by School of Life Sciences, Department of Plant Sciences, University of Hyderabad, Hyderabad, India-500046.
9. Presented the poster entitled "**Understanding the molecular circuitry underlying low phosphorous response in tomato"** in BioQuest-2017 held on 12th -13th October 2017 at School of Life Sciences, University of Hyderabad, Hyderabad , India-500046 .
10. Participant in the Nano3Bio dissemination event entitled **"The future of Chitosans"** held on 20th September 2017, organized by Department of Plant Sciences, School of Life Sciences, University of Hyderabad, Hyderabad, India-500046.

Functional characterization of SlRbohH and SlFBX2L1 genes for their roles in phosphorus starvation response in tomato

by Akash .

Submission date: 14-Dec-2022 11:59AM (UTC+0530)
Submission ID: 1980912933
File name: 17LPPH10_Thesis_141222.pdf (93.49M)
Word count: 42364
Character count: 242518

Functional characterization of SlRbohH and SlFBX2L1 genes for their roles in phosphorus starvation response in tomato

ORIGINALITY REPORT

18%	6%	18%	2%
SIMILARITY INDEX	INTERNET SOURCES	PUBLICATIONS	STUDENT PAPERS

PRIMARY SOURCES

1	Akash, Adwaita Prasad Parida, Alok Srivastva, Saloni Mathur, Arun Kumar Sharma, Rahul Kumar. "Identification, evolutionary profiling, and expression analysis of F-box superfamily genes under phosphate deficiency in tomato", Plant Physiology and Biochemistry, 2021 Publication	9%
2	Akash, Adwaita Prasad Parida, Alok Srivastava, Saloni Mathur, Arun Kumar Sharma, Rahul Kumar. "Identification, evolutionary profiling, and expression analysis of F-box superfamily genes under phosphate deficiency in tomato", Plant Physiology and Biochemistry, 2021 Publication	1%
3	www.ncbi.nlm.nih.gov Internet Source	<1%
4	Rajat Srivastava, Akash, Adwaita Prasad Parida, Pankaj Kumar Chauhan, Rahul Kumar. "Identification, structure analysis, and	<1%

R. Kumar

Dr. RAHUL KUMAR
Assistant Professor
Dept. of Plant Sciences
School of Life Sciences
University of Hyderabad
Hyderabad-500 046, INDIA.

R. Kumar

Dr. RAHUL KUMAR
Assistant Professor
Dept. of Plant Sciences
School of Life Sciences
University of Hyderabad
Hyderabad-500 046, INDIA.

R. Kumar

This is to certify that out of 18% overall similarity, 10% is from the student's own publications which includes 9% from Sl. No 1 and 1% from Sl. No 2, leaving less than 8% similarity

R. Kumar

Dr. RAHUL KUMAR
Assistant Professor
Dept. of Plant Sciences
School of Life Sciences
University of Hyderabad
Hyderabad-500 046, INDIA.

transcript profiling of purple acid phosphatases under Pi deficiency in tomato (Solanum lycopersicum L.) and its wild relatives", International Journal of Biological Macromolecules, 2020
Publication

5	link.springer.com Internet Source	<1%
6	Submitted to University of Hyderabad, Hyderabad Student Paper	<1%
7	"Plant Gene Silencing", Springer Science and Business Media LLC, 2022 Publication	<1%
8	Rajat Srivastava, Parul Sirohi, Harsh Chauhan, Rahul Kumar. "The enhanced phosphorus use efficiency in phosphate-deficient and mycorrhiza-inoculated barley seedlings involves activation of different sets of PHT1 transporters in roots", Planta, 2021 Publication	<1%
9	www.biorxiv.org Internet Source	<1%
10	Zhaopeng Song, Yong Luo, Weifeng Wang, Ningbo Fan, Daibin Wang, Chao Yang, Hongfang Jia. "NtMYB12 Positively Regulates Flavonol Biosynthesis and Enhances	<1%

Tolerance to Low Pi Stress in Nicotiana tabacum", Frontiers in Plant Science, 2020
Publication

11	plantmethods.biomedcentral.com Internet Source	<1%
12	www.frontiersin.org Internet Source	<1%
13	Zhang, Zhaoliang, Hong Liao, and William J. Lucas. "Molecular mechanisms underlying phosphate sensing, signaling, and adaptation in plants : Phosphate sensing and signaling in plants", Journal of Integrative Plant Biology, 2014. Publication	<1%
14	Ying Gao, Wei Wei, Xiaodan Zhao, Xiaoli Tan et al. "A NAC transcription factor, NOR-like1, is a new positive regulator of tomato fruit ripening", Horticulture Research, 2018 Publication	<1%
15	mail.journalcra.com Internet Source	<1%
16	"Legume Nitrogen Fixation in Soils with Low Phosphorus Availability", Springer Science and Business Media LLC, 2017 Publication	<1%
17	www.preprints.org Internet Source	<1%

18	"Climate Change and Plant Abiotic Stress Tolerance", Wiley, 2013 Publication	<1 %
19	www.plantphysiol.org Internet Source	<1 %
20	Hongfang Jia, Songtao Zhang, Lizhi Wang, Yongxia Yang, Hongying Zhang, Hong Cui, Huifang Shao, Guohua Xu. "OsPht1;8, a phosphate transporter, is involved in auxin and phosphate starvation response in rice", Journal of Experimental Botany, 2017 Publication	<1 %
21	Poonam Mehra, Bipin K. Pandey, Lokesh Verma, Jitender Giri. "A Novel Glycerophosphodiester Phosphodiesterase Improves Phosphate Deficiency Tolerance", Plant, Cell & Environment, 2018 Publication	<1 %
22	www.xdtrans.com Internet Source	<1 %
23	Yingchun Han, Na Liu, Chuang Li, Shuaiwu Wang, Lihua Jia, Rui Zhang, Hui Li, Jinfang Tan, Hongwei Xue, Wenming Zheng. "TaMADS2-3D, a MADS transcription factor gene, regulates phosphate starvation responses in plants", The Crop Journal, 2021 Publication	<1 %

24	coek.info Internet Source	<1%
25	Daniel Marino, Christophe Dunand, Alain Puppo, Nicolas Pauly. "A burst of plant NADPH oxidases", Trends in Plant Science, 2012 Publication	<1%
26	docplayer.net Internet Source	<1%
27	www.annualreviews.org Internet Source	<1%
28	Zhang, Y., X. Wang, S. Lu, and D. Liu. "A major root-associated acid phosphatase in Arabidopsis, AtPAP10, is regulated by both local and systemic signals under phosphate starvation", Journal of Experimental Botany, 2014. Publication	<1%
29	d-nb.info Internet Source	<1%
30	"Virus-Induced Gene Silencing in Plants", Springer Science and Business Media LLC, 2020 Publication	<1%
31	academic.oup.com Internet Source	<1%

32	Poonam Mehra, Bipin K. Pandey, Lokesh Verma, Jitender Giri. "A novel glycerophosphodiester phosphodiesterase improves phosphate deficiency tolerance in rice", Plant, Cell & Environment, 2018 Publication	<1 %
33	macsphere.mcmaster.ca Internet Source	<1 %
34	Lingyun Cheng, Bruna Bucciarelli, Junqi Liu, Kelly Zinn et al. "White Lupin Cluster Root Acclimation to Phosphorus Deficiency and Root Hair Development Involve Unique Glycerophosphodiester Phosphodiesterases", Plant Physiology, 2011 Publication	<1 %
35	spandidos-publications.com Internet Source	<1 %
36	Hanne Crombez, Hans Motte, Tom Beeckman. "Tackling Plant Phosphate Starvation by the Roots", Developmental Cell, 2019 Publication	<1 %
37	bmcplantbiol.biomedcentral.com Internet Source	<1 %
38	Hui Chen, Lingrui Zhang, Kangfu Yu, Aiming Wang. "Pathogenesis of Soybean mosaic virus in soybean carrying Rsv1 gene is associated with miRNA and siRNA pathways, and	<1 %

breakdown of AGO1 homeostasis", Virology, 2015
Publication

39	www.jove.com Internet Source	<1 %
40	www.mdpi.com Internet Source	<1 %
41	Bowen Luo, Peng Ma, Zhi Nie, Xiao Zhang et al. "Metabolite profiling and genome-wide association studies reveal response mechanisms of phosphorus deficiency in maize seedling", The Plant Journal, 2019 Publication	<1 %
42	Yeon Jae Hur, Doh Hoon Kim. "Overexpression of OsMAPK2 Enhances Low Phosphate Tolerance in Rice and Arabidopsis thaliana", American Journal of Plant Sciences, 2014 Publication	<1 %
43	archiv.ub.uni-heidelberg.de Internet Source	<1 %
44	Preman R. Soumya, Krishnapriya Vengavasi, Renu Pandey. "Adaptive strategies of plants to conserve internal phosphorus under P deficient condition to improve P utilization efficiency", Physiology and Molecular Biology of Plants, 2022 Publication	<1 %

45	www.curresweb.com Internet Source	<1%
46	discovery.ucl.ac.uk Internet Source	<1%
47	Jarosław Tyburski. "Reactive oxygen species localization in roots of Arabidopsis thaliana seedlings grown under phosphate deficiency", Plant Growth Regulation, 05/18/2009 Publication	<1%
48	Suren Deng, Jingyi Li, Zezhen Du, Zixuan Wu et al. " Rice 1 regulates Pi stress adaptation by maintaining intracellular Pi homeostasis ", Plant, Cell & Environment, 2021 Publication	<1%
49	Xue-qing WANG, Wen-yuan RUAN, Ke-ke YI. "Internal phosphate starvation signaling and external phosphate availability have no obvious effect on the accumulation of cadmium in rice", Journal of Integrative Agriculture, 2019 Publication	<1%
50	gxreferences.blogspot.com Internet Source	<1%
51	Ballachanda N. Devaiah, Athikkattuvalasu S. Karthikeyan, Kashchandra G. Raghothama. "WRKY75 Transcription Factor Is a Modulator	<1%

of Phosphate Acquisition and Root Development in Arabidopsis", Plant Physiology, 2007
Publication

52	Sihui Zhong, Kashif Mahmood, Yong-Mei Bi, Steven J. Rothstein, Kosala Ranathunge. "Altered Expression of OsNLA1 Modulates Pi Accumulation in Rice (Oryza sativa L.) Plants", Frontiers in Plant Science, 2017 Publication	<1 %
53	riunet.upv.es Internet Source	<1 %
54	Methods in Molecular Biology, 2015. Publication	<1 %
55	Synan AbuQamar, Mao-Feng Chai, Hongli Luo, Fengming Song, Tesfaye Mengiste. "Tomato Protein Kinase 1b Mediates Signaling of Plant Responses to Necrotrophic Fungi and Insect Herbivory", The Plant Cell, 2008 Publication	<1 %
56	onlinelibrary.wiley.com Internet Source	<1 %
57	C. Zhu. "Interactions between jasmonates and ethylene in the regulation of root hair development in Arabidopsis", Journal of Experimental Botany, 03/01/2006 Publication	<1 %

58	Hinako Takehisa, Fuminori Ando, Yohei Takara, Akifumi Ikehata, Yutaka Sato. "Transcriptome and hyperspectral profiling allows assessment of phosphorus nutrient status in rice under field conditions", Plant, Cell & Environment, 2022 Publication	<1 %
59	www.nature.com Internet Source	<1 %
60	www.science.org Internet Source	<1 %
61	Byung-Kook Ham, Jieyu Chen, Yan Yan, William J Lucas. "Insights into plant phosphate sensing and signaling", Current Opinion in Biotechnology, 2018 Publication	<1 %
62	Ghazanfar Abbas Khan, Evangelia Vogiatzaki, Gaétan Glauser, Yves Poirier. "Phosphate Deficiency Induces the Jasmonate Pathway and Enhances Resistance to Insect Herbivory", Plant Physiology, 2016 Publication	<1 %
63	Jin, C., C. Fang, H. Yuan, S. Wang, Y. Wu, X. Liu, Y. Zhang, and J. Luo. "Interaction between carbon metabolism and phosphate accumulation is revealed by a mutation of a	<1 %

cellulose synthase-like protein, CSLF6", Journal of Experimental Botany, 2015.
Publication

64	J. P. HAMMOND. "Genetic Responses to Phosphorus Deficiency", Annals of Botany, 08/03/2004 Publication	<1 %
65	Li, Xiaohui, Huijuan Zhang, Limei Tian, Lei Huang, Shixia Liu, Dayong Li, and Fengming Song. "Tomato SlRbohB, a member of the NADPH oxidase family, is required for disease resistance against Botrytis cinerea and tolerance to drought stress", Frontiers in Plant Science, 2015. Publication	<1 %
66	Steven Roberts. "Analysis of Genes Isolated from Plated Hemocytes of the Pacific Oyster, Crassostreas gigas", Marine Biotechnology, 02/2009 Publication	<1 %
67	elifesciences.org Internet Source	<1 %
68	Liangsheng Wang, Dong Liu. "Functions and regulation of phosphate starvation-induced secreted acid phosphatases in higher plants", Plant Science, 2018 Publication	<1 %

69	Zhaopeng Song, Huifang Shao, Huagang Huang, Yan Shen, Lizhi Wang, Feiyue Wu, Dan Han, Jiayong Song, Hongfang Jia. "Overexpression of the phosphate transporter gene OsPT8 improves the Pi and selenium contents in Nicotiana tabacum", Environmental and Experimental Botany, 2017 Publication	<1 %
70	eprints.qut.edu.au Internet Source	<1 %
71	pure.ulster.ac.uk Internet Source	<1 %
72	www.freepatentsonline.com Internet Source	<1 %
73	"Arbuscular Mycorrhizas and Stress Tolerance of Plants", Springer Science and Business Media LLC, 2017 Publication	<1 %
74	"Root Biology", Springer Science and Business Media LLC, 2018 Publication	<1 %
75	HYE-JI KIM. "Ethylene insensitivity impedes a subset of responses to phosphorus deficiency in tomato and petunia", Plant Cell & Environment, 12/2008 Publication	<1 %

76	Jinglong Zhang, Fangfang Jiang, Yixin Shen, Qiuwen Zhan, Binqiang Bai, Wei Chen, Yingjun Chi. "Transcriptome analysis reveals candidate genes related to phosphorus starvation tolerance in sorghum", BMC Plant Biology, 2019 Publication	<1 %
77	Tran, H.T.. "Feeding hungry plants: The role of purple acid phosphatases in phosphate nutrition", Plant Science, 201007/08 Publication	<1 %
78	Yongqiang Zhang, Yi Wang, Enhui Wang, Xueqian Wu, Qinghua Zheng, Yizhen Han, Weiwei Lin, Zhongjuan Liu, Wenxiong Lin. " , a transcription factor identified from tomato, positively regulates the phosphate starvation response ", Physiologia Plantarum, 2021 Publication	<1 %
79	ebin.pub Internet Source	<1 %
80	www.biomedcentral.com Internet Source	<1 %
81	A. J. Pieters. "Low sink demand limits photosynthesis under Pi deficiency", Journal of Experimental Botany, 05/01/2001 Publication	<1 %

82	Guoqiang Huang, Wanqi Liang, Craig J. Sturrock, Bipin K. Pandey et al. "Rice actin binding protein RMD controls crown root angle in response to external phosphate", Nature Communications, 2018 Publication	<1 %
83	Hongfang Jia, Jian'an Wang, Yongfeng Yang, Guoshun Liu, Yong Bao, Hong Cui. "Changes in flavonol content and transcript levels of genes in the flavonoid pathway in tobacco under phosphorus deficiency", Plant Growth Regulation, 2014 Publication	<1 %
84	Xiaoyan Dai, Yuanyuan Wang, An Yang, Wen-Hao Zhang. " , an R2R3 MYB Transcription Factor, Is Involved in the Regulation of Phosphate-Starvation Responses and Root Architecture in Rice ", Plant Physiology, 2012 Publication	<1 %
85	bmcgenomics.biomedcentral.com Internet Source	<1 %
86	intl-aem.asm.org Internet Source	<1 %
87	www.geneticsmr.com Internet Source	<1 %
88	Chandrika, Nulu Naga Prafulla, Kalaipandian Sundaravelpandian, Su-May Yu, and Wolfgang	<1 %

Schmidt. "ALFIN-LIKE 6 is involved in root hair elongation during phosphate deficiency in Arabidopsis", New Phytologist, 2013.
Publication

---

89 Dorota Kawa. "Hormonal solution for (root) hair extension", The Plant Cell, 2020 <1 %
Publication

---

90 JeeNa Hwang, Seonhee Lee, Joung-Ho Lee, Won-Hee Kang, Jin-Ho Kang, Min-Young Kang, Chang-Sik Oh, Byoung-Cheorl Kang. "Plant Translation Elongation Factor 1Bβ Facilitates Potato Virus X (PVX) Infection and Interacts with PVX Triple Gene Block Protein 1", PLOS ONE, 2015 <1 %
Publication

---

91 Kamal Tyagi, Anusha Sunkum, Prateek Gupta, Himabindu Vasuki Kilambi, Yellamaraju Sreelakshmi, Rameshwar Sharma. "Reduced γ-glutamyl hydrolase activity likely contributes to high folate levels in Periyakulam-1 tomato", Cold Spring Harbor Laboratory, 2022 <1 %
Publication

---

92 Plant Ecophysiology, 2005. <1 %
Publication

---

93 Wangfang Ping, Jian Hu, Gongcheng Hu, Yawei Song, Qing Xia, Mingze Yao, Shixin Gong, Cizhong Jiang, Hongjie Yao. "Genome-wide DNA methylation analysis reveals that mouse <1 %

chemical iPSCs have closer epigenetic features to mESCs than OSKM-integrated iPSCs", Cell Death & Disease, 2018
Publication

---

94 Xiaoning Cao, Fei Ma, Tingting Xu, Junjie Wang, Sichen Liu, Gaihong Li, Qian Su, Zhijun Qiao, XiaoFan Na. "Transcriptomic analysis reveals key early events of narciclasine signaling in Arabidopsis root apex", Plant Cell Reports, 2016 <1 %
Publication

---

95 repository.hkbu.edu.hk <1 %
Internet Source

---

96 "Antiviral Resistance in Plants", Springer Science and Business Media LLC, 2012 <1 %
Publication

---

97 Abidur Rahman, Satoko Hosokawa, Yutaka Oono, Taisaku Amakawa, Nobuharu Goto, Seiji Tsurumi. "Auxin and Ethylene Response Interactions during Arabidopsis Root Hair Development Dissected by Auxin Influx Modulators", Plant Physiology, 2002 <1 %
Publication

---

98 Andreas Leiherer, Kathrin Geiger, Axel Muendlein, Heinz Drexel. "Hypoxia induces a HIF-1α dependent signaling cascade to make a complex metabolic switch in SGBS- <1 %

adipocytes", Molecular and Cellular Endocrinology, 2014
Publication

---

99 Gurpreet Kaur, Harminder Pal Singh, Daizy R. Batish, Priyanka Mahajan, Ravinder Kumar Kohli, Valbha Rishi. "Exogenous Nitric Oxide (NO) Interferes with Lead (Pb)-Induced Toxicity by Detoxifying Reactive Oxygen Species in Hydroponically Grown Wheat (Triticum aestivum) Roots", PLOS ONE, 2015 <1 %
Publication

---

100 Kegui Chen. "Transcriptional Responses to Gibberellin and Abscisic Acid in Barley Aleurone", Journal of Integrative Plant Biology, 5/2006 <1 %
Publication

---

101 LEE, SANG SOOK, HYUN JI PARK, DAE HWA YOON, BEOM-GI KIM, JUN CHEUL AHN, SHENG LUAN, and HYE SUN CHO. "Rice cyclophilin OsCYP18-2 is translocated to the nucleus by an interaction with SKIP and enhances drought tolerance in rice and Arabidopsis : SKIP interacting cyclophilin enhances drought tolerance", Plant Cell & Environment, 2015. <1 %
Publication

---

102 Suvi Honkanen, Liam Dolan. "Growth regulation in tip-growing cells that develop on <1 %

the epidermis", Current Opinion in Plant Biology, 2016
Publication

103	Takafumi Narise. "Involvement of auxin signaling mediated by IAA14 and ARF7/19 in membrane lipid remodeling during phosphate starvation", Plant Molecular Biology, 12/31/2009 Publication	<1 %
104	Yaze Kong, Gang Wang, Xian Chen, Linying Li, Xueying Zhang, Sangtian Chen, Yuqing He, Gaojie Hong. " modulates phosphate starvation - induced signaling and resistance to pv. ", Plant, Cell & Environment, 2021 Publication	<1 %
105	cmjournal.biomedcentral.com Internet Source	<1 %
106	dennislab.lunenfeld.ca Internet Source	<1 %

Exclude quotes On
Exclude bibliography On
Exclude matches < 14 words

This is to certify that out of 18% similarity, 10% is from the student's own papers, which includes 9% from Sl. No 1 and 1% from Sl. No 2. That leaves 8% similarity.

R. Kumar

Dr. RAHUL KUMAR
Assistant Professor
Dept. of Plant Sciences
School of Life Sciences
University of Hyderabad
Hyderabad-500 046, INDIA.